"Give a man the answer and he will be momentarily satisfied. Teach a man to reason and he will think for a lifetime."

Aashish Priye

University of Alberta

State inference and Bayesian identification of non-linear state-space models

by

Aditya Tulsyan

A thesis submitted to the Faculty of Graduate Studies and Research
in partial fulfillment of the requirements for the degree of

Doctor of Philosophy

in

Chemical Engineering

Department of Chemical and Materials Engineering

©Aditya Tulsyan
Fall 2013
Edmonton, Alberta

This thesis is dedicated to my grandfather

Abstract

The main focus of this thesis is on state inference and identification of non-linear dynamical systems, which can be represented by discrete-time, stochastic state-space models (SSMs). We consider the state inference and identification as related, but two distinct problems. For identification of SSMs, we restrict ourselves only to the class of Bayesian methods. In this thesis, we develop a novel sequential Monte Carlo (SMC) based Bayesian method for simultaneous on-line state inference and identification of non-linear SSMs. Extension of the method to handle missing measurements in real-time is also provided. Using posterior Cramér-Rao lower bound (PCRLB), a minimum mean square error (MMSE) simultaneous state inferencing and identification strategy is developed for general non-linear systems. The PCRLB used here is derived for discrete-time, stochastic non-linear SSMs with unknown model parameters. It is shown that under some conditions, performing simultaneous state inferencing and identification according to the developed PCRLB based strategy yields a minimum mean square error state and parameter estimates.

To allow assessment of the quality of the parameter estimates, a PCRLB based tool is developed for error analysis. A distinct advantage of the developed tool is that it is general, and can be used to perform error analysis for an entire class of on-line Bayesian identification methods. In addition to the above developments, the problems of input design and prior design are also considered in this thesis. The input design problem helps to design optimal inputs for Bayesian identification of non-linear SSMs; whereas, the prior design problem helps to effectively organize a priori information available on the process and

model parameters. In this thesis, the problem of prior design is only considered in the context of designing optimal inputs for Bayesian identification of non-linear SSMs.

For state inferencing in non-linear SSMs, we develop a PCRLB based performance assessment and diagnosis tool for different non-linear state filters. The proposed assessment and diagnosis tool makes use of PCRLB, derived for discrete-time, stochastic non-linear SSMs with known model parameters. The utility of the above developments in devising an optimal state inferencing strategy for non-linear systems is also provided. To avoid using the true states in the computation of the PCRLB, an SMC based method is also developed to allow computation of the PCRLB in absence of true state information.

Finally, we show how the tools developed in this thesis can be put together into a unified framework to allow for efficient state inferencing and Bayesian identification of non-linear dynamical systems.

Acknowledgements

support, advise, and words of encouragement has definitely helped me in putting this thesis together. The errors and ambiguities in the papers we have published, including this thesis would have been much more severe and frequent if it were not for Biao, Fraser and Bhushan, who tirelessly proofread the papers and various parts of this thesis.

I would also like to thank Prof. Lakshminarayanan Samavedham from the Informatics and Process Control (IPC) unit at National University of Singapore for helping me take some of the difficult decisions during my time as an undergraduate student. My decision to pursue graduate studies at University of Alberta was made in consultation with him.

There are three persons who made a significant difference to my life in Edmonton-Dr. Anuj Narang, Dr. Swanand Khare and Tathagata Chakraborty. I am extremely thankful to Anuj and Swanand for patiently putting up with my constant bombardment of *'Okay. Tell me something,...'* questions (I do think that they used to get ruffled at times though). Despite their busy schedule at work, they diligently helped me with a variety of things; whether it be the subtle concepts in process control or the mysterious ways in which LATEX works. Swanand and Anuj never fell short of helping me understand it. I thoroughly enjoyed the brief, but intriguing *Saturday Sessions* with Swanand. Not only did we discuss a great deal of probability and irrational numbers over a cup of tea on Saturday evenings, we also had numerous philosophical discussions, which often ended in long awkward silence. I also had an opportunity to collaborate with Swanand on some of the interesting problems in systems theory. Other than academics, in Anuj's company, I learnt a number of cooking tricks and card games (I did beat him in a lot of games, including cards!). Tathagata was my room mate for almost two years and I cherish the memories of innumerable discussions we had on a spectrum of topics, although I did not agree with him on lot of things. I also cherish the *Friday Night* dinners we used to go out for without fail. They all deserve many thanks for making my stay in Edmonton comfortable and memorable.

I am also thankful to Aashish Priye and Vikram Bhandari, who have not only been

Contents

List of Tables

List of Figures

List of Abbreviations and Symbols

Abbreviations

a.s.	Almost surely
Ad-SIR	Adaptive sequential importance resampling
ADA	Artificial dynamics approach
ASIR	Auxiliary sequential importance resampling
CRLB	Cramér-Rao lower bound
CVP	Control vector parametrization
EKF	Extended Kalman filter
EM	Expectation maximization
EnKF	Ensemble Kalman filter
FIM	Fisher information matrix
GBF	Grid-based filter
HMM	Hidden Markov model
i.i.d.	Independent and identically distributed
ISF	Importance sampling function

KF	Kalman filter
KL	Kullback-Leibler
MC	Monte Carlo
MCMC	Markov chain Monte Carlo
ML	Maximum likelihood
MMSE	Minimum mean square error
MSE	Mean square error
NEES	Normalized estimation error squared
NIS	Normalized innovation square
NLP	Non-linear programming
OLFC	Open-loop feedback-control
PCRLB	Posterior Cramér-Rao lower bound
pdf	Probability density function
PF	Particle filter
PFIM	Posterior Fisher information matrix
R-ASIR	Redesigned auxiliary sequential importance resampling
R-SIR	Redesigned sequential importance resampling
RBPF	Rao-Blackwellised particle filter
RPF	Regularized particle filter

s.t.	Subject to
SIR	Sequential importance resampling
SMC	Sequential Monte Carlo
SMSE	Scalar mean square error
SNMSE	Sum of trace of normalized mean square error
SSM	State-space model
UKF	Unscented Kalman filter

State-space models

(A_t, B_t, C_t, D_t)	System matrices for a linear state-space model
$\mathcal{U}$	Input space
$\mathcal{X}$	State space
$\mathcal{Y}$	Measurement space
$\mathcal{Z}$	Joint state and parameter space
Θ	Parameter space
ζ	Experiment design space
$\{\eta_t\}_{t \in \mathbb{N}}$	Experiment design vector
$\{\theta_t\}_{t \in \mathbb{N}}$	r- dimensional parameter process
$\{\xi_t\}_{t \in \mathbb{N}}$	r- dimensional artificial parameter noise process
$\{U_t\}_{t \in \mathbb{N}}$	p- dimensional input process

$\{V_t\}_{t\in\mathbb{N}}$	n- dimensional state noise process
$\{W_t\}_{t\in\mathbb{N}}$	m- dimensional measurement noise process
$\{X_t\}_{t\in\mathbb{N}}$	n- dimensional state process
$\{Y_t\}_{t\in\mathbb{N}}$	m- dimensional measurement process
$\{Z_t\}_{t\in\mathbb{N}}$	s- dimensional joint state and parameter process
$f_t(\cdot)$	State transition function
$g_t(\cdot)$	Measurement function
Q_t	State noise covariance
R_t	Measurement noise covariance
T	Total experiment time
t	Discrete-time

Operators, functions and miscellaneous symbols

$:=, \leftarrow$	Assignment
$\approx$	Approximation
$\arg\max_x$	Argument x maximizing the operand
$\arg\min_x$	Argument x minimizing the operand
Card	Cardinality of a set
Δ	Laplacian operator
$\mathrm{diag}(v)$	n- dimensional diagonal matrix with entries given by $v \in \mathbb{R}^n$

$\wedge$	Logical conjunction
$\wedge$	Logical disjunction
$|x|$	Absolute value of x
$\mathcal{C}^k(\mathbb{R})$	Class of continuous function in $\mathbb{R}$ with k-order derivative in $\mathbb{R}$
$\mathcal{O}(\cdot)$	Time complexity of algorithm
∇	Gradient operator
$\otimes$	Kronecker product
$\propto$	Proportional
$\succ$	Partial order induced by cone of positive definite matrices
$\succeq$	Partial order induced by cone of semi-positive definite matrices
$\mathrm{supp}\, f$	Support of a function f
$\mathrm{Tr}[A]$	Trace of matrix A
$\triangleq$	Definition
$A \circ B$	Hadamard product of matrices A and B
A^T	Transpose of matrix A
$A^{\circ -1}$	Hadamard inverse of matrix A
h_t	Kernel parameter at time t
$I_{n \times n}$	n- dimensional identity matrix
J_t^{-1}	Posterior Cramér-Rao lower bound at time t

J_t	Posterior Fisher information matrix at time t
M	Number of Monte Carlo simulations
N	Number of particles
$P_{t|t}^{\theta}$	Mean square error for a parameter filter at time t
$P_{t|t}^{z}$	Mean square error for a state-parameter filter at time t
$P_{t|t}, P_{t|t}^{x}$	Mean square error for a state filter at time t
$||\cdot||_2$	2- norm operator
$W_{t|t}^{i}$	Importance weight i

Probability and distributions

$\mathbb{E}_{p(\cdot)}$	Expectation with respect to density $p(\cdot)$
$\mathbb{V}_{p(\cdot)}$	Covariance/variance with respect to density $p(\cdot)$
$\mathcal{R}_Z$	Mean square error Bayesian risk function for random variable Z
$\Pr(\cdot)$	Probability mass function for a discrete random variable
$\Pr_d$	Probability of detection
$\Pr_f$	Probability of false alarm
$\sim$	Sampled from or distributed according to
$\tilde{p}(\cdot)$	Approximation of a probability density function
$D_{q||p}$	Kullback-Leibler divergence between densities q and p
$p(\cdot)$	Probability density function for a continuous random variable

$\delta_x(dx)$	Point mass at x (Dirac δ- distribution)
$\mathcal{N}(x|m, \Sigma)$	Multi-variate Gaussian with mean m and covariance Σ
$\mathcal{R}(x|\Sigma)$	Rayleigh distribution with covariance Σ
$\widehat{X}_{t|t}$	point estimate of $\{X_t\}_{t\in\mathbb{N}}$ at t, given input-output data until t
P_Γ	Stochastic vector
P_Π	Stochastic matrix

Spaces

$\mathbb{F}^{m\times n}$	Space of $m \times n$ stochastic matrices
$\mathbb{N}$	Natural numbers
$\mathbb{N}_0$	Natural numbers with 0 included
$\mathbb{R}$	Real numbers
$\mathbb{R}^n$	n- dimensional Euclidean space
$\mathbb{R}^{m\times n}$	Space of $m \times n$ real matrices
$\mathbb{R}_+$	non-negative real numbers
$\mathcal{S}^n$	Symmetric $n \times n$ real matrices
$\mathcal{S}^n_+$	Non-negative definite, symmetric $n \times n$ matrices
$\mathcal{S}^n_{++}$	Positive definite, symmetric $n \times n$ matrices
L^p	Linear space of pth power absolutely integrable functions

Chapter 1

Introduction

Assume that for a given chemical process or a system, we have at our disposal a sensor, or a measuring device, from which we can record the values y_t for some important process variable (output), corresponding to the input action u_t implemented at some time point, indexed by $t \in \mathbb{N}$. Now based on the available input-output measurements, we are interested in learning something or drawing some conclusions about the underlying system, which generated the data. For example, let us assume that we have a sequence of recorded measurements $y_{1:t} \triangleq \{y_1, y_2, \ldots, y_t\}$ corresponding to the input sequence $u_{1:t} \triangleq \{u_1, u_2, \ldots, u_t\}$, and we are interested in predicting the future value of y_{t+1} for some known input action u_{t+1}. To solve this problem, we can either assume that the future value y_{t+1} will completely be independent of its past values $y_{1:t}$; in which case, the prediction of y_{t+1} will be impossible, or we can assume that the future value y_{t+1} will depend on the trend recorded in its past values $y_{1:t}$. For the latter assumption, using a model representation of a system aids in predicting the future values of measurements; however, in most practical systems, it is extremely difficult to find a process model that exactly describes the measurements. This is primarily because of the instrument or sensor noise present in measuring devices. To account for such random fluctuations in measurements, we can view the measurement sequence $y_{1:t}$ as some random realization of a stochastic measurement process $\{Y_t\}_{t \in \mathbb{N}}$, such that $\{Y_{1:t} = y_{1:t}\}$ represents one such random realization. Hence, a

model for the underlying system can be represented by the model for the stochastic process.

In this thesis, we work with a specific class of time-series model, known as state-space models (SSMs). SSMs are primarily stochastic difference equations, which can be used to represent a wide class of dynamical systems. For instance, assuming $\{X_t\}_{t \in \mathbb{N}}$ to be another stochastic process, a dynamical system with a SSM representation can be written as

$$X_{t+1} = f(X_t, \theta, u_t) + V_t, \tag{1.1a}$$

$$Y_t = g(X_t, \theta, u_t) + W_t. \tag{1.1b}$$

Equation (1.1a) is the state equation, which describes the time evolution of the internal states X_t of a system. Given state X_t and input u_t at time t, and model parameter θ, the state evolution at $t+1$ can be computed using the state transformation function $f(X_t, u_t, \theta)$, plus some process noise V_t. The process noise in (1.1a) accounts for all the unknown and unmeasured variations in the states not captured by the model. Note that since the state X_{t+1} depends on its past state X_t, (1.1a) captures the process dynamics, and is sometimes also called the dynamical state equation. Equation (1.1b) is a measurement equation; wherein the transformation $g(X_t, u_t, \theta)$ describes how the measurement or sensor reading Y_t relates to the internal state X_t and model parameter θ. In (1.1b), W_t accounts for the sensor noise, which corrupts the measurement readings. If f and g in model (1.1) are linear functions, the SSM is called linear, and for non-linear f and g, the SSM is non-linear.

In this thesis we will be concerned with the two key problems arising for non-linear systems-state inference and identification. These problems are briefly described next.

1.1   State inference

The state process $\{X_t\}_{t \in \mathbb{N}}$ in (1.1) is not measured directly and is sometimes referred to as a hidden or latent state. Therefore, given a fully specified SSM, any inference we wish to draw on the state process $\{X_t\}_{t \in \mathbb{N}}$ must be based on the sampled input-output data $\{u_t, y_t\}_{t \in \mathbb{N}}$ available for a given dynamical system. This is called state inferencing.

Based on the requirements, a state inferencing problem can be solved to estimate some past, present or future states of a dynamical system. In this thesis, we only focus on estimation of the present states.

For any generic sequence $\{k_t\}_{t\in\mathbb{N}}$, let $k_{i:j} \triangleq \{k_i, k_{i+1}, \ldots, k_j\}$. Given a sequence of input-output data $\{u_{1:t}, y_{1:t}\}$ generated from a process described by a SSM, the state inferencing problem can be solved by computing the state posterior probability density $p(x_t|y_{1:t}, u_{1:t}, \theta)$. The state posterior density contains all the statistical information about the state process X_t at time $t \in \mathbb{N}$ based on the process information available until $t \in \mathbb{N}$. Although a state posterior density gives us complete information about the state process $\{X_t\}_{t\in\mathbb{N}}$, in practice, we are often interested in computing a point estimate of $\{X_t\}_{t\in\mathbb{N}}$, rather than its density. For example, in state-feedback control, we only require point estimate of the states. A common choice for the point estimate in state inferencing, includes the mean or mode of the posterior density. These point estimates can be computed, once the state posterior density is made available. A recursive approach to compute a state posterior density is given by the Bayes' theorem, and the procedure involved is called state filtering.

For processes modelled by linear SSMs, the state posterior density can be exactly computed by Kalman filter (KF) using a finite number of moments (e.g., mean, variance); whereas, for non-linear SSMs, at least in theory, an infinite number of moments are required for exact representation of the posterior density. Thus, with finite computing capabilities, the state inferencing problem for non-linear SSMs cannot be optimally solved.

1.2   System identification

A key requirement in solving the state inferencing problem is that in addition to the input-output data, the model parameters θ of a SSM should be exactly known. This requirement is also evident from the posterior density $p(x_t|y_{1:t}, u_{1:t}, \theta)$ we are interested in computing for all $t \in \mathbb{N}$. In practice, this assumption might be a little restrictive, since for most of

the complex engineering systems, the model parameters are either not precisely known or they change over time. In such situations, estimating or identifying the present value of the model parameters is crucial to ensure acceptable filtering performance of the state filters. This is called a system identification problem.   More formally, a system identification problem aims at finding the model parameters θ, which explain the measurement $\{Y_t\}_{t \in \mathbb{N}}$ generated from the system based on the input $\{u_t\}_{t \in \mathbb{N}}$. System identification is a mature and broad area of research. Thus to keep the scope of this thesis focussed, we will only consider the use of Bayesian methods in estimating the unknown parameters of an SSM.

In the Bayesian framework, the identification problem is formulated by assuming the unknown and non-random parameters of the model as a set of random variables. This is followed by setting up a prior density for the parameters, such that $\theta \sim p(\theta)$. The prior density $p(\theta)$ is a probabilistic representation of the a priori information available for the parameters, before observing the input-output data. For example, if absolutely nothing is known about the value of the parameters, we can select a uniform density as a prior density. After the input-output data is made available, lets say $\{u_{1:t}, y_{1:t}\}$ is the sampled data set, we can refine our prior understanding of the parameters by computing an updated density, called parameter posterior density $p(\theta|y_{1:t}, u_{1:t})$. As in state inferencing, a parameter posterior density encapsulates all the statistical information available for the unknown parameters, given a set of input-output data and prior density $p(\theta)$. Although the Bayesian formulation of the identification problem is strikingly similar to the state inferencing problem, computing $p(\theta|y_{1:t}, u_{1:t})$ for all $t \in \mathbb{N}$ has proven to be much more complex. This is because in SSMs, since the state process $\{X_t\}_{t \in \mathbb{N}}$ is hidden, computing the parameter posterior density $p(\theta|y_{1:t}, u_{1:t})$ requires marginalization of a much more complex, multi-dimensional joint state and parameter posterior density $p(x_t, \theta|y_{1:t}, u_{1:t})$. The severity of the problem is highlighted from the fact that no closed form solution to $p(\theta|y_{1:t}, u_{1:t})$ exists even for linear SSMs. The main problems addressed in this thesis are

discussed next.

1.3   Problems of interest

Although there are many real world applications in which the process dynamics naturally manifest themselves in non-linear models; in engineering, the focus has traditionally been on linear models. This is because, compared to the linear models, non-linear models often require huge computational resources, and are, in general, much more difficult to work with. Interestingly, in the last decade or so, with the advent of high-speed computing technology, and the development of advanced and sophisticated computational tools, working with non-linear systems is no longer as formidable as it once used to be. Motivated by some of these developments, this thesis focuses on state inference and Bayesian identification of non-linear systems. Problems addressed in this thesis are:

1. **Identification methods:** In the past few decades, extensive work has been done to efficiently solve the state inferencing problem for non-linear SSMs; however, their extension to address the identification problem has received attention only recently. Despite the advances in numerical and simulation-based methods, identification of SSMs is a long-standing problem. This is due to the non-trivial complexities introduced with estimation of the model parameters. The first problem of interest is to develop an approach to on-line state and parameter estimation in non-linear SSMs.

2. **Prior design:** A major point of contention between the Frequentist and Bayesian statisticians is on the use of a prior density. Although a prior density plays a critical role in Bayesian methods, its selection and design is often termed by Frequentists as- 'mysterious' and 'ad-hoc'. The second problem of interest is to explore ways to organize available a priori information and systematically design the prior density.

3. **Input design:** The parameter posterior density $p(\theta|u_{1:t}, y_{1:t})$ required in Bayesian

identification of SSMs depends on the choice of the input sequence. By a judicious choice of the input sequence $\{u_{1:t}\}_{t\in\mathbb{N}}$, the density $p(\theta|u_{1:t}, y_{1:t})$ can be 'steered' in order to yield an accurate estimate of θ. This is called the Bayesian input design problem. Bayesian input design for regression models is a well established area of research; however, its extension to SSMs has been limited. Despite the success with regression models, no known Bayesian input design methods are available for identification of SSMs. This is due to the unobserved state process $\{X_t\}_{t\in\mathbb{N}}$, which makes the design problem difficult to solve. The third problem of interest is to develop input design methods for Bayesian identification of non-linear SSMs.

4. **Assessment problem:** Over the last few decades, several state filtering and identification methods based on statistical and analytical approximations of the posterior density have been developed to allow for inferencing and identification of non-linear SSMs. Although these numerical and simulation-based approximate methods can be used for general or specific type of non-linear SSMs, their performance is often restricted by the underlying numerical and statistical approximations used in their design. The forth problem aims at developing methods to assess the performance of different state filters and identification methods.

5. **Error analysis:** For researchers designing improved filtering and identification methods for non-linear SSMs, it is often in their interest to understand why the performance of existing methods is low or in which ways can the overall performance of a method be improved. This is particularly important for non-linear SSMs; wherein, any tractable state inferencing or identification method is only an approximation to the original problem. The fifth problem of interest is to develop a systematic error analysis method for performance diagnosis and quality monitoring of different state filters and Bayesian identification methods.

Table 1.1: Classification of thesis chapters based on their main content

Content	Chapters
System identification	2,3,4,5,6
State inference	7,8

6. **Selection problem:**   A recent surge of interest in developing advanced numerical and simulation-based methods for state inference and identification of non-linear SSMs has left researchers and practitioners inundated with a large number of sub-optimal methods to choose from. The problem of 'selection' is that there is no one single filtering or identification method, which is guaranteed to perform well for all non-linear systems, and at all operating conditions. The final problem of interest is to develop a strategy, which would allow us to select the 'best' state inference and Bayesian identification method for our system.

1.4   Thesis outline

This thesis is a collection of papers published by the author of this thesis. Given below is a short summary of each chapter. In Table 1.1, classification of thesis chapters based on their main content is provided.

Chapter 2: On simultaneous on-line state and parameter estimation in non-linear state-space models

Tulsyan, A., B. Huang, R.B. Gopaluni and J.F. Forbes (2013). On simultaneous on-line state and parameter estimation in non-linear state-space models. *Journal of Process Control* **23**(4), 516–526.

Summary: On-line estimation plays an important role in process control and monitoring. Obtaining a theoretical solution to the simultaneous state-parameter estimation problem for non-linear stochastic systems involves solving complex multi-dimensional integrals that are not amenable to analytical solution. While basic sequential Monte Carlo (SMC) or particle

filtering (PF) algorithms for simultaneous estimation exist, it is well recognized that there is a need for making these on-line algorithms non-degenerate, fast and applicable to processes with missing measurements. To overcome the deficiencies in traditional algorithms, this chapter proposes a Bayesian approach to on-line state and parameter estimation. Its extension to handle missing data in real-time is also provided. The simultaneous estimation is performed by filtering an extended vector of states and parameters using an adaptive sequential-importance-resampling (Ad-SIR) filter with a kernel density estimation method. The approach uses an on-line optimization algorithm based on Kullback-Leibler (KL) divergence to allow adaptation of the SIR filter for combined state-parameter estimation. An optimal rule to tune the kernel width and the variance of the artificial noise added to the parameters is also proposed. The approach is illustrated through numerical examples.

Chapter 3: Minimum mean square error non-linear target tracking strategy in presence of unknown static parameters

Tulsyan, A., S.R. Khare, B. Huang, R.B. Gopaluni and J.F. Forbes (2013). Minimum mean square error non-linear target tracking strategy in presence of unknown static parameters. *To be submitted for journal publication.*

Summary: Non-linear filters of different approximations and capabilities allow for real-time target tracking in non-linear systems. We propose a posterior Cramér-Rao lower bound (PCRLB) inequality based measure to simultaneously assess the tracking performance of different non-linear filters. Using the developed measure, average-optimal and optimal minimum mean square error (MMSE) tracking strategies are proposed for target tracking in non-linear state-space models (SSMs) with non-Gaussian noise and unknown target parameters. A systematic procedure to monitor the quality of the target estimates obtained with the proposed tracking strategies is also developed. The practical utility and efficacy of the developed PCRLB based tools are illustrated on a ballistic target tracking problem at re-entry phase with unknown ballistic coefficient.

Chapter 4: Error analysis in Bayesian identification of non-linear state-space models

Tulsyan, A., B. Huang, R.B. Gopaluni and J.F. Forbes (2013). Bayesian identification of non-linear state-space models: Part II-Error analysis. In: *Proceedings of the 10th IFAC International Symposium on Dynamics and Control of Process Systems*. Mumbai, India. Accepted for publication.

Summary: In the last two decades, several methods based on sequential Monte Carlo (SMC) and Markov chain Monte Carlo (MCMC) have been proposed for Bayesian identification of stochastic non-linear state-space models (SSMs). It is well known that the performance of these simulation-based identification methods depends on the numerical approximations used in their design. We propose the use of posterior Cramér-Rao lower bound (PCRLB) as a mean square error (MSE) bound. Using PCRLB, a systematic procedure is developed to analyse the estimates delivered by Bayesian identification methods in terms of bias, MSE, and efficiency. The efficacy and utility of the proposed approach is illustrated through a numerical example.

Chapter 5: Input design for Bayesian identification of non-linear state-space models

Tulsyan, A., S.R. Khare, B. Huang, R.B. Gopaluni and J.F. Forbes (2013). Bayesian identification of non-linear state-space models: Part I-Input design. In: *Proceedings of the 10th IFAC International Symposium on Dynamics and Control of Process Systems*. Mumbai, India. Accepted for publication.

Summary: We propose an algorithm for designing optimal inputs for on-line Bayesian identification of stochastic non-linear state-space models. The proposed method relies on minimization of the posterior Cramér Rao lower bound derived for the model parameters, with respect to the input sequence. To render the optimization problem computationally tractable, the inputs are parametrized as a multi-dimensional Markov chain in the input

space. The proposed approach is illustrated through a simulation example.

Chapter 6: Designing priors for robust Bayesian optimal input design

Tulsyan, A., J.F. Forbes and B. Huang (2012). Designing priors for robust Bayesian optimal experimental design. *Journal of Process Control* **22**(2), 450-462.

Summary: Building mathematical models is a common task in process systems engineering; wherein, parameter estimation is often the final step of the modelling exercise. Model-based input design has evolved as a potential statistical tool for reducing uncertainties in the parameter estimates. Designing optimal experiments for parameter estimation in non-linear dynamical systems is still an open research problem. Often a huge volume of process information is generated as an end result of an experiment design. This chapter deals with how information available a priori, can be organized and systematically used under the Bayesian framework for designing optimal experiments. Several novel techniques for organizing a priori process knowledge are also explored from a theoretical view point. The influence of the proposed prior designs on parameter estimates is demonstrated on a semi-continuous Baker's yeast fermenter problem.

Chapter 7: A particle filter approach to approximate posterior Cramér-Rao lower bound: The case of hidden states

Tulsyan, A., B. Huang, R.B. Gopaluni and J.F. Forbes (2013). A particle filter approach to approximate posterior Cramér-Rao lower bound: The case of hidden states. *IEEE Transactions on Aerospace and Electronic Systems* **49**(4), In press.

Summary: The posterior Cramér-Rao lower bound (PCRLB) derived in (Tichavský *et al.*, 1998) provides a bound on the mean square error (MSE) obtained with any non-linear state filter. Computing the PCRLB involves solving complex, multi-dimensional expectations, which do not lend themselves to an easy analytical solution. Furthermore, any attempt to approximate it using numerical or simulation based approaches requires a priori

access to the true states, which may not be available, except in simulations or in carefully designed experiments. To allow recursive approximation of the PCRLB when the states are hidden or unmeasured, a new approach based on sequential Monte Carlo (SMC) or particle filters (PF) is proposed. The approach uses SMC methods to estimate the hidden states using a sequence of the available sensor measurements. The developed method is general and can be used to approximate the PCRLB in non-linear state-space models (SSMs) with non-Gaussian state and sensor noise. The efficacy of the developed method is illustrated on two simulation examples, including a ballistic target tracking problem at re-entry phase.

Chapter 8: Assessment, diagnosis, and optimal selection of non-linear state filters

Tulsyan, A., B. Huang, R.B. Gopaluni and J.F. Forbes (2013). Assessment, diagnosis, and optimal selection of non-linear state filters. *Journal of Process Control*, In review.

Tulsyan, A., B. Huang, R.B. Gopaluni and J.F. Forbes (2012). Performance assessment of non-linear state filters. In: *Proceedings of the 8th IFAC International Symposium on Advanced Control of Chemical Processes*. Keynote paper. Singapore. pp. 371–376.

Summary: Non-linear state filters of different approximations and capabilities allow for real-time estimation of unmeasured states in non-linear stochastic processes. It is well known that the performance of these non-linear filters depends on the numerical and statistical approximations used in their design. Despite the practical interest in evaluating the performance of different non-linear filtering methods, it remains one of the most complex problems in the area of non-linear state estimation. We propose the use of the posterior Cramér-Rao lower bound (PCRLB) or mean square error (MSE) inequality as a filtering performance benchmark. Using the PCRLB inequality, an assessment and diagnosis tool is developed for monitoring and evaluating the performance of different non-linear filters. Based on the developed tool, a minimum MSE non-linear filter switching strategy is proposed to maintain high filtering performance under various operating

conditions. The complex, high dimensional integrals involved in the computation of the PCRLB inequality are approximated using sequential Monte Carlo (SMC) methods. The approach is illustrated through a numerical example.

1.5   Contributions

The main contributions in this thesis are briefly summarized below. The contributions are classified into two groups (see Table 1.1)- system identification and state inference.

System identification

- An adaptive sequential-importance-resampling filter (Ad-SIR) for simultaneous on-line state inference and Bayesian identification in general non-linear state-space models (SSMs) is developed. This method is presented in Chapter 2 together with its extension to handle on-line state and parameter estimation under missing data.

- A minimum mean square error strategy for simultaneous on-line state inference and identification strategy in general non-linear SSMs is presented in Chapter 3. Performance assessment for a class of on-line state inference and Bayesian identification methods is also discussed in Chapter 3.

- A new approach to systematically perform error analysis for a class of on-line Bayesian system identification methods is presented in Chapter 4.

- Input design for improving the performance of on-line Bayesian system identification methods in terms of mean square error is discussed in Chapter 5.

- A novel approach to design and organize a priori information in the context of input design for off-line Bayesian system identification is discussed in Chapter 6.

State inference

- A sequential Monte Carlo based posterior Cramér-Rao lower bound approximation for on-line state inferencing problem is presented in Chapter 7.

- A novel approach to performance assessment, diagnosis and optimal selection of on-line state inferencing methods is developed and discussed in Chapter 8.

Chapter 2

On simultaneous on-line state and parameter estimation in non-linear state-space models

On-line estimation plays an important role in process control and monitoring. Obtaining a theoretical solution to the simultaneous state-parameter estimation problem for non-linear stochastic systems involves solving complex multi-dimensional integrals that are not amenable to analytical solution. While basic sequential Monte Carlo (SMC) or particle filtering (PF) algorithms for simultaneous estimation exist, it is well recognized that there is a need for making these on-line algorithms non-degenerate, fast and applicable to processes with missing measurements. To overcome the deficiencies in traditional algorithms, this chapter proposes a Bayesian approach to on-line state and parameter estimation. Its extension to handle missing data in real-time is also provided. The simultaneous estimation is performed by filtering an extended vector of states and parameters using an adaptive sequential-importance-resampling (Ad-SIR) filter with a kernel density estimation method. The approach uses an on-line optimization algorithm based on Kullback-Leibler (KL) divergence to allow adaptation of the SIR filter for combined state-parameter estimation. An optimal rule to tune the kernel width and the variance of the artificial noise added to the

parameters is also proposed. The approach is illustrated through numerical examples.

2.1 Introduction

Recent advances in high speed computation have allowed the process industries to use complex high-fidelity non-linear dynamic models, such as in: a fermentation bioreactor (Chitralekha *et al.*, 2010); polymerization (Achilias and Kiparissides, 1992); and petroleum reservoirs (Evensen, 2007). Implementing advanced control strategies or monitoring process behaviour require real-time data processing for on-line estimation of the key process states and model parameters, which are either unmeasured or unknown. An extensive literature is available on on-line state estimation using sub-optimal Bayesian filters, such as extended Kalman filters (EKFs), unscented Kalman filters (UKFs), approximate grid-based filters (GBFs), and particle filters (PFs) (Soroush, 1998; Arulampalam *et al.*, 2002; Rawlings and Bakshi, 2006); however, their extension to on-line state-parameter estimation has received attention only recently.

In the past 15 years, several algorithms have been proposed to solve the simultaneous state-parameter estimation problem in real-time using likelihood and Bayesian derived methods. Despite the advances in SMC methods, which provide a good approximation to the optimal non-linear filter under weak assumption, simultaneous state-parameter estimation is a long-standing problem (Andrieu *et al.*, 2005). This is due to the non-trivial complexities introduced with on-line estimation of the unknown model parameters (Chen *et al.*, 2005). This chapter considers simultaneous on-line state-parameter estimation in non-linear stochastic systems under the Bayesian framework. The existing and current developments in both Bayesian and likelihood based methods for on-line state and parameter estimation are first briefly reviewed. An exposition of parameter estimation using Bayesian and likelihood based methods can be found in (Kantas *et al.*, 2009).

The central idea of simultaneous on-line Bayesian estimators is certainly not new.

A customary approach involves selecting a prior distribution for the model parameters followed by augmenting it with the states to form an extended state vector (Kitagawa, 1998). Theoretically, it casts the simultaneous state and parameter estimation problem into a unified filtering framework; however, due to lack of ergodicity and exponential forgetting of the joint state-parameter filter, coupled with successive resampling steps, employing this approach with any standard SMC algorithm often results in parameter sample degeneracy (Andrieu *et al.*, 2005; Doucet and Tadic, 2003). In other words, SMC approximation of the marginalized parameter posterior distribution is represented by a single Dirac delta function. It also causes error accumulation in successive Monte Carlo (MC) steps, which in terms of L^p norm, grows exponentially or polynomially in time (Kantas *et al.*, 2009).

A pragmatic approach to reduce parameter sample degeneracy and error accumulation in successive MC approximations is to introduce diversity to the parameter samples. This is done by adding artificial dynamics to the parameters (e.g., random walk) in the extended state vector (Kitagawa, 1998; Higuchi, 2001). In practice, artificial dynamics approach (ADA) has been implemented with several on-line Bayesian estimators (auxiliary SIR filter (ASIR) (Liu and West, 2001), Rao-Blackwellised particle filter (RBPF) (Gustafsson and Schön, 2003)). While this approach reduces parameter sample degeneracy and error accumulation in successive MC steps, adding artificial dynamics to the parameters, often results in over-dispersed posteriors, which is also commonly referred to as the variance inflation problem (Liu and West, 2001). To overcome the posterior variance inflation problem, a kernel density estimation method is proposed in (Liu and West, 2001; West, 1993), in which the degenerated approximation of the marginalized parameter posterior distribution is substituted by a kernel approximation (e.g., Gaussian or Epanechnikov). The artificial dynamics approach together with kernel density estimation method efficiently introduces parameter sample diversity and can be used for state-parameter estimation in general non-linear state-space models (SSMs) with non-Gaussian noise; however, there are

several limitations of this approach as summarized in (Kantas *et al.*, 2009): (a) transforming the problem by adding artificial noise modifies the original problem, so that, it becomes hard to quantify the bias introduced in the resulting parameter estimates; and (b) the dynamics of the parameters are related to the width of the kernel and the variance of the artificial noise, which are often difficult to fine tune. For the first issue, (Tulsyan *et al.*, 2013*b*) proposed the use of posterior Cramér-Rao lower bound (PCRLB) (Tichavský *et al.*, 1998) as a benchmark for error analysis of the parameter estimates obtained using the artificial approach; whereas, for the second issue, no practical solution exists.

The authors in (Chen *et al.*, 2005) used an ASIR filter for on-line state-parameter estimation with a priori knowledge based kernel width tuning rule. Compared to the SIR filter, an ASIR filter is a one-step look-ahead filter which offers an advantage by allowing importance sampling from the high likelihood region (Pitt and Shephard, 1999); however, the superiority of ASIR to SIR is case dependent (Johansen and Doucet, 2008). Most importantly, poor performance of ASIR filter for systems with large process noise (Ristic *et al.*, 2004) coupled with higher computational cost (compared to the SIR filter) (Chen, 2003), often renders it impractical for on-line applications.

The Resample-Move is an alternate on-line Bayesian estimation approach which introduces parameter sample diversity through a Markov chain Monte Carlo (MCMC) step (Gamerman, 1998; Gilks and Berzuini, 2001; Lee and Chia, 2002; Chopin, 2002). To avoid increase in the memory requirements with the MCMC step, use of a fixed dimensional sufficient statistics has also been proposed in the on-line Bayesian parameter estimation context (Andrieu *et al.*, 1999). As opposed to the methods based on kernel or artificial dynamics, Resampling-Move algorithm has the advantage of introducing diversity without perturbing the joint state-parameter target distribution. Unfortunately, MCMC/sufficient statistics based algorithms are known to result in approximation errors, which accumulate at least quadratically in time (Kantas *et al.*, 2009; Andrieu *et al.*, 1999). This problem has

also been illustrated in (Andrieu *et al.*, 2004) using a sufficient statistics method. Finally, unlike the ADA, applicability of the Resample-Move approach is restricted to a certain class of low dimensional non-linear models, for some of which, tractable solution to the estimation problem is also available (Djuric and Miguez, 2002; Storvic, 2002).

Apart from the developments in Bayesian estimation, maximum likelihood (ML) based algorithms for on-line parameter estimation is also an active area of research. Unlike the Bayesian estimators, where the focus is on the simultaneous state-parameter estimation, ML based methods are primarily focussed on solving the parameter estimation problem. A standard approach to on-line ML parameter estimation is the gradient method. The gradient method requires recursive computation of the likelihood of the measurements and its gradient with respect to the parameters, which is also referred to as the score function. Other than in simple models, such as in linear SSMs with Gaussian noise (Koopman and Shepard, 1992) or in finite state-space hidden Markov models (HMMs) (Lystig and Hughes, 2002), it is impossible to exactly solve the likelihood and the score functions (Poyiadjis *et al.*, 2011), and one has to resort to the use of some suitable approximations. In (Poyiadjis *et al.*, 2011; Poyiadjis *et al.*, 2005), use of SMC methods to approximate the likelihood and score functions for estimation using on-line gradient method is proposed. As pointed in (Kantas *et al.*, 2009; Andrieu *et al.*, 2004), for large dimensional problems, gradient approach scales poorly in terms of its components.

An alternate ML approach is the on-line expectation maximization (EM) algorithm, which unlike on-line gradient method, is known to be numerically more stable (Andrieu *et al.*, 2004). Unfortunately, like the gradient method, on-line EM algorithm can be implemented exactly only in linear SSMs with Gaussian noise (Elliott *et al.*, 2002) and in finite state-space HMMs (Cappé, 2011). Recently, SMC based on-line EM algorithm for parameter estimation in changepoint models (Yildirim *et al.*, 2012), and in certain classes of the non-linear SSMs (Moral *et al.*, 2009; Cappé, 2009), for which the likelihood

Table 2.1: Summary of the Bayesian and likelihood based methods for on-line state-parameter estimation (adapted from (Kantas *et al.*, 2009)). In this table, N is the number of particles used in SMC approximation, T is the final sampling time, and L is the number of measurements in each block of data (see (Andrieu *et al.*, 2005) for further details).

Method	Pros	Cons	Comp. cost
Artificial Dynamics (Bayesian)	Standard SMC applicable No optimization involved	Distribution altered Difficult to tune dynamics	$\mathcal{O}(NT)$
Resample-Move (Bayesian)	Distribution unaltered No optimization involved	Restricted model class Degeneracy problem Scalability issues	$\mathcal{O}(NT)$
On-line Gradient (ML)	Asymptotically efficient Generally applicable	Locally optimal Scalability issues Expensive	$\mathcal{O}(N^2)$ per update
On-line EM (ML)	Asymptotically efficient	Locally optimal Restricted model class Expensive	$\mathcal{O}(N^2)$ per update
On-line EM pseudo (ML)	Minimal tuning No degeneracy for small L	Needs stationary distribution Loss of efficiency	$\mathcal{O}(NL)$ per update

function belongs to the exponential family of distributions have appeared. Both on-line gradient and EM algorithms have computational complexity, which is quadratic in the number of particles used in the SMC approximation of the densities of interest. To develop computationally cheaper versions of the algorithm, pseudo on-line EM method for finite state-space HMMs (Rydén, 1997) and for non-linear SSMs (Andrieu *et al.*, 2005) have been proposed. Compared to the on-line gradient and EM algorithm, the pseudo on-line EM algorithm is computationally lighter, but fails to yield asymptotically efficient (unbiased and minimum variance) estimates. Finally, the pseudo on-line EM algorithm requires the stationary distribution of the states, which may not be always known in practice.

The key advantage of using ML estimators, such as on-line gradient (Poyiadjis *et al.*, 2011; Poyiadjis *et al.*, 2005) and EM algorithm (Moral *et al.*, 2009; Yildirim *et al.*, 2012) is that these methods yield asymptotically efficient estimates, at least in theory; however, in many situations, where the likelihood function is non-convex in model parameters (for e.g., in non-linear SSMs with non-Gaussian noise), numerical optimization routines either yield locally optimal (or biased) estimates (Andrieu *et al.*, 2004; Cappé, 2009) or require careful

tuning of the algorithm parameters (Kantas *et al.*, 2009). Finally, high computational cost of ML based algorithms (compared to Bayesian estimators) coupled with applicability to a restricted non-linear model class, renders ML based methods unsuitable for processes, that require fast on-line estimators. Bayesian methods, on the contrary are 'optimization-free' estimators, which allow these methods, to be fast, and free from issues related to optimization. Comparisons between the ML and Bayesian based methods for parameter estimation are further drawn in Section 2.9. A summary of different Bayesian and ML based algorithms, including their advantages and disadvantages is presented in Table 2.1.

In the next section, the motivation and the contributions of this chapter are provided.

2.2   Motivation and contributions

The existing literature on Bayesian and likelihood based methods for on-line state-parameter estimation assumes that measurement will be available at all sampling time; however, in practice, missing measurements are common in the process industries, where measurements may not arrive or be available at all sampling time instants. The importance of developing algorithms under missing measurements is well recognized (Gilks *et al.*, 1995). Existing literature addresses the issues related to missing data in linear (Shumway and Stoffer, 2000) and non-linear (Gopaluni, 2008) systems only under an off-line setting. Unfortunately, these methods cannot handle missing data in real-time.

In this chapter, a complete approach to on-line Bayesian state and parameter estimation in non-linear SSMs with non-Gaussian noise is developed, using an extended state vector representation with artificial dynamics for the parameters. Since this approach treats the simultaneous state and parameter estimation problems as the same, it will simply be referred to as an estimation problem unless otherwise warranted. Due to the inherent limitations of the EKF and UKF based simultaneous state-parameter estimators, a particle based SIR filtering approach is used. The choice of the SIR filter is motivated by the fact

that it is relatively (compared to ASIR filter) less sensitive to large process noise and is computationally less expensive. Furthermore, the importance weights are easily evaluated and the importance functions can be easily sampled (Ristic *et al.*, 2004).

It is emphasized that the PFs can be made arbitrarily accurate by simply increasing the number of particles; however, this comes at a computational cost. Several authors have focussed on this issue and developed methods, which either allows adaptation of the particle sample size (Straka and Šimandl, 2006; Fearnhead and Liu, 2007) or the adaptation of the proposal distribution from which the particles are sampled (Doucet *et al.*, 2000; Fearnhead, 2008). Performance of PFs is closely related to the ability to sample particles in state-space regions, where the posterior is significant (Pitt and Shephard, 1999). Perfect adaptation of the particle size or choice of an efficient proposal density for PFs is a long-standing topic (see (Cornebise *et al.*, 2008) for recent developments in this area).

The following are the main contributions of this chapter: (a) an adaptive SIR (Ad-SIR) filter for on-line state-parameter estimation in general non-linear SSMs with non-Gaussian noise is proposed and derived; (b) an optimal tuning rule to control the width of the kernel, and the variance of the artificial noise is proposed; (c) an on-line optimization algorithm based on KL divergence is used to project importance samples around the region of high likelihood, which allows adaptation of the SIR filter for on-line state-parameter estimation; (d) an extension of the algorithm to handle missing measurements in real-time is also presented; and (e) the efficacy of the algorithm is illustrated through numerical examples.

The proposed algorithm can estimate states and parameters of both time-invariant and slowly time-variant stochastic non-linear systems. It exhibits good performance even for systems with large process or measurement noise. A distinct advantage of the proposed algorithm is that it can also estimate parameters of the noise models. This particular feature is crucial, since filtering performance for any linear or non-linear filter depends on accurate characterization of the state and measurement noise models (Bavdekar *et al.*, 2011).

2.3   Problem formulation

Consider the following class of discrete-time, stochastic non-linear SSMs:

$$X_{t+1} = f_t(X_t, u_t, \theta_t, V_t), \tag{2.1a}$$

$$Y_t = g_t(X_t, u_t, \theta_t, W_t), \tag{2.1b}$$

where $X_t \in \mathcal{X} \subseteq \mathbb{R}^n$ and $Y_t \in \mathcal{Y} \subseteq \mathbb{R}^m$ for $t \in \mathbb{N}$ are the state and measurement processes, respectively. Here $\mathbb{R} := (-\infty, \infty)$ and $\mathbb{N} := \{1, 2, \ldots, \}$. $X_t \in \mathcal{X}$ is a Markov process, which is either partially or fully hidden, and $Y_t \in \mathcal{Y}$ may include missed measurements; $u_t \in \mathcal{U} \subseteq \mathbb{R}^p$ and $\theta_t \in \Theta \subseteq \mathbb{R}^r$ are the time-varying or time-invariant control variables and model parameters, respectively. The process and measurement noise are represented as $V_t \in \mathbb{R}^n$ and $W_t \in \mathbb{R}^m$, respectively. $f_t(\cdot)$ is a n-dimensional state mapping function and $g_t(\cdot)$ is a m-dimensional output mapping function, each being non-linear in its arguments, and possibly time-varying, such that $f_t := \mathcal{X} \times \mathcal{U} \times \Theta \times \mathbb{R}^n \to \mathcal{X}$ and $g_t := \mathcal{X} \times \mathcal{U} \times \Theta \times \mathbb{R}^m \to \mathcal{Y}$. The assumption on (2.1) is discussed next.

Assumption 2.3.1. *$V_t \in \mathbb{R}^n$ and $W_t \in \mathbb{R}^m$ are the mutually independent sequences of independent random variables described by the probability density functions (pdfs) $p(v_t|\cdot)$ and $p(w_t|\cdot)$, respectively. The pdfs are known a priori in their classes (e.g., Gaussian; Binomial) and are parametrized by a finite number of moments (e.g., mean; variance). If the moments are unknown, it can be augmented with the model parameter set $\theta_t \in \Theta$.*

Since $\theta_t \in \Theta$ does not have an explicit transition function like $f_t(\cdot)$ for $X_t \in \mathcal{X}$, artificial dynamics are introduced, such that $\theta_t \in \Theta$ evolves according to

$$\theta_{t+1} = \theta_t + \xi_t, \tag{2.2}$$

where $\xi_t \in \mathbb{R}^r$ is a sequence of independent Gaussian random variables realized from $\mathcal{N}(\xi_t|0, \Sigma_{\theta_t})$, independent of the noise sequences $V_t \in \mathbb{R}^n$ and $W_t \in \mathbb{R}^m$. The dynamics of θ_t in (2.2) is governed by the artificial noise variance $\Sigma_{\theta_t} \in \mathcal{S}_+^r$, where $\mathcal{S}_+^r$ is a cone

of positive semi-definite matrix. Often Σ_{θ_t} is unknown, and requires careful tuning. The formulation in (2.2) is the ADA, which avoids the parameter degeneracy problem discussed in Section 2.1, and further allows for estimation of time-varying parameters.

Equations (2.1) and (2.2) together represent an extended SSM. For notational simplicity, the extended state vector is defined as $Z_t \triangleq \{X_t, \theta_t\}$, such that $Z_t \in \mathcal{Z} \subseteq \mathbb{R}^{s=n+r}$. Throughout this chapter $Z_t \in \mathcal{Z}$ will be considered; however, distinction between the states and parameters will be made, as required. Equations (2.1) and (2.2) can be represented as:

$$X_0 \sim p(x_0); \quad X_{t+1}|Z_t \sim p(x_{t+1}|z_t); \tag{2.3a}$$

$$\theta_0 \sim p(\theta_0); \quad \theta_{t+1}|\theta_t \sim p(\theta_{t+1}|\theta_t); \tag{2.3b}$$

$$Y_t|Z_t \sim p(y_t|z_t), \tag{2.3c}$$

where: the Markov process $X_t \in \mathcal{X}$ is characterized by its initial density $p(x_0)$ and a transition density $p(x_{t+1}|z_t)$, while the Markov process $\theta_t \in \Theta$ is characterized by its initial density $p(\theta_0)$ and a transition density $p(\theta_{t+1}|\theta_t)$. The measurement $Y_t \in \mathcal{Y}$ is assumed to be conditionally independent given $Z_t \in \mathcal{Z}$, and is characterized by the conditional marginal density $p(y_t|z_t)$. The representation in (2.3) includes a wide class of non-linear time-series models, including (2.1). For the sake of clarity, the input signal $u_t \in \mathcal{U}$ is omitted in (2.3); however, all the derivations that appear in this chapter hold with $u_t \in \mathcal{U}$ included.

The main problems addressed in this chapter are stated next.

Problem 2.3.2. *The first problem aims at computing the state-parameter estimate of $Z_t \in \mathcal{Z}$ in real-time using $\{u_{1:t}; y_{1:t}\}$; wherein, $y_{1:t} \triangleq \{y_1, \ldots, y_t\}$ is a vector of measured outputs corresponding to the input sequence $u_{1:t} \triangleq \{u_1, \ldots, u_t\}$.*

Problem 2.3.3. *The second problem aims at computing the state-parameter estimate of $Z_t \in \mathcal{Z}$ in real-time using $\{u_{1:t}; y_{t_1:t_\gamma}\}$; wherein, the measurements arrive at random sampling time instants, such that only $\{y_{t_1}, \ldots, y_{t_\gamma}\}$ out of $y_{1:t}$ is available.*

2.4   Bayesian filtering

The Bayesian idea for solving Problems 2.3.2 and 2.3.3 is to construct a posterior pdf $Z_t|(Y_{1:t} = y_{1:t}) \sim p(z_t|y_{1:t})$ for all $t \in \mathbb{N}$. Here $p(z_t|y_{1:t})$ is a probabilistic representation of available statistical information on $Z_t \in \mathcal{Z}$ conditioned on $\{Y_{1:t} = y_{1:t}\}$. Using the Markov property of (2.3) and from the Bayes' theorem, $p(z_t|y_{1:t})$ can be computed as

$$p(z_t|y_{1:t}) = \frac{p(y_t|z_t)p(z_t|y_{1:t-1})}{p(y_t|y_{1:t-1})}, \tag{2.4}$$

where: $p(y_t|y_{1:t-1}) = \int_{\mathcal{Z}} p(y_t|z_t)p(dz_t|y_{1:t-1})$ is a constant; $p(dz_t|y_{1:t-1}) \triangleq p(z_t|y_{1:t-1})dz_t$ is a prior distribution; and $p(z_t|y_{1:t-1})$ is a prior density, which can be computed as

$$p(z_t|y_{1:t-1}) = \int_{\mathcal{Z}} p(z_t|z_{t-1})p(dz_{t-1}|y_{1:t-1}), \tag{2.5}$$

where $p(dz_{t-1}|y_{1:t-1}) \triangleq p(z_{t-1}|y_{1:t-1})dz_{t-1}$ is the posterior distribution at $t - 1$. Ignoring the constant term, (2.4) in compact form can be written as follows

$$p(z_t|y_{1:t}) \propto p(y_t|z_t)p(z_t|y_{1:t-1}). \tag{2.6}$$

In principle, the recurrence relation between the prediction and update equations in (2.5) and (2.6), respectively, provides a complete Bayesian solution to Problems 2.3.2 and 2.3.3.

To compute a point estimate from $p(z_t|y_{1:t})$, a common approach is to minimize the mean-square error (MSE) risk $\mathcal{R}_Z \triangleq \mathbb{E}_{p(Z_t, Y_{1:t})}[\|Z_t - \widehat{Z}_{t|t}\|_2^2]$, where $\widehat{Z}_{t|t} \in \mathbb{R}^s$ is the point estimate of the states and parameters at time $t \in \mathbb{N}$; $\|\cdot\|_2$ is a $2-$norm operator; and $\mathbb{E}_{p(\cdot)}$ is the expectation with respect to the pdf $p(\cdot)$. Minimizing $\mathcal{R}_Z$ over $\widehat{Z}_{t|t}$ yields conditional mean of $Z_t|(Y_{1:t} = y_{1:t}) \sim p(z_t|y_{1:t})$ as an optimal point estimate (Trees, 1968). For instance, if $\mathcal{R}_\theta$ is the MSE Bayes' risk then the MMSE parameter estimate is given by

$$\widehat{\theta}_{t|t} \triangleq \mathbb{E}_{p(\theta_t|Y_{1:t})}[\theta_t] = \int_{\Theta} \theta_t p(d\theta_t|y_{1:t}), \tag{2.7}$$

where $p(d\theta_t|y_{1:t})$ is the marginalized posterior distribution for the parameters, such that

$$p(d\theta_t|y_{1:t}) = \int_{\mathcal{X}} p(dz_t|y_{1:t}). \tag{2.8}$$

Remark 2.4.1. *Except for linear systems with Gaussian state and measurement noise or when $\mathcal{Z}$ is a finite set, with finite computing capabilities, Bayesian on-line state-parameter estimation solution given in (2.6) cannot be solved exactly.*

This chapter proposes an SMC based adaptive SIR filter to numerically approximate the Bayesian on-line state-parameter estimation solution given in (2.6).

2.5   Adaptive SIR filter

It is not our aim to review SMC methods in details, but simply to point out their intrinsic limitations, which have fundamental practical consequences on the ADA introduced in Section 2.3. The essential idea behind SMC methods is to generate a set of random particles and their associated weights from the target pdf. The target pdf of interest here is the posterior pdf $p(z_t|y_{1:t})$ in (2.6). Unfortunately, due to the non-Gaussian nature of $p(z_t|y_{1:t})$, generating set of random particles from the target pdf is non-trivial (Ristic *et al.*, 2004).

An alternate idea is to employ an importance sampling function (ISF) $q(z_t|y_{1:t}, z_{t-1})$, such that $q(z_t|y_{1:t}, z_{t-1})$ is a non-negative function on $\mathcal{Z}$ and $\operatorname{supp} q(z_t|y_{1:t}, z_{t-1}) \supseteq \operatorname{supp} p(z_t|y_{1:t})$. A standard SIR filter selects $q(z_t|y_{1:t}, z_{t-1}) = p(z_t|y_{1:t-1})$ (Arulampalam *et al.*, 2002), since it enables easy sampling from the ISF and easy evaluation of $p(z_t|y_{1:t-1})$ for any $\{Z_t, Y_{1:t-1}\} \in \mathcal{Z} \times \mathcal{Y}^{t-1}$. Now to generate a set of random particles from the ISF $p(z_t|y_{1:t-1})$, the multi-dimensional integral in (2.5) needs to be evaluated first. Using samples from $p(z_{t-1}|y_{1:t-1})$ (available from the recursive relation in (2.5) and (2.6)), an SMC approximation of $Z_{t-1}|(Y_{1:t-1} = y_{1:t-1}) \sim p(dz_{t-1}|y_{1:t-1})$ is given by

$$\tilde{p}(dz_{t-1}|y_{1:t-1}) = \sum_{i=1}^{N} W_{t-1|t-1}^{i} \delta_{Z_{t-1|t-1}^{i}}(dz_{t-1}), \tag{2.9}$$

where: $\tilde{p}(dz_{t-1}|y_{1:t-1})$ is an SMC approximation of the joint state-parameter posterior distribution $p(dz_{t-1}|y_{1:t-1})$; $\{Z_{t-1|t-1}^{i}; W_{t-1|t-1}^{i}\}_{i=1}^{N} \sim \tilde{p}(z_{t-1}|y_{1:t-1})$ is a set of N particles and their weights, distributed according to $\tilde{p}(z_{t-1}|y_{1:t-1})$, such that $\sum_{i=1}^{N} W_{t-1|t-1}^{i} = 1$ and

$\delta_{Z_{t-1|t-1}^i}(dz_{t-1})$ is the Dirac delta mass located at the random sample $Z_{t-1|t-1}^i$.

Using (2.9), an SMC approximation of the marginalized posterior distribution of the states and parameters at $t-1$ can also be computed as given in the next lemma.

Lemma 2.5.1. *Let the SMC approximation of the distribution of $Z_{t-1}|(Y_{1:t-1} = y_{1:t-1})$ be given by (2.9) then marginalizing (2.9) over $X_t \in \mathcal{X}$ and $\theta_t \in \Theta$ yields approximate distributions for $\theta_{t-1}|(Y_{1:t-1} = y_{1:t-1})$ and $X_{t-1}|(Y_{1:t-1} = y_{1:t-1})$, respectively, such that*

$$\tilde{p}(d\theta_{t-1}|y_{1:t-1}) = \sum_{i=1}^{N} W_{t-1|t-1}^i \delta_{\theta_{t-1|t-1}^i}(d\theta_{t-1}), \tag{2.10a}$$

$$\tilde{p}(dx_{t-1}|y_{1:t-1}) = \sum_{i=1}^{N} W_{t-1|t-1}^i \delta_{X_{t-1|t-1}^i}(dx_{t-1}), \tag{2.10b}$$

where $\tilde{p}(d\theta_{t-1}|y_{1:t-1})$ and $\tilde{p}(dx_{t-1}|y_{1:t-1})$ are the SMC approximations of the distributions $p(d\theta_{t-1}|y_{1:t-1})$ and $p(dx_{t-1}|y_{1:t-1})$, respectively.

Proof. Using the Law of Total Probability on posterior distribution $p(dz_{t-1}|y_{1:t-1})$ yields

$$p(d\theta_{t-1}|y_{1:t-1}) = \int_{\mathcal{X}} p(dz_{t-1}|y_{1:t-1}). \tag{2.11}$$

Substituting (2.9) into (2.11) and taking independent terms outside the integral yields

$$\tilde{p}(d\theta_{t-1}|y_{1:t-1}) = \sum_{i=1}^{N} W_{t-1|t-1}^i \int_{\mathcal{X}} \delta_{Z_{t-1|t-1}^i}(dz_{t-1}), \tag{2.12a}$$

$$= \sum_{i=1}^{N} W_{t-1|t-1}^i \delta_{\theta_{t-1|t-1}^i}(d\theta_{t-1}). \tag{2.12b}$$

The equality in (2.12b) is a result from marginalization of the joint state-parameter Dirac delta function over $\mathcal{X}$, which completes the proof. $\qquad\square$

Lemma 2.5.1 computes the marginal distributions of $\theta_{t-1}|(Y_{1:t-1} = y_{1:t-1})$ and $X_{t-1}|(Y_{1:t-1} = y_{1:t-1})$ using (2.9). Note that the weights in (2.10) are same as that in (2.9).

Remark 2.5.2. *From (2.10a), the mean and the covariance of $\theta_{t-1}|(Y_{1:t-1} = y_{1:t-1})$ can be approximated as $\mathbb{E}_{p(\theta_{t-1}|Y_{1:t-1})}[\theta_{t-1}] \triangleq \int_{\Theta} \theta_{t-1} p(d\theta_{t-1}|y_{1:t-1}) \approx \sum_{i=1}^{N} W_{t-1|t-1}^i \theta_{t-1|t-1}^i$*

$$= \widehat{\theta}_{t-1|t-1} \ and \ \mathbb{V}_{p(\theta_{t-1}|Y_{1:t-1})}\left[\theta_{t-1}\right] \triangleq \int_\Theta (\theta_{t-1} - \widehat{\theta}_{t-1|t-1})(\theta_{t-1} - \widehat{\theta}_{t-1|t-1})^T p(d\theta_{t-1}|y_{1:t-1})$$

$$\approx \sum_{i=1}^N W_{t-1|t-1}^i (\theta_{t-1|t-1}^i - \widehat{\theta}_{t-1|t-1})(\theta_{t-1|t-1}^i - \widehat{\theta}_{t-1|t-1})^T = V_{\theta_{t-1}}, \ respectively.$$

In Remark 2.5.2, $\widehat{\theta}_{t-1|t-1} \in \mathbb{R}^r$ is an MMSE parameter estimate at $t - 1$. Similarly, an MMSE state estimate $\widehat{X}_{t-1|t-1} \in \mathbb{R}^n$ at $t - 1$ can also be computed using (2.10b). Finally, to generate a set of random particles from the ISF, substituting (2.9) into (2.5) yields

$$\tilde{p}(z_t|y_{1:t-1}) = \int_{\mathcal{Z}} p(z_t|z_{t-1}) \sum_{i=1}^N W_{t-1|t-1}^i \delta_{Z_{t-1|t-1}^i}(dz_{t-1}), \tag{2.13a}$$

$$= \sum_{i=1}^N W_{t-1|t-1}^i p(z_t|Z_{t-1|t-1}^i), \tag{2.13b}$$

where $\tilde{p}(z_t|y_{1:t-1})$ is an SMC approximation of the ISF $p(z_t|y_{1:t-1})$. The approximation in (2.13b) is a mixture of N transitional pdfs, with a mixing ratio $\{W_{t-1|t-1}^i\}_{i=1}^N$ and centred at $\{Z_{t-1|t-1}^i\}_{i=1}^N$. Marginalization of the ISF $p(z_t|y_{1:t-1})$ over $X_t \in \mathcal{X}$ is discussed in next.

Lemma 2.5.3. *Let $\xi_t \in \mathbb{R}^r$ in (2.3b) be a sequence of independent Gaussian random variable, such that $\xi_t \sim \mathcal{N}(\xi_t|0, \Sigma_{\theta_t})$, where $\Sigma_{\theta_t} \in \mathcal{S}_+^r$ for all $t \in \mathbb{N}$ then marginalizing (2.13b) over $X_t \in \mathcal{X}$ yields a mixture Gaussian pdf for $\theta_t|(Y_{1:t-1} = y_{1:t-1})$ given by*

$$\tilde{p}(\theta_t|y_{1:t-1}) = \sum_{i=1}^N W_{t-1|t-1}^i \mathcal{N}(\theta_t|\theta_{t-1|t-1}^i, \Sigma_{\theta_t}), \tag{2.14}$$

where $\theta_t|\theta_{t-1|t-1}^i \sim \mathcal{N}(\theta_t|\theta_{t-1|t-1}^i, \Sigma_{\theta_t})$ follws a Gaussian density with mean $\theta_{t-1|t-1}^i \in \mathbb{R}^r$ and covariance $\Sigma_{\theta_t} \in \mathcal{S}_+^r$.

Proof. Using the Law of Total Probability on the ISF $p(z_t|y_{1:t-1})$ yields

$$p(\theta_t|y_{1:t-1}) = \int_{\mathcal{X}} p(z_t|y_{1:t-1})dx_t. \tag{2.15}$$

Substituting (2.13b) into (2.15) and pulling independent terms out of the integral yields

$$\tilde{p}(\theta_t|y_{1:t-1}) = \sum_{i=1}^N W_{t-1|t-1}^i \int_{\mathcal{X}} p(z_t|Z_{t-1|t-1}^i)dx_t, \tag{2.16a}$$

$$= \sum_{i=1}^N W_{t-1|t-1}^i p(\theta_t|\theta_{t-1|t-1}^i) \int_{\mathcal{X}} p(x_t|Z_{t-1|t-1}^i)dx_t, \tag{2.16b}$$

where $\tilde{p}(\theta_t|y_{1:t-1})$ is an estimate. Since, $\int_{\mathcal{X}} p(dx_t|Z^i_{t-1|t-1}) = 1$, (2.16b) simplifies to

$$\tilde{p}(\theta_t|y_{1:t-1}) = \sum_{i=1}^{N} W^i_{t-1|t-1} p(\theta_t|\theta^i_{t-1|t-1}), \tag{2.17a}$$

$$= \sum_{i=1}^{N} W^i_{t-1|t-1} \mathcal{N}(\theta_t|\theta^i_{t-1|t-1}, \Sigma_{\theta_t}). \tag{2.17b}$$

The equality in (2.17b) follows from the fact that the pdf $p(\theta_t|\theta^i_{t-1|t-1})$ models the noise distribution $\xi_t \sim \mathcal{N}(\xi_t|0, \Sigma_{\theta_t})$ (see (2.3b)). $\qquad\square$

(Liu and West, 2001; West, 1993) refer to (2.14) as Gaussian kernel estimate of the marginalized ISF, whose kernel width is controlled by the noise covariance Σ_{θ_t}. Statistics of (2.14) are given next to highlight the implications of using SMC methods with ADA.

Lemma 2.5.4. *Let the artificial noise in (2.3b) be $\xi_t \sim \mathcal{N}(\xi_t|0, \Sigma_{\theta_t})$ and let $\widehat{\theta}_{t-1|t-1} \in \mathbb{R}^r$ and $V_{\theta_{t-1}} \in \mathcal{S}^r_+$ be the mean and covariance of $\theta_{t-1}|(Y_{1:t-1} = y_{1:t-1}) \sim \tilde{p}(\theta_{t-1}|y_{1:t-1})$ as computed in Remark 2.5.2. Also, let the SMC approximation of the marginalized ISF be given by (2.14), such that $\theta_t|(Y_{1:t-1} = y_{1:t-1}) \sim \tilde{p}(\theta_t|y_{1:t-1})$ then the first and second moment of $\theta_t|(Y_{1:t-1} = y_{1:t-1})$ is given by*

$$\mathbb{E}_{p(\theta_t|Y_{1:t-1})}[\theta_t] = \widehat{\theta}_{t-1|t-1}, \tag{2.18a}$$

$$\mathbb{V}_{p(\theta_t|Y_{1:t-1})}[\theta_t] = V_{\theta_{t-1}} + \Sigma_{\theta_t}. \tag{2.18b}$$

Proof. Expectation of $\theta_t|(Y_{1:t-1} = y_{1:t-1})$ is given by

$$\mathbb{E}_{p(\theta_t|Y_{1:t-1})}[\theta_t] = \int_{\Theta} \theta_t p(d\theta_t|y_{1:t-1}). \tag{2.19}$$

Substituting (2.17b) into (2.19) yields

$$\mathbb{E}_{p(\theta_t|Y_{1:t-1})}[\theta_t] = \int_{\Theta} \theta_t \sum_{i=1}^{N} W^i_{t-1|t-1} \mathcal{N}(d\theta_t|\theta^i_{t-1|t-1}, \Sigma_{\theta_t}), \tag{2.20a}$$

$$= \sum_{i=1}^{N} W^i_{t-1|t-1} \int_{\Theta} \theta_t \mathcal{N}(d\theta_t|\theta^i_{t-1|t-1}, \Sigma_{\theta_t}), \tag{2.20b}$$

$$= \sum_{i=1}^{N} W^i_{t-1|t-1} \theta^i_{t-1|t-1} = \widehat{\theta}_{t-1|t-1}, \tag{2.20c}$$

where (2.20c) follows from Remark 2.5.2, which completes the proof for (2.18a). Now the

covariance of $\theta_t|(Y_{1:t-1} = y_{1:t-1})$ is given by

$$\mathbb{V}_{p(\theta_t|Y_{1:t-1})}[\theta_t] = \int_{\Theta} (\theta_t - \mathbb{E}_{p(\theta_t|Y_{1:t-1})}[\theta_t])(\theta_t - \mathbb{E}_{p(\theta_t|Y_{1:t-1})}[\theta_t])^T p(d\theta_t|y_{1:t-1}). \quad (2.21)$$

Substituting (2.17b) and (2.20c) into (2.21) yields

$$\mathbb{V}_{p(\theta_t|Y_{1:t-1})}[\theta_t] = \sum_{i=1}^{N} W_{t-1|t-1}^i \int_{\Theta} (\theta_t - \widehat{\theta}_{t-1|t-1})(\theta_t - \widehat{\theta}_{t-1|t-1})^T \mathcal{N}(d\theta_t|\theta_{t-1|t-1}^i, \Sigma_{\theta_t}).$$

$$(2.22)$$

Simple algebraic manipulation of (2.22) yields

$$\mathbb{V}_{p(\theta_t|Y_{1:t-1})}[\theta_t] = \sum_{i=1}^{N} W_{t-1|t-1}^i \int_{\Theta} (\theta_t - \theta_{t-1|t-1}^i + \theta_{t-1|t-1}^i - \widehat{\theta}_{t-1|t-1})$$

$$\times (\theta_t - \theta_{t-1|t-1}^i + \theta_{t-1|t-1}^i - \widehat{\theta}_{t-1|t-1})^T \mathcal{N}(d\theta_t|\theta_{t-1|t-1}^i, \Sigma_{\theta_t}). \quad (2.23)$$

Simplifying the terms in (2.23) and representing the integral solution as

$$\mathbb{V}_{p(\theta_t|Y_{1:t-1})}[\theta_t] = I_1 + I_2 + I_3 + I_4, \quad (2.24)$$

where:

$$I_1 = \sum_{i=1}^{N} W_{t-1|t-1}^i \int_{\Theta} (\theta_t - \theta_{t-1|t-1}^i)(\theta_t - \theta_{t-1|t-1}^i)^T \mathcal{N}(d\theta_t|\theta_{t-1|t-1}^i, \Sigma_{\theta_t}) = \sum_{i=1}^{N} W_{t-1|t-1}^i \Sigma_{\theta_t}$$

$$= \Sigma_{\theta_t}; \quad (2.25a)$$

$$I_2 = \sum_{i=1}^{N} W_{t-1|t-1}^i \int_{\Theta} (\theta_{t-1|t-1}^i - \widehat{\theta}_{t-1|t-1})(\theta_{t-1|t-1}^i - \widehat{\theta}_{t-1|t-1})^T \mathcal{N}(d\theta_t|\theta_{t-1|t-1}^i, \Sigma_{\theta_t}) =$$

$$\sum_{i=1}^{N} W_{t-1|t-1}^i (\theta_{t-1|t-1}^i - \widehat{\theta}_{t-1|t-1})(\theta_{t-1|t-1}^i - \widehat{\theta}_{t-1|t-1})^T \int_{\Theta} \mathcal{N}(d\theta_t|\theta_{t-1|t-1}^i, \Sigma_{\theta_t}) = V_{\theta_{t-1}};$$

$$(2.25b)$$

$$I_3 = \sum_{i=1}^{N} W_{t-1|t-1}^i \int_{\Theta} (\theta_t - \theta_{t-1|t-1}^i)(\theta_{t-1|t-1}^i - \widehat{\theta}_{t-1|t-1})^T \mathcal{N}(d\theta_t|\theta_{t-1|t-1}^i, \Sigma_{\theta_t}) =$$

$$\sum_{i=1}^{N} W_{t-1|t-1}^i \int_{\Theta} (\theta_t - \theta_{t-1|t-1}^i) \mathcal{N}(d\theta_t|\theta_{t-1|t-1}^i, \Sigma_{\theta_t})(\theta_{t-1|t-1}^i - \widehat{\theta}_{t-1|t-1})^T = 0; \quad (2.25c)$$

$$I_4 = \sum_{i=1}^{N} W_{t-1|t-1}^i \int_\Theta (\theta_{t-1|t-1}^i - \widehat{\theta}_{t-1|t-1})(\theta_t - \theta_{t-1|t-1}^i)^T \mathcal{N}(d\theta_t|\theta_{t-1|t-1}^i, \Sigma_{\theta_t}) =$$

$$\sum_{i=1}^{N} W_{t-1|t-1}^i (\theta_{t-1|t-1}^i - \widehat{\theta}_{t-1|t-1}) \int_\Theta (\theta_t - \theta_{t-1|t-1}^i)^T \mathcal{N}(d\theta_t|\theta_{t-1|t-1}^i, \Sigma_{\theta_t}) = 0. \qquad (2.25\text{d})$$

Here (2.25a) and (2.25b) are based on Remark 2.5.2, and (2.25c) and (2.25d) use the relation $\int_\Theta \theta_t \mathcal{N}(\theta_t|\theta_{t-1|t-1}^i, \Sigma_{\theta_t}) d\theta_t = \theta_{t-1|t-1}^i$. Finally, substituting (2.25a), (2.25b), (2.25c) and (2.25d) into (2.24) yields (2.18b), which completes the proof. $\qquad \square$

Remark 2.5.5. *From Remark 2.5.2 and Lemma 2.5.4, while computing $\tilde{p}(\theta_t|y_{1:t-1})$ from $\tilde{p}(\theta_{t-1}|y_{1:t-1})$, the mean is unchanged, i.e., $\mathbb{E}_{p(\theta_{t-1}|Y_{1:t-1})}[\theta_{t-1}] = \mathbb{E}_{p(\theta_t|Y_{1:t-1})}[\theta_t]$, while the covariance disperses by Σ_{θ_t}, such that $\mathbb{V}_{p(\theta_t|Y_{1:t-1})}[\theta_t] - \mathbb{V}_{p(\theta_{t-1}|Y_{1:t-1})}[\theta_{t-1}] = \Sigma_{\theta_t}$.*

Remark 2.5.5 highlights the variance inflation problem associated with the ADA. In (Liu and West, 2001), the authors implied similar results. Note that the results presented here are important, since they are the key aspects underlying the Ad-SIR filter proposed here.

2.5.1   Kernel smoothing

It is well known that using particles sampled from an over-dispersed ISF will yield a poor approximation of the posterior pdf (Liu and West, 2001). From Remark 2.5.5, it is clear that the SMC approximation of the marginalized ISF in (2.14) suffers from a similar dispersion problem. To overcome the issue of dispersion, use of a kernel method is proposed. The idea behind this approach is the shrinkage of the kernel width according to

$$\tilde{\theta}_{t-1|t-1}^i = \sqrt{1 - h_t^2}\, \theta_{t-1|t-1}^i + \left(1 - \sqrt{1 - h_t^2}\right) \widehat{\theta}_{t-1|t-1}, \qquad (2.26)$$

where $\{\tilde{\theta}_{t-1|t-1}^i\}_{i=1}^N$ are the shrinkage locations and $h_t \in [0, 1]$ is a kernel parameter. Therefore replacing $\{\theta_{t-1|t-1}^i\}_{i=1}^N$ with $\{\tilde{\theta}_{t-1|t-1}^i\}_{i=1}^N$ in (2.14) and setting $\Sigma_{\theta_t} = h_t^2 V_{\theta_{t-1}}$, the SMC approximation of the marginalized ISF in (2.14) can now be represented as

$$\tilde{p}(\theta_t|y_{1:t-1}) = \sum_{i=1}^{N} W_{t-1|t-1}^i \mathcal{N}(\theta_t|\tilde{\theta}_{t-1|t-1}^i, h_t^2 V_{\theta_{t-1}}). \qquad (2.27)$$

Note that by setting $\Sigma_{\theta_t} = h_t^2 V_{\theta_{t-1}}$, the kernel width Σ_{θ_t} becomes a non-linear function of the kernel parameter h_t. Tuning of h_t is discussed in Section 2.5.2, but first the statistics of (2.27) as a plausible SMC approximation of the marginalized ISF are discussed next.

Corollary 2.5.6. *Let the SMC approximation of $p(\theta_t|y_{1:t-1})$ with kernel smoothing be represented by (2.27) then the first two moments of $\theta_t|(Y_{1:t-1} = y_{1:t-1}) \sim \tilde{p}(\theta_t|y_{1:t-1})$ are given by $\mathbb{E}_{p(\theta_t|(Y_{1:t-1})}[\theta_t] = \widehat{\theta}_{t-1|t-1}$ and $\mathbb{V}_{p(\theta_t|(Y_{1:t-1})}[\theta_t] = V_{\theta_{t-1}}$, respectively.*

Proof. The proof is based on using (2.26) and setting $\Sigma_{\theta_t} = h_t^2 V_{\theta_{t-1}}$ in Lemma 2.5.4.   □

With kernel smoothing, the SMC approximations of $\theta_t|(Y_{1:t-1} = y_{1:t-1}) \sim \tilde{p}(\theta_t|y_{1:t-1})$ and $\theta_{t-1}|(Y_{1:t-1} = y_{1:t-1}) \sim \tilde{p}(\theta_t|y_{1:t-1})$ have the same first two moments (see Corollary 2.5.6). Finally, defining $\tilde{Z}^i_{t-1|t-1} \triangleq \{X^i_{t-1|t-1};\ \tilde{\theta}^i_{t-1|t-1}\}$, the SMC approximation of the ISF density in (2.13b) with kernel smoothing can be represented as

$$\tilde{p}(z_t|y_{1:t-1}) = \sum_{i=1}^{N} W^i_{t-1|t-1} p(z_t|\tilde{Z}^i_{t-1|t-1}). \tag{2.28}$$

Note that the random particle set $\{Z^i_{t|t-1}; W^i_{t|t-1}\}_{i=1}^{N} \sim \tilde{p}(z_t|y_{1:t-1})$ from (2.28) can be generated by passing $\{\tilde{Z}^i_{t-1|t-1}\}_{i=1}^{N}$ through the transition pdfs, such that

$$X^i_{t|t-1} \sim p(x_t|\tilde{Z}^i_{t-1|t-1}), \tag{2.29a}$$

$$\theta^i_{t|t-1} \sim p(\theta_t|\tilde{\theta}^i_{t-1|t-1}), \tag{2.29b}$$

where $1 \leq i \leq N$. Using the generated random particle set $\{Z^i_{t|t-1}; W^i_{t-1}\}_{i=1}^{N}$ from (2.28), an SMC approximation of the ISF distribution $p(dz_t|y_{1:t-1})$ can be represented as

$$\tilde{p}(dz_t|y_{1:t-1}) = \sum_{i=1}^{N} W^i_{t|t-1} \delta_{Z^i_{t|t-1}}(dz_t), \tag{2.30}$$

where $\{W^i_{t|t-1} = W^i_{t-1|t-1}\}_{i=1}^{N}$. Now to obtain an SMC approximation of the target posterior distribution $p(dz_t|y_{1:t})$, substituting (2.30) into (2.6) yields

$$\tilde{p}(dz_t|y_{1:t}) \propto p(y_t|z_t) \sum_{i=1}^{N} W^i_{t|t-1} \delta_{Z^i_{t|t-1}}(dz_t), \tag{2.31a}$$

$$= \sum_{i=1}^{N} W^i_{t|t} \delta_{Z^i_{t|t-1}}(dz_t), \tag{2.31b}$$

where the weight $W_{t|t}^i$ in (2.31b) is given by

$$W_{t|t}^i = \frac{W_{t|t-1}^i p(y_t|Z_{t|t-1}^i)}{\sum_{i=1}^N W_{t|t-1}^i p(y_t|Z_{t|t-1}^i)}. \tag{2.32}$$

Note that in (2.31b) the importance weights $\{W_{t|t}^i\}_{i=1}^N$ are computed using the likelihood function. Finally, the MMSE point estimates for the states and parameters at $t \in \mathbb{N}$ can be computed from (2.31b) using the procedure outlined in Lemma 2.5.1 and Remark 2.5.2.

2.5.2   Optimal tuning of kernel parameter

Although over-dispersion in the SMC approximation of the ISF is corrected using the kernel smoothing, optimal tuning of the kernel parameter $h_t \in [0, 1]$ remains unclear.

Remark 2.5.7. *The tuning practices for h_t are largely ad-hoc. (Liu and West, 2001) suggested selecting $h_t = 0.1$; whereas, in (Chen et al., 2005), h_t was optimized based on historical data-set, and then applied to future batches. These ad-hoc rules deliver a constant h_t, for which, optimality cannot be established with respect to the incoming data.*

An optimal tuning rule for h_t based on an on-line optimization procedure is proposed in this chapter. The tuning rule is based on minimization of the KL divergence between the ISF and the target posterior density at each sampling time. The objective of the optimizer is not only to tune h_t, but to also project the particles sampled from the ISF in the region of high posterior density. This is to allow for adaptation of the SIR filter for combined state-parameter estimation. A similar idea of adaptive filtering is also proposed in (Cornebise *et al.*, 2008). In a standard SIR filter, if $\operatorname{supp} p(z_t|y_{1:t-1})$ is larger or smaller compared to $\operatorname{supp} p(y_t|z_t)$ then only a few particles in (2.32) are assigned higher weights. This is due to insufficient number of particles in the overlapping region (see Figure 2.1). As discussed in (Ristic *et al.*, 2004), a standard SIR filter is inefficient in handling such situations. This is because in an SIR filter, the particles from the ISF are generated without taking the current measurement into consideration (see (2.5)). Methods

(a) $\Phi_t \approx 1$ $(\mathbb{V}[z_t|y_{1:t-1}] \approx \mathbb{V}[y_t|z_t])$ (b) $\Phi_t < 1$ $(\mathbb{V}[z_t|y_{1:t-1}] < \mathbb{V}[y_t|z_t])$ (c) $\Phi_t > 1$ $(\mathbb{V}[z_t|y_{1:t-1}] > \mathbb{V}[y_t|z_t])$
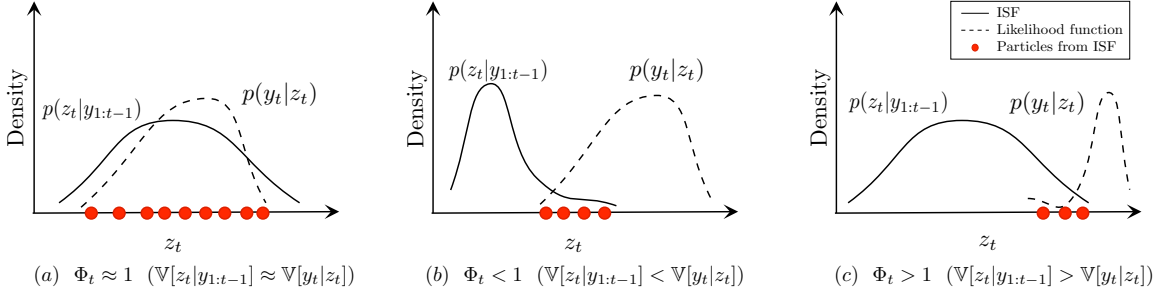
Figure 2.1: A schematic diagram to highlight the possible scenarios for different values of $\Omega_t \in \mathbb{R}_+$, where $\Omega_t \triangleq \mathrm{Tr}[\mathbb{V}_{p(Z_t|Y_{1:t-1})}[Z_t]]/\,\mathrm{Tr}[\mathbb{V}_{p(Y_t|Z_t)}[Y_t]]$ and $\mathrm{Tr}[\cdot]$ is the trace operator. In Case (a), when $\Omega_t \approx 1$, the ISF is mapped in the high likelihood region, which represents an ideal estimation scenario for SIR filters. In Cases (b) and (c), either the ISF is peaked $(\Omega_t < 1)$ or the likelihood function is peaked $(\Omega_t > 1)$ compared to the other distribution, such that only few number of particles generated from the ISF falls in the likelihood region.

such as ASIR filter (Chen *et al.*, 2005; Liu and West, 2001; Pitt and Shephard, 1999); progressive correction (Oudjane and Musso, 2000); and bridging densities (Clapp and Godsill, 2001) make use of current measurements to allow sampling from high-likelihood regions. Proposition 2.5.8 provides an optimal tuning rule for controlling the kernel width and for making an SIR filter adaptive and efficient for different values of $\Omega_t \in \mathbb{R}_+$, where: $\Omega_t \triangleq \mathrm{Tr}[\mathbb{V}_{p(Z_t|Y_{1:t-1})}[Z_t]]/\,\mathrm{Tr}[\mathbb{V}_{p(Y_t|Z_t)}[Y_t]]$; $\mathbb{R}_+ := [0, \infty)$; and $\mathrm{Tr}[\cdot]$ is the trace operator.

Proposition 2.5.8. *An optimal tuning for h_t at $t \in \mathbb{N}$ based on minimization of the KL divergence between the ISF $p(z_t|y_{1:t-1})$ and target posterior density $p(z_t|y_{1:t})$ is given by*

$$h_t^\star = \underset{h_t \in [0,1]}{\arg\min} \left[-\sum_{i=1}^{N} W_{t|t-1}^i \log[W_{t|t}^i] \right], \tag{2.33}$$

where: $h_t^\star$ is the optimal kernel parameter at $t \in \mathbb{N}$; and $\{W_{t|t-1}^i\}_{i=1}^N$ and $\{W_{t|t}^i\}_{i=1}^N$ are the particle weights given in (2.30) and (2.31b), respectively.

Proof. The KL divergence between $p(z_t|y_{1:t-1})$ and $p(z_t|y_{1:t})$ at $t \in \mathbb{N}$ is given by

$$D_{q||p}(t) = \int_{\mathcal{Z}} \log \left[\frac{p(z_t|y_{1:t-1})}{p(z_t|y_{1:t})} \right] p(dz_t|y_{1:t-1}), \tag{2.34}$$

where $D_{q||p}(t)$ is the KL divergence at $t \in \mathbb{N}$. Substituting (2.4) into (2.34) yields

$$D_{q||p}(t) = \int_{\mathcal{Z}} \log \left[\frac{p(y_t|y_{1:t-1})}{p(y_t|z_t)} \right] p(dz_t|y_{1:t-1}), \tag{2.35a}$$

$$= \int_{\mathcal{Z}} \log \left[\frac{\int_{\mathcal{Z}} p(y_t|z_t) p(dz_t|y_{1:t-1})}{p(y_t|z_t)} \right] p(dz_t|y_{1:t-1}). \tag{2.35b}$$

Computing (2.35b) in closed form is non-trivial for the model considered in (2.1); however, substituting (2.30) into (2.35b) yields an SMC approximation of (2.35b), such that

$$\widehat{D}_{q||p}(h_t) = \int_{\mathcal{Z}} \log \left[\frac{\int_{\mathcal{Z}} p(y_t|z_t) \sum_{j=1}^{N} W_{t|t-1}^i \delta_{Z_{t|t-1}^i}(dz_t)}{p(y_t|z_t)} \right] \sum_{i=1}^{N} W_{t|t-1}^i \delta_{Z_{t|t-1}^i}(dz_t), \tag{2.36a}$$

$$= \sum_{i=1}^{N} W_{t|t-1}^i \log \left[\frac{\sum_{j=1}^{N} W_{t|t-1}^i p(y_t|Z_{t|t-1}^i)}{p(y_t|Z_{t|t-1}^i)} \right], \tag{2.36b}$$

where $\widehat{D}_{q||p}(h_t)$ is an SMC estimate of $D_{q||p}(t)$. Note that the dependence of $\widehat{D}_{q||p}(h_t)$ on h_t can be established from (2.26) and (2.29). Several algebraic manipulations in (2.36b) followed by substituting (2.32) into (2.36b) yields

$$\widehat{D}_{q||p}(h_t) = -\sum_{i=1}^{N} W_{t|t-1}^i \log \left[\frac{W_{t|t}^i}{W_{t|t-1}^i} \right]. \tag{2.37}$$

Finally, a constrained optimization problem can be formulated based on minimization of $\widehat{D}_{q||p}(h_t)$ with respect to h_t, such that

$$h_t^\star = \arg\min_{h_t \in [0,1]} \widehat{D}_{q||p}(h_t). \tag{2.38}$$

Substituting (2.37) into (2.38) yields

$$h_t^\star = \arg\min_{h_t \in [0,1]} \left[-\sum_{i=1}^{N} W_{t|t-1}^i \log \left[\frac{W_{t|t}^i}{W_{t|t-1}^i} \right] \right], \tag{2.39a}$$

$$= \arg\min_{h_t \in [0,1]} \left[-\sum_{i=1}^{N} W_{t|t-1}^i \log \left[W_{t|t}^i \right] \right], \tag{2.39b}$$

where (2.39b) follows from the fact that $\sum_{i=1}^{N} W_{t|t-1}^i \log \left[W_{t|t-1}^i \right]$ is independent of h_t, which completes the proof. $\qquad\square$

Remark 2.5.9. *Proposition 2.5.8 provides an optimal tuning rule for (a) correcting over-dispersion in ISF and; (b) making Ad-SIR filter efficient for different values of $\Omega_t \in \mathbb{R}_+$. Note that other tuning rules for $h_t \in [0,1]$ can also be readily used in place of Proposition 2.5.8, provided, it is compatible with the developments of previous sections.*

2.5.3   Resampling

In importance sampling, degeneracy is a very common problem; wherein, after a few sampling time instances, the distribution of the weights in (2.31b) becomes skewed. As a result, the variance of the weights in (2.31b) increases over time (Doucet *et al.*, 2001); thereby, requiring a large computational effort to update the particles, whose contributions are negligible. See (Chen, 2003; Ristic *et al.*, 2004) for further details. A systematic resampling scheme (Kitagawa, 1996) is adopted here that eliminates the low weighted particles by replacing them with particles with large weight. The choice of systematic resampling is supported by an easy implementation procedure and a lower order of computational complexity $\mathcal{O}(N)$ (Arulampalam *et al.*, 2002). A systematic resampling step involves drawing N new particles $\{Z_{t|t}^i\}_{i=1}^N$, with replacement from a set of particles $\{Z_{t|t-1}^i\}_{i=1}^N$ realized from the ISF, such that the following equality holds

$$\Pr(Z_{t|t}^i = Z_{t|t-1}^i) = W_{t|t}^i \tag{2.40}$$

for all $1 \leq i \leq N$. Here $\Pr(\cdot)$ is the probability measure. The resampled particles $\{Z_{t|t}^i\}_{i=1}^N \sim p(z_t|y_{1:t})$ are identically distributed with weights reset to $\{W_{t|t}^i = N^{-1}\}_{i=1}^N$.

Remark 2.5.10. *A key feature of the resampling step in (2.40) is that it takes an independent set of particles $\{Z_{t|t-1}^i\}_{i=1}^N$ and returns a set of dependent particles $\{Z_{t|t}^i\}_{i=1}^N$. This is due to the large number of replications of highly weighted particles. As discussed in (Schön et al., 2011), using correlated particles $\{Z_{t|t}^i; W_{t|t}^i = N^{-1}\}_{i=1}^N$ in (2.31b) further degrades the accuracy of the MMSE point estimate computed in Remark 2.5.2. In (Ninness, 2000), the authors showed that the rate of convergence of the MMSE point estimates to the true*

posterior mean decreases as correlation in $\{Z_{t|t}^i\}_{i=1}^N$ increases. To avoid any performance degradation, the MMSE point estimates are computed before the resampling step.

Remark 2.5.11. *Stratified (Kitagawa, 1996; Liu and Chen, 1998) or residual (Liu and Chen, 1998) resampling can also be used as an alternative to the systematic resampling used here. See (Chen, 2003) for other resampling methods.*

2.6   Missing measurements

Missing measurements are common in the process industries, where measurements may not become available at all sampling time instants. An approach to allow Bayesian state-parameter estimation with real-time missing measurements is presented in this section.

From (2.32) it is clear that if $\{Y_t = y_t\}$ at $t \in \mathbb{N}$ is missing then (2.32) can no longer be used to compute (2.31b) or the MMSE estimates obtained therefrom. To address this, if $\{Y_t = y_t\}$ at $t \in \mathbb{N}$ is missing then the ISF $p(z_t|y_{1:t-1})$ in (2.5) is used instead to compute a one-step ahead predicted MMSE point estimate for the states and parameters at $t \in \mathbb{N}$. The procedure to obtain an MMSE estimate under missing measurements is outlined next.

Remark 2.6.1. *Let the SMC approximation of the ISF $p(dz_t|y_{1:t-1})$ be represented by (2.30) then a one-step ahead predicted MMSE point estimate for the states and parameters at $t \in \mathbb{N}$ can be computed as $\widehat{Z}_{t|t-1} \triangleq \int_{\mathcal{Z}} z_t p(dz_t|y_{1:t-1}) \approx \sum_{i=1}^N W_{t|t-1}^i Z_{t|t-1}^i$.*

It is important to note that if $\{Y_t = y_t\}$ at $t \in \mathbb{N}$ is missing then the posterior $p(z_t|y_{1:t})$ or its KL divergence with $p(z_t|y_{1:t-1})$ at $t \in \mathbb{N}$ cannot be computed either. In other words, h_t cannot be optimally tuned (based on Proposition 2.5.8) under missing measurements.

Note that with Proposition 2.5.8, optimal tuning for h_t under missing measurement is not necessary. This is because tuning h_t according to Proposition 2.5.8 corrects the variance inflation problem in the SMC approximation of $p(z_t|y_{1:t-1})$ and also projects the particles from it onto the region of high posterior density $p(z_t|y_{1:t})$ (see Remark 2.5.9); however, if

$p(z_t|y_{1:t})$ is unavailable at $t \in \mathbb{N}$, Proposition 2.5.8 only addresses the variance inflation in the SMC approximation of $p(z_t|y_{1:t-1})$, which can be corrected with any $h_t \in [0,1]$ value.

Remark 2.6.2. *As a general rule, if $\{Y_t = y_t\}$ at $t \in \mathbb{N}$ is missing, h_t will be assigned its previous optimal value $h_{t-1}^\star$. Note that, if necessary, the user can choose any $h_t \in [0,1]$ value, or can optimize it based on other tuning rules as well (see Remark 2.5.9).*

After computing the one-step ahead predicted MMSE state-parameter point estimate at $t \in \mathbb{N}$ (see Remark 2.6.1), the Law of Total Probability on $p(z_t|y_{1:t-1})$ yields

$$p(z_{t+1}|y_{1:t-1}) = \int_{\mathcal{Z}} p(z_{t+1}|z_t)p(dz_t|y_{1:t-1}), \tag{2.41}$$

where $p(z_{t+1}|y_{1:t-1})$ is a two-step ahead prior density, and also the ISF for the sampling time $t+1$ under missing $\{Y_t = y_t\}$. Since (2.41) does not have a closed form solution, an SMC approximation of it can be obtained by substituting (2.30) into (2.41), such that

$$\tilde{p}(z_{t+1}|y_{1:t-1}) = \sum_{i=1}^{N} W_{t|t-1}^i p(z_{t+1}|Z_{t|t-1}^i). \tag{2.42}$$

To correct the variance inflation in (2.42), kernel smoothing discussed in Section 2.5.1 is applied, such that with kernel smoothing the ISF can now be approximated as follows

$$\tilde{p}(z_{t+1}|y_{1:t-1}) = \sum_{i=1}^{N} W_{t|t-1}^i p(z_{t+1}|\tilde{Z}_{t|t-1}^i), \tag{2.43}$$

where $\{\tilde{Z}_{t|t-1}^i\}_{i=1}^N = \{X_{t|t-1}^i; \tilde{\theta}_{t|t-1}^i\}_{i=1}^N$, and

$$\tilde{\theta}_{t|t-1}^i = \sqrt{1 - h_{t+1}^2}\, \theta_{t|t-1}^i + (1 - \sqrt{1 - h_{t+1}^2})\, \widehat{\theta}_{t|t-1}. \tag{2.44}$$

In (2.44), h_{t+1} can be tuned based on Proposition 2.5.8, using the next available measurement $\{Y_{t+1} = y_{t+1}\}$. Note that from (2.43), random particles can be generated by passing $\tilde{Z}_{t|t-1}^i$ through $p(z_{t+1}|\tilde{Z}_{t|t-1}^i)$ for all $1 \le i \le N$. Using the set of generated random particles, the ISF distribution $p(dz_{t+1}|y_{1:t-1})$ can be represented as

$$\tilde{p}(dz_{t+1}|y_{1:t-1}) = \sum_{i=1}^{N} W_{t+1|t-1}^i \delta_{Z_{t+1|t-1}^i}(dz_{t+1}), \tag{2.45}$$

Algorithm 1 Complete measurements

1: Select a prior pdf $Z_0 \sim p(z_0)$ for the states and parameters.
2: Generate N independent and identically distributed particles $\{Z_{0|-1}^i\}_{i=1}^N \sim p(z_0)$ and
   set the associated weights to $\{W_{0|-1}^i = N^{-1}\}_{i=1}^N$. Set $t \leftarrow 1$.
3: Sample $\{Z_{t|t-1}^i\}_{i=1}^N \sim p(z_t|y_{1:t-1})$ using (2.28). Set $\{W_{t|t-1}^i = N^{-1}\}_{i=1}^N$.
4: **while** $t \in \mathbb{N}$ **do**
5:    Use $\{Y_t = y_t\}$ and compute the importance weights $\{W_{t|t}^i\}_{i=1}^N$ from (2.32).
6:    Compute the point estimate $\widehat{Z}_{t|t}$ using the procedure outlined in Remark 2.5.2.
7:    Resample the particle set $\{Z_{t|t-1}^i; W_{t|t}^i\}_{i=1}^N$ with replacement using (2.40).
8:    Compute $h_{t+1}^\star$ using Proposition 2.5.8 and generate $\{\tilde{\theta}_{t|t}^i\}_{i=1}^N$ using (2.26).
9:    Sample $\{Z_{t+1|t}^i\}_{i=1}^N \sim p(z_{t+1}|y_{1:t})$ using (2.28). Set $\{W_{t+1|t}^i = N^{-1}\}_{i=1}^N$.
10:   Set $t \leftarrow t + 1$.
11: **end while**

---

where $\{Z_{t+1|t-1}^i; W_{t+1|t-1}^i = w_{t|t-1}^i\}_{i=1}^N$ is a set of N random particles from (2.43).

Finally, using the next available measurement $\{Y_{t+1} = y_{t+1}\}$, the posterior distribution $p(dz_{t+1}|y_{1:t-1}, y_{t+1})$ at $t + 1$ can be approximated using SMC methods, such that

$$\tilde{p}(dz_{t+1}|y_{1:t-1}, y_{t+1}) = \sum_{i=1}^N W_{t+1|t+1}^i \delta_{Z_{t+1|t-1}^i}(dz_{t+1}), \tag{2.46}$$

where $\{W_{t+1|t+1}^i\}_{i=1}^N$ are computed using (2.32).

Remark 2.6.3. *The on-line Bayesian state-parameter estimation method presented in this section assumes that measurements are missing at random time instants. Note that, the proposed method can also handle cases with multiple consecutively missed measurements.*

2.7   On-line estimation algorithm

Algorithms 1 and 2 outlines the procedure for estimating $Z_t \in \mathcal{Z}$ in (2.1) for complete and missing measurements, respectively. Convergence of these algorithms is discussed next.

2.8   Convergence

Computing the conditional mean of $Z_t|(Y_{1:t} = y_{1:t}) \sim p(z_t|y_{1:t})$ requires evaluating the multi-dimensional integral over $\mathcal{Z}$. As stated earlier, obtaining an analytical solution to

---

Algorithm 2 Missing measurements

1: Select a prior pdf $Z_0 \sim p(z_0)$ for the states and parameters.
2: Generate N independent and identically distributed particles $\{Z_{0|-1}^i\}_{i=1}^N \sim p(z_0)$ and set the associated weights to $\{W_{0|-1}^i = N^{-1}\}_{i=1}^N$. Set $t \leftarrow 1$.
3: Sample $\{Z_{t|t-1}^i\}_{i=1}^N \sim p(z_t|y_{1:t-1})$ using (2.28). Set $\{W_{t|t-1}^i = N^{-1}\}_{i=1}^N$.
4: **while** $t \in \mathbb{N}$ **do**
5:     **if** $\{Y_t = y_t\}$ is available **then**
6:         Use $\{Y_t = y_t\}$ and compute the importance weights $\{W_{t|t}^i\}_{i=1}^N$ from (2.32).
7:         Compute the point estimate $\widehat{Z}_{t|t}$ using the procedure outlined in Remark 2.5.2.
8:         Resample the particle set $\{Z_{t|t-1}^i; W_{t|t}^i\}_{i=1}^N$ with replacement using (2.40).
9:     **end if**
10:    **if** $\{Y_t = y_t\}$ is unavailable **then**
11:        Compute the predicted point estimate $\widehat{Z}_{t|t-1}$ using the procedure in Remark 2.6.1.
12:    **end if**
13:    **if** $\{Y_{t+1} = y_{t+1}\}$ is available **then**
14:        Compute $h_{t+1}^\star$ using Proposition 2.5.8 and generate $\{\tilde{\theta}_{t|t}^i\}_{i=1}^N$ using (2.26).
15:        Sample $\{Z_{t+1|t}^i\}_{i=1}^N \sim p(z_{t+1}|y_{1:t})$ using (2.28). Set $\{W_{t+1|t}^i = N^{-1}\}_{i=1}^N$.
16:    **end if**
17:    **if** $\{Y_{t+1} = y_{t+1}\}$ is unavailable **then**
18:        Set $h_{t+1}^\star \leftarrow h_t^\star$ and generate $\{\tilde{\theta}_{t|t-1}^i\}_{i=1}^N$ using (2.44).
19:        Sample $\{Z_{t+1|t-1}^i\}_{i=1}^N \sim p(z_{t+1}|y_{1:t-1})$ using (2.43). Set $\{W_{t+1|t-1}^i = w_{t|t-1}^i\}_{i=1}^N$.
20:    **end if**
21:    Set $t \leftarrow t + 1$.
22: **end while**

---

the MMSE estimate is not possible for the model considered in (2.1). Algorithms 1 and 2 deliver an N-particle approximation to the MMSE estimates. Establishing theoretical convergence for Algorithms 1 and 2 is beyond the scope of this chapter; however, some of the practical issues affecting their convergence, include:

- Finding an optimal $N < \infty$, for which the N-particle MMSE estimate $\widehat{Z}_{t|t}^N$ would converge to true MMSE estimate $Z_{t|t}^\star$ in a ball of some predefined radius is non-trivial; however, note that the estimates can be made accurate for sufficiently large N.

- Inaccurate noise model can prevent the estimates from converging to their true values. To circumvent this problem the noise models are known in their distribution class and their parameters estimated along with model parameters (see Assumption 2.3.1).

- Poor choice of $Z_0 \sim p(z_0)$ can cause serious convergence issues. The problem is particularly severe while estimating the discrete states of hybrid systems. Any discrete change in the state require an adaptive mechanism for redefining the ISF for the states. Since estimation in hybrid systems is not included in the scope of this chapter, it will not be considered here. Consideration will be made in selecting $p(z_0)$ in Section 2.10.

The procedure to reduce computational complexity of Algorithms 1 and 2 is discussed next.

Remark 2.8.1. *Algorithms 1 and 2 compute an estimate of $Z_t \in \mathcal{Z}$. Note for time-invariant systems, estimation of θ_t can be bypassed if $\exists t_\alpha \in \mathbb{N}$, $\lim_{N \to +\infty} \widehat{\theta}_{t|t}^N - \theta^\star = 0 \ \forall t \geq t_\alpha$, where $\theta^\star \in \Theta$ is a vector of true system parameters. The rationale behind this approach is to reduce the computational complexity of Algorithms 1 and 2 by simply selecting $\widehat{\theta}_{t|t} = \widehat{\theta}_{t_\alpha|t_\alpha} \ \forall t \geq t_\alpha$. Caution is required while estimating in a time-varying systems.*

In the next section, some of the key features of the on-line estimation algorithm presented in this chapter are compared against that of an off-line parameter estimation algorithm.

2.9   Comparison with off-line algorithm

In processes, where developing an efficient off-line parameter estimator is required, an EM algorithm has been very successful. The EM algorithm is a popular off-line ML based method for parameter estimation in non-linear SSMs with non-Gaussian noise. The key advantage with EM is that it can be adopted under a variety of industry relevant situations. In (Chitralekha *et al.*, 2010; Schön *et al.*, 2011), the authors used the off-line EM algorithm to estimate the process and noise model parameters (e.g., mean and covariance) under complete measurements. Extension of the EM algorithm for estimation under missing measurements was considered in (Gopaluni, 2008).

In terms of computational complexity, the particle smoothing step in EM requires $\mathcal{O}(N^2Tn)$ calculations at each iteration (Chitralekha *et al.*, 2010; Gopaluni, 2008; Schön

et al., 2011), where n is the state dimension and T is the total number of measurements. Smoothing step with computational complexity $\mathcal{O}(NTn)$ has also appeared (Douc *et al.*, 2011). This highlights the scalability issues with the EM algorithm when n is large. The brute-force optimization in the M step of EM further adds to the computational cost. From a theoretical perspective, EM has an advantage in terms of asymptotic efficiency and consistency; however, in practice, solving the maximization step of EM can be prohibitive, especially in large dimensional dynamical systems with long measurement sequence. Depending on the dimension of the system, the number of particles and samples used, the algorithm may take hours to run on a state-of-the art desktop computer (Gopaluni, 2008).

Focussing only on the parameter estimation aspect of Algorithms 1 and 2, the developed method can estimate the process and noise model parameters in real-time with either complete or missing measurement set. The efficacy of the proposed method in dealing with these cases is demonstrated in Section 2.10. A distinct advantage of the proposed algorithm is that it can also be used for estimating time-varying systems. Computational complexity of Algorithms 1 and 2 until time T is of the order $\mathcal{O}(NTs)$ whereas the optimization approach introduced in Proposition 2.5.8 has complexity $\mathcal{O}(N)$, where r is the dimension of unknown parameters. Also, by including Remark 2.8.1, the computational cost can further be reduced. Direct quantification of the bias introduced through the use of artificial dynamics approach might be difficult as pointed in (Kantas *et al.*, 2009); however, (Tulsyan *et al.*, 2013*b*) proposed the use of PCRLB for assessing the quality of the parameter estimates. This assessment is done by comparing the MSE for the estimates against the theoretical PCRLB. Experiments in (Tulsyan *et al.*, 2013*b*) have confirmed that using ADA, with the tuning rule in Proposition 1 yields numerically reliable estimates.

Remark 2.9.1. *Comparison is not intended to draw conclusions on the validity of the involved algorithms. Instead, it is provided to highlight key features of the Ad-SIR filter in handling situations, which have been considered so far only under off-line settings.*

2.10   Numerical illustrations

In this section, efficacy of Algorithms 1 and 2 is illustrated through two numerical examples. The first example is taken from (Gopaluni, 2008) and the second example from (Schön *et al.*, 2011). In this study, the estimation problem is formulated to estimate both states and parameters of a non-linear system, but the analysis is focussed mainly on on-line parameter estimation as it has been less studied compared to the state estimation problem.

2.10.1   Example 1: A non-linear and non-Gaussian system

Consider the following stochastic SSM (Gopaluni, 2008; Goodwin and Agüero, 2005)

$$X_{t+1} = \alpha_t X_t + \beta_t U_t + V_t, \tag{2.47a}$$

$$Y_t = \gamma_t \cos X_t + W_t, \tag{2.47b}$$

where: $U_t \sim \mathcal{N}(u_t|0,1)$; $V_t \sim \mathcal{N}(v_t|0,Q_t)$; and $W_t \sim \mathcal{N}(w_t|0,R_t)$. The process and measurement noise models in (2.47a) and (2.47b), respectively, are known in their distribution class and mean, but unknown in their respective variances $Q_t \in \mathbb{R}_+$ and $R_t \in \mathbb{R}_+$. (Gopaluni, 2008) used this example for off-line estimation of process and noise model parameters under complete and missing measurements using EM algorithm. In this study, real-time state-parameter estimation will be setup using Algorithms 1 and 2.

For comparison with results reported in (Gopaluni, 2008), similar simulation conditions are maintained to the extent possible. As in (Gopaluni, 2008), the initial condition for the true state and true parameters in (2.47) are selected as $x_0^\star = 1$ and $\theta_t^\star \triangleq [\alpha_t^\star; \beta_t^\star; \gamma_t^\star; Q_t^\star; R_t^\star] = [0.9; 1; 1; 0.1; 0.1] \ \forall t \in [1,T]$, respectively.

To estimate $\theta_t \in \mathbb{R}^5$, MC simulations are performed using 45 random realizations of input-output data $\{u_{1:T}; \ y_{1:T}\}$. For each input-output data set, MMSE estimates $\widehat{\theta}_{t|t} \ \forall t \in [1,T]$ are computed. For this study a finite filtering time $T = 1000$ is selected with $N = 20000$ particles. A large T and N values help reduce variation in $\widehat{\theta}_{t|t}$ arising

Table 2.2: Parameter estimates and standard error computed using Algorithms 1 and 2 based on 45 MC simulations.

Parameter	True	Parameter estimates $\pm$ standard deviation $(\widehat{\theta}_{T|T} \pm V_{\theta_T}^{0.5})$			
θ_t	$\theta_t^\star$	0% Missing	10% Missing	25% Missing	50% Missing
α_t	0.90	0.9027 ± 0.0060	0.9017 ± 0.0074	0.9014 ± 0.0077	0.9041 ± 0.0079
β_t	1.0	0.9926 ± 0.0210	0.9946 ± 0.0203	0.9913 ± 0.0278	0.9865 ± 0.0367
γ_t	1.0	1.0179 ± 0.0225	1.0145 ± 0.0208	1.0105 ± 0.0275	0.9743 ± 0.0415
Q_t	0.10	0.1068 ± 0.0124	0.1054 ± 0.0145	0.1037 ± 0.0167	0.0915 ± 0.0197
R_t	0.10	0.1068 ± 0.0090	0.0892 ± 0.0076	0.0932 ± 0.0129	0.1101 ± 0.0216

due to randomness in measurement and error associated with SMC approximations, respectively. The prior density $\theta_0 \sim \mathcal{N}(\theta_0 | M_\theta, C_\theta)$ is selected as a mutually independent multi-variate normal distribution with mean $M_\theta = [0.5; \ 0.5; \ 0.5; \ 0.2; \ 0.2]$ and covariance $C_\theta = \mathrm{diag}([1; \ 1; \ 1; \ 0.05; \ 0.05])$, where $\mathrm{diag}(\cdot)$ is a diagonal matrix.

In this simulation study, estimation is performed on four different experiment runs each with 0%, 10%, 25% and 50% randomly missing measurements. A MC based MMSE parameter estimates $\widehat{\theta}_{T|T}$ along with the standard estimation error at sampling time $t = T$ are given in Table 2.2. In each of the four experiments the estimated parameters $\widehat{\theta}_{T|T}$ are in the neighbourhood of $\theta_T^\star$. Also, comparing with the results reported in (Gopaluni, 2008), the proposed method delivers $\widehat{\theta}_{T|T}$ in the neighbourhood of $\theta_T^\star$ with high statistical reliability. Higher parameter accuracy can be attributed to large T and N values used here in contrast to $T = 100$ and $N = 150$ used by (Gopaluni, 2008). This highlights the advantage of Ad-SIR filter over EM algorithm; wherein, large N can be used to approximate the posterior without significant increase in the computational load.

Figure 2.2 shows the MMSE estimates $\widehat{\alpha}_{t|t}$ and $\widehat{R}_{t|t}$ $\forall t \in [1, T]$ computed using Algorithm 1 (for 0% missing measurements) and Algorithm 2 (for 50% missing measurements). Under 0% missing measurements, the estimates converge in the neighbourhood of $\theta_T^\star$ within a few sampling time instants; whereas, as the percentage of missing measurements increases to 50%, the estimates take longer to convergence.

Computation of $\widehat{\theta}_{t|t}$ $\forall t \in [1, T]$ took 210 seconds (for 0% missing measurements) on
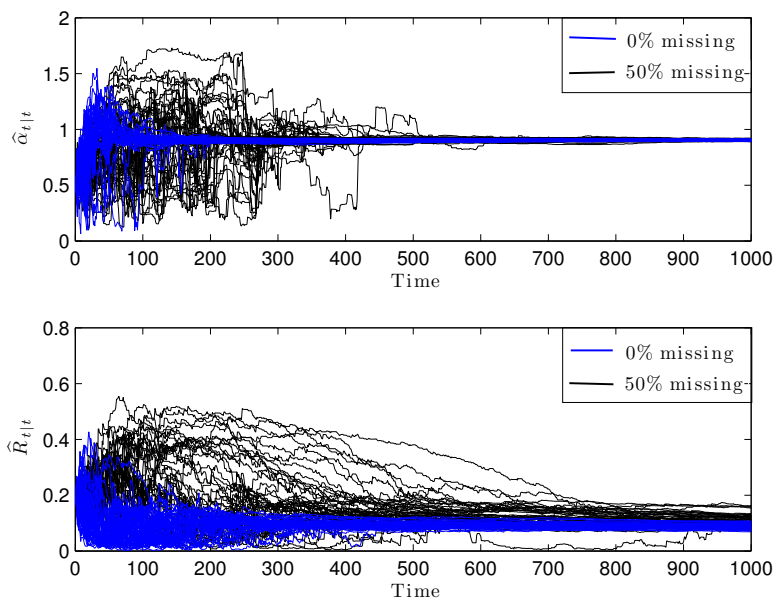
Figure 2.2: MMSE estimates of: [Top] $\widehat{\alpha}_{t|t}$ and [Bottom] $\widehat{R}_{t|t}$ computed using Algorithms 1 and 2 based on 45 simulations.
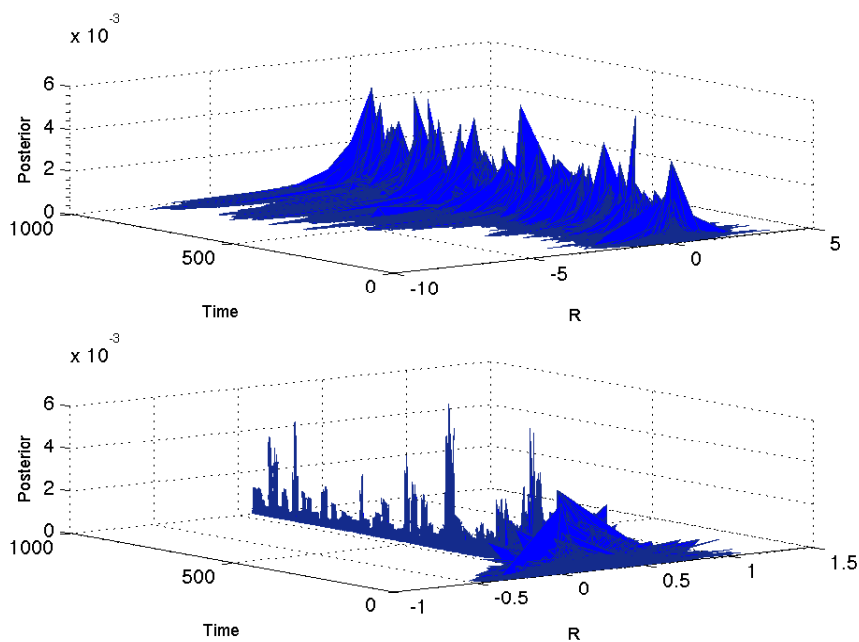
Figure 2.3: Posterior distribution $\tilde{p}(R_t|y_{1:t}) \ \forall t \in [1, T]$ under 0% missing measurements computed using Algorithm 1: [Top] without kernel smoothing method, and [Bottom] with kernel smoothing method and tuning rule selected as Proposition 2.5.8.
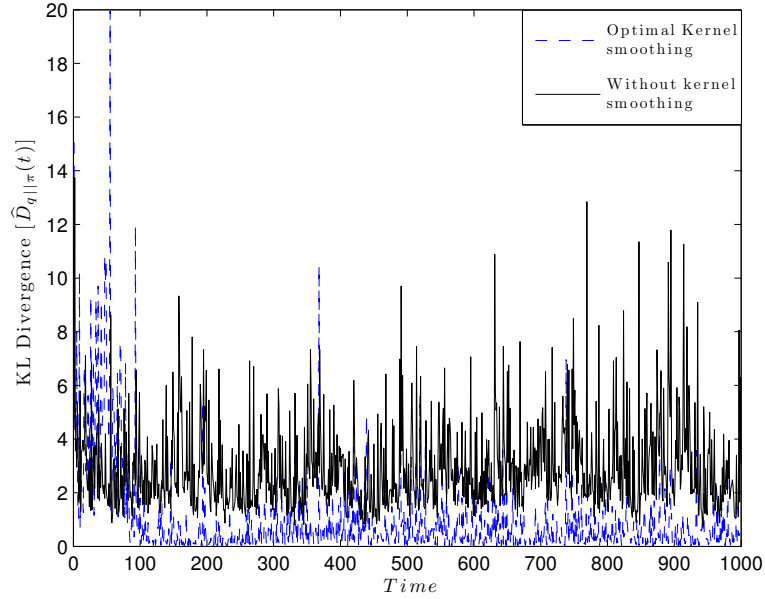
Figure 2.4: KL divergence between $\tilde{p}(z_t|y_{1:t-1})$ and $\tilde{p}(z_t|y_{1:t})$ $\forall t \in [1, T]$ computed using Algorithm 1. The divergence is computed with $T = 1000$ and $N = 20000$.

a 3.33 GHz Intel Core i5 processor running on Windows 7. Computation under missing measurements is even faster, as the optimization step for tuning the kernel parameter is not required at all sampling time instants.

Figure 2.3[Top] validates the comment made in Remark 2.5.5 that without correcting the inflation problem, SMC based marginalized posterior density estimate would continue to disperse over time. The advantage of using the kernel smoothing method with Proposition 2.5.8 is evident from Figure 2.3[Bottom]; wherein, the proposed method not only corrects dispersion in the marginalized posterior density, but also reduces it substantially around the estimates. In Figure 2.4, KL divergence between $\tilde{p}(z_t|y_{1:t-1})$ and $\tilde{p}(z_t|y_{1:t})$ is shown. Comparing the mean and variance of the two trajectories in Figure 2.4 it is clear that Proposition 2.5.8 significantly reduces divergence between the ISF and posterior density.

In summary, Figures 2.2 through 2.4 validate the usefulness of Proposition 2.5.8 in achieving convergence of $\widehat{\theta}_{T|T}$ in the neighbourhood of $\theta_T^\star$ under compete and missing measurements. Another non-linear and non-Gaussian example is considered next.

2.10.2   Example 2: A non-linear and non-Gaussian system

In Section 2.10.1, efficacy of Algorithms 1 and 2 was established under different percentage of missing measurements. In this study, estimation capability of Algorithm 1 is demonstrated for different values of $\Gamma_t \in \mathbb{R}_+$, where $\Gamma_t \triangleq \mathbb{V}_{p(Z_t|Z_{t-1})}[Z_t]/\mathbb{V}_{p(Y_t|Z_t)}[Y_t]$. Consider the following discrete-time, stochastic non-linear autonomous SSM (Doucet *et al.*, 2001; Schön *et al.*, 2011)

$$X_{t+1} = \frac{X_t}{\alpha_t} + \frac{\beta_t X_t}{1 + X_t^2} + \kappa_t \cos(1.2t) + V_t, \tag{2.48a}$$

$$Y_t = \gamma_t X_t^2 + W_t, \tag{2.48b}$$

where: $V_t \sim \mathcal{N}(v_t|0, Q_t)$; and $W_t \sim \mathcal{N}(w_t|0, R_t)$. The initial condition for the true state is chosen as $x_0^\star = 5$ and the true parameters are selected as $\theta_t^\star \triangleq [\alpha_t^\star; \beta_t^\star; \kappa_t^\star; \gamma_t^\star; Q_t^\star; R_t^\star] = [2.0; 25; 8.0; 0.05; \{0.10; 1.0\}; \{0.10; 1.0\}]\ \forall t \in [1, T]$, where $\{\cdot; \cdot\}$ denote a set of possible discrete values for Q_t and R_t, considered in this study. In the simulation, the algorithm parameters are selected as $T = 100$ seconds and $N = 20000$ particles.

On-line estimation of process and noise model parameters in (2.48) is considered for three independent cases, with each differing in the choice of $\Gamma_t\ \forall t \in [1, T]$. In the first experiment $\Gamma_t = 1$ (with $Q_t = 0.1$; $R_t = 0.1$) is selected. For the second and third experiment, $\Gamma_t = 0.1$ (with $Q_t = 0.1$; $R_t = 1$) and $\Gamma_t = 10$ (with $Q_t = 1$; $R_t = 0.1$) is selected, respectively. The choice of the experiments denote the cases in Figure 2.1.

The prior density $\theta_0 \sim \mathcal{N}(\theta_0|M_\theta, C_\theta)$ is selected as a mutually independent multivariate normal distribution with mean $M_\theta = [1; 20; 10; 1; 0.5; 0.5]$ and covariance $C_\theta = \mathrm{diag}([1; 15; 5; 1; 1; 1])$. Large variance ensures that $\theta_0^\star$ is included in the $\mathrm{supp}\, p(\theta_0)$.

As in Section 2.10.1, 45 MC simulations are performed. Using Algorithm 1, a MC MMSE parameter estimates $\widehat{\theta}_{T|T}$ for the three experiments are given in Table 2.3. Small uncertainties associated with $\widehat{\theta}_{T|T}$ across the range of Γ_t values suggest high statistical reliability of the estimates. Moreover, comparing the estimates with the true values it is evident that the estimate $\widehat{\theta}_{T|T}$ is in the neighbourhood of $\theta_{T|T}^\star$. Algorithm 1 yields the most

Table 2.3: Parameter estimates and standard error computed using Algorithms 1 for different $\Gamma_t \; \forall t \in [1, T]$ based on 45 MC simulations.

Parameter	True	Parameter estimates $\pm$ standard deviation $(\widehat{\theta}_{T|T} \pm V_{\theta_T}^{0.5})$		
θ_t	$\theta_t^\star$	$\Gamma_t = 1$	$\Gamma_t = 0.1$	$\Gamma_t = 10$
		$(Q_t = 0.1; \; R_t = 0.1)$	$(Q_t = 0.1; \; R_t = 1)$	$(Q_t = 1; \; R_t = 0.1)$
α_t	2.0	2.0358 ± 0.0400	2.0694 ± 0.0812	2.0845 ± 0.0791
β_t	25	24.250 ± 1.5273	23.686 ± 1.5997	23.916 ± 1.6806
κ_t	8.0	7.9004 ± 0.3873	7.7611 ± 0.4154	7.6728 ± 0.5329
γ_t	0.05	0.0530 ± 0.0052	0.0557 ± 0.0061	0.0566 ± 0.0067
Q_t	–	0.1202 ± 0.0154	0.1284 ± 0.0204	0.9144 ± 0.1543
R_t	–	0.1084 ± 0.0151	0.9054 ± 0.1126	0.1072 ± 0.0157

reliable estimates for $\Gamma_t = 1$. This is because $\Gamma_t = 1$ presents an ideal scenario for filtering.

Estimates of $\widehat{\gamma}_{t|t}$ and $\widehat{Q}_{t|t}$ for $\Gamma_t = 10$ are given in Figure 2.5. On average, $\widehat{\gamma}_{t|t}$ converges in the neighbourhood of $\gamma_T^\star$ in about $t = 10$ seconds, whereas $\widehat{Q}_{t|t}$ takes $t = 65$ seconds to converge. For this simulation, computation of $\widehat{\theta}_{t|t} \; \forall t \in [1, T]$ took 21 seconds of CPU time to complete. Figure 2.6 gives the kernel parameter computed using Proposition 2.5.8.

The advantage of using KL divergence based tuning rule for h_t is highlighted in Figure 2.7. Figure 2.7 gives the SMC based approximate marginalized posterior distribution $\tilde{p}(\beta_T|y_{1:T})$ for different choices of $h_t \; \forall t \in [1, T]$. It is clear that with the proposed tuning rule, Algorithm 1 projects $\tilde{p}(\beta_T|y_{1:T})$ around the true parameter $\beta_T^\star = 25$ (see Table 2.3).

Interestingly, with $h_t = 0.01 \; \forall t \in [1, T]$, a single particle representation of $\tilde{p}(\beta_T|y_{1:T})$ is obtained (see Figure 2.7). This is because as $h_t \to 0$, $\Sigma_{\theta_t} = h_t^2 V_{\theta_{t-1}} \to 0 \; \forall t \in [1, T]$. In the limiting case, when $h_t = 0$, β_t has a stationary dynamics. It is well known that using SMC methods in such situations result in parameter sample degeneracy (see Section 2.1).

Studying the other extreme case, with $h_t = 0.99 \; \forall t \in [1, T]$ the posterior density $\tilde{p}(\beta_T|y_{1:T})$ in Figure 2.7 has a wide support. This can again be understood by analysing $\tilde{p}(\beta_t|y_{1:t}) \; \forall t \in [1, T]$ in limits. As $h_t \to 1$, the set of smoothed particles in (2.26) are projected closer to the mean $\widehat{\theta}_{t-1|t-1}$. Under the limiting case, when $h_t = 1$ the marginalized ISF is given by $\tilde{p}(\theta_t|y_{1:t-1}) = \sum_{i=1}^{N} W_{t-1|t-1}^i \mathcal{N}(\theta_t|\widehat{\theta}_{t-1|t-1}, V_{\theta_{t-1}})$. Note that, generating particles from $\tilde{p}(\theta_t|y_{1:t-1})$ under the limiting case only depends on the
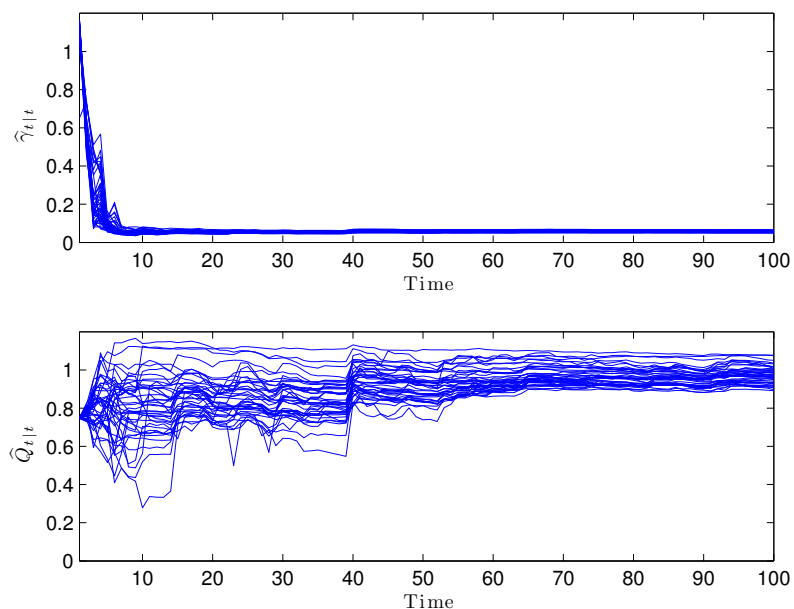
Figure 2.5: MMSE estimates of: [Top] $\widehat{\gamma}_{t|t}$ and [Bottom] $\widehat{Q}_{t|t}$ computed using Algorithm 1 for $\Gamma_t = 10 \ \forall t \in [1, T]$. It is based on 45 MC simulations with 0% missing measurements.
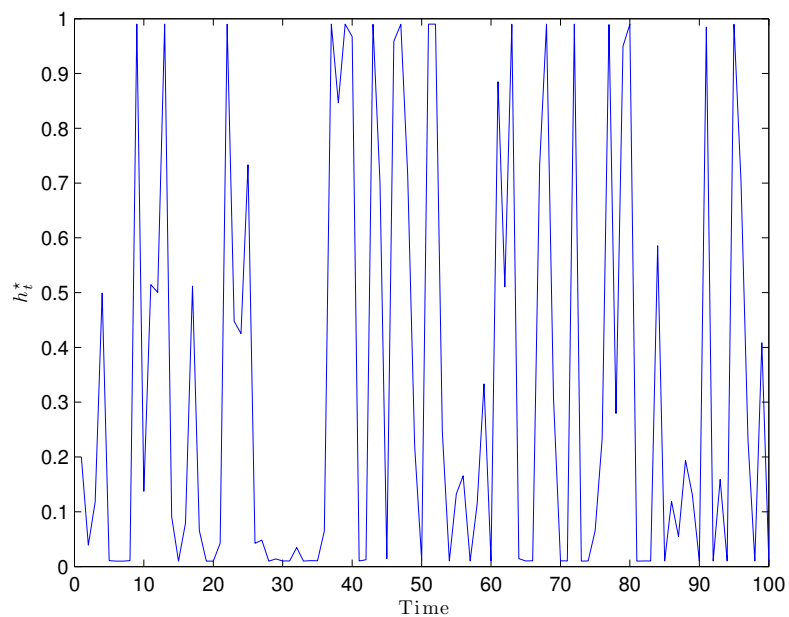
Figure 2.6: Optimal kernel $h_t \ \forall t \in [1, T]$ tuned using Proposition 2.5.8 for $\Gamma_t = 10 \ \forall t \in [1, T]$ and 0% missing measurements.
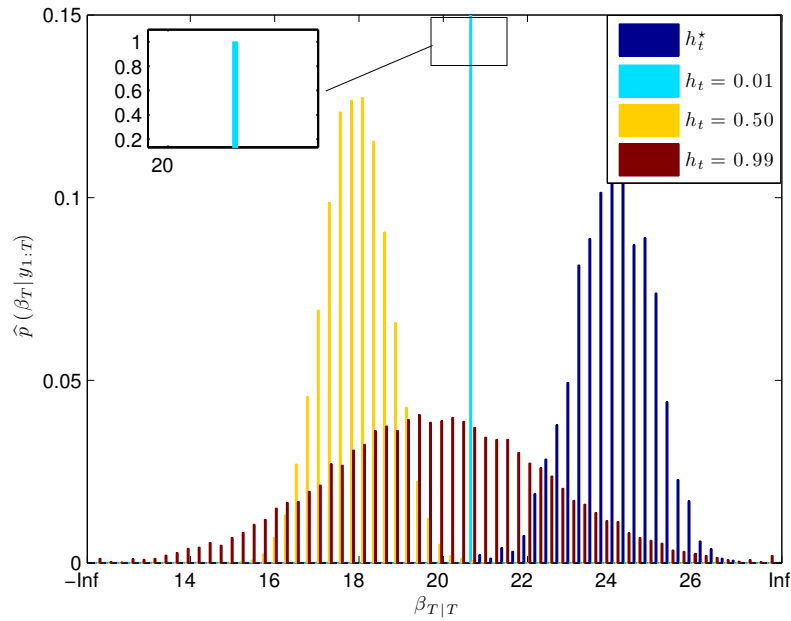
Figure 2.7: Approximate marginalized posterior distribution $\tilde{p}(\beta_t|y_{1:t})$ at $t = T$ computed based on different tuning rules for h_t $\forall t \in [1, T]$. In the graph, h_t^* represents the optimal tuning based on Proposition 2.5.8 (see Figure 2.6).

estimated parameter covariance $V_{\theta_{t-1}}$. It is easy to see that in such situations, arbitrarily wide distributions for the SMC based approximate marginalized posterior density can be obtained depending on $V_{\theta_{t-1}}$ values.

In summary, this simulation study demonstrates the efficacy of the proposed optimal tuning rule for a range of process to measurement noise variance ratio.

2.11   Conclusions

In this chapter, a Bayesian algorithm for on-line state and parameter estimation in discrete-time, stochastic non-linear state-space models is presented. The proposed algorithm uses an adaptive SIR filter to deliver an minimum mean-square error estimate at each filtering time. The extension of the algorithm to handle missing measurements in real-time is also presented. The usual variance inflation problem introduced by adding artificial parameter dynamics is corrected by introducing a kernel smoothing algorithm. An optimal tuning rule

for the kernel smoothing parameter is presented under an on-line optimization framework. The usual degeneracy issues with sequential-importance-resampling filter under different process to measurement noise ratios are avoided through the kernel smoothing process based on Kullback-Leibler divergence. The proposed algorithm is an 'optimization-free' estimator, which makes it efficient and computationally fast, which is a major advantage over the traditional maximum-likelihood based methods. Finally, the performance of the proposed method was demonstrated on two non-linear simulation examples.

Bibliography

Achilias, D.S. and C. Kiparissides (1992). Development of a general mathematical framework for modeling diffusion controlled free-radical polymerization reactions. *Macromolecules* **25**(14), 3739–3750.

Andrieu, C., A. Doucet and V.B. Tadic (2005). Online parameter estimation in general state-space models. In: *Proceedings of the 44th IEEE Conference on Decision and Control and European Control Conference*. Seville, Spain. pp. 332–337.

Andrieu, C., A. Doucet, S.S. Singh and V.B. Tadic (2004). Particle methods for change detection, system identification, and control. *Proceedings of the IEEE* **92**(3), 423–438.

Andrieu, C., N. de Freitas and A. Doucet (1999). Sequential MCMC for Bayesian model selection. In: *Proceedings of the IEEE Signal Processing Workshop on Higher-Order Statistics*. Ceasarea, Israel. pp. 130–134.

Arulampalam, M.S., S. Maskell, N. Gordon and T. Clapp (2002). A tutorial on particle filters for online non-linear/non-Gaussian Bayesian tracking. *IEEE Transactions on Signal Processing* **50**(2), 174–188.

Bavdekar, V.A., A.P. Deshpande and S.C. Patwardhan (2011). Identification of process and measurement noise covariance for state and parameter estimation using extended Kalman filter. *Journal of Process Control* **21**(4), 585–601.

Cappé, O. (2009). Online sequential Monte Carlo EM algorithm. In: *Proceedings of the 15th IEEE Workshop on Statistical Signal Processing*. Cardiff, U.K.. pp. 37–40.

Cappé, O. (2011). Online EM algorithm for hidden Markov models. *Journal of Computational and Graphical Statistics* **20**(3), 728–749.

Chen, T., J. Morris and E. Martin (2005). Particle filters for state and parameter estimation in batch processes. *Journal of Process Control* **15**(6), 665–673.

Chen, Z. (2003). Bayesian filtering: from Kalman filters to particle filters, and beyond. Technical report. Communications Research Laboratory, McMaster University. Hamilton, Canada.

Chitralekha, S.B., J. Prakash, H. Raghavan, R.B. Gopaluni and S.L. Shah (2010). A comparison of simultaneous state and parameter estimation schemes for a continuous fermentor reactor. *Journal of Process Control* **20**(8), 934–943.

Chopin, N. (2002). A sequential particle filter method for static models. *Biometrika* **89**(3), 539–551.

Clapp, T. and S. Godsill (2001). *Sequential Monte Carlo Methods in Practice*. Chap. Improvement strategies for Monte Carlo particle filters. Springer–Verlag, New York.

Cornebise, J., É. Moulines and J. Olsson (2008). Adaptive methods for sequential importance sampling with application to state-space models. *Statistics and Computing* **18**(4), 461–480.

Djuric, P.M. and J. Miguez (2002). Sequential particle filtering in the presence of additive Gaussian noise with unkown parameters. In: *Proceedings of the IEEE International Conference on Acoustics, Speech and Signal Processing*. Orlando, USA. pp. 1621–1624.

Douc, R., A. Garivier, E. Moulines and J. Olsson (2011). Sequential Monte Carlo smoothing for general state-space hidden Markov models. *Annals of Applied Probability* **21**(6), 2109–2145.

Doucet, A. and V.B. Tadic (2003). Parameter estimation in general state-space models using particle methods. *Annals of the Institute of Statistical Mathematics* **55**(2), 409–422.

Doucet, A., N. de Freitas and N.J. Gordon (2001). *Sequential Monte Carlo Methods in Practice*. Chap. An introduction to sequential Monte Carlo methods. Springer–Verlag, New York.

Doucet, A., S. Godsill and C. Andrieu (2000). On Sequential Monte Carlo Sampling Methods for Bayesian Filtering. *Statistics and Computing* **10**(3), 197–208.

Elliott, R.J., J.J. Ford and J.B. Moore (2002). On-line almost-sure parameter estimation for partially observed discrete-time linear systems with known noise characteristics. *International Journal of Adaptive Control and Signal Processing* **16**(6), 435–453.

Evensen, G. (2007). *Data Assimilation: The Ensemble Kalman Filter*. Chap. Estimation in an oil reservoir simulator. Springer, Berlin/Heidelberg.

Fearnhead, P. (2008). Computational methods for complex stochastic systems: A review of some alternatives to MCMC. *Statistics and Computing* **18**(2), 151–171.

Fearnhead, P. and Z. Liu (2007). On-line inference for multiple change points problems. *Journal of the Royal Statistical Society: Series B* **69**(4), 589–605.

Gamerman, D. (1998). Markov chain Monte Carlo for dynamic generalized models. *Biometrika* **85**(1), 215–227.

Gilks, W.R. and C. Berzuini (2001). Following a moving target–Monte Carlo inference for dynamic Bayesian models. *Journal of the Royal Statistical Society: Series B* **63**(1), 127–146.

Goodwin, G.C. and J.C. Agüero (2005). Approximate EM algorithms for parameter and state estimation in non-linear stochastic models. In: *Proceedings of the 44th IEEE Conference on Decision and Control*. Seville, Spain. pp. 368–373.

Gopaluni, R.B. (2008). A particle filter approach to identification of non-linear processes under missing observations. *The Canadian Journal of Chemical Engineering* **86**(6), 1081–1092.

Gudi, R.D., S.L. Shah and M.R. Gray (1995). Adaptive multirate state and parameter estimation strategies with application to a bioreactor. *AIChE Journal* **41**(11), 2451–2464.

Gustafsson, F. and T.B. Schön (2003). Particle filters for system identification of state-space models linear in either parameters or states. In: *Proceedings of the 13th IFAC Symposium on System Identification*. Rotterdam, The Netherlands. pp. 1287–1292.

Higuchi, T. (2001). *Sequential Monte Carlo Methods in Practice*. Chap. Self organizing time series model. Springer–Verlag, New York.

Johansen, A.M. and A. Doucet (2008). A note on the auxiliary particle filter. *Statistics and Probability Letters* **78**(12), 1498–1504.

Kantas, N., A. Doucet, S.S. Singh and J. Maciejowski (2009). An overview of sequential Monte Carlo methods for parameter estimation in general state-space models. In: *Proceedings of the 15th IFAC Symposium on System Identification*. Saint-Malo, France. pp. 774–785.

Kitagawa, G. (1996). Monte Carlo filter and smoother for non-Gaussian non-linear state-space models. *Journal of Computational and Graphical Statistics* **5**(1), 1–25.

Kitagawa, G. (1998). Self organizing state–space models. *Journal of the American Statistical Association* **93**(443), 1203–1215.

Koopman, S. and N. Shepard (1992). Exact score for time series models in state-space form. *Biometrika* **79**(4), 823–826.

Lee, D.S. and N.K.K. Chia (2002). A particle algorithm for sequential Bayesian parameter estimation and model selection. *IEEE Transactions on Signal Processing* **50**(2), 326–336.

Liu, J. and M. West (2001). *Sequential Monte Carlo Methods in Practice*. Chap. Combined parameter and state estimation in simulation–based filtering. Springer–Verlag, New York.

Liu, J.S. and R. Chen (1998). Sequential Monte Carlo methods for dynamics systems. *Journal of the American Statistical Association* **93**(443), 1032–1044.

Lystig, T.C. and J.P. Hughes (2002). Exact computation of the observed information matrix for hidden Markov models. *Journal of Computational and Graphical Statistics* **11**(3), 678–689.

Moral, P. Del, A. Doucet and S.S. Singh (2009). Forward smoothing using sequential Monte Carlo. Technical report. Department of Engineering, Cambridge University. Cambridge, U.K.

Ninness, B. (2000). Strong laws of large numbers under weak assumptions with application. *IEEE Transactions on Automatic Control* **45**(11), 2117–2122.

Oudjane, N. and C. Musso (2000). Progressive correction for regularized particle filters. In: *Proceedings of the 3rd International Conference on Information Fusion*. Paris, France. pp. 10–17.

Pitt, M. and N. Shephard (1999). Filtering via simulation: Auxillary particle filters. *Journal of the American Statistical Association* **94**(446), 550–599.

Poyiadjis, G., A. Doucet and S.S. Singh (2005). Maximum likelihood parameter estimation in general state-space models using particle methods. In: *Proceedings of the American Statistical Association*. Minneapolis, USA.

Poyiadjis, G., A. Doucet and S.S. Singh (2011). Particle approximations of the score and observed information matrix in state-space models with application to parameter estimation. *Biometrika* **98**(1), 65–80.

Rawlings, J.B. and R.B. Bakshi (2006). Particle filtering and moving horizon estimation. *Computers and Chemical Engineering* **30**(10–12), 1529–1541.

Ristic, B., S. Arulampalam and N. Gordon (2004). *Beyond the Kalman Filter: Particle Filters for Tracking Applications*. Chap. A tutorial on particle filters. Artech House, Boston.

Rydén, T. (1997). On recursive estimation for hidden Markov models. *Stochastic Processes and their Applications* **66**(1), 79–96.

Schön, T.B., A. Wills and B. Ninness (2011). System identification of non-linear state-space models. *Automatica* **47**(1), 39–49.

Shumway, R.H. and D.S. Stoffer (2000). *Time Series Analysis and its Applications*. Springer, New York.

Soroush, M. (1998). State and parameter estimations and their applications in process control. *Computers and Chemical Engineering* **23**(2), 229–245.

Storvic, G. (2002). Particle filters in state-space models with the presence of unknown static parameters. *IEEE Transactions on Signal Processing* **50**(2), 281–289.

Straka, O. and M. Šimandl (2006). Particle filter adaptation based on efficient sample size. In: *Proceedings of the 14th IFAC Symposium on System Identication*. Newcastle, Australia. pp. 991–996.

Tichavský, P., C. Muravchik and A. Nehorai (1998). Posterior Cramér-Rao bounds for discrete-time non-linear filtering. *IEEE Transactions on Signal Processing* **46**(5), 1386–1396.

Trees, H.L. Van (1968). *Detection, Estimation and Modulation Theory Part I*. Wiley, New York.

Tulsyan, A., B. Huang, R.B. Gopaluni and J.F. Forbes (2013). Bayesian identification of non-linear state-space models: Part II- Error analysis. In: *Proceedings of the 10th International Symposium on Dynamics and Control of Chemical Processes*. Mumbai, India.

West, M. (1993). Mixture models, Monte Carlo, Bayesian updating and dynamic models. *Computing Science and Statistics* **24**, 325–333.

Yildirim, S., S.S. Singh and A. Doucet (2012). An online Expectation-Maximization algorithm for changepoint models. *Journal of Computational and Graphical Statistics, In press*.

Chapter 3

Minimum mean square error non-linear target tracking strategy in presence of unknown static parameters

Non-linear filters of different approximations and capabilities allow for real-time target tracking in non-linear systems. We propose a posterior Cramér-Rao lower bound (PCRLB) inequality based measure to simultaneously assess the tracking performance of different non-linear filters. Using the developed measure, average-optimal and optimal minimum mean square error (MMSE) tracking strategies are proposed for target tracking in non-linear state-space models (SSMs) with non-Gaussian noise and unknown target parameters. A systematic procedure to monitor the quality of the target estimates obtained with the proposed tracking strategies is also developed. The practical utility and efficacy of the developed PCRLB based tools are illustrated on a ballistic target tracking problem at re-entry phase with unknown ballistic coefficient.

3.1 Introduction and problem formulation

Recent advances in high-speed computing technology have enabled the aerospace industry to use complex, high-fidelity non-linear stochastic models for their targets. The

---

This chapter is to be submitted as Tulsyan, A., S.R. Khare, B. Huang, R.B. Gopaluni and J.F. Forbes (2013). Minimum mean square error non-linear target tracking strategy in presence of unknown static parameters, for journal publication.

implementation of advanced control and monitoring strategies using such complex target models require real-time data processing for tracking key target states and parameters, which are either unmeasured or unknown. Here, we consider the problem of target tracking in non-linear SSM, with non-Gaussian noise and in presence of unknown target parameters.

Let $\{X_t\}_{t\in\mathbb{N}}$ and $\{Y_t\}_{t\in\mathbb{N}}$ be $\mathcal{X}(\subseteq \mathbb{R}^n)$ and $\mathcal{Y}(\subseteq \mathbb{R}^m)$ valued stochastic processes defined on a measurable space $(\Omega, \mathcal{F})$. The discrete-time state process $\{X_t\}_{t\in\mathbb{N}}$ is an unobserved Markov process with initial density $p_\theta(x)$ and Markovian transition density $p_\theta(x'|x)$:

$$X_0 \sim p_\theta(\cdot) \quad \text{and} \quad X_{t+1}|(X_t = x_t) \sim p_\theta(\cdot|x_t) \quad (t \in \mathbb{N}). \tag{3.1}$$

The state process $\{X_t\}_{t\in\mathbb{N}}$ is hidden, but observed through a sensor process $\{Y_t\}_{t\in\mathbb{N}}$. It is assumed that the process $\{Y_t\}_{t\in\mathbb{N}}$ is conditionally independent given $\{X_t\}_{t\in\mathbb{N}}$, with marginal density $p_\theta(y|x)$:

$$Y_t|(X_0,\ldots,X_t = x_t,\ldots,X_T) \sim p_\theta(\cdot|x_t) \quad (t \in \mathbb{N}). \tag{3.2}$$

θ in (3.1) and (3.2) is a vector of target parameters, such that $\theta \in \Theta$ is an open subset of $\mathbb{R}^r$. All the densities are with respect to suitable dominating measures, such as Lebesgue measure. Although (3.1) and (3.2) represent a wide class of non-linear time-series models, the model form and the assumptions considered in this chapter are given below:

Model 3.1.1. *Stochastic non-linear and non-Gaussian SSM*

$$X_{t+1} = f_t(X_t, \theta_t, V_t); \tag{3.3a}$$

$$\theta_{t+1} = \theta_t; \tag{3.3b}$$

$$Y_t = g_t(X_t, \theta_t, W_t), \tag{3.3c}$$

where $\{\theta_t\}_{t\in\mathbb{N}} = \theta$ in Model 3.1.1 is a vector of static target parameters.

Assumption 3.1.2. *$\{V_t\}_{t\in\mathbb{N}}$, $\{W_t\}_{t\in\mathbb{N}}$ are mutually independent sequences of independent random variables known a priori in their distribution classes (e.g., Gaussian; Rayleigh) and parametrized by a known and finite number of moments (e.g., mean; variance).*

Assumption 3.1.3. *$\{f_t; g_t\}_{t \in \mathbb{N}}$ is a pair of non-linear functions, such that in $\mathcal{X}$ and Θ, $\{f_t; g_t\}_{t \in \mathbb{N}}$ is $\mathcal{C}^k(\mathcal{X})$ and $\mathcal{C}^k(\Theta)$, and in $\mathbb{R}^n$ and $\mathbb{R}^m$, $\{f_t\}_{t \in \mathbb{N}}$ is $\mathcal{C}^{k-1}(\mathbb{R}^n)$ and $\{g_t\}_{t \in \mathbb{N}}$ is $\mathcal{C}^{k-1}(\mathbb{R}^m)$, where $k \geq 2$.*

Assumption 3.1.4. *For a random realization $(x_{t+1}, x_t, \theta_t, v_t) \in \mathcal{X} \times \mathcal{X} \times \Theta \times \mathbb{R}^n$ and $(y_t, x_t, \theta_t, w_t) \in \mathcal{Y} \times \mathcal{X} \times \Theta \times \mathbb{R}^m$ satisfying (3.3a) and (3.3c), respectively, $\nabla_{v_t} f_t^T(x_t, \theta_t, v_t)$ and $\nabla_{w_t} g_t^T(x_t, \theta_t, w_t)$ have rank n and m, such that using implicit function theorem, $p_\theta(x_{t+1}|x_t) = p(V_t = \tilde{f}_t(x_t, \theta_t, x_{t+1}))$ and $p_\theta(y_t|x_t) = p(W_t = \tilde{g}_t(x_t, \theta_t, y_t))$ are defined and do not involve Dirac delta functions.*

Assumption 3.1.5. *The sensor measurement $\{Y_t\}_{t \in \mathbb{N}}$ is target-oriented with probability of false alarm $\mathrm{Pr}_f = 0$ and that of detection $\mathrm{Pr}_d = 1$.*

For any generic sequence $\{u_t\}_{t \in \mathbb{N}}$, let $u_{i:j} \triangleq \{u_i, u_{i+1}, \ldots, u_j\}$. Our aim is to perform Bayesian inference in Model 3.1.1, conditional on measurement sequence $\{Y_{1:t}\}_{t \in \mathbb{N}}$. When $\{\theta_t\}_{t \in \mathbb{N}} = \theta$ is known, Bayesian inference on process $\{X_t\}_{t \in \mathbb{N}}$ relies on the posterior density $\{p_\theta(x_t|Y_{1:t})\}_{t \in \mathbb{N}}$. A recursive method to compute $\{p_\theta(x_t|Y_{1:t})\}_{t \in \mathbb{N}}$ is given by the optimal state tracking equations (Andrieu *et al.*, 2004). When Model 3.1.1 is linear, Gaussian SSM or when $\mathcal{X}$ is a finite set, $\{p_\theta(x_t|Y_{1:t})\}_{t \in \mathbb{N}}$ can be solved in closed form. Unfortunately, in many tracking applications $\theta \in \Theta$ is often unknown, and its estimation is required before the target states can be tracked. In practical settings, on-line tracking of θ is often the only realistic solution, since it avoids processing of large dataset, and allows for adaptation to change in target dynamics.

Joint target state and parameter tracking in Model 3.1.1 is an active area of research (Minvielle *et al.*, 2010). Let $\theta^\star$ be the true, but unknown target parameter vector generating $\{Y_{1:t}\}_{t \in \mathbb{N}}$, such that $X_{t+1}|(X_t = x_t) \sim p_{\theta^\star}(\cdot|x_t)$ and $Y_t|(X_t = x_t) \sim p_{\theta^\star}(\cdot|x_t)$, then in Bayesian settings, the joint target state and parameter tracking problem is formulated by first ascribing an initial prior density $\theta_0 \sim p(\theta_0)$, such that $\theta^\star \in \mathrm{supp}\, p(\theta_0)$, and then computing $\{p(z_t|Y_{1:t})\}_{t \in \mathbb{N}}$, where: $Z_t \triangleq \{X_t; \theta_t\}$ is a

$\mathcal{Z}(\subseteq \mathbb{R}^{s=n+r})$ valued extended Markov process with $(Z_0 = z_0) \sim p_{\theta_0}(x_0)p(\theta_0)$ and $Z_t|(Z_{t-1} = z_{t-1}) \sim p_{\theta_{t-1}}(\cdot|x_{t-1})\delta_{\theta_{t-1}}(\cdot)$. The Bayesian inference on $\{Z_t\}_{t \in \mathbb{N}}$ then relies on the joint posterior density $\{p(z_t|Y_{1:t})\}_{t \in \mathbb{N}}$, which provides a real-time inference on the target states and parameters. Although apparently similar to the target state tracking problem, joint target state and parameter tracking has proved to be a non-trivial problem (Kantas *et al.*, 2009; Minvielle *et al.*, 2010). No analytical solution to $\{p(z_t|Y_{1:t})\}_{t \in \mathbb{N}}$ is available, even for linear and Gaussian SSM, or when $\mathcal{X}$ is a finite set. In other words, an optimal filter, which solves $\{p(z_t|Y_{1:t})\}_{t \in \mathbb{N}}$ in closed form is not realizable for Model 3.1.1.

Over the years many non-linear tracking methods have developed to approximate the joint density $\{p(z_t|Y_{1:t})\}_{t \in \mathbb{N}}$. Although tractable, the quality of the target state and parameter estimates obtained with these filters depend on the underlying numerical and statistical approximation techniques used in their design. An exposition of these methods and related approximations can be found in (Kantas *et al.*, 2009; Minvielle *et al.*, 2010).

A recent surge of interest in developing methods to approximate $\{p(z_t|Y_{1:t})\}_{t \in \mathbb{N}}$ for Model 3.1.1 has left researchers and practitioners inundated with a large number of filters to choose from. Unfortunately, there is no single filter that is guaranteed to provide best tracking performance on a given system (Minvielle *et al.*, 2010). Moreover, it is not even possible to choose a filter that retains high tracking performance under all target conditions. A practitioner is thus left with no clear substitute for the optimal non-linear filter.

Optimal selection of a target tracking strategy in presence of unknown target parameters is still an open problem. An approach to resolve this dilemma is to start with a family of non-linear tracking filters and switch between them as and when required, so as to maintain high tracking performance. Naturally, this approach has to depend on a performance measure, which accounts for the uncertainty in unknown target parameters, and is also independent of the tracking method or any target specific conditions. Despite the strong practical interest in evaluating the performance of non-linear filters, it remains one of the

most complex problems in Bayesian inference theory (Šimandl *et al.*, 2001).

In this chapter, we propose: (i) a PCRLB based performance measure for assessment of different tracking filters; (ii) average-optimal and optimal MMSE target tracking strategies for Model 3.1.1 in presence of unknown target parameters; and (iii) a systematic approach to monitor the quality of the target estimates obtained with the proposed tracking strategies. Initial results reported in (Tulsyan *et al.*, 2013*c*) use PCRLB inequality for assessment of tracking filters under known target parameters case. The focus of this chapter is to generalize the results in (Tulsyan *et al.*, 2013*c*) for tracking in SSMs with unknown target parameters.

Notation: $\mathbb{N} := \{1, 2, \dots\}$; $\mathbb{R}_+ := [0, \infty)$; $\mathbb{R}^{s \times s}$ is the set of real valued $s \times s$ matrices; $\mathcal{S}^s \subset \mathbb{R}^{s \times s}$ is the space of symmetric matrices; $I_{s \times s}$ is the identity matrix; $\mathcal{S}^s_+$ is the cone of symmetric positive semi-definite matrices in $\mathcal{S}^s$; and $\mathcal{S}^s_{++}$ is its interior, i.e., the positive definite matrices. The partial order on $\mathcal{S}^s$ induced by $\mathcal{S}^s_+$ and $\mathcal{S}^s_{++}$ are denoted by $\succcurlyeq$ and $\succ$, respectively. Let $A = A(i, j)$, $B = B(i, j)$ be two matrices in $\mathbb{R}^{s \times s}$ then Hadamard product of A and B is denoted by $A \circ B = A(i, j)B(i, j)$, where $1 \leq i, j \leq s$; and A has a Hadamard inverse, denoted by $A^{\circ-1} = 1/A(i, j)$, where $1 \leq i, j \leq s$, if and only if $A(i, j) \neq 0$ for all $1 \leq i, j \leq s$. $\text{Tr}[A]$ represents trace of A. Let $v \in \mathbb{R}^s$ be a column vector then $v(i)$ indicates ith-entry of v and $\text{diag}(v) \in \mathbb{R}^{s \times s}$ is a diagonal matrix with elements in $v \in \mathbb{R}^s$ as its diagonal entries. $|\cdot|$ is the absolute value. $\wedge$ and $\vee$ are logical conjunction and disjunction operators. Also, $\Delta^y_x \triangleq \nabla_x \nabla^T_y$ is the Laplacian and $\nabla_x \triangleq \left[\frac{\partial}{\partial x}\right]$ is the gradient.

3.2   Main results

3.2.1   Assessment of tracking filters in presence of unknown parameters

The conventional Cramér-Rao lower bound (CRLB) provides a lower bound on the MSE of any maximum-likelihood (ML) based estimator. An analogous extension of the CRLB to

the class of Bayesian estimators is called the PCRLB inequality. Extension of the PCRLB inequality to discrete-time, non-linear tracking in presence of unknown target parameters was provided by (Tichavský *et al.*, 1998), and is given next.

Lemma 3.2.1. *Let $\{Y_{1:t}\}_{t \in \mathbb{N}}$ be a measurement sequence generated from Model 3.1.1 under Assumption 3.1.5, then MSE of any tracking filter at $t \in \mathbb{N}$ is bounded from below by the following matrix inequality*

$$P_{t|t} \triangleq \mathbb{E}_{p(Z_t, Y_{1:t})}[(Z_t - \widehat{Z}_{t|t})(Z_t - \widehat{Z}_{t|t})^T] \succcurlyeq J_t^{-1} \quad (t \in \mathbb{N}), \tag{3.4}$$

where: $P_{t|t} \in \mathcal{S}_{++}^s$ is the MSE; $\widehat{Z}_{t|t} \triangleq \widehat{Z}_t(Y_{1:t}) := \mathbb{R}^{tm} \to \mathbb{R}^s$ is the target estimate; $J_t \in \mathcal{S}_{++}^s$ is the posterior Fisher information matrix (PFIM); and $J_t^{-1} \in \mathcal{S}_{++}^s$ is the PCRLB for Model 3.1.1.

Proof. See (Tichavský *et al.*, 1998) for the complete proof. □

Lemma 3.2.1 guarantees $P_{t|t} - J_t^{-1} \in \mathcal{S}_+^s$. A recursive approach to compute PFIM for Model 3.1.1 was derived by (Tichavský *et al.*, 1998), and is given next.

Lemma 3.2.2. *A recursive approach to compute the PFIM for Model 3.1.1 under Assumptions 3.1.2 through 3.1.5 is given as follows:*

$$J_{t+1}^{11} = H_t^{33} - (H_t^{13})^T [J_t^{11} + H_t^{11}]^{-1} H_t^{13}; \tag{3.5a}$$

$$J_{t+1}^{12} = (H_t^{23})^T - (H_t^{13})^T [J_t^{11} + H_t^{11}]^{-1} (J_t^{12} + H_t^{12}); \tag{3.5b}$$

$$J_{t+1}^{22} = J_t^{22} + H_t^{22} - (J_t^{12} + H_t^{12})^T [J_t^{11} + H_t^{11}]^{-1} (J_t^{12} + H_t^{12}), \tag{3.5c}$$

where:

$$J_{t+1} = \begin{bmatrix} J_{t+1}^{11} & J_{t+1}^{12} \\ (J_{t+1}^{12})^T & J_{t+1}^{22} \end{bmatrix}; \qquad (s \times s) \qquad (3.6a)$$

$$H_t^{11} = \mathbb{E}_{p(X_{0:t+1}, \theta_t, Y_{1:t+1})}[-\Delta_{X_t}^{X_t} \log p_t]; \qquad (n \times n) \qquad (3.6b)$$

$$H_t^{12} = \mathbb{E}_{p(X_{0:t+1}, \theta_t, Y_{1:t+1})}[-\Delta_{X_t}^{\theta_t} \log p_t]; \qquad (n \times r) \qquad (3.6c)$$

$$H_t^{13} = \mathbb{E}_{p(X_{0:t+1}, \theta_t, Y_{1:t+1})}[-\Delta_{X_t}^{X_{t+1}} \log p_t]; \qquad (n \times n) \qquad (3.6d)$$

$$H_t^{22} = \mathbb{E}_{p(X_{0:t+1}, \theta_t, Y_{1:t+1})}[-\Delta_{\theta_t}^{\theta_t} \log p_t]; \qquad (r \times r) \qquad (3.6e)$$

$$H_t^{23} = \mathbb{E}_{p(X_{0:t+1}, \theta_t, Y_{1:t+1})}[-\Delta_{\theta_t}^{X_{t+1}} \log p_t]; \qquad (r \times n) \qquad (3.6f)$$

$$H_t^{33} = \mathbb{E}_{p(X_{0:t+1}, \theta_t, Y_{1:t+1})}[-\Delta_{X_{t+1}}^{X_{t+1}} \log p_t]; \qquad (n \times n) \qquad (3.6g)$$

and $p_t = p(X_{t+1}|Z_t)p(Y_{t+1}|\theta_t, X_{t+1})$. The PFIM at $t = 0$ can be computed using the relation $J_0 = \mathbb{E}_{p(Z_0)}[-\Delta_{Z_0}^{Z_0} \log p(Z_0)]$.

Proof. See (Tichavský *et al.*, 1998; Šimandl *et al.*, 2001) for the detailed proof. $\square$

$J_{t+1}^{11} \in \mathcal{S}_{++}^n$ and $J_{t+1}^{22} \in \mathcal{S}_{++}^r$ in (3.6a) are the PFIMs for the states and parameters, respectively. Here, Assumptions 3.1.2 through 3.1.4 are regulatory conditions to ensure $J_{t+1} \in \mathcal{S}_{++}^s$ or $J_{t+1}^{-1} \in \mathcal{S}_{++}^s$ exists.

Remark 3.2.3. *Expectation with respect to $\{Z_{0:t+1}, Y_{1:t+1}\}$ makes (3.6) independent of $(z_{0:t+1}, y_{1:t+1}) \in \mathcal{Z}^{t+2} \times \mathcal{Y}^{t+1}$. In fact, the PCRLB only depends on: the dynamics in Model 3.1.1; the noise characteristics of $\{V_t\}_{t \in \mathbb{N}}$ and $\{W_t\}_{t \in \mathbb{N}}$; and $Z_0 \sim p(z_0)$. The PCRLB is thus a system property, independent of the non-linear tracking filter used.*

Remark 3.2.4. *An optimal non-linear filter for Model 3.1.1 may not be realisable with finite computing capabilities, the PCRLB can be regarded as its second-order performance limit. Using (3.4), the MSE of a filter can be compared against that of an optimal filter.*

Using the inequality (3.4), a PCRLB based performance measure for simultaneous assessment of multiple non-linear tracking filters is defined next.

Definition 3.2.5. *Let J_t^{-1} be the PCRLB for a system described by Model 3.1.1 and $P_{t|t}$ be the MSE of a filter used for tracking the target states and parameters of Model 3.1.1, such that J_t^{-1} and $P_{t|t}$ satisfy (3.4), then the performance of the filter at $t \in \mathbb{N}$ can be defined as*

$$\Phi_t = J_t^{-1} \circ P_{t|t}^{\circ -1}, \tag{3.7}$$

where: Φ_t is the performance measure; $P_{t|t}^{\circ -1}$ is the Hadamard inverse of $P_{t|t}$; and $J_t^{-1} \circ P_{t|t}^{\circ -1}$ is the Hadamard product of J_t^{-1} and $P_{t|t}^{\circ -1}$.

Theorem 3.2.6. *Let $J_t^{-1} \in \mathcal{S}_{++}^s$ and $P_{t|t} \in \mathcal{S}_{++}^s$ be such that they satisfy the PCRLB inequality (3.4), then Φ_t in Definition 3.2.5 at $t \in \mathbb{N}$ satisfies $0 < \Phi_t(i,i) \leq 1$ for all $1 \leq i \leq s$ and is such that: (a) $\Phi_t \in \mathcal{S}^s$ if $P_{t|t}^{\circ -1} \in \mathcal{S}^s$; and (b) $\Phi_t \in \mathcal{S}_{++}^s$, if $P_{t|t}^{\circ -1} \in \mathcal{S}_{++}^s$.*

Proof. Note that since $P_{t|t}(i,i) > 0$ and $J_t^{-1}(i,i) > 0$, we have $\Phi_t(i,i) = J_t^{-1}(i,i)[P_{t|t}(i,i)]^{-1} > 0$ for all $1 \leq i \leq s$. Also, since J_t^{-1} and $P_{t|t}$ satisfy (3.4), we have $P_{t|t}(i,i) \geq J_t^{-1}(i,i)$, which implies $\Phi_t(i,i) = J_t^{-1}(i,i)[P_{t|t}(i,i)]^{-1} \leq 1$ for all $1 \leq i \leq s$. Combining the two yields, $0 < \Phi_t(i,i) \leq 1$ for all $1 \leq i \leq s$, which completes the first part of the proof. Now for part (a) $P_{t|t} \in \mathcal{S}_{++}^s$ implies $P_{t|t}^{\circ -1} \in \mathcal{S}^s$, which with $J_t^{-1} \in \mathcal{S}_{++}^s$ implies $\Phi_t = J_t^{-1} \circ P_{t|t}^{\circ -1} \in \mathcal{S}^s$. For part (b), if $P_{t|t} \in \mathcal{S}_{++}^s$ has positive off-diagonal entries and just one positive eigenvalue then from Corollary 2.8 in (Reams, 1999), $P_{t|t}^{\circ -1} \in \mathcal{S}_{++}^s$. From Schur Product Theorem (Bapat and Raghavan, 1997), we have $\Phi_t \in \mathcal{S}_{++}^s$, if and only if $P_{t|t}^{\circ -1} \in \mathcal{S}_{++}^s$, which completes the proof. $\square$

Theorem 3.2.6 shows that the diagonal entries of the measure in Definition 3.2.5 are bounded, with $0 < \Phi_t(i,i) \leq 1$ for all $1 \leq i \leq s$ and $t \in \mathbb{N}$. From Theorem 3.2.6, efficiency of a tracking filter is defined next.

Definition 3.2.7. *A filter is partially efficient if for at least one target state or parameter $1 \leq i \leq s$ at $t \in \mathbb{N}$, $\Phi_t(i,i) = 1$ (i.e., $P_{t|t}(i,i) = J_t^{-1}(i,i)$) and is efficient, if $\mathrm{Tr}[\Phi_t] = s$ (i.e., $\mathrm{Tr}[P_{t|t} - J_t^{-1}] = 0$).*

Remark 3.2.8. *Performance of a tracking filter can also be defined in terms of $\Phi'_t :=$ $J_t^{-1} P_{t|t}^{-1}$, with $\Phi'_t = I_{s \times s}$ indicating efficiency; however, with this definition, partial efficiency of a tracking filter is not easy to define, since it involves inverting the matrix $P_{t|t} \in \mathcal{S}_{++}^s$.*

The choice of the target state and parameter estimate $\widehat{Z}_{t|t} \in \mathbb{R}^s$, for which $\mathrm{Tr}[\Phi_t] \in (0, s]$ at $t \in \mathbb{N}$ is maximized is discussed next.

Remark 3.2.9. *A common method to compute $\widehat{Z}_{t|t} \in \mathbb{R}^s$ is to minimize $\mathrm{Tr}[P_{t|t}] \in \mathbb{R}_+$. The optimal target estimate minimizing $\mathrm{Tr}[P_{t|t}] \in \mathbb{R}_+$ is the MMSE estimate, and is the mean of the joint posterior density $Z_t | Y_{1:t} \sim p(\cdot | Y_{1:t})$, i.e., $\widehat{Z}_{t|t} = Z_{t|t}^\star \triangleq \mathbb{E}_{p(Z_t | Y_{1:t})}[Z_t]$.*

Theorem 3.2.10. *Let $J_t^{-1} \in \mathcal{S}_{++}^s$ and $P_{t|t} \in \mathcal{S}_{++}^s$ be such that it satisfies the inequality (3.4), then the estimate $\widehat{Z}_{t|t} \in \mathbb{R}^s$ obtained by minimizing $\mathrm{Tr}[P_{t|t}] \in \mathbb{R}_+$ also maximizes $\mathrm{Tr}[\Phi_t] \in (0, s]$, such that*

$$\widehat{Z}_{t|t} = \operatorname*{arg\,min}_{\widehat{Z}_{t|t} \in \mathbb{R}^s} \mathrm{Tr}[P_{t|t}] = \operatorname*{arg\,max}_{\widehat{Z}_{t|t} \in \mathbb{R}^s} \mathrm{Tr}[\Phi_t], \tag{3.8}$$

where $\widehat{Z}_{t|t} \in \mathbb{R}^s$ is an MMSE estimate given a sequence $\{Y_{1:t}\}_{t \in \mathbb{N}}$.

Proof. An MMSE estimate $\widehat{Z}_{t|t}$ at $t \in \mathbb{N}$ is obtained by solving the following optimization problem: $\widehat{Z}_{t|t} = \arg\min_{\widehat{Z}_{t|t} \in \mathbb{R}^s} \mathrm{Tr}[P_{t|t}] = \arg\min_{\widehat{Z}_{t|t} \in \mathbb{R}^s} \sum_{i=1}^s [P_{t|t}(i,i) - J_t^{-1}(i,i)] = \arg\min_{\widehat{Z}_{t|t} \in \mathbb{R}^s} \sum_{i=1}^s [\Phi_t(i,i)]^{-1} J_t^{-1}(i,i)$. Here we used the fact that J_t^{-1} is independent of $\widehat{Z}_{t|t}$ (see Lemma 3.2.2). Now note that $[\Phi_t(i,i)]^{-1} J_t^{-1}(i,i) > 0$. This is because $0 < \Phi_t(i,i) \leq 1$ (from Theorem 3.2.6) and $J_t^{-1}(i,i) > 0$ (since $J_t^{-1} \in \mathcal{S}_{++}^s$) for all $1 \leq i \leq s$. Since the terms in the optimization are positive and independent, we can minimize them separately (Trees, 1968), such that $\widehat{Z}_{t|t} = \sum_{i=1}^s \arg\min_{\widehat{Z}_{t|t}(i) \in \mathbb{R}} [\Phi_t(i,i)]^{-1} J_t^{-1}(i,i) = \sum_{i=1}^s \arg\max_{\widehat{Z}_{t|t}(i) \in \mathbb{R}} [\Phi_t(i,i)]$, where $\widehat{Z}_{t|t}(i) \in \mathbb{R}$ is ith-entry in $\widehat{Z}_{t|t} \in \mathbb{R}^s$. Again, since $0 < \Phi_t(i,i) \leq 1$ for all $1 \leq i \leq s$, the optimization can be written as $\widehat{Z}_{t|t} = \arg\max_{\widehat{Z}_{t|t} \in \mathbb{R}^s} \sum_{i=1}^s [\Phi_t(i,i)] = \arg\max_{\widehat{Z}_{t|t} \in \mathbb{R}^s} \mathrm{Tr}[\Phi_t]$, which completes the proof. $\qquad\square$

Algorithm 3 Average-case tracking strategy

Input: Performance measure $\Phi_t^i \in \mathcal{S}^s$ and target estimate $\widehat{Z}_{t|t}^i \in \mathbb{R}^s$ for all the tracking filters in the filter bank $\mathcal{B}$ at $t \in \mathbb{N}$, where $i \in \mathcal{F}$.

Output: Target estimate $\widehat{Z}_{t|t}^o \in \mathbb{R}^s$ to be selected at $t \in \mathbb{N}$.

1: Compute $\mathrm{Tr}[\Phi_t^i]$ for all $i \in \mathcal{F}$.

2: Solve: $\widehat{Z}_{t|t}^o \triangleq \widehat{Z}_{t|t}^i = \arg\max_{i \in \mathcal{F}} \mathrm{Tr}[\Phi_t^i]$.

Algorithm 4 Best-case tracking strategy

Input: Performance measure $\Phi_t^i \in \mathcal{S}^s$ and target estimate $\widehat{Z}_{t|t}^i \in \mathbb{R}^s$ for all the tracking filters in the filter bank $\mathcal{B}$ at $t \in \mathbb{N}$, where $i \in \mathcal{F}$.

Output: Target estimate $\widehat{Z}_{t|t}^o \in \mathbb{R}^s$ to be selected at $t \in \mathbb{N}$.

1: **for** $j = 1$ to s **do**

2:     Solve: $\widehat{Z}_{t|t}^o(j) \triangleq \widehat{Z}_{t|t}^i(j) = \arg\max_{i \in \mathcal{F}}[\Phi_t^i(j, j)]$.

3: **end for**

Theorem 3.2.10 shows that the performance of a tracking filter in terms of the measure in Definition 3.2.5 can be maximized for the choice of an MMSE target state and parameter estimate. Now, since calculating the MMSE estimate requires computation of $\{p(z_t|Y_{1:t})\}_{t \in \mathbb{N}}$, obtaining such an estimate for Model 3.1.1 in closed form is non-trivial.

Remark 3.2.11. *Non-linear filters only provide an approximation to $\{p(z_t|Y_{1:t})\}_{t \in \mathbb{N}}$ thus in practice, the estimate delivered by these filters may not be the MMSE estimate, i.e., $\widehat{Z}_{t|t} \triangleq \mathbb{E}_{\widehat{p}(z_t|Y_{1:t})}[Z_t] \neq Z_{t|t}^\star$ almost surely, where $\widehat{Z}_{t|t}$ is the mean of $Z_t|Y_{1:t} \sim \widehat{p}(\cdot|Y_{1:t})$ and $\widehat{p}(z_t|Y_{1:t})$ is an approximation of $p(z_t|Y_{1:t})$ given by the filter.*

Remark 3.2.12. *Since $\Phi_t \in \mathcal{S}^s$ is a function of $\widehat{Z}_{t|t} \in \mathbb{R}^s$, tracking filters of different approximations and capabilities have different Φ_t matrices. Thus, while comparing different tracking filters, ideally, the best performing filter is the one that is efficient; however, this is rarely achieved in non-linear tracking problems (see Remark 3.2.11).*

Equation (3.7) not only provides a tool to assess the performance of various tracking filters, it can also be used to design the tracking strategy itself. Design of optimal tracking strategy is discussed next.

3.2.2   Optimal tracking strategy in presence of unknown parameters

In this chapter, a filter switching strategy is proposed for target tracking in Model 3.1.1 in presence of unknown target parameters. The strategy is motivated by the fact that there is no one single tracking filter, which is guaranteed to perform well for all tracking systems, and in all target conditions. Let $\mathcal{B}$ be any arbitrarily chosen bank containing $F \in \mathbb{N}$ different tracking filters, such that $\mathcal{F} = \{1, 2, \ldots, F\}$ indicates the filter index in $\mathcal{B}$. In the filter switching strategy, the performance of F tracking filters in $\mathcal{B}$ is first assessed based on (3.7), and then the filter with highest measure is selected for delivering the target state and parameter estimate at $t \in \mathbb{N}$. There are different ways in which the switching strategy can be implemented, as given in Algorithms 3 and 4.

In Algorithm 3, switching is based on the average filter performance in estimating all the states and parameters of Model 3.1.1; however, switching can also be based on the filter performance in estimating individual states and parameters, as given in Algorithm 4.

Theorem 3.2.13. *Let $F \in \mathbb{N}$ be the number of filters in an arbitrarily chosen filter bank $\mathcal{B}$, then with respect to $\mathcal{B}$, the filter switching implemented with Algorithms 3 and 4 gives average-optimal and optimal MMSE tracking strategies for Model 3.1.1, respectively.*

Proof. The very construction of Algorithms 3 and 4 based on (3.7), makes them average-optimal and optimal MMSE target tracking strategies, with respect to the filter bank $\mathcal{B}$.   □

Theorem 3.2.14. *Let $F \in \mathbb{N}$ be the number of tracking filters in an arbitrarily chosen bank $\mathcal{B}$ and $s \in \mathbb{N}$ be the number of target states and parameters in Model 3.1.1. If the average-case computational complexity of Algorithms 3 and 4 is N_1 and N_2, respectively, then:*

(a) $N_1 = F(s - 1) + F \log_2 F$ and $N_2 = Fs \log_2 F$.

(b) N_1 and N_2 satisfy the following conditions

$$\begin{cases} N_1 = N_2 & \text{if } s = 1 \vee F = 2; \\ N_1 > N_2 & \text{if } s \geq 2 \wedge F = 1; \\ N_1 < N_2 & \text{otherwise.} \end{cases}$$

Proof. (a) Computing $\text{Tr}[\Phi_t^i]$ for all $1 \leq i \leq F$ in Step 1 of Algorithm 3 requires $F(s-1)$ computations, while sorting an F dimensional vector in Step 2 with quicksort requires $F \log_2 F$ computations (Knuth, 1973). Thus Algorithm 3 has an average-case computational complexity $N_1 = F(s-1) + F \log_2 F$. Similarly, Algorithm 4 only requires to sort an F dimensional vector, s times; thus it has a complexity $N_2 = Fs \log_2 F$. (b) Note that N_1 can be written as $N_1 = F(s-1) - F(s-1) \log_2 F + Fs \log_2 F$, which can be further simplified to $N_1 = F(s-1)[1 - \log_2 F] + N_2$. Now from this it clear that $N_1 = N_2$, if $s = 1 \vee F = 2$. Now, for $s \geq 2 \wedge F = 1$, $[1 - \log_2 F] > 0$, which implies $N_1 > N_2$, and for all other values of F and s, $F(s-1)[1 - \log_2 F] < 0$, which implies $N_1 < N_2$. $\square$

Remark 3.2.15. *Theorems 3.2.13 and 3.2.14 suggest that although Algorithm 3 has less average-case computational complexity than Algorithm 4, it only computes the average-optimal target estimates, in contrast to the optimal target estimates obtained with Algorithm 4. This result will further be illustrated in the simulation section (see Section 3.4).*

Remark 3.2.16. *If only state tracking in Model 3.1.1 is of interest then the switching strategy can be implemented by replacing Step 2 of Algorithm 3 with $\widehat{X}_{t|t}^o \triangleq \widehat{X}_{t|t}^i = \arg\max_{i \in \mathcal{F}} \text{Tr}[\Omega_t^i]$, or that of Algorithm 4 with $\widehat{X}_{t|t}^o(j) \triangleq \widehat{X}_{t|t}^i(j) = \arg\max_{i \in \mathcal{F}}[\Omega_t^i(j,j)]$ for all $1 \leq j \leq n$. Here $\Omega_t^i \in \mathcal{S}^n$ is the top-left sub-matrix of $\Phi_t^i \in \mathcal{S}^s$ and $\widehat{X}_{t|t}^o$ is the target state estimate selected at $t \in \mathbb{N}$. The average-case computational complexity of implementing this algorithm is $F(n-1) + F \log_2 F$ or $Fn \log_2 F$ (see Theorem 3.2.14).*

Remark 3.2.17. *If only parameter tracking in Model 3.1.1 is of interest then the switching strategy can be implemented by replacing Step 2 of Algorithm 3 with $\widehat{\theta}_{t|t}^o \triangleq \widehat{\theta}_{t|t}^i = \arg\max_{i \in \mathcal{F}} \text{Tr}[\Psi_t^i]$, or that of Algorithm 4 with $\widehat{\theta}_{t|t}^o(j) \triangleq \widehat{\theta}_{t|t}^i(j) = \arg\max_{i \in \mathcal{F}}[\Psi_t^i(j,j)]$*

for all $1 \leq j \leq r$. Here $\Psi_t^i \in \mathcal{S}^r$ is the bottom-right sub-matrix of $\Phi_t^i \in \mathcal{S}^s$ and $\widehat{\theta}_{t|t}^o$ is the target parameter estimate selected at $t \in \mathbb{N}$. The average-case computational complexity of this algorithm is $F(r-1) + F \log_2 F$ or $Fr \log_2 F$ (see Theorem 3.2.14).

Algorithms 3 and 4 only provide a tracking strategy for Model 3.1.1. Monitoring the quality of the target state and parameter estimates obtained with these strategies is critical, and is discussed next.

3.2.3   Quality monitoring of target state and parameter estimates

The second-order estimation error associated with any tracking strategy is completely characterized by its MSE. Thus monitoring the quality of the target state and parameter estimates obtained with a tracking strategy requires clear analysis of the MSE. Decomposition of the MSE into its sources of errors is given in the next theorem.

Theorem 3.2.18. *Let $Z_{t|t}^\star \in \mathbb{R}^s$ and $V_{t|t}^\star \in \mathcal{S}_{++}^s$ be the mean and covariance of $Z_t | Y_{1:t} \sim p(\cdot | Y_{1:t})$ and $\widehat{Z}_{t|t}^o \in \mathbb{R}^s$ be the mean of $Z_t | Y_{1:t} \sim \widehat{p}(\cdot | Y_{1:t})$ as computed by Algorithm 3, then for $\widehat{Z}_{t|t}^o \neq Z_{t|t}^\star$ almost surely, $P_{t|t}$ at $t \in \mathbb{N}$ can be written as follows:*

$$P_{t|t} = \mathbb{E}_{p(Y_{1:t})}[V_{t|t}^\star] + \mathbb{E}_{p(Y_{1:t})}[B_{t|t}^\star [B_{t|t}^\star]^T], \tag{3.9}$$

where $B_{t|t}^\star \triangleq [Z_{t|t}^\star - \widehat{Z}_{t|t}^o] \in \mathbb{R}^s$ is the conditional bias in estimating the mean of the posterior density $Z_t | Y_{1:t} \sim p(\cdot | Y_{1:t})$ at $t \in \mathbb{N}$.

Proof. Using $p(Z_t, Y_{1:t}) = p(Y_{1:t}) p(Z_t | Y_{1:t})$, the MSE can be written as: $P_{t|t} = \mathbb{E}_{p(Y_{1:t})} \mathbb{E}_{p(Z_t | Y_{1:t})}[(Z_t - \widehat{Z}_{t|t}^o)(Z_t - \widehat{Z}_{t|t}^o)^T]$. Adding and subtracting $Z_{t|t}^\star$ in $P_{t|t}$, followed by algebraic manipulations yield $P_{t|t} = \mathbb{E}_{p(Y_{1:t})} \mathbb{E}_{p(Z_t | Y_{1:t})}[K_{t|t}^\star + L_{t|t}^\star + [L_{t|t}^\star]^T + B_{t|t}^\star [B_{t|t}^\star]^T]$, where $K_{t|t}^\star = [Z_t - Z_{t|t}^\star][Z_t - Z_{t|t}^\star]^T$; $L_{t|t}^\star = [Z_t - Z_{t|t}^\star][Z_{t|t}^\star - \widehat{Z}_{t|t}^o]^T$. Now $\mathbb{E}_{p(Z_t | Y_{1:t})}[K_{t|t}^\star] = V_{t|t}^\star$; $\mathbb{E}_{p(Z_t | Y_{1:t})}[L_{t|t}^\star] = 0$, since $\mathbb{E}_{p(Z_t | Y_{1:t})}[Z_t - Z_{t|t}^\star] = 0$; and $\mathbb{E}_{p(Z_t | Y_{1:t})}[B_{t|t}^\star][B_{t|t}^\star]^T = [B_{t|t}^\star][B_{t|t}^\star]^T$, since $[B_{t|t}^\star][B_{t|t}^\star]^T$ is independent of $Z_t | Y_{1:t}$. Substituting the results into $P_{t|t}$ yields (3.9), which completes the proof. $\square$

Note that Theorem 3.2.18 is the Bayesian equivalent of the classical MSE decomposition results available for the likelihood based estimators (Trees, 1968). Using Theorem 3.2.18, bias in the target estimates is defined next.

Definition 3.2.19. *The target estimate at $t \in \mathbb{N}$ is unconditionally unbiased if $\mathbb{E}_{p(Y_{1:t})}[B_{t|t}^\star] = 0$, and conditionally unbiased if $B_{t|t}^\star = 0$ almost surely. The target estimate which is both unconditionally and conditionally unbiased is said to be unbiased in target states and parameters. Bias in the target estimate can be similarly defined.*

The condition under which a tracking strategy yields unbiased target state and parameter estimates is discussed in the next lemma.

Lemma 3.2.20. *Let $\widehat{Z}_{t|t}^o \in \mathbb{R}^s$ be the estimate delivered by Algorithm 3 at $t \in \mathbb{N}$, and let $B_{t|t}^\star \in \mathbb{R}^s$ be the corresponding conditional bias in estimating the mean of $Z_t | Y_{1:t} \sim p(\cdot | Y_{1:t})$, then $B_{t|t}^\star = 0$ almost surely is: (a) a necessary condition for $\mathbb{E}_{p(Y_{1:t})}[B_{t|t}^\star] = 0$; whereas, (b) necessary and sufficient condition for $\mathbb{E}_{p(Y_{1:t})}[B_{t|t}^\star[B_{t|t}^\star]^T] = 0$.*

Proof. (a) is from Theorem 15.2 in (Billingsley, 1995), while the proof of (b) is a straightforward use of Theorem 15.2 in (Billingsley, 1995) in conjunction with the fact that $B_{t|t}^\star \in \mathbb{R}^s$ implies $\mathbb{E}_{p(Y_{1:t})}[B_{t|t}^\star[B_{t|t}^\star]^T] \in \mathcal{S}_+^s$. □

Remark 3.2.21. *Lemma 3.2.20(a) shows that if the estimates are unconditionally unbiased, it does not imply it is unbiased as well, but if it is conditionally unbiased, it implies the estimates are unbiased as well.*

The MSE for an unbiased target estimate is given next.

Corollary 3.2.22. *Let $\widehat{Z}_{t|t}^o \in \mathbb{R}^s$ obtained with Algorithm 3 be unbiased, such that $B_{t|t}^\star = 0$ almost surely, then $P_{t|t} = \mathbb{E}_{p(Y_{1:t})}[V_{t|t}^\star]$. This is obtained using Lemma 3.2.20(b), and substituting $B_{t|t}^\star = 0$ into (3.9).*

Theorem 3.2.23. *Let the filter $i \in \mathcal{F}$ in Algorithm 3 be such that $\widehat{Z}^o_{t|t} \triangleq \widehat{Z}^i_{t|t}$, and let $B^\star_{t|t} \in \mathbb{R}^s$ be the conditional bias in estimating the mean of $Z_t|Y_{1:t} \sim p(\cdot|Y_{1:t})$, then the condition $B^\star_{t|t} = 0$ almost surely ensures that the filter $i \in \mathcal{F}$ is efficient at $t \in \mathbb{N}$.*

Proof. If the estimate $\widehat{Z}^o_{t|t} \triangleq \widehat{Z}^i_{t|t}$ delivered by the filter $i \in \mathcal{F}$ in Algorithm 3 satisfies the condition $B^\star_{t|t} = 0$ almost surely, then from Corollary 3.2.22, its MSE is given by $P_{t|t} = \mathbb{E}_{p(Y_{1:t})}[V^\star_{t|t}]$. Since $P_{t|t}$ only depends on the covariance of $Z_t|Y_{1:t} \sim p(\cdot|Y_{1:t})$, it cannot be reduced any further i.e., $P_{t|t} = J_t^{-1}$. In fact the MSE is independent of the choice of the filter. Thus the filter $i \in \mathcal{F}$ is efficient at $t \in \mathbb{N}$. This completes the proof. □

Remark 3.2.24. *In Definition 3.2.7, filter efficiency at $t \in \mathbb{N}$ is defined using measure Φ_t; whereas, in Theorem 3.2.23 it is defined based on $P_{t|t}$ value. Note that the two definitions of efficiency are equivalent, since Φ_t and $P_{t|t}$ at $t \in \mathbb{N}$ are related by Theorem 3.2.10.*

The procedure to monitor the quality of the target estimates obtained with any tracking strategy is summarized in the next theorem.

Theorem 3.2.25. *Let $Z^\star_{t|t} \in \mathbb{R}^s$ and $V^\star_{t|t} \in \mathcal{S}^s_{++}$ be the mean and covariance of $Z_t|Y_{1:t} \sim p(\cdot|Y_{1:t})$ and $\widehat{Z}^o_{t|t} \triangleq \widehat{Z}^i_{t|t}$ be the target state and parameter estimate computed by filter $i \in \mathcal{F}$ at $t \in \mathbb{N}$, then the quality of $\widehat{Z}^o_{t|t} \in \mathbb{R}^s$ can be assessed as follows:*

(a) If $B^\star_{t|t} = 0$ almost surely then the PCRLB inequality in (3.4) is given by $P_{t|t} = \mathbb{E}_{p(Y_{1:t})}[V^\star_{t|t}] = J_t^{-1}$, such that the filter $i \in \mathcal{F}$ is efficient, and the corresponding estimate $\widehat{Z}^o_{t|t}$ is unbiased and MMSE.

(b) If $B^\star_{t|t} \neq 0$ almost surely, and $\mathbb{E}_{p(Y_{1:t})}[B^\star_{t|t}] \neq 0$ then (3.4) is given by $P_{t|t} = \mathbb{E}_{p(Y_{1:t})}[V^\star_{t|t} + [B^\star_{t|t}[B^\star_{t|t}]'] \succ J_t^{-1}$, such that the filter is not efficient, and the estimate is biased (only conditionally biased if $\mathbb{E}_{p(Y_{1:t})}[B^\star_{t|t}] = 0$) and fails to yield an MMSE estimate.

Proof. (a) If the filter $i \in \mathcal{F}$, delivering $\widehat{Z}^o_{t|t} \in \mathbb{R}^s$ at $t \in \mathbb{N}$ satisfies $B^\star_{t|t} = 0$ almost surely, then its MSE is given by $P_{t|t} = \mathbb{E}_{p(Y_{1:t})}[V^\star_{t|t}]$ (see Corollary 3.2.22). This implies that the filter $i \in \mathcal{F}$ is efficient (see Theorem 3.2.23). Also, $B^\star_{t|t} = 0$ almost surely

implies the filter yields unbiased (see Lemma 3.2.20(a) and Remark 3.2.21) and MMSE (see Remark 3.2.9) estimate. (2) If the filter $i \in \mathcal{F}$ satisfies $B_{t|t}^{\star} \neq 0$ almost surely, then from Lemma 3.2.20(b), we have $\mathbb{E}_{p(Y_{1:t})}[B_{t|t}^{\star}[B_{t|t}^{\star}]^T] \neq 0$. This implies its MSE is $P_{t|t} = \mathbb{E}_{p(Y_{1:t})}[V_{t|t}^{\star} + [B_{t|t}^{\star}[B_{t|t}^{\star}]'] \succ \mathbb{E}_{p(Y_{1:t})}[V_{t|t}^{\star}]$. Now, since $P_{t|t} \succ J_t^{-1}$, the filter $i \in \mathcal{F}$ is not efficient. Moreover, if the estimate satisfies $\mathbb{E}_{p(Y_{1:t})}[B_{t|t}^{\star}] \neq 0$, then the estimate is biased and only conditionally biased if $\mathbb{E}_{p(Y_{1:t})}[B_{t|t}^{\star}] = 0$ (see Definition 3.2.19). $\qquad\square$

Remark 3.2.26. *The results in Theorem 3.2.25 are general, and can also be used to monitor the quality of the estimates obtained with Algorithm 4, Remarks 3.2.16 and 3.2.17 or any other on-line Bayesian tracking methods.*

Although the PCRLB inequality allow for assessment, monitoring, and selection of a tracking strategy, computing it in closed form is non-trivial, and require numerical methods.

3.3   Numerical computation

Computing PCRLB inequality (3.4) involves solving multi-dimensional integrals, which do not admit any closed form solution for Model 3.1.1. The Monte Carlo (MC) method is a popular numerical approach (Bergman, 2001); wherein, the MSE and PCRLB at $t \in \mathbb{N}$ can be approximated by simulating M i.i.d. sample paths $(z_{0:t}^j, y_{1:t}^j)_{j=1}^M \in \mathcal{Z}^{t+1} \times \mathcal{Y}^t$ using Model 3.1.1, starting at M i.i.d. initial positions drawn from $Z_0 \sim p(z_0)$. It can be shown that the MC estimate asymptotically converges to its true value (Moral, 2004). The practical issues with MC based MSE and PCRLB estimates are given next.

Remark 3.3.1. *With $M < +\infty$, the MC based MSE and PCRLB will not necessarily satisfy the condition $P_{t|t} - J_t^{-1} \succcurlyeq 0$ for all $t \in \mathbb{N}$.*

Remark 3.3.2. *Since $M < +\infty$, the conditions in Theorem 3.2.25 are relaxed to $|B_{t|t}^{\star}(i)| \leq \epsilon(i)$ and $|\mathbb{E}_{p(Y_{1:t})}[B_{t|t}^{\star}(i)]| \leq \alpha(i)$, where $1 \leq i \leq s$, and $\epsilon \in \mathbb{R}_+^s$ and $\alpha \in \mathbb{R}_+^s$ are pre-defined tolerance levels set based on M and the required degree of accuracy.*

Remark 3.3.3. *A tracking filter satisfying* $|B_{t|t}^{\star}(i)| \leq \epsilon(i)$ *for all* $1 \leq i \leq s$, *is* ϵ-*efficient at* $t \in \mathbb{N}$ *and the resulting tracking estimate is* ϵ-*unbiased and* ϵ-*MMSE (see Theorem 3.2.25(a)). Similarly, if the target estimate only satisfies* $|\mathbb{E}_{p(Y_{1:t})}[B_{t|t}^{\star}(i)]| \leq \alpha(i)$ *for all* $1 \leq i \leq s$, *then it is* α-*unconditionally unbiased (see Theorem 3.2.25(b)).*

3.4   Numerical illustration

3.4.1   Target tracking at re-entry phase with unknown ballistic coefficient

We illustrate the efficacy of the tools developed in Section 3.2 on a ballistic target tracking problem at re-entry phase with unknown ballistic coefficient.

3.4.1.1   Simulation setup

Consider a target launched along a ballistic flight whose kinematics are described in a 2-D Cartesian coordinate system. This particular description of the kinematics assumes that the only forces acting on the target at any given time are the forces due to gravity and drag. All other forces such as: centrifugal acceleration; Coriolis acceleration; wind; lift force; and spinning motion are assumed to have a small effect on the target dynamics. With the position and the velocity of the target at time $t \in \mathbb{N}$ given as $(\mathrm{X}_t, \mathrm{H}_t)$ and $(\dot{\mathrm{X}}_t, \dot{\mathrm{H}}_t)$, respectively, its motion in the re-entry phase can be described by (Tulsyan *et al.*, 2013a): $X_{t+1} = AX_t + GF_t(X_t) + G[0 \ -g]^T + V_t$, where: $X_t \triangleq [\mathrm{X}_t \ \dot{\mathrm{X}}_t \ \mathrm{H}_t \ \dot{\mathrm{H}}_t]^T$; $A = I_{2\times2} \otimes \begin{bmatrix} 1 & \Delta \\ 0 & 1 \end{bmatrix}$; $G = I_{2\times2} \otimes [\Delta^2/2 \ \ \Delta]^T$; $\otimes$ is the Kronecker product; Δ is time lapse between radar measurements; $F_t(X_t) = -\dfrac{g\rho(\mathrm{H}_t)}{2\theta}(\dot{\mathrm{X}}_t^2 + \dot{\mathrm{H}}_t^2)^{0.5}[\dot{\mathrm{X}}_t \ \ \dot{\mathrm{H}}_t]^T$ is the drag force on the target; g is the acceleration due to gravity; $\theta \in \mathbb{R}$ is the unknown ballistic coefficient, whose value depends on the shape, mass and the cross sectional area of the target; and $\rho(\mathrm{H}_t)$ is the air density, such that $\rho(\mathrm{H}_t) = \alpha_1 e^{(-\alpha_2 \mathrm{H}_t)}$, where: $\alpha_1 = 1.227\mathrm{kgm}^{-3}$, $\alpha_2 = 1.09310 \times 10^{-4}\mathrm{m}^{-1}$ for $\mathrm{H}_t < 9144\mathrm{m}$; and $\alpha_1 = 1.754\mathrm{kgm}^{-3}$, $\alpha_2 = 1.4910 \times 10^{-4}\mathrm{m}^{-1}$ for $\mathrm{H}_t \geq 9144\mathrm{m}$. $V_t \sim \mathcal{N}(0, Q_t)$ is a zero mean multivariate

Gaussian noise with covariance $Q_t = \gamma I_{2 \times 2} \otimes \Psi$, where $\Psi = \begin{bmatrix} \Delta^3/3 & \Delta^2/2 \\ \Delta^2/2 & \Delta \end{bmatrix}$ and $\gamma \in \mathbb{R}_+$

is the noise intensity. The target measurements $Y_t = [L_t \quad E_t]^T$, where L_t is the range and

E_t the elevation are collected by a dish radar assumed to be stationed at the origin, such

that $Y_t = [(\mathbf{X}_t^2 + \mathbf{H}_t^2)^{0.5} \arctan(\mathbf{H}_t/\mathbf{X}_t)]^T + W_t$, where $W_t \sim \mathcal{N}(0, R_t)$ is a zero mean

multivariate Gaussian noise with covariance $R_t = \mathrm{diag}(\sigma_l^2, \sigma_e^2)$, where $\sigma_l \in \mathbb{R}_+$ and $\sigma_e \in$

$\mathbb{R}_+$ are the standard deviation for the range and elevation readings. The target elevation

angle is assumed to be between 0 and $\pi/2$ radians. The parameters used here are: $g =$

$9.8\mathrm{ms}^{-2}$; $\Delta = 2\mathrm{s}$; $T = 120\mathrm{s}$; $\gamma = 1$; $\sigma_l = 0.1\mathrm{km}$; and $\sigma_e = 0.017\mathrm{rad}$. Let $Z_t = [X_t^T \ \theta_t]^T$

be a vector of unknown target states and ballistic coefficient, such that $Z_0 \sim \mathcal{N}(M_{z_0}, C_{z_0})$,

where $M_{z_0} = [232\mathrm{km} \ 2.290\cos 190^o\mathrm{kms}^{-1} \ 88\mathrm{km} \ 2.290\sin 190^o\mathrm{kms}^{-1} \ 40000\mathrm{kgm}^{-1}s^{-2}]^T$

and $[C_{z_0}]^{0.5} = \mathrm{diag}(1\mathrm{km}, 20\mathrm{ms}^{-1}, 1\mathrm{km}, 20\mathrm{ms}^{-1}, 20\mathrm{kgm}^{-1}s^{-2})$. The results presented in

the next section are valid only under the above settings.

3.4.1.2   Results

Starting with $Z_0 \sim \mathcal{N}(M_{z_0}, C_{z_0})$, Fig.3.1 gives the PCRLB for $\{Z_t\}_{t \in \mathbb{N}}$ for all $0 \leq t \leq T$,

obtained as $J_t^{-1}(i, i)$, where $1 \leq i \leq 5$. In the interval $0 \leq t \leq 60$, the PCRLB for

$\{\theta_t\}_{t \in \mathbb{N}}$ is almost constant. This is due to absence of drag at higher altitude, where the

target dynamics are linear and no additional information is available to estimate θ. In

$60 < t \leq 90$, due to higher levels of air density, the drag force increases and the PCRLB

for $\{X_t\}_{t \in \mathbb{N}}$ grows, but that of $\{\theta_t\}_{t \in \mathbb{N}}$ decreases sharply. In $90 < t \leq T$, the PCRLB for

$\{Z_t\}_{t \in \mathbb{N}}$ decreases. Since the PCRLB of $\{Z_t\}_{t \in \mathbb{N}}$ in $0 \leq t \leq T$ is bounded, it suggests that,

at least in theory, it is possible to use Bayesian methods to track $\{Z_t\}_{t \in \mathbb{N}}$ effectively.

Amongst the class of Bayesian methods for computing the posterior density

$\{p(z_t|Y_{1:t}\}_{t \in \mathbb{N}}$, the artificial dynamics approach (ADA) is a widely used method (Kantas

et al., 2009). The key advantage of ADA is that it can be implemented with both Kalman

and Sequential Monte Carlo (SMC) based tracking filters; however, there are two long-

standing problems with ADA approach as summarized in (Kantas *et al.*, 2009): (a) the

dynamics of the parameters are related to the width of the kernel and the variance of the artificial noise, which are often difficult to fine tune; and (b) transforming the problem by adding artificial noise modifies the original problem, so that, it becomes hard to quantify the bias introduced in the resulting estimates. The first issue was addressed in (Tulsyan *et al.*, 2013*b*); wherein, an approach to auto-tune the kernel width was developed. For the second issue, we will see how the developments of Section 3.2.3 can be used to quantify bias in the resulting estimates. For solely illustrative purposes, the following ADA based Kalman and SMC non-linear filters are tested for their tracking performance: (1) extended Kalman filter (EKF) (Ristic *et al.*, 2003); (2) unscented Kalman filter (UKF) (Ristic *et al.*, 2003); (3) sequential importance resampling filter (SIR) (Ristic *et al.*, 2003); and (4) adaptive sequential importance resampling filter (ASIR) (Tulsyan *et al.*, 2013*b*).

To assess the performance of filters in approximating $\{p(z_t|Y_{1:t})\}_{t\in\mathbb{N}}$, we construct a filter bank $\mathcal{B}$, with $\mathcal{F} = \{1, 2, 3, 4\}$. Fig.3.2 gives $\mathrm{Tr}[\Phi_t]$ values for all the tracking filters in $\mathcal{B}$. From Fig.3.2, it is clear that the tracking performance of all the filters is high in the interval $0 \leq t \leq 70$ (with EKF being efficient (see Definition 3.2.7)), but plummets in the interval $70 < t \leq 120$. This is again due to the large drag force at lower altitude, which shifts the target dynamics from linear to non-linear regime, and thus making tracking difficult. Note that in Fig.3.2, $\mathrm{Tr}[\Phi_t]) > 5$ for certain tracking filters (see Remark 3.3.1).

Figs.3.3(a) and (b) give the average-case and best-case tracking strategies (see Algorithms 3 and 4) for this problem. At higher altitude, where the target dynamics are linear, both the strategies suggest using EKF, but recommend switching to advanced filters, such as SIR and ASIR at lower altitude. Although Algorithm 4 extensively uses UKF in tracking $\{Z_t(4)\}_{t\in\mathbb{N}}$ and $\{Z_t(5)\}_{t\in\mathbb{N}}$ (see Fig.3.3(b)), due to the poor overall performance of UKF (see Fig.3.2), its use is not recommended by Algorithm 3 (see Fig.3.3(a)).

Table 3.1 compares different tracking strategies based on their SNMSE values. It is clear that Algorithm 3 outperforms all other 'single filter use' strategies; however, amongst all
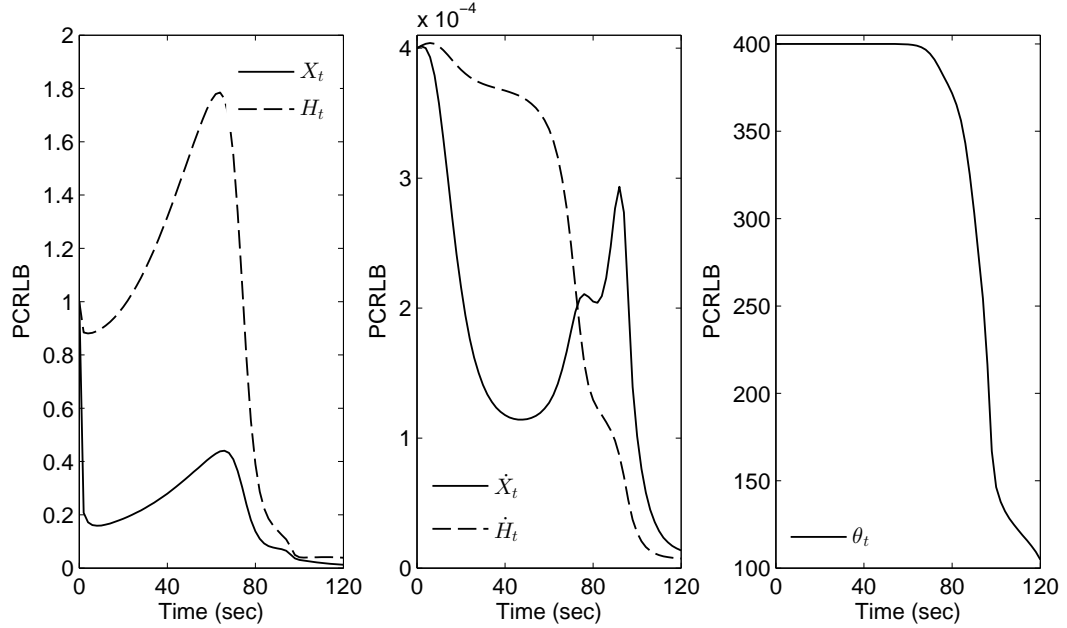
Figure 3.1: The PCRLB associated with the target states and ballistic coefficient. The results are based on $M = 2000$ MC simulations.

the tracking strategies implemented, Algorithm 4 yields the smallest SNMSE. In fact the SNMSE for Algorithm 4 reflects the optimal performance achievable with the four filters in the bank. Note that the SNMSE for Algorithm 4 is about 13% less than that obtained with Algorithm 3, but then, computationally, it is 1.5 times slower (see Remark 3.2.15).

Figs.3.3(c) and (e) and Figs.3.3(d) and (f) give the quality assessment of the target estimates obtained with Algorithms 3 and 4, respectively. Based on the assumed tolerance levels ϵ and α (see Remark 3.3.2), Algorithms 3 and 4 are ϵ-efficient ($> 75\%$ of the simulations in Figs.3.3(c) and (d) are within the set tolerance limit ϵ) in the interval $0 \leq t \leq 70$, and the resulting target estimates are ϵ-unbiased and ϵ-MMSE (see Figs.3.3(e) and (f), Theorem 3.2.25(a) and Remark 3.3.3). In the interval $70 < t \leq 120$, Algorithms 3 and 4 are not efficient (see Figs.3.3(c) and (d)), and the resulting estimates are neither MMSE nor unbiased (see Theorem 3.2.25(b)), except in $85 < t \leq 105$ and $100 < t \leq 120$, where Algorithms 3 and 4 are α-unconditionally unbiased, respectively (see Figs.3.3(e) and (f), and Remark 3.3.3). Note that although Algorithms 3 and 4 are not efficient in
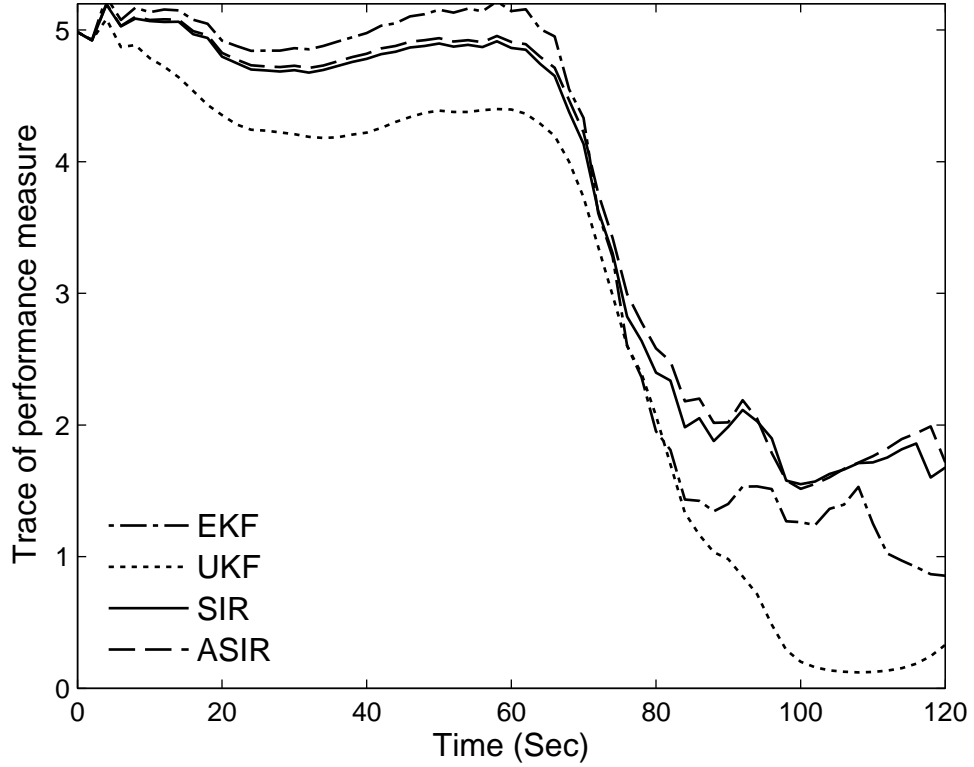
Figure 3.2: Performance assessment of all tracking filters in the bank.

Table 3.1: Comparing strategies using sum of the trace of normalized MSE (SNMSE), i.e., $\sum_{t=1}^{T} \text{Tr}[P_{t|t} \circ [J_{t|t}^{-1}]^{\circ -1} = \sum_{t=1}^{T} \text{Tr}[\Phi_t^{\circ -1}]$

	EKF	UKF	SIR	ASIR	Algorithm 3	Algorithm 4
SNMSE	798	5915	668	670	562	489

$70 < t \leq 120$, around 50% of the simulations in Fig.3.3(d) are within the set tolerance limit ϵ, as compared to 40% in Fig.3.3(c). This suggests that compared to Algorithm 3, quality of tracking with Algorithm 4 is better.

In summary, the results suggest that, at least in theory, it is possible to achieve higher tracking performance at lower altitude. This can be achieved by either choosing new filters or by carefully redesigning the existing ones. Note that choosing new non-linear filters or redesigning existing ones with certain specific properties (e.g., low estimation bias) requires a thorough understanding of the statistical and numerical approximations.
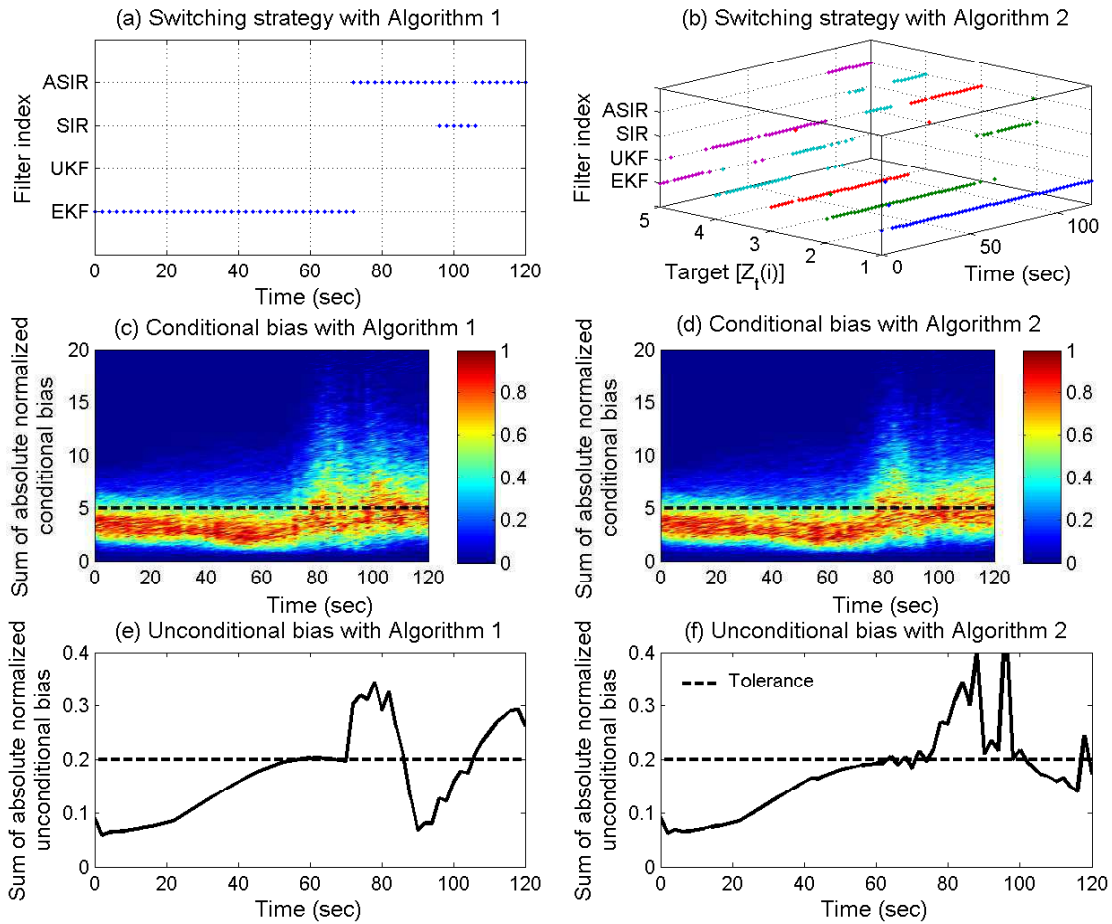
Figure 3.3: Filter assessment, optimal filter switching strategy, and quality assessment of the target estimates obtained with Algorithms 3 and 4.

3.5   Conclusions

A PCRLB inequality based tool for performance assessment of multiple non-linear tracking filters is developed. Based on the developed measure, average-optimal and optimal MMSE filtering strategy for target tracking in non-linear SSMs with non-Gaussian noise and unknown target parameters are proposed. An approach to monitor the quality of the target estimates obtained using the proposed tracking strategy is also provided. The monitoring procedure presented here is general, and can be used to monitor the quality of the estimates obtained with any on-line Bayesian methods. The utility of the tools were illustrated on a ballistic target tracking problem at re-entry phase with unknown ballistic coefficient.

Bibliography

Andrieu, C., A. Doucet, S.S. Singh and V.B. Tadic (2004). Particle methods for change detection, system identification, and control. *Proceedings of IEEE* **92**(3), 423–438.

Bapat, R.B. and T.E.S. Raghavan (1997). *Nonnegative Matrices and Applications*. Cambridge University Press, New York.

Bergman, N. (2001). *Sequential Monte Carlo Methods in Practice*. Chap. Posterior Cramér-Rao bounds for sequential estimation. Springer–Verlag, New York.

Billingsley, P. (1995). *Probability and Measure*. Chap. The integral. Wiley, New York.

Kantas, N., A. Doucet, S.S. Singh and J. Maciejowski (2009). An overview of sequential Monte Carlo methods for parameter estimation in general state-space models. In: *Proceedings of the 15th IFAC Symposium on System Identification*. Saint-Malo, France. pp. 774–785.

Knuth, D.E. (1973). *The Art of Computer Programming–Part III*. Chap. Sorting. Addison-Wesley, Reading, MA.

Minvielle, P., A. Doucet, A. Marrs and S. Maskell (2010). A Bayesian approach to joint tracking and identification of geometric shapes in video sequences. *Image and Vision Computing* **28**(1), 111–123.

Moral, P. Del (2004). *Feynman-Kac Formulae: Genealogical and Interacting Particle Systems with Applications*. Springer–Verlag, New York.

Reams, R. (1999). Hadamard inverses, square roots and products of almost semidefinite matrices. *Linear Algebra and its Applications* **288**(1), 35–43.

Ristic, B., A. Farina, D. Benvenuti and M.S. Arulampalam (2003). Performance bounds and comparison of non-linear filters for tracking a ballistic object on re-entry. *IEE Proceedings-Radar, Sonar and Navigation* **150**(2), 65–70.

Tichavský, P., C. Muravchik and A. Nehorai (1998). Posterior Cramér-Rao bounds for discrete-time non-linear filtering. *IEEE Transactions on Signal Processing* **46**(5), 1386–1396.

Trees, H.L.V. (1968). *Detection, Estimation and Modulation Theory–Part I*. Chap. Classical detection and estimation theory. Wiley, New York.

Tulsyan, A., B. Huang, R.B. Gopaluni and J.F. Forbes (2013*a*). A particle filter approach to approximate posterior Cramér-Rao lower bound: The case of hidden states. *IEEE Transactions on Aerospace and Electronic Systems, In press*.

Tulsyan, A., B. Huang, R.B. Gopaluni and J.F. Forbes (2013*b*). On simultaneous on-line state and parameter estimation in non-linear state-space models. *Journal of Process Control* **23**(4), 516–526.

Tulsyan, A., B. Huang, R.B. Gopaluni and J.F. Forbes (2013*c*). Performance assessment, diagnosis, and optimal selection of non-linear state filters. *Journal of Process Control, In Review*.

Šimandl, M., J. Královec and P. Tichavský (2001). Filtering, predictive, and smoothing Cramér-Rao bounds for discrete-time non-linear dynamic systems. *Automatica* **37**(11), 1703–1716.

Chapter 4

Error analysis in Bayesian identification of non-linear state-space models

In the last two decades, several methods based on sequential Monte Carlo (SMC) and Markov chain Monte Carlo (MCMC) have been proposed for Bayesian identification of stochastic non-linear state-space models (SSMs). It is well known that the performance of these simulation based identification methods depends on the numerical approximations used in their design. We propose the use of posterior Cramér-Rao lower bound (PCRLB) as a mean square error (MSE) bound. Using PCRLB, a systematic procedure is developed to analyse the estimates delivered by Bayesian identification methods in terms of bias, MSE, and efficiency. The efficacy and utility of the proposed approach is illustrated through a numerical example.

4.1   Introduction

Bayesian identification has a long history, dating at least as far back as (Peterka, 1981). Despite this, it is not commonly used in practice, except for the linear, Gaussian SSM case; wherein, Kalman filter based Bayesian estimate is routinely employed (Ninness and Henriksen, 2010). This is due to the computational complexities associated with

the computation of the posterior densities, their marginals, and associated functions, such as posterior mean and variance (Juloski *et al.*, 2005). Recent developments in statistical methods, such as SMC and MCMC along with advances in computing technology have allowed researchers to use Bayesian methods in both on-line (Chen *et al.*, 2005; Tulsyan *et al.*, 2013*b*) and off-line (Jones *et al.*, 2011; Geweke and Tanizaki, 2001) identification of SSMs. This chapter is directed towards the class of Bayesian identification methods for parameter estimation in stochastic SSMs.

The notation used in this chapter is introduced next.

Notation: $\mathbb{N} := \{1, 2, \dots\}$; $\mathbb{R}_+ := [0, \infty)$; $\mathbb{R}^{s \times s}$ is the set of real-valued $s \times s$ matrices; $\mathcal{S}^s \subset \mathbb{R}^{s \times s}$ is the space of symmetric matrices; $\mathcal{S}^s_+$ is the cone of symmetric positive semi-definite matrices in $\mathcal{S}^s$; and $\mathcal{S}^s_{++}$ is its interior. The partial order on $\mathcal{S}^s$ induced by $\mathcal{S}^s_+$ and $\mathcal{S}^s_{++}$ are denoted by $\succcurlyeq$ and $\succ$, respectively. For $A \in \mathbb{R}^{s \times s}$, $\mathrm{Tr}[A]$ denotes its trace. For a vector $y \in \mathbb{R}^p$, $\mathrm{diag}(y) \in \mathcal{S}^p$ is a diagonal matrix with $y \in \mathbb{R}^p$ as its entries. $|\cdot|$ is the absolute value. $\Delta^y_x \triangleq \nabla_x \nabla^T_y$ is Laplacian and $\nabla_x \triangleq \left[\frac{\partial}{\partial x}\right]$ is gradient.

4.2 Bayesian identification

Let $\{X_t\}_{t \in \mathbb{N}}$ and $\{Y_t\}_{t \in \mathbb{N}}$ be $\mathcal{X}(\subseteq \mathbb{R}^n)$ and $\mathcal{Y}(\subseteq \mathbb{R}^m)$ valued stochastic processes defined on a measurable space $(\Omega, \mathcal{F})$. Let these stochastic processes depend on unknown parameter vector $\theta \in \Theta$, where Θ is an open subset of $\mathbb{R}^q$. The discrete-time state $\{X_t\}_{t \in \mathbb{N}}$ is an unobserved process, with initial density $p_\theta(x)$ and transition density $p_\theta(x'|x)$:

$$X_0 \sim p_\theta(\cdot); \;\; X_{t+1}|(X_t = x_t) \sim p_\theta(\cdot|x_t, u_t) \;\; (t \in \mathbb{N}). \tag{4.1}$$

$\{Y_t\}_{t \in \mathbb{N}}$ is conditionally independent given $\{X_t\}_{t \in \mathbb{N}}$ and have a marginal density $p_\theta(y|x)$:

$$Y_t|(X_0, \dots, X_t = x_t, \dots, X_T) \sim p_\theta(\cdot|x_t) \;\;\;\; (t \in \mathbb{N}). \tag{4.2}$$

All the densities are with respect to suitable dominating measures, such as Lebesgue measure, which are denoted generically as dx and dy. Although (4.1) and (4.2) represent a

wide class of non-linear time-series models, the model considered here is given below.

Model 4.2.1. *Consider the following discrete-time, stochastic non-linear SSM*

$$X_{t+1} = f_t(X_t, \theta_t, V_t); \tag{4.3a}$$

$$\theta_{t+1} = \theta_t; \tag{4.3b}$$

$$Y_t = g_t(X_t, \theta_t, W_t), \tag{4.3c}$$

where $\{\theta_t\}_{t\in\mathbb{N}} = \theta$ is a vector of unknown parameters, and $\{V_t\}_{t\in\mathbb{N}}$ and $\{W_t\}_{t\in\mathbb{N}}$ are the state and measurement noise.

Remark 4.2.2. *To minimize use of notation, signal $\{u_t\}_{t\in\mathbb{N}}$ is not included in Model 4.2.1; however, all the results that appear in this chapter hold with signal $\{u_t\}_{t\in\mathbb{N}}$ included.*

For a generic sequence $\{r_t\}_{t\in\mathbb{N}}$, let $r_{i:j} \triangleq \{r_i, r_{i+1}, \ldots, r_j\}$. In Bayesian identification, the problem of estimating the parameter vector $\theta \in \Theta \subseteq \mathbb{R}^q$ in Model 4.2.1, given a measurement sequence $\{Y_{1:t} = y_{1:t}\}_{t\in\mathbb{N}}$ is formulated as a joint state and parameter estimation problem. This is done by ascribing a prior density $\theta_0 \sim p(\theta_0)$, such that $\theta \in \operatorname{supp} p(\theta_0)$, and computing the density $Z_t|(Y_{1:t} = y_{1:t}) \sim p(\cdot|y_{1:t})$, where $Z_t \triangleq \{X_t; \theta_t\}$ is a $\mathcal{Z}(\subseteq \mathbb{R}^{s=n+q})$ valued extended Markov process with $(Z_0 = z_0) \sim p_{\theta_0}(x_0)p(\theta_0)$, $Z_t|(Z_{t-1} = z_{t-1}) \sim p_{\theta_{t-1}}(\cdot|x_{t-1})\delta_{\theta_{t-1}}(\cdot)$. A recursive method to compute $\{p(z_t|y_{1:t})\}_{t\in\mathbb{N}}$ is given by the optimal filtering equation. Having computed $\{p(z_t|y_{1:t})\}_{t\in\mathbb{N}}$, inference on $\{\theta_t\}_{t\in\mathbb{N}}$ relies on the marginal density $\{p(\theta_t|y_{1:t})\}_{t\in\mathbb{N}}$.

Although computing $\theta_t|(Y_{1:t} = y_{1:t}) \sim p(\cdot|y_{1:t})$ appears similar to computing $X_t|(Y_{1:t} = y_{1:t}) \sim p_\theta(\cdot|y_{1:t})$ (under known parameter case) in the state estimation problem, calculating $\{p(\theta_t|y_{1:t})\}_{t\in\mathbb{N}}$ for Model 4.2.1 has proved to be a non-trivial problem (Kantas *et al.*, 2009; Minvielle *et al.*, 2010). No analytical solution to $\{p(\theta_t|y_{1:t})\}_{t\in\mathbb{N}}$ is available, even for linear and Gaussian SSM, or when $\mathcal{X}$ is a finite set (Kantas *et al.*, 2009). There are several simulation and numerical methods (e.g., SMC, MCMC, Kalman based filters), which allow for recursive approximation of $\{p(\theta_t|y_{1:t})\}_{t\in\mathbb{N}}$. Although tractable, the

quality of these identification methods depends on the underlying numerical and statistical approximations used in their design.

Despite the widespread interest in developing advanced simulation and numerical methods for Bayesian identification of Model 4.2.1, there have been no elaborate study on the quality of these methods. With this background, this chapter proposes the use of PCRLB as an error bound. Using PCRLB, a systematic approach to assess the quality of a Bayesian identification method, in terms of bias, MSE, and efficiency is developed. Initial results reported by the authors in (Tulsyan *et al.*, 2013*c*), use PCRLB for assessment of state (but not parameter) estimation algorithms. The focus of this chapter is to extend the results in (Tulsyan *et al.*, 2013*c*) to the Bayesian parameter estimation algorithms.

4.3   PCRLB as an error bound

The conventional Cramér-Rao lower bound (CRLB) provides a theoretical lower bound on the MSE of any maximum-likelihood (ML) based unbiased parameter estimator. An analogous extension of the CRLB to the Bayesian estimators was derived by (Trees, 1968), and is commonly referred to as the PCRLB inequality. The PCRLB, derived recently by (Tichavský *et al.*, 1998) for Model 4.2.1, provides a bound on the MSE associated with the estimation of the states and parameters from $\{p(z_t|u_{1:t}, y_{1:t})\}_{t\in\mathbb{N}}$, and is given next.

Lemma 4.3.1. *Let* $\{Y_{1:t} = y_{1:t}\}_{t\in\mathbb{N}}$ *be an output sequence generated from Model 4.2.1, then the MSE associated with the estimation of* $\{Z_t\}_{t\in\mathbb{N}}$ *from* $\{p(z_t|y_{1:t})\}_{t\in\mathbb{N}}$ *is bounded by*

$$P_{t|t}^z \triangleq \mathbb{E}_{p(Z_t, Y_{1:t})}[(Z_t - \widehat{Z}_{t|t})(Z_t - \widehat{Z}_{t|t})^T] \succcurlyeq [J_t^z]^{-1}, \tag{4.4}$$

where: $\widehat{Z}_{t|t} := \mathbb{R}^{tm} \to \mathbb{R}^s$ *is a point estimate of* $\{Z_t\}_{t\in\mathbb{N}}$; $P_{t|t}^z \triangleq \begin{bmatrix} P_{t|t}^x & P_{t|t}^{x\theta} \\ (P_{t|t}^{x\theta})^T & P_{t|t}^\theta \end{bmatrix} \in \mathcal{S}_{++}^s$,

$J_t^z \triangleq \begin{bmatrix} J_t^x & J_t^{x\theta} \\ (J_t^{x\theta})^T & J_t^\theta \end{bmatrix} \in \mathcal{S}_{++}^s$, $[J_t^z]^{-1} \triangleq \begin{bmatrix} L_t^x & L_t^{x\theta} \\ (L_t^{x\theta})^T & L_t^\theta \end{bmatrix} \in \mathcal{S}_{++}^s$ *are the MSE, posterior Fisher information matrix (PFIM), and PCRLB, respectively.*

Proof. See (Tichavský *et al.*, 1998) for proof.   □

A recursive approach to compute $J_t^z \in \mathcal{S}_{++}^s$ was derived by (Tichavský *et al.*, 1998), and is given next. But first, we give the assumptions on the model considered in Model 4.2.1.

Assumption 4.3.2. $\{V_t\}_{t\in\mathbb{N}}$ *and* $\{W_t\}_{t\in\mathbb{N}}$ *are mutually independent sequences of independent random variables known a priori in their distribution classes (e.g., Gaussian) and parametrized by a known and finite number of moments.*

Assumption 4.3.3. $f_t := \mathcal{X} \times \Theta \times \mathbb{R}^m \to \mathbb{R}^n$ *and* $g_t := \mathcal{X} \times \Theta \times \mathbb{R}^m \to \mathbb{R}^m$ *are non-linear functions, such that in the open set* $\mathcal{X}$ *and* Θ, $\{f_t; g_t\}$ *is* $\mathcal{C}^k(\mathcal{X})$ *and* $\mathcal{C}^k(\Theta)$, *and in* $\mathbb{R}^n$ *and* $\mathbb{R}^m$, f_t *is* $\mathcal{C}^{k-1}(\mathbb{R}^n)$, *and* g_t *is* $\mathcal{C}^{k-1}(\mathbb{R}^m)$, *where* $k \geq 2$.

Assumption 4.3.4. *For* $(x_{t+1}, x_t, \theta_t, v_t) \in \mathcal{X} \times \mathcal{X} \times \Theta \times \mathbb{R}^n$ *and* $(y_t, x_t, \theta_t, w_t) \in \mathcal{Y} \times \mathcal{X} \times \Theta \times \mathbb{R}^m$ *satisfying Model 4.2.1,* $\nabla_{v_t} f_t^T(x_t, \theta_t, v_t)$ *and* $\nabla_{w_t} g_t^T(x_t, \theta_t, w_t)$ *have rank* n *and* m, *respectively, such that using implicit function theorem,* $p_\theta(x_{t+1}|x_t) = p(V_t = \tilde{f}_t(x_t, \theta_t, x_{t+1}))$ *and* $p_\theta(y_t|x_t) = p(W_t = \tilde{g}_t(x_t, \theta_t, y_t))$ *are defined.*

Lemma 4.3.5. *A recursive approach to compute* $J_t^z \in \mathcal{S}_{++}^s$ *for Model 4.2.1 under Assumptions 4.3.2 through 4.3.4 is given as follows:*

$$J_{t+1}^x = H_t^{33} - (H_t^{13})^T[J_t^x + H_t^{11}]^{-1}H_t^{13}; \tag{4.5a}$$

$$J_{t+1}^{x\theta} = (H_t^{23})^T - (H_t^{13})^T[J_t^x + H_t^{11}]^{-1}(J_t^{x\theta} + H_t^{12}); \tag{4.5b}$$

$$J_{t+1}^\theta = J_t^\theta + H_t^{22} - (J_t^{x\theta} + H_t^{12})^T[J_t^x + H_t^{11}]^{-1}(J_t^{x\theta} + H_t^{12}), \tag{4.5c}$$

where:

$$H_t^{11} = \mathbb{E}_{p(X_{0:t+1}, \theta_t, Y_{1:t+1})}[-\Delta_{X_t}^{X_t} \log p_t]; \tag{4.6a}$$

$$H_t^{12} = \mathbb{E}_{p(X_{0:t+1}, \theta_t, Y_{1:t+1})}[-\Delta_{X_t}^{\theta_t} \log p_t]; \tag{4.6b}$$

$$H_t^{13} = \mathbb{E}_{p(X_{0:t+1}, \theta_t, Y_{1:t+1})}[-\Delta_{X_t}^{X_{t+1}} \log p_t]; \tag{4.6c}$$

$$H_t^{22} = \mathbb{E}_{p(X_{0:t+1}, \theta_t, Y_{1:t+1})}[-\Delta_{\theta_t}^{\theta_t} \log p_t]; \tag{4.6d}$$

$$H_t^{23} = \mathbb{E}_{p(X_{0:t+1}, \theta_t, Y_{1:t+1})}[-\Delta_{\theta_t}^{X_{t+1}} \log p_t]; \tag{4.6e}$$

$$H_t^{33} = \mathbb{E}_{p(X_{0:t+1}, \theta_t, Y_{1:t+1})}[-\Delta_{X_{t+1}}^{X_{t+1}} \log p_t]; \tag{4.6f}$$

and: $p_t = p(X_{t+1}|Z_t)p(Y_{t+1}|\theta_t, X_{t+1})$*; and the PFIM at* $t = 0$ *can be computed using*

$$J_0 = \mathbb{E}_{p(Z_0)}[-\Delta_{Z_0}^{Z_0} \log p(Z_0)].$$

Proof. See (Tichavský *et al.*, 1998) for proof.   □

Since the focus here is on $\{\theta\}_{t\in\mathbb{N}}$ alone, a lower bound on the MSE associated with the estimation of $\{\theta\}_{t\in\mathbb{N}}$ is of interest to us. Using Lemmas 4.3.1 and 4.3.5, a bound on the MSE for parameter estimates can be derived, as given next.

Corollary 4.3.6. *Let* $P_{t|t}^z \in \mathcal{S}_{++}^s$ *and* $J_t^z \in \mathcal{S}_{++}^s$ *be such that they satisfy (4.4), then the MSE associated with the estimation of* $\{\theta_t\}_{t\in\mathbb{N}}$ *from* $\{p(\theta_t|y_{1:t})\}_{t\in\mathbb{N}}$*, is bounded by*

$$P_{t|t}^\theta = \mathbb{E}_{p(\theta_t, Y_{1:t})}[(\theta_t - \widehat{\theta}_{t|t})(\theta_t - \widehat{\theta}_{t|t})^T] \succcurlyeq L_t^\theta, \tag{4.7}$$

where $\theta_{t|t} := \mathbb{R}^{tm} \to \mathbb{R}^q$ *is the parameter estimate delivered by a Bayesian identification algorithm, and* $L_t^\theta \in \mathcal{S}_{++}^q$ *is the lower right matrix of* $[J_t^z]^{-1} \in \mathcal{S}_{++}^s$ *in Lemma 4.3.1.*

Proof. The proof is based on the fact that Lemma 4.3.1 ensures $P_{t|t}^z - [J_t^z]^{-1} \in \mathcal{S}_+^s$.   □

A recursive approach to compute $L_t^\theta \in \mathcal{S}_{++}^q$ is given next.

Theorem 4.3.7. *Let* $J_t^z \in \mathcal{S}_{++}^s$ *be the PFIM for* $\{Z_t\}_{t\in\mathbb{N}}$*, and* $L_t^\theta \in \mathcal{S}_{++}^q$ *be the lower bound on the MSE associated with the estimation of* $\{\theta_t\}_{t\in\mathbb{N}}$ *in Model 4.2.1, then given* $J_t^z \in \mathcal{S}_{++}^s$*, the lower bound* $L_t^\theta \in \mathcal{S}_{++}^q$ *at* $t \in \mathbb{N}$ *can be recursively computed as follows:*

$$L_t^\theta = [J_t^\theta - (J_t^{x\theta})^T (J_t^x)^{-1} J_t^{x\theta}]^{-1}, \tag{4.8}$$

where J_t^θ*,* $J_t^{x\theta}$ *and* J_t^x *are the PFIMs given in Lemma 4.3.1.*

Proof. The proof is based on matrix inversion lemma (Bapat and Raghavan, 1997).   □

Remark 4.3.8. *Theorem 4.3.7 shows that for Model 4.2.1,* L_t^θ *is not only a function of the PFIM for* $\{\theta_t\}_{t\in\mathbb{N}}$*, i.e.,* J_t^θ*, but it also depends on the PFIMs for* $\{X_t\}_{t\in\mathbb{N}}$*, i.e.,* $J_t^{x\theta}$ *and* J_t^x*.*

Remark 4.3.9. *Integral in (4.6) with respect to* $p(x_{0:t}, \theta_{t-1}, y_{1:t})$ *makes* L_t^θ *in (4.8) independent of any random sample from* $\mathcal{X}^{t+1}$, Θ, *and* $\mathcal{Y}^t$. L_t^θ *in fact only depends on: the process dynamics in Model 4.2.1; noise characteristics of* $V_t \sim p(v_t)$ *and* $W_t \sim p(w_t)$; *and the choice of* $Z_0 \sim p(z_0)$. *This makes* L_t^θ *a system property, independent of any Bayesian identification method or any specific realization from* $\mathcal{X}$, Θ *or* $\mathcal{Y}$. *This motivates the use of PCRLB as a benchmark for error analysis of Bayesian identification algorithms.*

Using PCRLB inequality (4.7), the MSE for the parameter estimates obtained with any Bayesian identification method can be compared against the theoretical lower bound. A systematic approach to compare and analyse the MSE and PCRLB is discussed next.

4.4   PCRLB inequality based error analysis

A common approach to compute $\widehat{\theta}_{t|t} \in \mathbb{R}^q$, is to minimize $\mathrm{Tr}[P_{t|t}^\theta] \in \mathbb{R}_+$. This ensures that $\mathrm{Tr}[P_{t|t}^\theta - L_t^\theta] \geq 0$ is minimized. The optimal estimate that minimizes $\mathrm{Tr}[P_{t|t}^\theta] \in \mathbb{R}_+$ is referred to as the minimum MSE (MMSE) estimate, and is the conditional mean of $\theta_t|(Y_{1:t} = y_{1:t}) \sim p(\cdot|y_{1:t})$, i.e., $\theta_{t|t} = \theta_{t|t}^\star \triangleq \mathbb{E}_{p(\theta_t|Y_{1:t})}[\theta_t]$ (see (Trees, 1968) for derivation).

Remark 4.4.1. *Bayesian identification methods only approximate the true density* $\{p(\theta_t|y_{1:t})\}_{t\in\mathbb{N}}$, *thus in practice, the estimate delivered by identification methods may not be an MMSE estimate, i.e.,* $\widehat{\theta}_{t|t} \triangleq \mathbb{E}_{\tilde{p}(\theta_t|Y_{1:t})}[\theta_t] \neq \theta_{t|t}^\star$ *almost surely, where* $\widehat{\theta}_{t|t}$ *is the mean of* $\theta_t|(Y_{1:t} = y_{1:t}) \sim \tilde{p}(\cdot|y_{1:t})$ *and* $\{\tilde{p}(\theta_t|y_{1:t})\}_{t\in\mathbb{N}}$ *is the approximate posterior.*

The second-order error associated with $\{\theta_{t|t}\}_{t\in\mathbb{N}}$ is completely characterized by its MSE. A thorough assessment of Bayesian estimates requires clear understanding of the MSE. The next theorem shows decomposition of the MSE into its sources of errors.

Theorem 4.4.2. *Let* $\theta_{t|t}^\star \in \mathbb{R}^q$ *and* $V_{t|t}^\star \in \mathcal{S}_{++}^q$ *be the mean and covariance of* $\theta_t|(Y_{1:t} = y_{1:t}) \sim p(\cdot|y_{1:t})$ *and* $\widehat{\theta}_{t|t} \in \mathbb{R}^q$ *be the mean of* $\theta_t|(Y_{1:t} = y_{1:t}) \sim \tilde{p}(\cdot|y_{1:t})$ *computed by a Bayesian identification method, then for* $\widehat{\theta}_{t|t} \neq \theta_{t|t}^\star$ *almost surely,* $P_{t|t}^\theta$ *at*

$t \in \mathbb{N}$ *can be decomposed and written as*

$$P_{t|t}^{\theta} = \mathbb{E}_{p(Y_{1:t})}[V_{t|t}^{\star}] + \mathbb{E}_{p(Y_{1:t})}[B_{t|t}^{\star}[B_{t|t}^{\star}]^{T}], \tag{4.9}$$

where $B_{t|t}^{\star} \triangleq [\theta_{t|t}^{\star} - \widehat{\theta}_{t|t}] \in \mathbb{R}^q$ *is the conditional bias in estimating the true conditional mean* $\theta_{t|t}^{\star} \in \mathbb{R}^q$ *at* $t \in \mathbb{N}$.

Proof. The proof is adapted from (Tulsyan *et al.*, 2013c). From the definition of expectation, MSE in (4.7) can be written as $P_{t|t}^{\theta} = \mathbb{E}_{p(Y_{1:t})}\mathbb{E}_{p(\theta_t|Y_{1:t})}[(\theta_t - \widehat{\theta}_{t|t})(\theta_t - \widehat{\theta}_{t|t})^{T}]$, where we have used $p(\theta_t, y_{1:t}) = p(y_{1:t})p(\theta_t|y_{1:t})$. Adding and subtracting $\theta_{t|t}^{\star}$ in $P_{t|t}^{\theta}$, followed by several algebraic manipulations yield $P_{t|t}^{\theta} = \mathbb{E}_{p(Y_{1:t})}\mathbb{E}_{p(\theta_t|Y_{1:t})}[F_{t|t}^{\star} + G_{t|t}^{\star} + [G_{t|t}^{\star}]^{T} + B_{t|t}^{\star}[B_{t|t}^{\star}]^{T}]$, where $F_{t|t}^{\star} = [\theta_t - \theta_{t|t}^{\star}][\theta_t - \theta_{t|t}^{\star}]^{T}$; $G_{t|t}^{\star} = [\theta_t - \theta_{t|t}^{\star}][\theta_{t|t}^{\star} - \widehat{\theta}_{t|t}]^{T}$. Now $\mathbb{E}_{p(\theta_t|Y_{1:t})}[F_{t|t}^{\star}] = V_{t|t}^{\star}$; $\mathbb{E}_{p(\theta_t|Y_{1:t})}[G_{t|t}^{\star}] = 0$, since $\mathbb{E}_{p(\theta_t|Y_{1:t})}[\theta_t - \theta_{t|t}^{\star}] = 0$; and $\mathbb{E}_{p(\theta_t|Y_{1:t})}[B_{t|t}^{\star}][B_{t|t}^{\star}]^{T} = [B_{t|t}^{\star}][B_{t|t}^{\star}]^{T}$, since $[B_{t|t}^{\star}][B_{t|t}^{\star}]^{T}$ is independent of $\theta_t|(Y_{1:t} = y_{1:t})$. Substituting the results into $P_{t|t}^{\theta}$ yields (4.9), which completes the proof. $\square$

Note that Theorem 4.4.2 is the Bayesian equivalent of the classical MSE decomposition results available for the likelihood based estimators. Using Theorem 4.4.2, bias in the Bayesian parameter estimates $\{\theta_{t|t}\}_{t \in \mathbb{N}}$ is defined next.

Definition 4.4.3. $\{\theta_{t|t}\}_{t \in \mathbb{N}} \in \mathbb{R}^q$ *is unconditionally unbiased if* $\mathbb{E}_{p(Y_{1:t})}[B_{t|t}^{\star}] = 0$, *and conditionally unbiased if* $B_{t|t}^{\star} = 0$ *almost surely. The estimate which is both conditionally and unconditionally unbiased is an unbiased estimate.*

Bias in $\theta_{t|t} \in \mathbb{R}^q$ can be similarly defined as Definition 4.4.3. The condition under which an identification method delivers unbiased parameter estimate is discussed next.

Theorem 4.4.4. *Let* $\widehat{\theta}_{t|t} \in \mathbb{R}^q$ *be the estimate of* $\theta_{t|t}^{\star} \in \mathbb{R}^q$, *as computed by an identification method, where* $\theta_{t|t}^{\star} \in \mathbb{R}^q$ *is the mean of* $\theta_t|(Y_{1:t} = y_{1:t}) \sim p(\cdot|y_{1:t})$, *and let* $B_{t|t}^{\star} \in \mathbb{R}^q$ *be the corresponding conditional bias, then* $B_{t|t}^{\star} = 0$ *almost surely is only a necessary condition for* $\mathbb{E}_{p(Y_{1:t})}[B_{t|t}^{\star}] = 0$, *but necessary and sufficient for* $\mathbb{E}_{p(Y_{1:t})}[B_{t|t}^{\star}[B_{t|t}^{\star}]^{T}] = 0$.

Proof. See (Tulsyan *et al.*, 2013c) for proof.   □

Remark 4.4.5. *Theorem 4.4.4 shows that if the parameter estimate $\widehat{\theta}_{t|t} \in \mathbb{R}^q$ is unconditionally unbiased, it does not imply it is unbiased as well, but if it is conditionally unbiased, it implies $\widehat{\theta}_{t|t} \in \mathbb{R}^q$ is unbiased as well.*

The MSE for an unbiased estimate $\widehat{\theta}_{t|t} \in \mathbb{R}^q$ is given next.

Corollary 4.4.6. *Let $\widehat{\theta}_{t|t} \in \mathbb{R}^q$ be the estimate of the mean of $\theta_t|(Y_{1:t} = y_{1:t}) \sim p(\cdot|y_{1:t})$ computed by a Bayesian identification method, such that $B_{t|t}^\star = 0$ almost surely, then the MSE associated with $\widehat{\theta}_{t|t} \in \mathbb{R}^q$ is $P_{t|t}^\theta = \mathbb{E}_{p(Y_{1:t})}[V_{t|t}^\star]$.*

Proof. Since $B_{t|t}^\star = 0$ almost surely is a necessary and sufficient condition for $\mathbb{E}_{p(Y_{1:t})}[B_{t|t}^\star[B_{t|t}^\star]^T] = 0$ (see Theorem 4.4.4), substituting $\mathbb{E}_{p(Y_{1:t})}[B_{t|t}^\star[B_{t|t}^\star]^T] = 0$ into (4.9) gives $P_{t|t}^\theta = \mathbb{E}_{p(Y_{1:t})}[V_{t|t}^\star]$, which completes the proof.   □

Efficiency of a Bayesian identification method is defined next.

Definition 4.4.7. *A Bayesian identification method delivering an estimate $\widehat{\theta}_{t|t} \in \mathbb{R}^q$ is efficient at $t \in \mathbb{N}$ if the estimate satisfies the equality $\text{Tr}[P_{t|t}^\theta - L_t^\theta] = 0$.*

Theorem 4.4.8. *Let $\widehat{\theta}_{t|t} \in \mathbb{R}^q$ be the estimate of $\theta_{t|t}^\star \in \mathbb{R}^q$ computed by a Bayesian method, and let $B_{t|t}^\star \in \mathbb{R}^s$ be the conditional bias in estimating $\theta_{t|t}^\star \in \mathbb{R}^q$, then $B_{t|t}^\star = 0$ almost surely is both necessary and sufficient condition for the identification method to be efficient.*

Proof. For $\widehat{\theta}_{t|t} \in \mathbb{R}^q$ satisfying $B_{t|t}^\star = 0$ almost surely, the MSE is given by $P_{t|t}^\theta = \mathbb{E}_{p(Y_{1:t})}[V_{t|t}^\star]$ (see Corollary 4.4.6). Since $P_{t|t}^\theta$ only depends on $V_{t|t}^\star$, which is the covariance of $\theta_t|(Y_{1:t} = y_{1:t}) \sim p(\cdot|Y_{1:t})$, $P_{t|t}^\theta$ cannot be reduced any further i.e., $P_{t|t}^\theta = L_t^\theta$. Thus from Definition 4.4.7 the estimator delivering $\widehat{\theta}_{t|t} \in \mathbb{R}^q$ is efficient at $t \in \mathbb{N}$.   □

Finally, the procedure to systematically assess the quality of the parameter estimates obtained with any Bayesian identification method is summarized in the next theorem.

Theorem 4.4.9. *Let $L_t^\theta \in \mathcal{S}_{++}^q$ be the PCRLB on Model 4.2.1, and let $\theta_{t|t}^\star \in \mathbb{R}^q$ and*

$V_{t|t}^\star \in \mathcal{S}_{++}^q$ be the mean and covariance of $\theta_t | (Y_{1:t} = y_{1:t}) \sim p(\cdot | y_{1:t})$. Now if $\widehat{\theta}_{t|t} \in \mathbb{R}^q$

is an estimate of $\theta_{t|t}^\star \in \mathbb{R}^q$, as computed by an identification method, such that $B_{t|t}^\star \in \mathbb{R}^q$ is

the conditional bias in estimating $\theta_{t|t}^\star \in \mathbb{R}^q$, then for $P_{t|t}^\theta \in \mathcal{S}_{++}^q$ as the associated MSE, the

quality of the estimate $\widehat{\theta}_{t|t} \in \mathbb{R}^q$ can be assessed as follows:

(a) If $B_{t|t}^\star = 0$ almost surely, then the PCRLB inequality (4.7) is given by

$$P_{t|t}^\theta = \mathbb{E}_{p(Y_{1:t})}[V_{t|t}^\star] = L_t^\theta, \tag{4.10}$$

which implies the identification method is efficient, and the corresponding estimate

$\widehat{\theta}_{t|t} \in \mathbb{R}^q$ is unbiased and MMSE.

(b) If $B_{t|t}^\star \neq 0$ almost surely, then the PCRLB inequality (4.7) is given by

$$P_{t|t}^\theta = \mathbb{E}_{p(Y_{1:t})}[V_{t|t}^\star] + \mathbb{E}_{p(Y_{1:t})}[B_{t|t}^\star [B_{t|t}^\star]'] \succ L_t^\theta, \tag{4.11}$$

which implies the identification method is not efficient, and the estimate $\widehat{\theta}_{t|t} \in \mathbb{R}^q$ is biased

(only conditionally biased if $\mathbb{E}_{p(Y_{1:t})}[B_{t|t}^\star] = 0$) and not an MMSE estimate.

Proof. The proof is based on the collective developments of Section 4.4, and is omitted

here for the sake of brevity. □

The PCRLB inequality based error analysis tool developed in this section allows

for assessment of parameter estimates obtained with Bayesian identification methods;

however, obtaining a closed form solution to (4.7) is non-trivial for Model 4.2.1. Use

of numerical methods is discussed next.

4.5   Numerical methods

It is well known that computing the MSE and PCRLB in (4.7) in closed form is non-trivial

for the model considered in (4.3) (see (Tichavský *et al.*, 1998; Bergman, 2001)). This is

because of the complex, high-dimensional integrals in the MSE with respect to $p(\theta_t, y_{1:t})$

(see Corollary 4.3.6) and in the PCRLB with respect to $p(x_{0:t}, \theta_{t-1}, y_{1:t})$ (see (4.6a) through (4.6f)) do not admit any analytical solution.

To address this issue, we use Monte Carlo (MC) perfect sampling to numerically compute the MSE and PCRLB in (4.7). For the sake of brevity, a detailed procedure for MC approximation of the PCRLB is not provided here, but can be found in (Tulsyan *et al.*, 2013*a*); however, for completeness, we provide the following example.

Example 4.5.1. *Simulating samples* $\{(\theta_t = \theta_t^j, Y_{1:t} = y_{1:t}^j)\}_{j=1}^M \sim p(\theta_t, y_{1:t})$, *M times using Model 4.2.1, starting at* M *i.i.d. initial draws from* $\{\theta_0\}_{i=1}^M \sim p(\theta_0)$ *and computing the estimates* $\{\theta_{t|t}^j\}_{j=1}^M$, *the MSE* $P_{t|t}^\theta$ *at* $t \in \mathbb{N}$ *can be approximated as*

$$\tilde{P}_{t|t}^\theta = \frac{1}{M} \sum_{j=1}^M (\theta_t^j - \theta_{t|t}^j)(\theta_t^j - \theta_{t|t}^j)^T, \tag{4.12}$$

where $\tilde{P}_{t|t}^\theta \in \mathcal{S}_{++}^q$ *is an* M*-sample MC estimate of* $P_{t|t}^\theta$.

Since (4.12) is based on perfect sampling, using strong law of large numbers $\tilde{P}_{t|t}^\theta \xrightarrow{a.s.} P_{t|t}^\theta$ as $M \to +\infty$, where $\xrightarrow{a.s.}$ denotes almost sure convergence (see (Moral, 2004)). Note that $\tilde{L}_t^\theta$, which is an M-sample MC estimate of L_t^θ can also be similarly approximated using MC sampling. Details are omitted here, but can be found in (Tulsyan *et al.*, 2013*a*). There are practical issues with the use of MC methods, as given next.

Remark 4.5.2. *With* $M < +\infty$, *the MC estimate of the MSE and PCRLB may not necessarily satisfy the positive semi definite condition* $\tilde{P}_{t|t}^\theta - \tilde{L}_t^\theta \succeq 0$ *for all* $t \in \mathbb{N}$.

Remark 4.5.3. *Since* $M < +\infty$, *the conditions in Theorem 4.4.9 are relaxed to* $|B_{t|t}^\star| \leq \epsilon$ *and* $|\mathbb{E}_{p(Y_{1:t})}[B_{t|t}^\star]| \leq \alpha$, *and* $\epsilon \in \mathbb{R}_+^q$ *and* $\alpha \in \mathbb{R}_+^q$ *are pre-defined tolerance levels set based on* M *and the required degree of accuracy.*

Remark 4.5.4. *An identification method satisfying* $|B_{t|t}^\star| \leq \epsilon$ *is* ϵ-*efficient at* $t \in \mathbb{N}$ *and the corresponding estimate is* ϵ-*unbiased and* ϵ-*MMSE (see Theorem 4.4.9(a)). Similarly, if the estimate only satisfies* $|\mathbb{E}_{p(Y_{1:t})}[B_{t|t}^\star]| \leq \alpha$, *then it is* α-*unconditionally unbiased (see Theorem 4.4.9(b)).*

4.6   Final algorithm

A systematic approach to assess the quality of a Bayesian identification method, proposed in Sections 4.3 through 4.5 is formally outlined in Algorithm 5.

4.7   Numerical illustration

In this section we use a simulated system to assess the quality of a Bayesian identification method using the procedure outlined in Algorithm 5.   A brief introduction to the identification method considered here, is given next.

4.7.1   Bayesian identification: artificial dynamics approach

Artificial dynamics approach (ADA) is a popular Bayesian identification method to compute $\{p(\theta_t|y_{1:t})\}_{t\in\mathbb{N}}$. In ADA, artificial dynamics is introduced to the otherwise static parameters, such that $\{\theta_t\}_{t\in\mathbb{N}}$ in (4.3b) evolves according to

$$\theta_{t+1}|\theta_t \sim \mathcal{N}(\cdot|\theta_t, Q_t^\theta), \tag{4.13}$$

where $\theta_{t+1}|\theta_t \sim \mathcal{N}(\cdot|\theta_t, Q_t^\theta)$ is a sequence of independent Gaussian random variable, realized independent of $\{V_t\}_{t\in\mathbb{N}}$ and $\{W_t\}_{t\in\mathbb{N}}$. By appending (4.3a) and (4.3c) with (4.13), methods such as SMC, EKF, UKF can be used to recursively compute $\{p(\theta_t|y_{1:t})\}_{t\in\mathbb{N}}$. A detailed review on ADA can be found in (Tulsyan *et al.*, 2013*b*; Kantas *et al.*, 2009).

Even though ADA is the most widely used approach amongst the class of Bayesian identification methods, there are several standing limitations of this approach as summarized in (Kantas *et al.*, 2009) (a) the dynamics of $\{\theta_t\}_{t\in\mathbb{N}}$ in (4.13) is related to the artificial noise covariance Q_t^θ, which is often difficult to tune; and (b) adding dynamics to $\{\theta_t\}_{t\in\mathbb{N}}$ modifies the original problem, which means, it is hard to quantify the bias introduced in the parameter estimates.

For the former problem, (Tulsyan *et al.*, 2013*b*) proposed an optimal rule to tune Q_t^θ for

---

Algorithm 5 Analysis of Bayesian identification methods

Module 1: Computing the lower bound for Model 4.2.1

Input: Given Model 4.2.1, define $Z_t = \{X_t, \theta_t\}$ and assume a prior density on $\{Z_t\}_{t \in \mathbb{N}}$, such that $(Z_0 = z_0) \sim p(z_0)$

Output: Lower bound on the system in Model 4.2.1

1: Generate M i.i.d. samples from the assumed prior density $Z_0 \sim p(\cdot)$, such that $\{(Z_0 = z_0^i)\}_{i=1}^{M} \sim p(z_0^i)$

2: **for** $t = 1$ to T **do**

3:    Generate M random samples from the state $\{X_t = x_t^i | (Z_{t-1} = z_{t-1})\}_{i=1}^{M} \sim p(x_t^i | z_{t-1})$ using (4.3a)

4:    Generate M random samples from the parameters $\{\theta_t = \theta_t^i | (Z_{t-1} = z_{t-1})\}_{i=1}^{M} \sim p(\theta_t^i)$ using (4.3b). Note that in this step $\theta_t^i = \theta_0^i$ for all $1 \le i \le M$ (see (4.3b))

5:    Generate M random samples from the measurements $\{Y_t = y_t^i | (Z_t = z_t^i)\}_{i=1}^{M} \sim p(y_t^i | z_t^i)$ using (4.3c)

6:    Compute an M-sample MC estimate of $\tilde{J}_t^z$

7:    Compute an M-sample MC estimate of $\tilde{L}_t^\theta$

8: **end for**

Module 2: Computing Bayesian parameter estimates

Input: Measurement sequences from Module 1, denoted as $\{(Y_{1:T} = y_{1:T}^i)\}_{i=1}^{M}$ and a Bayesian identification method, which can compute $\{p(\theta_t | y_{1:t})\}_{t \in \mathbb{N}}$ (e.g., SMC, MCMC, EKF, and UKF)

Output: Parameter estimates

9: **for** $i = 1$ to M **do**

10:    **for** $t = 1$ to T **do**

11:       Compute $p(\theta_t | y_{1:t}^i)$ using an identification method and denote density approximation by $\tilde{p}(\theta_t | y_{1:t}^i)$

12:       Using $\tilde{p}(\theta_t | y_{1:t}^i)$, compute parameter point estimate as $\theta_{t|t}^i = \mathbb{E}_{\tilde{p}(\theta_t | Y_{1:t}^i)}[\theta_t]$

13:    **end for**

14: **end for**

Module 3: Error Analysis of Bayesian identification method

Input: Parameter sequences from Module 1, denoted by $\{(\theta_{1:T} = \theta_{1:T}^i)\}_{i=1}^{M}$ and their estimates from Module 2, denoted as $\{(\theta_{t|t} = \theta_{t|t}^i)\}_{i=1,t=1}^{M,T}$. Matrices $\tilde{L}_t^\theta \in \mathcal{S}_{++}^q$ and $\tilde{P}_{t|t}^\theta \in \mathcal{S}_{++}^q$ and tolerance level $\epsilon \in \mathbb{R}_+^q$ and $\alpha \in \mathbb{R}_+^q$

Output: Error analysis of identification method

15: **for** $t = 1$ to T **do**

16:    Compute an M-sample MC estimate of $\tilde{P}_{t|t}^\theta$

17:    Compare $\tilde{P}_{t|t}^\theta$ against $\tilde{L}_t^\theta$

18:    Compute $\{B_{t|t}^{\star,i}\}_{i=1}^{M}$ and compare against $\epsilon \in \mathbb{R}_+^q$

19:    Compute an M-sample MC estimate of $\mathbb{E}_{p(Y_{1:t})}[B_{t|t}^\star]$ and compare against $\alpha \in \mathbb{R}_+^q$

20:    Use Theorem 4.4.9 for error analysis

21: **end for**

---

all $t \in \mathbb{N}$; however, for the later problem, we will see how the developments of this chapter can be used to assess the quality of ADA based Bayesian methods.

4.7.2 Simulation setup

Consider a univariate, non stationary, non-linear stochastic SSM (Tulsyan *et al.*, 2013*a*)

$$X_{t+1} = aX_t + \frac{X_t}{b + X_t^2} + u_t + V_t, \quad V_t \sim \mathcal{N}(0, Q_t), \tag{4.14a}$$

$$Y_t = cX_t + dX_t^2 + W_t, \qquad W_t \sim \mathcal{N}(0, R_t), \tag{4.14b}$$

where $\theta \triangleq [a\ b\ c\ d]$ is a vector of unknown static model parameters. The noise covariances are constant, and selected as $Q_t = 10^{-3}$ and $R_t = 10^{-3}$ for all $t \in [1, T]$, where $T = 300$. $\{u_t\}_{t\in[1,T]}$ is a sequence of optimal input (see (Tulsyan *et al.*, 2013*a*)). For Bayesian identification of θ, we define $\{\theta_t = \theta_{t-1}\}_{t\in[1,T]} = \theta$ as a stochastic process, such that $Z_t = \{X_t,\ \theta_t\}$ is a $\mathcal{Z}$ valued extended Markov process with $Z_0 \sim \mathcal{N}(z_m, z_c)$, where $z_m = [1\ 0.7\ 0.6\ 0.5\ 0.4]$, $z_c = \mathrm{diag}(0.01,\ 0.01,\ 0.01,\ 0.01,\ 0.01)$. Starting at $t = 0$, we are interested in assessing the ADA based SMC method proposed in (Tulsyan *et al.*, 2013*b*).

4.7.3 Results

Using $M = 1000$ MC simulations, we compute the PCRLB for (4.14) using Module 1 of Algorithm 5. Figure 4.1 gives the diagonal entries of $\{\tilde{L}_t^\theta\}_{t\in[1,T]}$. Note that amongst the four PCRLBs, the PCRLB for b is the highest for all $t \in [1, T]$. This suggest estimation difficulties with parameter b. This result is not surprising, since (4.14) is non-linear in parameter b; however, the overall decaying trend of PCRLBs in Figure 4.1 suggests that starting with $\theta_0 \sim p(\theta_0)$, theoretically, it is possible for a Bayesian identification method to reduce the MSE associated with the parameter estimates. Figure 4.2 compares the PCRLB against the MSE for b and d, computed using Module 2 of Algorithm 5. Despite the MC approximations involved, the MSE is greater than the PCRLB at all sampling time instants (see Remark 4.5.2) and Figure 4.2). It is instructive to highlight that at $T = 300$, the MSE
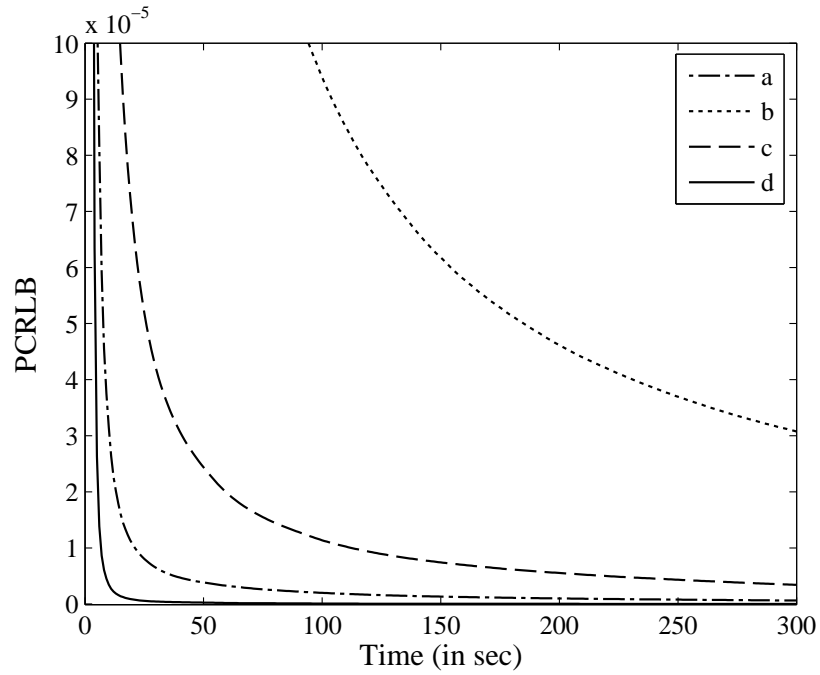
Figure 4.1: PCRLB for parameters as a function of time. Note that the vertical axis has been appropriately scaled for clarity.
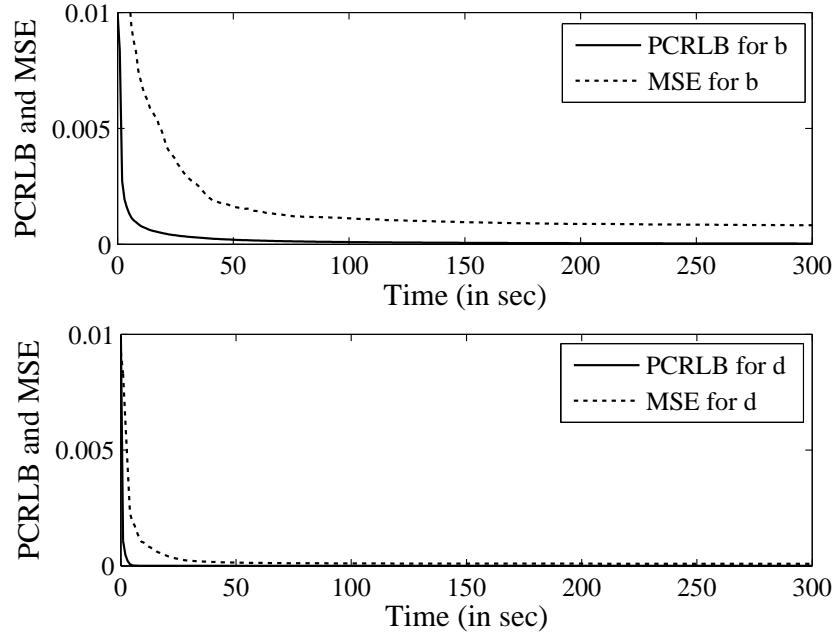
Figure 4.2: Comparing PCRLB against the MSE computed using the ADA based SMC identification method. Graphs are shown only for parameters b and d. Results for a and c are similar.

associated with the estimation of d is about 89% less than that for b, which validates the claim made earlier about estimation difficulties with parameter b. It is also important to point that for the ADA based SMC method, $\text{Tr}[\tilde{P}^\theta_{t|t} - \tilde{L}^\theta_t] \neq 0$ for all $t \in [1, T]$. Since the ADA based SMC method fails to satisfy the condition in Definition 4.4.7, it is not efficient, and therefore requires error analysis.

Figures 4.3 and 4.4 give the conditional and unconditional bias with ADA based SMC method. The results are obtained using Module 3 of Algorithm 5. Based on an assumed tolerance level $\epsilon = [0.01;\ 0.01;\ 0.01;\ 0.01]$ and $\alpha = [0.001;\ 0.001;\ 0.001;\ 0.001]$, in the interval $t = [1, 50]$, less than 70% of the simulations are within the specified ϵ limit (see Figure 4.3). Thus from Theorem 4.4.9(b), for $t = [1, 50]$, the ADA based SMC method is not even ϵ-efficient, and fails to yield ϵ-unbiased (except for d, which is α-unconditionally unbiased, see Figure 4.4) or ϵ-MMSE estimates. Another interesting interval is $t = [100, T]$; wherein, more than 70% of the simulations are within the specified ϵ limit (except for parameter b, where only 60% of simulations are within ϵ, see Figure 4.3). Thus from Theorem 4.4.9(a), the ADA based SMC method is ϵ-efficient for all the parameters, except for b, and the resulting estimates are ϵ-unbiased and ϵ-MMSE; whereas, for b, the estimates are are not MMSE, but are α-unconditionally unbiased.

In summary, the results suggest that for model given in (4.14), the ADA based SMC method at $t = T$ yields ϵ-unbiased, ϵ-MMSE estimates for all the parameters, except for parameter b, which is only α-unconditionally unbiased.

4.8   Conclusions

A PCRLB based approach is proposed for error analysis in Bayesian identification methods of non-linear SSMs. Using the proposed tool it was illustrated how the quality of the parameter estimates obtained using artificial dynamics approach, which is a popular Bayesian identification method can be assessed in terms of bias, MSE and efficiency.
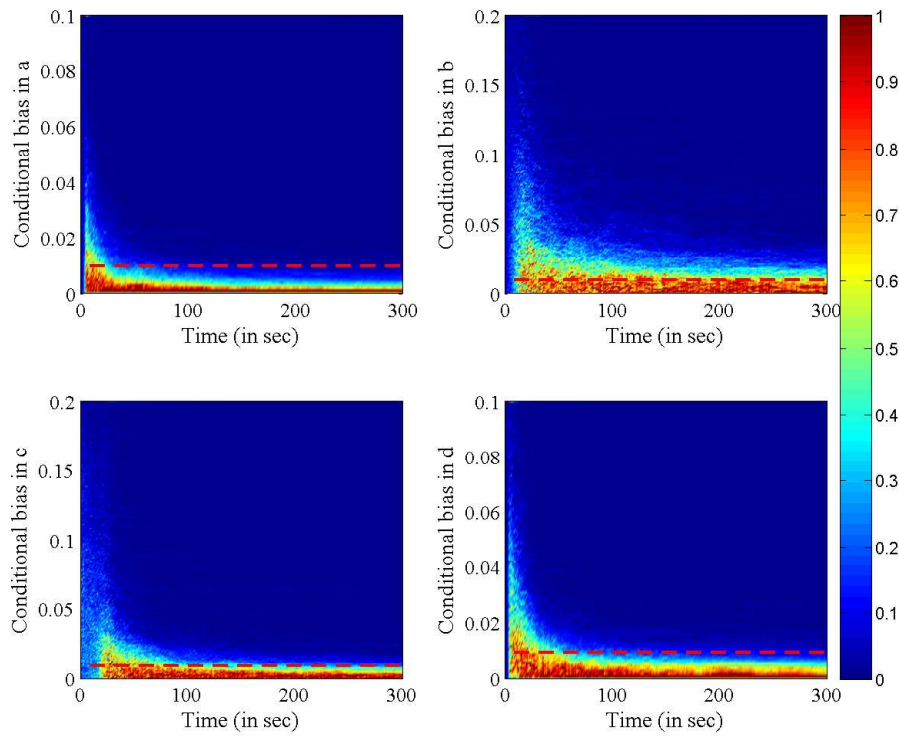
Figure 4.3: Conditional bias in parameter estimates with ADA based SMC method. The broken red line is the ϵ value.
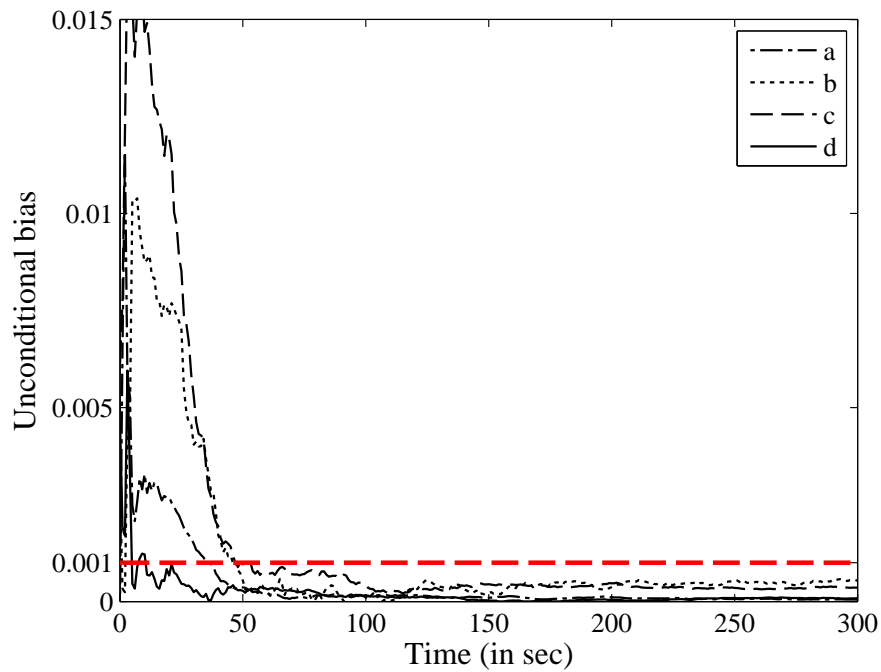
Figure 4.4: Unconditional bias in parameter estimates with ADA based SMC method. The broken red line is the α value.

Bibliography

Bapat, R.B. and T.E.S. Raghavan (1997). *Nonnegative Matrices and Applications*. Cambridge University Press, New York.

Bergman, N. (2001). *Sequential Monte Carlo Methods in Practice*. Chap. Posterior Cramér-Rao bounds for sequential estimation. Springer–Verlag, New York.

Chen, T., J. Morris and E. Martin (2005). Particle filters for state and parameter estimation in batch processes. *Journal of Process Control* **15**(6), 665–673.

Geweke, J. and H. Tanizaki (2001). Bayesian estimation of state-space models using the Metropolis–Hastings algorithm within Gibbs sampling. *Computational Statistics & Data Analysis* **37**(2), 151–170.

Jang, S.S. and R.B. Gopaluni (2011). Parameter estimation in non-linear chemical and biological processes with unmeasured variables from small data sets. *Chemical Engineering Science* **66**(12), 2774–2787.

Juloski, A.L., S. Weiland and W.P.M.H. Heemels (2005). A Bayesian approach to identification of hybrid systems. *IEEE Transactions on Automatic Control* **50**(10), 1520–1533.

Kantas, N., A. Doucet, S.S. Singh and J. Maciejowski (2009). An overview of sequential Monte Carlo methods for parameter estimation in general state-space models. In:

Proceedings of the 15th IFAC Symposium on System Identification. Saint-Malo, France. pp. 774–785.

Minvielle, P., A. Doucet, A. Marrs and S. Maskell (2010). A Bayesian approach to joint tracking and identification of geometric shapes in video sequences. *Image and Vision Computing* **28**(1), 111–123.

Moral, P. Del (2004). *Feynman-Kac Formulae: Genealogical and Interacting Particle Systems with Applications*. Springer–Verlag, New York.

Ninness, B. and S. Henriksen (2010). Bayesian system identification via Markov chain Monte Carlo techniques. *Automatica* **46**(1), 40–51.

Peterka, V. (1981). Bayesian system identification. *Automatica* **17**(1), 41–53.

Tichavský, P., C. Muravchik and A. Nehorai (1998). Posterior Cramér-Rao bounds for discrete-time non-linear filtering. *IEEE Transactions on Signal Processing* **46**(5), 1386–1396.

Trees, H.L.V. (1968). *Detection, Estimation and Modulation Theory–Part I*. Chap. Classical detection and estimation theory. Wiley, New York.

Tulsyan, A., B. Huang, R.B. Gopaluni and J.F. Forbes (2013*a*). Bayesian identification of non-linear state-space models: Part I- Input design. In: *Proceedings of 10th International Symposium on Dynamics and Control of Process Systems*. Mumbai, India.

Tulsyan, A., B. Huang, R.B. Gopaluni and J.F. Forbes (2013*b*). On simultaneous on-line state and parameter estimation in non-linear state-space models. *Journal of Process Control* **23**(4), 516–526.

Tulsyan, A., B. Huang, R.B. Gopaluni and J.F. Forbes (2013*c*). Performance assessment, diagnosis, and optimal selection of non-linear state filters. *Journal of Process Control, In Review*.

Chapter 5

Input design for Bayesian identification of non-linear state-space models

We propose an algorithm for designing optimal inputs for on-line Bayesian identification of stochastic non-linear state-space models. The proposed method relies on minimization of the posterior Cramér Rao lower bound derived for the model parameters, with respect to the input sequence. To render the optimization problem computationally tractable, the inputs are parametrized as a multi-dimensional Markov chain in the input space. The proposed approach is illustrated through a simulation example.

5.1   Introduction

Bayesian system identification has a long history, dating at least as far back as (Peterka, 1981). Despite this, it is not commonly used in practice, except for the linear, Gaussian state-space model (SSM) case; wherein, Kalman filter-based Bayesian estimation is routinely employed (Ninness and Henriksen, 2010). This is due to the computational complexities associated with the computation of the posterior densities, their marginals, and associated functions, such as posterior mean and variance (Juloski *et al.*, 2005).

Over the last decade, great progress has been made within the statistics community

in overcoming the computational issues, and making Bayesian identification tractable for a wide range of complicated models arising in demographic and population studies, image processing, and drug response modelling (Gilks *et al.*, 1995). Recent developments in methods, such as sequential Monte Carlo (SMC) and Markov chain Monte Carlo (MCMC) along with advances in computing have allowed researchers to use Bayesian methods in both on-line (Tulsyan *et al.*, 2013*b*; Chen *et al.*, 2005) and off-line (Jones *et al.*, 2011; Geweke and Tanizaki, 2001) identification of stochastic state-space models (SSMs). An exposition of off-line and on-line Bayesian methods for identification of non-linear SSMs can be found in a recent review paper by (Kantas *et al.*, 2009).

This chapter is directed towards the class of on-line methods for Bayesian identification of stochastic non-linear SSMs, the procedure for which is briefly introduced here first. Let $\{X_t\}_{t\in\mathbb{N}}$ and $\{Y_t\}_{t\in\mathbb{N}}$ be $\mathcal{X}(\subseteq \mathbb{R}^n)$ and $\mathcal{Y}(\subseteq \mathbb{R}^m)$ valued stochastic processes, and let $\{u_t\}_{t\in\mathbb{N}}$ be the sequence of inputs in $\mathbb{R}^p$, such that the state $\{X_t\}_{t\in\mathbb{N}}$ is an unobserved or unmeasured process, with initial density $p_\theta(x)$ and transition density $p_\theta(x'|x, u)$:

$$X_0 \sim p_\theta(x_0); \quad X_{t+1}|(x_t, u_t) \sim p_\theta(x_{t+1}|x_t, u_t) \quad (t \in \mathbb{N}). \tag{5.1}$$

$\{X_t\}_{t\in\mathbb{N}}$ is an unobserved process, but is observed through $\{Y_t\}_{t\in\mathbb{N}}$, such that $\{Y_t\}_{t\in\mathbb{N}}$ is conditionally independent given $\{X_t, u_t\}_{t\in\mathbb{N}}$, with marginal density $p_\theta(y|x, u)$:

$$Y_t|(x_t, u_t) \sim p_\theta(y_t|x_t, u_t) \quad (t \in \mathbb{N}). \tag{5.2}$$

θ in (5.1) and (5.2) is a vector of unknown model parameters, such that $\theta \in \Theta$ is an open subset of $\mathbb{R}^q$. All the densities are with respect to suitable dominating measures, such as Lebesgue measure. (5.1) and (5.2) represent a wide class of non-linear time-series models, the model form and the assumptions considered in this chapter are given below.

Model 5.1.1. *Consider a discrete-time, stochastic non-linear SSM:*

$$X_{t+1} = f_t(X_t, u_t, \theta_t, V_t); \tag{5.3a}$$

$$Y_t = g_t(X_t, u_t, \theta_t, W_t), \tag{5.3b}$$

where: $\{\theta_{t+1} = \theta_t\}_{t\in\mathbb{N}} = \theta$ *is a vector of unknown static model parameters, and* $\{V_t\}_{t\in\mathbb{N}}$ *and* $\{W_t\}_{t\in\mathbb{N}}$ *are state and measurement noise sequences.*

Assumption 5.1.2. $\{V_t\}_{t\in\mathbb{N}}$ *and* $\{W_t\}_{t\in\mathbb{N}}$ *are mutually independent sequences of independent random variables known a priori in their distribution classes (e.g., Gaussian) and parametrized by a known and finite number of moments.*

Assumption 5.1.3. $\{f_t; g_t\}_{t\in\mathbb{N}}$ *are such that in the open sets* $\mathcal{X}$ *and* Θ, $\{f_t; g_t\}_{t\in\mathbb{N}}$ *is* $\mathcal{C}^k(\mathcal{X})$ *and* $\mathcal{C}^k(\Theta)$, *respectively, and in* $\mathbb{R}^p$, $\{f_t; g_t\}_{t\in\mathbb{N}}$ *is* $\mathcal{C}^{k-1}(\mathbb{R}^p)$, *and in* $\mathbb{R}^n$ *and* $\mathbb{R}^m$, $\{f_t\}_{t\in\mathbb{N}}$ *is* $\mathcal{C}^{k-1}(\mathbb{R}^n)$, *and* $\{g_t\}_{t\in\mathbb{N}}$ *is* $\mathcal{C}^{k-1}(\mathbb{R}^m)$, *where* $k \geq 2$.

Assumption 5.1.4. *For any random sample* $(x_{t+1}, x_t, u_t, \theta_t, v_t) \in \mathcal{X} \times \mathcal{X} \times \mathbb{R}^p \times \Theta \times \mathbb{R}^n$ *and* $(y_t, x_t, u_t, \theta_t, w_t) \in \mathcal{Y} \times \mathcal{X} \times \mathbb{R}^p \times \Theta \times \mathbb{R}^m$ *satisfying (5.3),* $\nabla_{v_t} f_t^T(x_t, u_t, \theta_t, v_t)$ *and* $\nabla_{w_t} g_t^T(x_t, u_t, \theta_t, w_t)$ *have rank* n *and* m, *respectively, such that using implicit function theorem,* $p_\theta(x_{t+1}|x_t, u_t) = p(V_t = \tilde{f}_t(x_t, u_t, \theta_t, x_{t+1}))$ *and* $p_\theta(y_t|x_t, u_t) = p(W_t = \tilde{g}_t(x_t, u_t, \theta_t, y_t))$ *do not involve any Dirac delta functions.*

For a generic sequence $\{r_t\}_{t\in\mathbb{N}}$, let $r_{i:j} \triangleq \{r_i, r_{i+1}, \ldots, r_j\}$. Let $\theta^\star \in \Theta \subseteq \mathbb{R}^q$ be the true, but unknown parameter vector generating a measurement sequence $\{Y_{1:t} = y_{1:t}\}_{t\in\mathbb{N}}$ given $\{u_{1:t}\}_{t\in\mathbb{N}}$, such that $X_{t+1}|(x_t, u_t) \sim p_{\theta^\star}(x_{t+1}|x_t, u_t)$ and $Y_t|(x_t, u_t) \sim p_{\theta^\star}(y_t|x_t, u_t)$. In Bayesian identification of Model 5.1.1, the problem of estimating the parameter vector $\theta^\star \in \Theta \subseteq \mathbb{R}^q$ in real-time, given a sequence of input-output data $\{u_{1:t}, y_{1:t}\}_{t\in\mathbb{N}}$ is formulated as a joint state and parameter estimation problem. This is done by ascribing a prior density $\theta_0 \sim p(\theta_0)$, such that $\theta^\star \in \text{supp}\, p(\theta_0)$, and computing $\{p(z_t|u_{1:t}, y_{1:t})\}_{t\in\mathbb{N}}$, where: $Z_t \triangleq \{X_t; \theta_t\}$ is a $\mathcal{Z}(\subseteq \mathbb{R}^{s=n+q})$ valued extended Markov process with $Z_0 \sim p_{\theta_0}(x_0)p(\theta_0)$ and $Z_t|(z_{t-1}, u_{t-1}) \sim p_{\theta_{t-1}}(x_t|x_{t-1}, u_{t-1})\delta_{\theta_{t-1}}(\theta_t)$. The inference on $\{\theta_t\}_{t\in\mathbb{N}}$ then relies on the marginal posterior $\{p(\theta_t|u_{1:t}, y_{1:t})\}_{t\in\mathbb{N}}$. Although a recursive method to compute $\{p(z_t|U_{1:t}, Y_{1:t})\}_{t\in\mathbb{N}}$ is given by the optimal filtering equation, computing it or its marginal density for Model 5.1.1, in closed-form is non-trivial (Tulsyan *et al.*, 2013*b*).

There are several Bayesian methods, such as SMC, MCMC, extended Kalman filter (EKF) and unscented Kalman filter (UKF), which allow for recursive approximation of $\{p(z_t|U_{1:t}, Y_{1:t})\}_{t\in\mathbb{N}}$. Note that by a judicious choice of the input sequence $\{u_{1:t}\}_{t\in\mathbb{N}}$, $\{p(z_t|u_{1:t}, y_{1:t})\}_{t\in\mathbb{N}}$ can be 'steered' in order to yield $\{p(\theta_t|u_{1:t}, y_{1:t})\}_{t\in\mathbb{N}}$, which gives more accurate inference on $\{\theta_t\}_{t\in\mathbb{N}}$. This is called the input design problem for Bayesian identification or simply, the Bayesian input design problem. A detailed review on this subject can be found in (Chaloner and Verdinelli, 1995).

Bayesian input design for linear and non-linear regression models is an active area of research (see (Huan and Marzouk, 2012; Kück *et al.*, 2006; Müller and Parmigiani, 1995) and references cited therein); however, its extension to SSMs has been limited. Recently, Bayesian input design procedure for non-linear SSMs, where $\{X_t\}_{t\in\mathbb{N}}$ is completely observed was developed by (Tulsyan *et al.*, 2012). Despite the success with regression models, to the best of authors' knowledge, no known Bayesian input design methods are available for identification of stochastic non-linear SSMs. This is due to the unobserved state process $\{X_t\}_{t\in\mathbb{N}}$, which makes the design problem difficult to solve.

This chapter deals with the Bayesian input design for identification of stochastic non-linear systems given by Model 5.1.1. The proposed method is based on minimization of the posterior Cramér-Rao lower bound (PCRLB), derived by (Tichavský *et al.*, 1998). First, we use Monte Carlo (MC) methods to obtain an approximation of the PCRLB, and then parametrize the inputs as a multi-dimensional Markov chain in $\mathbb{R}^p$, to render the optimization problem computationally tractable. Markov chain parametrization not only allows to include amplitude constraints on the input, it can be easily implemented using a standard PID controller or any other regulator. The notation used here is given next.

Notation: $\mathbb{N} := \{1, 2, \dots\}$; $\mathbb{N}_0 := \{0\} \cup \mathbb{N}$; $\mathbb{R}^{s\times s}$ is the set of real-valued $s \times s$ matrices of cardinality $\mathrm{Card}(\mathbb{R}^{s\times s})$; $\mathcal{S}^s \subset \mathbb{R}^{s\times s}$ is the space of symmetric matrices; $\mathcal{S}_+^s$ is the cone of symmetric positive semi-definite matrices in $\mathcal{S}^s$; and $\mathcal{S}_{++}^s$ is its interior. The partial order

on $\mathcal{S}^s$ induced by $\mathcal{S}^s_+$ and $\mathcal{S}^s_{++}$ are denoted by $\succcurlyeq$ and $\succ$, respectively. $\mathbb{F}^{s\times s} \subset \mathbb{R}^{s\times s}$ is a set of $s \times s$ stochastic matrix. For $A \in \mathbb{R}^{s\times s}$, $\mathrm{Tr}[A]$ denotes its trace. For vectors $x \in \mathbb{R}^p$, $y \in \mathbb{R}^p$, and $z \in \mathbb{R}^p$, $x \leq y \leq z$ denotes element-wise inequality, and $\mathrm{diag}(y) \in \mathcal{S}^p$ is a $p \times p$ diagonal matrix with elements of $y \in \mathbb{R}^p$ as its diagonal entries. Finally, $\Delta^y_x \triangleq \nabla_x \nabla^T_y$ is a Laplacian and $\nabla_x \triangleq \left[\frac{\partial}{\partial x}\right]$ is a gradient.

5.2   Problem formulation

Bayesian input design for regression models is a well studied problem in statistics (Chaloner and Verdinelli, 1995); wherein, the problem is often formulated as follows

$$\psi(u^\star_{1:N}) = \max_{u_{1:N}\in\mathbb{R}^{pN}} \sum_{t=1}^{N} \mathbb{E}_{p(\theta_t, Y_{1:t}|u_{1:t})}[\psi(Y_{1:t}, u_{1:t}, \theta_t)] \tag{5.4}$$

where $\{u^\star_{1:N}\}_{N\in\mathbb{N}}$ is an N-step ahead optimal input sequence, and $\psi(\cdot)$ is a utility function. When inference on $\{\theta_t\}_{t\in\mathbb{N}}$ is of interest, (Lindley, 1956) suggested using the mean-square error (MSE) as a utility function, such that

$$\psi(u^\star_{1:N}) = \max_{u_{1:N}\in\mathbb{R}^{pN}} \sum_{t=1}^{N} -\Phi(P^\theta_{t|t}(u_{1:t})), \tag{5.5}$$

where $P^\theta_{t|t}(u_{1:t}) = \mathbb{E}_{p(\theta_t, Y_{1:t}|u_{1:t})}[(\theta_t - \widehat{\theta}_{t|t})(\theta_t - \widehat{\theta}_{t|t})^T]$ is the MSE associated with the parameter estimate given by $\widehat{\theta}_{t|t} = \mathbb{E}_{p(\theta_t|u_{1:t}, Y_{1:t})}[\theta_t]$, and $\Phi : \mathcal{S}^q_{++} \to \mathbb{R}$ is a test function.

Remark 5.2.1. *For the model considered in Model 5.1.1, the marginal posterior density $\{p(\theta_t|u_{1:t}, y_{1:t})\}_{t\in\mathbb{N}}$, or the expectation with respect to it, does not admit any analytical solution, and thus, (5.5) cannot be computed in closed form.*

Remark 5.2.2. *Methods such as SMC and MCMC can be used to approximate $\{p(\theta_t|u_{1:t}, y_{1:t})\}_{t\in\mathbb{N}}$; however, it makes the computation in (5.5) formidable (Kück et al., 2006). Moreover, the input $\{u^\star_{1:N}\}_{N\in\mathbb{N}}$ is optimal only for the Bayesian estimator used to approximate $\{p(\theta_t|u_{1:t}, y_{1:t})\}_{t\in\mathbb{N}}$.*

To address the issues in Remarks 5.2.1 and 5.2.2, we propose to define a lower bound on the MSE first, and minimize the lower bound instead. The PCRLB, derived by (Tichavský *et al.*, 1998), provides a lower bound on the MSE associated with the estimation of $\{Z_t\}_{t \in \mathbb{N}}$ from $\{p(z_t|u_{1:t}, y_{1:t})\}_{t \in \mathbb{N}}$, and is given in the next lemma.

Lemma 5.2.3. *Let $\{Y_{1:t} = y_{1:t}\}_{t \in \mathbb{N}}$ be an output sequence generated from Model 5.1.1 using $\{u_{1:t}\}_{t \in \mathbb{N}}$, then the MSE associated with the estimation of $\{Z_t\}_{t \in \mathbb{N}}$ from $\{p(z_t|u_{1:t}, y_{1:t})\}_{t \in \mathbb{N}}$ is bounded from below by the following matrix inequality*

$$P_{t|t}^z \triangleq \mathbb{E}_{p(Z_t, Y_{1:t}|u_{1:t})}[(Z_t - \widehat{Z}_{t|t})(Z_t - \widehat{Z}_{t|t})^T] \succeq [J_t^z]^{-1}, \tag{5.6}$$

where: $\widehat{Z}_{t|t} = \mathbb{E}_{p(Z_t|u_{1:t}, Y_{1:t})}[Z_t]$ is an estimate of $\{Z_t\}_{t \in \mathbb{N}}$; $P_{t|t}^z \triangleq \begin{bmatrix} P_{t|t}^x & P_{t|t}^{x\theta} \\ (P_{t|t}^{x\theta})^T & P_{t|t}^\theta \end{bmatrix} \in \mathcal{S}_{++}^s$,

$J_t^z \triangleq \begin{bmatrix} J_t^x & J_t^{x\theta} \\ (J_t^{x\theta})^T & J_t^\theta \end{bmatrix} \in \mathcal{S}_{++}^s$, $[J_t^z]^{-1} \triangleq \begin{bmatrix} L_t^x & L_t^{x\theta} \\ (L_t^{x\theta})^T & L_t^\theta \end{bmatrix} \in \mathcal{S}_{++}^s$ are the MSE, posterior Fisher information matrix (PFIM), and PCRLB, respectively.

Proof. See (Tichavský *et al.*, 1998) for proof. □

A recursive approach to compute the lower bound $\{J_t^{-1}\}_{t \in \mathbb{N}}$ in Lemma 5.2.3 was derived by (Šimandl *et al.*, 2001; Tichavský *et al.*, 1998), and is given next.

Lemma 5.2.4. *Let a discrete-time, stochastic non-linear system be represented by Model 5.1.1, such that it satisfies Assumptions 5.1.2 through 5.1.4, then the PFIM $\{J_t^z\}_{t \in \mathbb{N}}$ for Model 5.1.1 can be recursively computed as follows:*

$$J_{t+1}^x = H_t^{33} - (H_t^{13})^T[J_t^x + H_t^{11}]^{-1}H_t^{13}; \tag{5.7a}$$

$$J_{t+1}^{x\theta} = (H_t^{23})^T - (H_t^{13})^T[J_t^x + H_t^{11}]^{-1}(J_t^{x\theta} + H_t^{12}); \tag{5.7b}$$

$$J_{t+1}^\theta = J_t^\theta + H_t^{22} - (J_t^{x\theta} + H_t^{12})^T[J_t^x + H_t^{11}]^{-1}(J_t^{x\theta} + H_t^{12}), \tag{5.7c}$$

where:

$$H_t^{11} = \mathbb{E}_{p(X_{0:t+1}, \theta_t, Y_{1:t+1}|u_{1:t+1})}[-\Delta_{X_t}^{X_t} \log p_t]; \tag{5.8a}$$

$$H_t^{12} = \mathbb{E}_{p(X_{0:t+1}, \theta_t, Y_{1:t+1}|u_{1:t+1})}[-\Delta_{X_t}^{\theta_t} \log p_t]; \tag{5.8b}$$

$$H_t^{13} = \mathbb{E}_{p(X_{0:t+1}, \theta_t, Y_{1:t+1}|u_{1:t+1})}[-\Delta_{X_t}^{X_{t+1}} \log p_t]; \tag{5.8c}$$

$$H_t^{22} = \mathbb{E}_{p(X_{0:t+1}, \theta_t, Y_{1:t+1}|u_{1:t+1})}[-\Delta_{\theta_t}^{\theta_t} \log p_t]; \tag{5.8d}$$

$$H_t^{23} = \mathbb{E}_{p(X_{0:t+1}, \theta_t, Y_{1:t+1}|u_{1:t+1})}[-\Delta_{\theta_t}^{X_{t+1}} \log p_t]; \tag{5.8e}$$

$$H_t^{33} = \mathbb{E}_{p(X_{0:t+1}, \theta_t, Y_{1:t+1}|u_{1:t+1})}[-\Delta_{X_{t+1}}^{X_{t+1}} \log p_t]; \tag{5.8f}$$

Also: $p_t = p(X_{t+1}|Z_t, u_t) \, p(Y_{t+1}|\theta_t, X_{t+1}, u_{t+1})$; *and* $J_0 = \mathbb{E}_{p(Z_0)}[-\Delta_{Z_0}^{Z_0} \log p(Z_0)]$.

Proof. See (Šimandl *et al.*, 2001; Tichavský *et al.*, 1998) for proof. □

Using Lemmas 5.2.3 and 5.2.4, a bound on the MSE associated with estimation of unknown model parameters $\{\theta_t\}_{t\in\mathbb{N}}$ can also be derived, as given next.

Corollary 5.2.5. *Let* $P_{t|t}^z \in \mathcal{S}_{++}^s$, $[J_t^z]^{-1} \in \mathcal{S}_{++}^s$ *be such that they satisfy the PCRLB inequality (5.6), then the MSE associated with the point estimation of* $\{\theta_t\}_{t\in\mathbb{N}}$, *computed from* $\{p(\theta_t|u_{1:t}, y_{1:t})\}_{t\in\mathbb{N}}$, *is bounded from below by the following matrix inequality*

$$P_{t|t}^\theta = \mathbb{E}_{p(\theta_t, Y_{1:t}|u_{1:t})}[(\theta_t - \widehat{\theta}_{t|t})(\theta_t - \widehat{\theta}_{t|t})^T] \succcurlyeq L_t^\theta, \tag{5.9}$$

where $L_t^\theta \in \mathcal{S}_{++}^q$ *is the lower-right sub-matrix of* $[J_t^z]^{-1} \in \mathcal{S}_{++}^s$ *in (5.6).*

Proof. The proof is based on the fact that (5.6) ensures $P_{t|t}^z - [J_t^z]^{-1} \in \mathcal{S}_+^s$. □

A recursive approach to compute $L_t^\theta \in \mathcal{S}_{++}^q$ is given next.

Theorem 5.2.6. *Let* $J_t^z \in \mathcal{S}_{++}^s$ *be the PFIM for model in Model 5.1.1 and* $L_t^\theta \in \mathcal{S}_{++}^q$ *be the lower bound on the MSE associated with the estimation of* $\{\theta_t\}_{t\in\mathbb{N}}$ *in Model 5.1.1, then given* $J_t^z \in \mathcal{S}_{++}^s$, *the lower bound* $L_t^\theta \in \mathcal{S}_{++}^q$ *at* $t \in \mathbb{N}$ *can be computed as*

$$L_t^\theta = [J_t^\theta - (J_t^{x\theta})^T (J_t^x)^{-1} J_t^{x\theta}]^{-1}, \tag{5.10}$$

where J_t^θ, $J_t^{x\theta}$ *and* J_t^x *are the PFIMs given in Lemma 5.2.4.*

Proof. The proof is based on the matrix inversion lemma (Bapat and Raghavan, 1997). □

Remark 5.2.7. *Theorem 5.2.6 shows that for Model 5.1.1,* L_t^θ *is not only a function of the PFIM for* $\{\theta_t\}_{t\in\mathbb{N}}$, *i.e.,* J_t^θ, *but it also depends on the PFIMs for* $\{X_t\}_{t\in\mathbb{N}}$, *i.e.,* $J_t^{x\theta}$ *and* J_t^x.

Formulation 5.2.8. *An* $N-$*step ahead input design problem for Bayesian identification of* $\{\theta_t\}_{t\in\mathbb{N}}$ *in Model 5.1.1 can be formulated as follows*

$$\psi(u_{1:N}^\star) = \min_{u_{1:N}\in\mathbb{R}^{pN}} \sum_{t=1}^{N} \Phi(L_t^\theta(u_{1:t})) \tag{5.11}$$

$$s.t. \quad u_{min} \leq \{u_i\}_{t\in[1,N]} \leq u_{max},$$

where $L_t^\theta(u_{1:t}) \triangleq L_t^\theta$*; and* $u_{max} \in \mathbb{R}^p$ *and* $u_{min} \in \mathbb{R}^p$ *are the maximum and minimum magnitude of the input.*

Remark 5.2.9. *The optimization problem in Formulation 5.2.8 allows to impose magnitude constraints on the inputs. Although constraints on* $(x_{0:N}) \in \mathcal{X}^{N+1}$ *and* $(y_{1:N}) \in \mathcal{Y}^N$ *are not included, but if required, they can also be appended.*

Remark 5.2.10. *Integral in (5.8), with respect to* $p(x_{0:t}, \theta_{t-1}, y_{1:t}|u_{1:t})$*, makes (5.11) independent of the random realizations from* $\mathcal{X}^{t+1}$*,* Θ*, and* $\mathcal{Y}^t$*. The optimization in (5.11) in fact only depends on: the process dynamics represented in Model 5.1.1; noise densities* $V_t \sim p(v_t)$ *and* $W_t \sim p(w_t)$*; and the choice of* $Z_0 \sim p(z_0)$ *and* $u_{1:N} \in \mathbb{R}^{pN}$*. This makes (5.11) independent of* $\theta^\star \in \Theta \subseteq \mathbb{R}^q$ *or the Bayesian estimator used for estimating* $\{\theta_t\}_{t\in\mathbb{N}}$*.*

Remark 5.2.11. *Formulation 5.2.8 yields a sequence* $\{u_{1:N}^\star\}_{N\in\mathbb{N}}$*, which is (a) optimal for all the Bayesian identification methods that approximate* $\{p(\theta_t|u_{1:t}^\star, y_{1:t})\}_{t\in\mathbb{N}}$*; and (b) independent of* $\theta^\star \in \mathbb{R}^q$ *(see Remark 5.2.10), such that the resulting input* $\{u_{1:N}^\star\}_{N\in\mathbb{N}}$ *is optimal for all* $\theta^\star \in \text{supp } p(\theta_0)$*.*

Remark 5.2.12. *The input design problem in Formulation 5.2.8 is an open-loop stochastic control problem. In order to utilize feedback in implementation, (5.11) can also be implemented using the open-loop feedback-control (OLFC) approach (see (Bertsekas, 1995)). This is done by using the information in the estimate of* $\{\theta_t\}_{t\in[1,N]}$ *to update* $\theta_0 \sim p(\theta_0)$*. Note that we will not observe OLFC implementation here.*

There are two challenges that need to be addressed in order to make (5.11) tractable: (a) computing the lower bound $\{L_t^\theta\}_{t \in \mathbb{N}}$; and (b) solving the high-dimensional optimization problem in $\mathbb{R}^{pN}$. Our approach to address the above challenges is discussed next.

5.3   Computing the lower bound

The first challenge is to compute the lower bound L_t^θ in (5.11). It is well known that computing L_t^θ in closed form is non-trivial for the model form considered in Model 5.1.1 (see (Tichavský *et al.*, 1998; Bergman, 2001)). This is because of the complex, high-dimensional integrals in (5.8a) through (5.8f), which do not admit any analytical solution.

MC sampling is a popular numerical method to solve integrals of the form $F(u_{1:t}) = \mathbb{E}_{p(X_{0:t}|u_{1:t})}[h(X_{0:t}, u_{1:t})]$, where $h : \mathcal{X}^{t+1} \times \mathbb{R}^{pt} \to \mathbb{R}$. Using M i.i.d. state trajectories $\{X_{0:t}^i|u_{1:t}\}_{i=1}^M \sim p(x_{0:t}|u_{1:t})$ generated from the density $p(x_{0:t}|u_{1:t})$, the probability distribution $p(x_{0:t}|u_{1:t})dx_{0:t} \triangleq p(dx_{0:t}|u_{1:t})$, can be approximated as

$$\tilde{p}(dx_{0:t}|u_{1:t}) = \frac{1}{M} \sum_{i=1}^M \delta_{X_{0:t}^i|u_{1:t}}(dx_{0:t}), \tag{5.12}$$

where $\tilde{p}(dx)$ is a MC estimate of $p(dx)$ and $\delta_{x_0}(dx)$ is the Dirac delta. Substituting (5.12) into $F(u_{1:t})$, we get $\tilde{F}(u_{1:t}) \triangleq \tilde{F}(\{X_{0:t}^i|u_{1:t}\}_{i=1}^M) = \int h(x_{0:t}, u_{1:t})\tilde{p}(dx_{0:t}|u_{1:t}) = \frac{1}{M} \sum_{i=1}^M h(X_{0:t}^i, u_{1:t})$, where $\tilde{F}(u_{1:t})$ is an estimate of $F(u_{1:t})$.

Remark 5.3.1. *Using MC methods, the integrals in (5.8a) through (5.8f), with respect to the density $p(x_{0:t}, \theta_{t-1}, y_{1:t}|u_{1:t})$ can be approximated by simulating M i.i.d. sample paths $\{X_{0:t}^i, \theta_{t-1}^i, Y_{1:t}^i|u_{1:t}\}_{i=1}^M \sim p(x_{0:t}, \theta_{t-1}, y_{1:t}|u_{1:t})$ using Model 5.1.1, starting at M i.i.d. initial positions drawn from $\{Z_0^i\}_{i=1}^M \sim p(z_0)$.*

Model 5.3.2. *Consider a SSM with additive Gaussian state and measurement noise*

$$X_{t+1} = f_t(X_t, \theta_t, u_t) + V_t, \tag{5.13a}$$

$$Y_t = g_t(X_t, \theta_t, u_t) + W_t, \tag{5.13b}$$

where $\{V_t\}_{t\in\mathbb{N}}$ and $\{W_t\}_{t\in\mathbb{N}}$ are mutually independent sequences of independent zero mean Gaussian random variables, such that $V_t \sim \mathcal{N}(v_t|0, Q_t)$ and $W_t \sim \mathcal{N}(w_t|0, R_t)$, where $Q_t < \infty$ and $R_t < \infty$ for all $t \in \mathbb{N}$.

Note that for Model 5.3.2, using the Markov property of the states and conditional independence of the measurements, the dimension of the integrals in (5.8a) through (5.8f) can be reduced, as given in the next theorem.

Theorem 5.3.3. *For a stochastic non-linear system represented by Model 5.3.2 and satisfying Assumptions 5.1.2 through 5.1.4, (5.8a) through (5.8f) can be written as*

$$H_t^{11} = \mathbb{E}_{p(X_t,\theta_t|u_{1:t+1})}[\nabla_{X_t} f_t^T(X_t, \theta_t, u_t)]Q_t^{-1}[\nabla_{X_t} f_t^T(X_t, \theta_t, u_t)]^T; \tag{5.14a}$$

$$H_t^{12} = \mathbb{E}_{p(X_t,\theta_t|u_{1:t+1})}[\nabla_{X_t} f_t^T(X_t, \theta_t, u_t)]Q_t^{-1}[\nabla_{\theta_t} f_t^T(X_t, \theta_t, u_t)]^T; \tag{5.14b}$$

$$H_t^{13} = \mathbb{E}_{p(X_t,\theta_t|u_{1:t+1})}[-\nabla_{X_t} f_t^T(X_t, \theta_t, u_t)]Q_t^{-1}; \tag{5.14c}$$

$$H_t^{22} = \mathbb{E}_{p(X_t,\theta_t|u_{1:t+1})}[\nabla_{\theta_t} f_t^T(X_t, \theta_t, u_t)]Q_t^{-1}[\nabla_{\theta_t} f_t^T(X_t, \theta_t, u_t)]^T$$
$$+ \mathbb{E}_{p(X_{t+1},\theta_t|u_{1:t+1})}[\nabla_{\theta_t} g_t^T(X_{t+1}, \theta_t, u_{t+1})]R_{t+1}^{-1}[\nabla_{\theta_t} g_t^T(X_{t+1}, \theta_t, u_{t+1})]^T \tag{5.14d}$$

$$H_t^{23} = \mathbb{E}_{p(X_t,\theta_t|u_{1:t+1})}[-\nabla_{\theta_t} f_t^T(X_t, \theta_t, u_t)]Q_t^{-1}$$
$$+ \mathbb{E}_{p(X_{t+1},\theta_t|u_{1:t+1})}[\nabla_{\theta_t} g_t^T(X_{t+1}, \theta_t, u_{t+1})]R_{t+1}^{-1}[\nabla_{X_{t+1}} g_t^T(X_{t+1}, \theta_t, u_{t+1})]^T \tag{5.14e}$$

$$H_t^{33} = Q_t^{-1} + \mathbb{E}_{p(X_{t+1},\theta_t|u_{1:t+1})}[\nabla_{X_{t+1}} g_t^T(X_{t+1}, \theta_t, u_{t+1})]R_{t+1}^{-1}[\nabla_{X_{t+1}} g_t^T(X_{t+1}, \theta_t, u_{t+1})]^T \tag{5.14f}$$

Proof. (5.14a): First note that the matrix (5.8a) can be alternatively written as $H_t^{11} = \mathbb{E}_{p(X_{0:t+1},\theta_t,Y_{1:t+1}|u_{1:t+1})}[-\Delta_{X_t}^{X_t} \log p_t] = \mathbb{E}_{p(X_{0:t+1},\theta_t,Y_{1:t+1}|u_{1:t+1})}[\nabla_{X_t} \log p_t][\nabla_{X_t} \log p_t]^T$ (see (Tichavský *et al.*, 1998)). On simplifying, we have $H_t^{11} = \mathbb{E}_{p(X_{t+1}|X_t,\theta_t,u_t)P(X_t,\theta_t|u_{1:t+1})}$ $[\nabla_{X_t} \log p(X_{t+1}|X_t, \theta_t, u_t)][\nabla_{X_t} \log p(X_{t+1}|X_t, \theta_t, u_t)]^T$. This is because $\nabla_{X_t} \log p(Y_{t+1}|X_{t+1}, \theta_t, u_{t+1}) = 0$. For Model 5.3.2, $\nabla_{X_t} \log p(X_{t+1}|X_t, \theta_t, u_t)$ $= [\nabla_{X_t} f_t^T(X_t, \theta_t, u_t)] \; Q_t^{-1}[X_{t+1} - f_t(X_t, \theta_t, u_t)]^T$. Substituting it into H_t^{11}, and using $E_{p(X_{t+1}|X_t,\theta_t,u_t)}[X_{t+1} - f_t(X_t, \theta_t, u_t)][X_{t+1} - f_t(X_t, \theta_t, u_t)]^T = Q_t$, we have (5.14a). Note that the expression in (5.14b) through (5.14f) can be similarly derived. □

Theorem 5.3.3 reduces the dimension of the integral in (5.8) for Model 5.3.2 from $(t + 1)(n + m) + s$ to s. Using MC sampling, (5.14a), for instance, can be computed as $\tilde{H}_t^{11} = \frac{1}{M} \sum_{i=1}^{M} [\nabla_{X_t} f^T(X_t^i, \theta_t^i, u_t)] Q_t^{-1} [\nabla_{X_t} f^T(X_t^i, \theta_t^i, u_t)]^T$. Here $\{X_t^i, \theta_t^i | u_{1:t+1}\}_{i=1}^{M} \sim p(x_t, \theta_t | u_{1:t+1})$ and $\tilde{H}_t^{11}$ is an M-sample MC estimate of H_t^{11}. Note that the MC estimates of (5.14b) through (5.14f) can be similarly computed. Substituting the MC estimates of (5.8a) through (5.8f) first into Lemma 5.2.4, and then into Theorem 5.2.6, yields

$$\tilde{L}_t^\theta = [\tilde{J}_t^\theta - (\tilde{J}_t^{x\theta})^T (\tilde{J}_t^x)^{-1} \tilde{J}_t^{x\theta}]^{-1}, \tag{5.15}$$

where $\tilde{L}_t^\theta$ is an estimate of L_t^θ, and $\tilde{J}_t^\theta$, $\tilde{J}_t^{x\theta}$ and $\tilde{J}_t^x$ are the estimates of the PFIMs in Lemma 5.2.4. Finally, substituting (5.15) into (5.11) gives the following optimization problem

$$\tilde{\psi}(u_{1:N}^\star) = \min_{u_{1:N} \in \mathbb{R}^{pN}} \sum_{t=1}^{N} \Phi(\tilde{L}_t^\theta(u_{1:t})) \tag{5.16a}$$

$$\text{s.t.} \quad u_{min} \leq \{u_i\}_{t \in [1,N]} \leq u_{max}. \tag{5.16b}$$

Theorem 5.3.4. *Let $\psi(u_{1:N}^\star)$ and $\tilde{\psi}(u_{1:N}^\star)$ be the optimal utility functions, computed by solving the optimization problem in (5.11) and (5.16), respectively, then we have*

$$\tilde{\psi}(u_{1:N}^\star) \xrightarrow[M \to +\infty]{a.s.} \psi(u_{1:N}^\star), \tag{5.17}$$

where $\xrightarrow{a.s.}$ denotes almost sure convergence.

Proof. Since (5.15) is based on perfect MC sampling, using the strong law of large numbers, we have $\tilde{L}_t^\theta \xrightarrow{a.s.} L_t^\theta$ as $M \to +\infty$. Equation (5.17) follows from this result, which completes the proof. $\qquad \square$

A natural approach to solve (5.16) is to treat $\{u_{1:N}\}_{N \in \mathbb{N}}$ as a vector of continuous variables in $\mathbb{R}^{pN}$; however, this will render (5.16) computationally inefficient for large $N \in \mathbb{N}$. A relaxation method to make (5.16) tractable is given next.

5.4   Input parametrization

To overcome the complications due to continuous valued input $\{u_t\}_{t\in\mathbb{N}} \in \mathbb{R}^p$, we discretize the input space from $\mathbb{R}^p$ to $\mathcal{U} \subseteq \mathbb{R}^p$, such that $\mathrm{Card}(\mathcal{U}) = r$, where $r = b^p$, and $b \in \mathbb{N}$ is the number of discrete values for each input in $\mathbb{R}$. If we denote $\mathcal{U} = \{s_1, \ldots, s_r\}$, then $u_{min} \le s_i \le u_{max}$, for all $1 \le i \le r$, such that (5.16) can be written as follows

$$\tilde{\psi}(u_{1:N}^{\star}) = \min_{u_{1:N}\in\mathcal{U}^N} \sum_{t=1}^{N} \Phi(\tilde{L}_t^{\theta}(u_{1:t})). \tag{5.18}$$

Although $\{u_{1:N}\}_{N\in\mathbb{N}}$ in (5.18) is defined on a discrete input space $\mathcal{U}^N$ of $\mathrm{Card}(\mathcal{U}^N) = r^N$, (5.18) is still intractable for large $N \in \mathbb{N}$. To address this, a multi-dimensional Markov chain input parametrization, first proposed by (Brighenti *et al.*, 2009), is used here.

Definition 5.4.1. *For* $k \in \mathbb{N}_0$ *and* $\mathbb{S} := \{k+1, k+2, \cdots\}$, *let* $\{U_t\}_{t\in\mathbb{S}} = \{u_{t-k:t}\}_{k\in\mathbb{N}_0}$ *be a* $\mathcal{U}^{k+1}$ *valued first-order finite Markov chain, where* $\mathrm{Card}(\mathcal{U}^{k+1}) = r^{k+1}$, *such that the sample values of* $\{U_t\}_{k\in\mathbb{N}_0, t\in\mathbb{S}\setminus\{k+1\}} \in \mathcal{U}^{k+1}$, *depend on the past only through the sample values of* $\{U_{t-1}\}_{t-1\in\mathbb{S}} \in \mathcal{U}^{k+1}$, *such that for all* $\{U_t\}_{k\in\mathbb{N}_0, t\in\mathbb{S}\setminus\{k+1\}} \in \mathcal{U}^{k+1}$ *and* $\{U_{k+1:t-1}\}_{k\in\mathbb{N}_0, t-1\in\mathbb{S}} \in \mathcal{U}^{t-1}$, *we have the following*

$$\Pr(U_t = \{u_{t-k:t}\}|U_{k:t-1} = \{u_{1:t-1}\}) = P_{\Pi}(U_t = \{u_{t-k:t}\}|U_{t-1} = \{u_{t-k-1:t-1}\}), \tag{5.19}$$

where $\Pr(\cdot)$ *is probability, and* $P_{\Pi} \in \mathbb{F}^{r^{k+1}\times r^{k+1}}$ *is a probability transition matrix.*

In Definition 5.4.1, $P_{\Pi}(U_t = s_2)|U_{t-1} = s_1)$, where $\{s_1, s_2\} \in \mathcal{U}^{k+1}$ represents the probability that the Markov chain transits from $\{U_{t-1}\}_{k\in\mathbb{N}_0, t-1\in\mathbb{S}} = s_1$ to the input state $\{U_t\}_{k\in\mathbb{N}_0, t\in\mathbb{S}\setminus\{k+1\}} = s_2$. Consider the following example.

Example 5.4.2. *For* $p = 1$, $k = 0$, *and* $b \in \mathbb{N}$, *we have* $r = b$ *and* $\mathbb{S} = \mathbb{N}$, *such that* $\{U_t\}_{t\in\mathbb{S}} = \{u_t\}$ *is a Markov chain on the input space* $\mathcal{U} = \{s_1, s_2, \ldots, s_b\}$ *of* $\mathrm{Card}(\mathcal{U}) = b$, *then the probability matrix* $P_{\Pi} \in \mathbb{F}^{b\times b}$ *can be represented as*

$$P_{\Pi} = \begin{bmatrix} p_{s_1,s_1} & p_{s_1,s_2} & \cdots & p_{s_1,s_b} \\ p_{s_2,s_1} & p_{s_2,s_2} & \cdots & p_{s_2,s_b} \\ \vdots & \vdots & & \vdots \\ p_{s_b,s_1} & p_{s_b,s_2} & \cdots & p_{s_b,s_b} \end{bmatrix},$$

where $p_{s_i, s_j} \triangleq P_{\Pi}(U_t = s_j)|U_{t-1} = s_i) \; \forall 1 \leq i, j \leq b.$

Example 5.4.3. *For $p = 1$, $k = 1$, and $b \in \mathbb{N}$, $r = b$ and $\mathbb{S} = \mathbb{N} \setminus \{1\}$, such that $\{U_t\}_{t \in \mathbb{S}} = \{u_{t-1:t}\}$ is a Markov chain on $\mathcal{U}^2 = \{\{s_1, s_1\}, \{s_1, s_2\}, \ldots, \{s_2, s_1\}, \ldots, \{s_b, s_b\}\}$ of $\mathrm{Card}(\mathcal{U}^2) = b^2$, then $P_{\Pi} \in \mathbb{F}^{b^2 \times b^2}$ can be represented as*

$$P_{\Pi} = \begin{bmatrix} p_{\{s_1,s_1\},\{s_1,s_1\}} & p_{\{s_1,s_1\},\{s_1,s_2\}} & \cdots & p_{\{s_1,s_1\},\{s_b,s_b\}} \\ p_{\{s_1,s_2\},\{s_1,s_1\}} & p_{\{s_1,s_2\},\{s_1,s_2\}} & \cdots & p_{\{s_1,s_2\},\{s_b,s_b\}} \\ \vdots & \vdots & & \vdots \\ p_{\{s_1,s_g\},\{s_1,s_1\}} & p_{\{s_1,s_g\},\{s_1,s_2\}} & \cdots & p_{\{s_1,s_g\},\{s_g,s_g\}} \\ p_{\{s_2,s_1\},\{s_1,s_1\}} & p_{\{s_2,s_1\},\{s_1,s_2\}} & \cdots & p_{\{s_2,s_1\},\{s_g,s_g\}} \\ \vdots & \vdots & & \vdots \\ \vdots & \vdots & & \vdots \\ p_{\{s_g,s_g\},\{s_1,s_1\}} & p_{\{s_g,s_g\},\{s_1,s_2\}} & \cdots & p_{\{s_g,s_g\},\{s_g,s_g\}} \end{bmatrix}.$$

where $p_{\{s_i,s_j\},\{s_l,s_m\}} \triangleq P_{\Pi}(U_t = \{s_i, s_j\})|U_{t-1} = \{s_l, s_m\}) \; \forall 1 \leq i, j, l, m \leq b.$

Assumption 5.4.4. *The Markov chain $\{U_t\}_{t \in \mathbb{S}} = \{u_{t-k:t}\}_{k \in \mathbb{N}_0}$ considered in Definition 5.4.1 is time-homogeneous.*

Assumption 5.4.5. *The Markov chain $\{U_t\}_{t \in \mathbb{S}} = \{u_{t-k:t}\}_{k \in \mathbb{N}_0}$ in Definition 5.4.1 has a prior probability distribution $U_{k+1} \sim P_{\Gamma}(\{u_{1:k+1}\})$, where P_{Γ} is a $1 \times r^{k+1}$ vector.*

Theorem 5.4.6. *For $k \in \mathbb{N}_0$ and $\mathbb{S} := \{k+1, k+2, \cdots\}$, let $\{U_t\}_{t \in \mathbb{S}} = \{u_{t-k:t}\}_{k \in \mathbb{N}_0}$ be a Markov chain defined in Definition 5.4.1, and satisfying Assumptions 5.4.4 and 5.4.5, such that $U_t|(\{u_{t-k-1:t-1}\}) \sim P_{\Pi}(\{u_{1:k+1}\}|\{u_{t-k-1:t-1}\})$ for all $t \in \mathbb{S} \setminus \{k+1\}$ and $U_{k+1} \sim P_{\Gamma}(\{u_{1:k+1}\})$ then $\{U_{k+1:N}\}_{N \in \mathbb{N}} \sim P_{\Gamma,\Pi}^{k+1:N}$ has a probability distribution*

$$P_{\Gamma,\Pi}^{k+1:N} = P_{\Gamma}(\{u_{1:k+1}\}) \prod_{t=k+2}^{N} P_{\Pi}(\{u_{t-k:t}\}|\{u_{t-k-1:t-1}\}). \tag{5.20}$$

Proof. Using probability chain rule, $U_{k+1:N} \sim P_{\Gamma,\Pi}^{k+1:N}$ can be written as

$$P_{\Gamma,\Pi}^{k+1:N} = P(\{u_{1:k+1}\}, \{u_{2:k+2}\}, \ldots, \{u_{N-k:N}\})$$

$$= P(\{u_{N-k:N}\}|\{u_{1:k+1}\}, \{u_{2:k+2}\}, \ldots, \{u_{N-k-1:N-1}\})$$

$$\times P(\{u_{1:k+1}\}, \{u_{2:k+2}\}, \ldots, \{u_{N-k-1:N-1}\}), \tag{5.21a}$$

$$= P_{\Pi_{k,r}}(\{u_{N-k:N}\}|\{u_{N-k-1:N-1}\}) P(\{u_{1:k+1}\}, \{u_{2:k+2}\}, \ldots, \{u_{N-k-1:N-1}\}), \tag{5.21b}$$

where in (5.21b), we have used the first-order Markov property of $\{U_t\}_{t\in\mathbb{S}}$. Noting the time-homogeneous property of $\{U_t\}_{t\in\mathbb{S}}$ and repeatedly appealing to the probability chain rule in (5.21b), we get (5.20), which completes the proof. $\square$

Remark 5.4.7. *From Theorem 5.4.6, it is clear that: (i) the sample values of the random variables $\{U_{k+1:N}\}_{k\in\mathbb{N}_0,N\in\mathbb{N}}$ is an ordered sequence constructed from $\{u_{1:N}\}_{N\in\mathbb{N}}$; (ii) the probability distribution of the sequence $\{U_{k+1:N}\}_{k\in\mathbb{N}_0,N\in\mathbb{N}}$ given in (5.20) is uniquely defined by P_Π and P_Γ.*

Formulation 5.4.8. *Using Definition 5.4.1 and Theorem 5.4.6, the input design problem in (5.18) can be reformulated to the following stochastic programming problem*

$$\tilde{\psi}(U^\star_{k+1:N}) = \arg\min_{P_\Pi,P_\Gamma} \left\{ \sum_{t=1}^{k+1} \Phi(\mathbb{E}_{P_\Gamma}[\tilde{L}^\theta_t(\{U_{k+1}\})]) + \sum_{t=k+2}^{N} \Phi(\mathbb{E}_{P^{k+1:t}_{\Gamma,\Pi}}[\tilde{L}^\theta_t(U_{k+1:t})]) \right\}$$
(5.22a)

$$s.t. \qquad 0 \leq P_\Pi(s_i|s_j) \leq 1 \quad \forall\, 1 \leq i,j \leq r^{k+1},$$
(5.22b)

$$\sum_{i=1}^{r^{k+1}} P_\Pi(s_i|s_j) = 1 \quad \forall\, 1 \leq j \leq r^{k+1},$$
(5.22c)

$$0 \leq P_\Gamma(s_i) \leq 1 \quad \forall\, 1 \leq i \leq r^{k+1},$$
(5.22d)

$$\sum_{i=1}^{r^{k+1}} P_\Gamma(s_i) = 1.$$
(5.22e)

Note that the expectation in (5.22a), with respect to P_Γ and $P^{k+1:t}_{\Gamma,\Pi}$ can again be approximated using a perfect MC sampling, such that

$$\tilde{P}^{k+1:t}_{\Gamma,\Pi} = \frac{1}{M_u} \sum_{i=1}^{M_u} \delta_{U^i_{k+1:t}}(U_{k+1:t})$$
(5.23)

where $\tilde{P}^{k+1:t}_{\Gamma,\Pi}$ is a M_u-sample MC approximation of $P^{k+1:t}_{\Gamma,\Pi}$. Now marginalizing (5.23), with respect to $\{U_{k+2:N}\}_{k\in\mathbb{N}_0,N\in\mathbb{N}}$ yields

$$\tilde{P}_\Gamma = \frac{1}{M_u} \sum_{i=1}^{M_u} \delta_{U^i_{k+1}}(U_{k+1}),$$
(5.24)

where $\tilde{P}_\Gamma$ is a M_u-sample MC approximation of P_Γ.

Formulation 5.4.9. *Substituting the MC approximation of $\tilde{P}_{\Gamma,\Pi}^{k+1:t}$ and $\tilde{P}_\Gamma$, given in (5.23)*

and (5.24), respectively into (5.22a) in Formulation 5.4.8 yields

$$\overline{\psi}(U_{k+1:N}^\star) = \underset{P_\Pi, P_\Gamma}{\arg\min} \frac{1}{M_u} \left\{ \sum_{t=1}^{k+1} \Phi\left(\sum_{i=1}^{M_u} \tilde{L}_t^\theta(U_{k+1}^i)\right) + \sum_{t=k+2}^{N} \Phi\left(\sum_{i=1}^{M_u} \tilde{L}_t^\theta(U_{k+1:t}^i)\right) \right\}$$
(5.25a)

$$\text{s.t.} \qquad 0 \le P_\Pi(s_i|s_j) \le 1 \quad \forall\, 1 \le i,j \le r^{k+1}, \tag{5.25b}$$

$$\sum_{i=1}^{r^{k+1}} P_\Pi(s_i|s_j) = 1 \qquad \forall\, 1 \le j \le r^{k+1}, \tag{5.25c}$$

$$0 \le P_\Gamma(s_i) \le 1 \qquad \forall\, 1 \le i \le r^{k+1}, \tag{5.25d}$$

$$\sum_{i=1}^{r^{k+1}} P_\Gamma(s_i) = 1. \tag{5.25e}$$

Note that solving the stochastic optimization problem in Formulation 5.4.9 yields

$U_{k+1:N}^\star \sim P_{\Gamma^\star,\Pi^\star}^{k+1:N}$, which is the optimal distribution of the input sequence.

Corollary 5.4.10. *Let $\overline{\psi}(U_{k+1:N}^\star)$ and $\tilde{\psi}(U_{k+1:N}^\star)$ be the optimal utility functions, computed*

by solving the optimization problem in Formulations 5.4.8 and 5.4.9, respectively, then

$$\overline{\psi}(U_{k+1:N}^\star) \xrightarrow[M_u \to +\infty]{a.s.} \tilde{\psi}(U_{k+1:N}^\star), \tag{5.26}$$

where $\xrightarrow{a.s.}$ denotes almost sure convergence.

Proof. Proof is similar to Theorem 5.3.4. $\qquad\qquad\qquad\qquad\qquad\qquad\qquad\Box$

Remark 5.4.11. *There are several advantages of using the formulation given in (5.25): (a)*

the optimization is independent of $N \in \mathbb{N}$, as the number of parameters to be estimated

are $r^{k+1}(1 + r^{k+1})$; (b) easy to include magnitude and other transition constraints on

the inputs; and (c) samples from the optimal distribution can be easily sampled, and

implemented using a PID or any classical regulator; and (d) although the input is designed

in probability domain, the input spectrum is shaped by the choice of $P_{\Pi_{k,r}}$ and $P_{\Gamma_{k,r}}$ (Bilardi

et al., *1983; Brighenti* et al., *2009).*

Algorithm 6 Input design for Bayesian identification of Model 5.1.1

1: Choose an initial value for the input design parameters $P_\Gamma = P_\Gamma^{(0)}$ and $P_\Pi = P_\Pi^{(0)}$. Set $c \leftarrow 0$.
2: **while** converged **do**
3:     **for** $i = 1$ to M_u **do**
4:         Generate a random input sequence $U_{k+1:N}^i \sim P_{\Gamma,\Pi}^{k+1:N}$ using the distribution given in (5.20).
5:         Generate M random samples of states and parameters from the prior density $\{Z_0^j\}_{j=1}^M \sim p(z_0)$.
6:         **for** $t = 1$ to N **do**
7:             Generate M random samples of the process states $\{X_t^j|(Z_{t-1}^j, u_{t-1}^i)\}_{j=1}^M \sim p(x_t|Z_{t-1}^j, u_{t-1}^i)$ and parameters $\{\theta_t^j = \theta_{t-1}^j\}_{j=1}^M$ using Model 5.1.1.
8:             Generate M random samples of the measurements $\{Y_t^j|(Z_t^j, u_t^i)\}_{j=1}^M \sim p(y_t|Z_t^j, u_t^i)$ using Model 5.1.1.
9:             Approximate the lower bound $\tilde{L}_t^\theta$ using (5.15).
10:         **end for**
11:     **end for**
12:     Evaluate the approximate cost function in (5.25a).
13:     Use any standard constrained non-linear optimization algorithm to find a new input design parameters $P_\Gamma = P_\Gamma^{(c)}$ and $P_\Pi = P_\Pi^{(c)}$. Set $c \leftarrow c + 1$.
14: **end while**

5.5 Final algorithm

In this chapter, the optimization problem in Formulation 5.4.9 is implemented through an iterative approach, that involves standard numerical solvers (Nocedal and Wright, 2006). The proposed method for input design, including the iterations in the optimization, is summarized in Algorithm 6. Next we illustrate the efficacy of the input design procedure, outlined in Algorithm 6 on a simulation example.

5.6 Numerical illustration

Consider a univariate, and non-stationary stochastic SSM (Tulsyan *et al.*, 2013*a*)

$$X_{t+1} = aX_t + \frac{X_t}{b + X_t^2} + u_t + V_t, \quad V_t \sim \mathcal{N}(0, Q_t), \tag{5.27a}$$

$$Y_t = cX_t + dX_t^2 + W_t, \qquad W_t \sim \mathcal{N}(0, R_t), \tag{5.27b}$$

where $\theta \triangleq [a \ b \ c \ d]$ is a vector of model parameters to be estimated, with $\theta^\star = [0.8 \ 0.7 \ 0.6 \ 0.5]$ being the true parameter vector. The noise covariances are selected as $Q_t = 0.01$ and $R_t = 0.01$, for all $t \in \mathbb{N}$. For Bayesian identification, $\{\theta_t = \theta_{t-1}\}_{t \in \mathbb{N}} = \theta$ in (5.25) is a random process, with $Z_t = \{X_t, \theta_t\}$, such that $Z_0 \sim \mathcal{N}(z_m, z_c)$, where $z_m = [1 \ 0.7 \ 0.6 \ 0.5 \ 0.4]$, $z_c = \text{diag}(0.01, \ 0.01, \ 0.01, \ 0.01, \ 0.01)$. Here we assume that $u_{min} \leq \{u_t\}_{t \in \mathbb{N}} \leq u_{max}$, where $u_{min} = -0.8$ and $u_{max} = 0.8$. Starting at $t = 0$, we are interested in choosing an input sequence $\{u_{1:N}\}_{N \in \mathbb{N}}$ that would eventually lead to minimization of the MSE of the parameter estimates, computed using an SMC based Bayesian estimator given in (Tulsyan *et al.*, 2013*b*). Algorithm 6 was implemented with $N = 100$, $M = 2000$, and $M_u = 2000$. The input is parametrized according to Example 5.4.2, with $g = 2$, such that $\mathcal{U} = \{u_{min}, u_{max}\}$. Here $\{U_t\}_{t \in \mathbb{N}} = \{u_t\}$ have the following initial and transition probability

$$\textbf{Case 1: } P_\Gamma = [p_1 \ 1 - p_1], \quad P_\Pi = \begin{bmatrix} p_1 & 1 - p_1 \\ 1 - p_1 & p_1 \end{bmatrix}; \tag{5.28a}$$

$$\textbf{Case 2: } P_\Gamma = [p_1 \ 1 - p_1], \quad P_\Pi = \begin{bmatrix} p_1 & 1 - p_1 \\ 1 - p_2 & p_2 \end{bmatrix}; \tag{5.28b}$$

$$\textbf{Case 3: } P_\Gamma = [p_0 \ 1 - p_0], \quad P_\Pi = \begin{bmatrix} p_1 & 1 - p_1 \\ 1 - p_2 & p_2 \end{bmatrix}, \tag{5.28c}$$

where p_i, where $i = \{0, 1, 2\}$ in Cases 1 through 3 are the probabilities. For comparison purposes, we also consider a pseudo-random binary signal, which can be represented as

$$\textbf{Case 4: } P_\Gamma = [0.5 \quad 0.5], \quad P_\Pi = \begin{bmatrix} 0.5 & 0.5 \\ 0.5 & 0.5 \end{bmatrix}. \tag{5.28d}$$

For all of the above cases, $\Phi(\cdot)$ in (5.25a) was selected as the trace. Table 5.1 gives $P_{\Gamma^\star}$ and $P_{\Pi^\star}$ for Cases 1 through 3 as computed by Algorithm 6, and Figure 5.1(a) gives the corresponding trace of the lower bound. It is clear from Table 5.1 and Figure 5.1(a) that Case 3 yields the lowest objective function value. Although the objective value for Case 2 is comparable to Case 3; Case 3 provides the most general form of the Markov chain in $\mathcal{U}$.

Figure 5.1(b) validates the quality of the designed inputs based on the performance of the Bayesian estimator. From Figure 5.1(b), it is clear that with Case 3, the estimator yields

(a) Trace of the lower bound with different input designs

(b) Trace of the MSE with different input designs
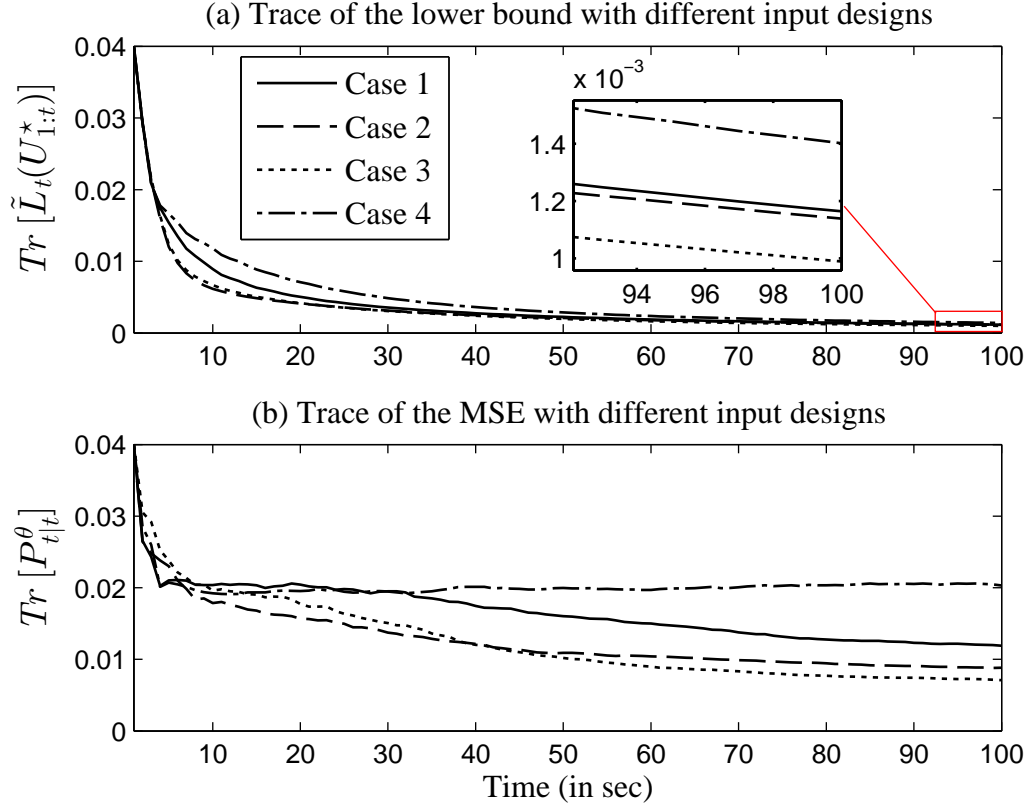
Figure 5.1: (a) Trace of the approximate lower bound; (b) trace of the MSE. Magnification of the key region of (a) is provided as inset.

the lowest trace of MSE at all sampling time. The same is also evident from Table 5.1; wherein, the sum of the trace of MSE is smallest with Case 3 as the input. The Results are based on 500 MC simulations, starting with 500 i.i.d. input path trajectories generated from $\{U_{1:N}\} \sim P^{1:N}_{\Gamma^\star,\Pi^\star}$ for Cases 1 through 4. If required, a more rigorous validation of the designed input can be performed using the approach proposed in (Tulsyan *et al.*, 2013*a*).

The results appear promising; however, we faced problems in solving the optimization. As discussed earlier, (5.25) is a stochastic programming problem, as a result (5.25a) tends to be non-smooth, and have many local minima. In future, we will consider use of stochastic gradient-based methods.

Table 5.1: Results as computed by Algorithm 6.

	Case 1	Case 2	Case 3	Case 4
p_0	N.A.	N.A.	0.34	N.A.
p_1	0.62	0.63	0.61	N.A.
p_2	N.A.	0.92	0.72	N.A.
$\overline{\psi}(U_{1:100}^{\star})$	0.42	0.37	0.36	0.51
$\sum_{t=1}^{100} \mathrm{Tr}[P_{t|t}^{\theta}]$	1.66	1.27	1.25	2.02

5.7   Conclusions

An algorithm for input design for Bayesian identification of stochastic non-linear SSM is proposed. The developed algorithm is based on minimization of the PCRLB with respect to inputs. One of the distinct advantages of the proposed method is that the designed input is independent of the Bayesian estimator used for identification. Simulation results suggest that the method can be used to deliver accurate inference on the parameter estimates.

Bibliography

Bapat, R.B. and T.E.S. Raghavan (1997). *Nonnegative Matrices and Applications*. Cambridge University Press, New York.

Bergman, N. (2001). *Sequential Monte Carlo Methods in Practice*. Chap. Posterior Craḿer-Rao bounds for sequential estimation. Springer–Verlag, New York.

Bertsekas, D.P. (1995). *Dynamic Programming and Optimal Control*. Athena Scientific.

Bilardi, G., R. Padovani and G. Pierobon (1983). Spectral analysis of functions of Markov chains with applications. *IEEE Transactions on Communications* **31**(7), 853–861.

Brighenti, C., B. Wahlberg and C.R. Rojas (2009). Input design using Markov chains for system identification. In: *Proceedings of the 48th IEEE Conference on Decision and Control and 28th Chinese Control Conference*. Shanghai, China. pp. 1557–1562.

Chaloner, K. and I. Verdinelli (1995). Bayesian experimental design: A review. *Statistical Science* **10**(3), 273–304.

Chen, T., J. Morris and E. Martin (2005). Particle filters for state and parameter estimation in batch processes. *Journal of Process Control* **15**(6), 665–673.

Geweke, J. and H. Tanizaki (2001). Bayesian estimation of state-space models using the Metropolis–Hastings algorithm within Gibbs sampling. *Computational Statistics & Data Analysis* **37**(2), 151–170.

Gilks, W.R., S. Richardson and D. Spiegelhalter (1995). *Markov Chain Monte Carlo in Practice*. Chapman & Hall.

Huan, X. and Y.M. Marzouk (2012). Simulation-based optimal Bayesian experimental design for non-linear systems. *Journal of Computational Physics* **232**(1), 288–317.

Jang, S.S. and R.B. Gopaluni (2011). Parameter estimation in non-linear chemical and biological processes with unmeasured variables from small data sets. *Chemical Engineering Science* **66**(12), 2774–2787.

Juloski, A.L., S. Weiland and W.P.M.H. Heemels (2005). A Bayesian approach to identification of hybrid systems. *IEEE Transactions on Automatic Control* **50**(10), 1520–1533.

Kantas, N., A. Doucet, S.S. Singh and J. Maciejowski (2009). An overview of sequential Monte Carlo methods for parameter estimation in general state-space models. In: *Proceedings of the 15th IFAC Symposium on System Identification*. Saint-Malo, France. pp. 774–785.

Kück, H., N. de Freitas and A. Doucet (2006). SMC samplers for Bayesian optimal non-linear design. In: *Proceedings of the IEEE non-linear Statistical Signal Processing Workshop*. Cambridge, UK. pp. 99–102.

Lindley, D.V. (1956). On a measure of the information provided by an experiment. *The Annals of Mathematical Statistics* **27**(4), 986–1005.

Müller, P. and G. Parmigiani (1995). Optimal design via curve fitting of Monte Carlo experiments. *Journal of the American Statistical Association* **90**(432), 1322–1330.

Ninness, B. and S. Henriksen (2010). Bayesian system identification via Markov chain Monte Carlo techniques. *Automatica* **46**(1), 40–51.

Nocedal, J. and S.J. Wright (2006). *Numerical Optimization: Springer Series in Operations Research*. Springer, New York.

Peterka, V. (1981). Bayesian system identification. *Automatica* **17**(1), 41–53.

Tichavský, P., C. Muravchik and A. Nehorai (1998). Posterior Cramér-Rao bounds for discrete-time non-linear filtering. *IEEE Transactions on Signal Processing* **46**(5), 1386–1396.

Tulsyan, A., B. Huang, R.B. Gopaluni and J.F. Forbes (2013*a*). Bayesian identification of non-linear state-space models: Part II- Error Analysis. In: *Proceedings of the 10th International Symposium on Dynamics and Control of Process Systems, In Review*. Mumbai, India.

Tulsyan, A., B. Huang, R.B. Gopaluni and J.F. Forbes (2013*b*). On simultaneous on-line state and parameter estimation in non-linear state-space models. *Journal of Process Control* **23**(4), 516–526.

Tulsyan, A., J.F. Forbes and B. Huang (2012). Designing priors for robust Bayesian optimal experimental design. *Journal of Process Control* **22**(2), 450–462.

Šimandl, M., J. Královec and P. Tichavský (2001). Filtering, predictive and smoothing Crámer-Rao bounds for discrete-time non-linear dynamic systems. *Automatica* **37**(11), 1703–1716.

Chapter 6

Designing priors for robust Bayesian optimal input design

Building mathematical models is a common task in process systems engineering; wherein, parameter estimation is often the final step of the modelling exercise. Model based input design has evolved as a potential statistical tool for reducing uncertainties in the parameter estimates. Designing optimal experiments for parameter estimation in non-linear dynamical systems is still an open research problem. Often a huge volume of process information is generated as an end result of an experiment design. This chapter deals with how information available a priori, can be organized and systematically used under the Bayesian framework for designing optimal experiments. Several novel techniques for organizing a priori process knowledge are also explored from a theoretical view point. The influence of the proposed prior designs on parameter estimates is demonstrated on a semi-continuous Baker's yeast fermenter problem.

6.1 Introduction

In last few decades, dynamic modelling has attracted a lot of interest amongst researchers in both academia and industries. These dynamic models are useful in describing the underlying chemical, physical or biological laws governing the process. Thus, obtaining a

reliable model is very important from product design, optimization and control perspective. The capability of a model to mimic a real system, depends heavily on its structural parameters, thereby making it of paramount interest to estimate them precisely. Both parameter estimation and model validation exercises require sampling of appropriate experimental data set; however, conducting experiments is expensive both in terms of time and resources. This motivates the need to design informative input with limited resources (e.g., materials, cost, analyses and time).

Classical input design methods aim at systematic minimization of the joint confidence region formed by the estimates in the parameter space. Design criteria developed based on this principle can be found in (Box and Lucas, 1959; Hill and Hunter, 1974). Earlier, the research in input design was more focussed for linear and non-linear steady-state models (Box and Lucas, 1959; Hill *et al.*, 1968; Box, 1970). Later, (Draper and Hunter, 1966) extended its use to multi-response models. Eventually, the potential of input design for dynamical systems was recognized by (Mehra, 1974; Goodwin and Payne, 1977). Relevant work in input design for identification of state-space models (SSMs) was presented by (Hosten and Emig, 1975; Espie and Macchietto, 1989). An excellent review on classical input design for both steady-state and dynamic models can be found in (Franceschini and Macchietto, 2008*a*).

The concept of Bayesian alphabetical input design evolved in parallel with the classical input design (Draper and Hunter, 1967*a*; Draper and Hunter, 1967*b*). In the Bayesian approach, the input design criterion is formulated based on available a priori process information. In (Chaloner and Verdinelli, 1995), the authors provide a good review on Bayesian input design for both linear and non-linear models.

Unlike the standard input design, the robust version of the classical and Bayesian design criteria accounts for the uncertainties in the parameter information available a priori. Ignoring parameter uncertainties often yields sub-optimal or even poor designs, as

pointed out by (Walter and Pronzato, 1990). In (Fedorov, 1972; Fedorov, 1980; Goodwin and Payne, 1977), the authors consider taking mathematical expectation of the design criterion over the prior parameter space; however, evaluating the expectation is a non-trivial problem as it often lacks an analytical solution. To avoid evaluating multiple integrals, (Mehra, 1974) suggested approximating the information matrix directly, or its determinant (Ng and Goodwin, 1976) by a second order expansion term around the available parameter estimate. Unfortunately, these methods result in only approximate solution, as pointed by (Walter and Pronzato, 1990). Recently, (Asprey and Macchietto, 2002) used a robust version of classical D-optimal criterion to design dynamic input. The authors in (Asprey and Macchietto, 2002) summarized the parameter uncertainty under a Gaussian distribution, and used a 3-point multi-dimensional Gauss quadrature rule to numerically approximate the expectation. To simplify the case further, (Asprey and Macchietto, 2002) ignored information on parameter correlations while setting up the Gaussian distribution. Several drawbacks of using the quadrature rule as emphasized by Geweke (Geweke, 1996) include: 1) results are adequate only in lower dimensional marginals of the functions; 2) the integrand should be smooth to apply the tensor product rule; and 3) the method suffers from the curse of dimensionality. Moreover, classical input design criterion adopted by (Asprey and Macchietto, 2002), in general lacks the necessary mathematical framework to include prior process information, which is often desirable in designing informed input.

This chapter considers a robust Bayes' ED-optimal input design for sequential identification of deterministic SSMs. The sequential Bayesian setting helps in designing the input sequence based on process and parameter information amassed from previous experiments. To circumvent the limitations of the quadrature rule, the complex, multi-dimensional integrals are numerically approximated used Monte Carlo methods. This class of numerical techniques provides (Veach, 1977) higher convergence rates in all dimensions, irrespective of the smoothness of integrand and an easy two-step implementation process

requiring appropriate sampling and point evaluation.

We propose evaluating the expectation of the Bayesian design criterion over the parameter space defined based on information available from previous input design. Often, for real processes, hyper-rectangular constraints in the form of upper and lower bounds are available a priori for model parameters. Failing to contain the parameter space within the specified hyper-rectangular constraint has serious drawbacks in robust input design, including: 1) the information contributed by samples outside the hyper-rectangular constraints may be misleading; 2) implementing the computed design based on infeasible sampled points may result in unexpected results, such as unstable dynamics; and 3) sampling from a larger parameter space, by ignoring the hyper-rectangular constraints may make the design computationally more intensive.

In order to address the above issues, we need to systematically organize parameter information available from previous input design into the hyper-rectangular constraints. This is important for achieving an efficient integration of available parameter information with the input design algorithm. The key challenge is to map information from original parameter space to a smaller sub-space with minimal loss of information. In this chapter, we propose three different projection techniques: circular, truncated and directional. These prior designs differ in the way they project information unto the constrained space. Finally, the effectiveness of all three priors in estimating parameters of a Baker's yeast fermenter model is demonstrated.

6.2   Problem formulation

This chapter considers the problem of Bayesian input design for parameter estimation in the following class of non-linear systems.

Model 6.2.1. *Consider a discrete-time, non-linear deterministic SSM given by*

$$x_{t+1} = f(x_t, u_t, \bar{u}, \theta, t), \tag{6.1a}$$

$$Y_t = g(x_t, \theta) + W_t, \tag{6.1b}$$

where $x_t \in \mathcal{X} \subseteq \mathbb{R}^n$ and $Y_t \in \mathcal{Y} \subseteq \mathbb{R}^m$ are the state variables and system outputs, respectively. Also, $u_t \in \mathcal{U} \subseteq \mathbb{R}^p$ and $\bar{u} \in \mathcal{W} \subseteq \mathbb{R}^q$ are the exogenous control variables and time-invariant control parameters (e.g., initial condition, sampling rate), respectively. Also, $\theta \in \Theta \subseteq \mathbb{R}^r$ is a set of unknown model parameters, such that $\theta_{LB} \leq \theta \leq \theta_{UB}$, where θ_{LB} and θ_{UB} are the hyper-rectangular parameter constraints, assumed to be known a priori. $W_t \in \mathbb{R}^m$ is the measurement noise, assumed to follow a zero-mean, finite variance Gaussian distribution, such that $W_t \sim \mathcal{N}(w_t|0, R)$. f and g are n and m dimensional non-linear state and output vector function, respectively, such that f and g are at least one time differentiable with respect to $x_t \in \mathcal{X}$ and $\theta \in \Theta$.

For Model 6.2.1, let $\eta_t = \{u_t, \bar{u}, x_0\}$ be a set of design variables, such that $\eta_t \in \zeta$, where x_0 is the initial condition for state variables and ζ is the feasible design space. The problem addressed in this chapter is discussed next.

Problem 6.2.2. *To design sequential Bayesian input, which would provide a maximally precise Bayesian estimate of $\theta \in \Theta$ using a set of sampled input-output data.*

6.3   Sequential Bayesian input design

Sequential Bayesian input design is an iterative procedure in which the information available at the current time step is used for designing input for the next run. In this section, we consider a robust Bayesian sequential design criterion for parameter estimation in processes represented by Model 6.2.1.

Definition 6.3.1. *Let a N sample data set from experiment k be denoted as $\mathcal{D}^{(k)} = \{\eta_{1:N}^{(k)}, y_{1:N}^{(k)}\}$, where $y_{1:N}^{(k)} = \{y_1^{(k)}, y_2^{(k)}, \ldots, y_N^{(k)}\}^T$ is a set of observed outputs*

corresponding to the design sequence $\eta_{1:N}^{(k)} = \{\eta_1^{(k)}, \eta_2^{(k)}, \ldots, \eta_N^{(k)}\}^T$. *Let* $\widehat{\theta}^{(k)} \in \mathbb{R}^r$ *be a Bayesian estimate computed based on the data set* $\mathcal{D}^{(k)}$, *then the design* $\eta_{1:N}^{(k+1)}$ *for experiment* $k + 1$ *based on Bayesian ED-optimal design can be computed as*

$$\eta_{1:N}^{(k+1)} = \underset{\eta_{1:N}^{(k+1)} \in \zeta}{\arg\max} \ \mathbb{E}_{p(\theta)} |M(\eta_{1:N}^{(k+1)}, \theta)|, \tag{6.2}$$

where $M(\eta_{1:N}^{(k+1)}, \theta)|$ *is a Bayesian information matrix, which is inverse of the covariance of the parameter posterior density;* $p(\theta)$ *is the prior density associated with the parameters;* $\mathbb{E}_{p(\cdot)}$ *denotes expectation with respect to the density* $p(\cdot)$; *and* $|\cdot|$ *is the determinant.*

Based on Definition 6.3.1, a sequential Bayesian design problem aims at finding an optimal design, which minimizes the covariance of the parameter posterior density.

Remark 6.3.2. *The input design obtained by solving the optimization in Definition 6.3.1 is robust as it accounts for uncertainties associated with estimation of* θ. *Note that* $p(\theta)$ *in (6.2) is a prior density, which can be constructed based on experiment* k *results.*

Derivation of the Bayesian information matrix for Model 6.2.1 is discussed next.

6.3.1   Bayesian information matrix

In this section, we derive an analytical expression for the Bayesian information matrix or the posterior covariance used in Definition 6.3.1. First attempt to derive such a covariance expression was made by (Draper and Hunter, 1967*b*) for static input-output, non-linear models. (Zullo, 1991) later extended the results for dynamic non-linear models.

We present a rigorous derivation of the posterior covariance of the parameters of Model 6.2.1. This allows us to introduce the prior design problem addressed in this chapter. Consider a set of sampled data from experiment k, represented by $\mathcal{D}^{(k)} = \{\eta_{1:N}^{(k)}, y_{1:N}^{(k)}\}$. Using Bayes' rule, the parameter posterior density at experiment k can be computed as

$$p(\theta|\mathcal{D}^{(k)}) \propto p(y_{1:N}^{(k)}|\theta, \eta_{1:N}^{(k)}) p(\theta|\eta_{1:N}^{(k)}), \tag{6.3a}$$

$$\propto p(y_{1:N}^{(k)}|\theta, \eta_{1:N}^{(k)}) p(\theta), \tag{6.3b}$$

where: $p(\theta|\mathcal{D}^{(k)})$ is the posterior density for the parameters; $p(y^{(k)}_{1:N}|\theta, \eta^{(k)}_{1:N})$ is a likelihood function; and $p(\theta)$ is a prior density, available from previous input design, independent of $\eta^{(k)}_{1:N}$. Note that the posterior density $p(\theta|\mathcal{D}^{(k)})$ in (6.3b) summarizes our knowledge of $\theta \in \Theta$ based on information available from experiment k. In absence of no or limited a priori knowledge about the parameters, a uniform or Gaussian prior density can be assumed for $\theta \in \Theta$. This chapter assumes that (6.3b) is a Gaussian density, such that

$$p(\theta|\mathcal{D}^{(k)}) \propto \exp\left(-\frac{1}{2}[\theta - \widehat{\theta}^{(k)}]^T \Sigma^{-1}_{\theta^{(k)}}[\theta - \widehat{\theta}^{(k)}]\right), \tag{6.4}$$

where $\widehat{\theta}^{(k)}$ and $\Sigma_{\theta^{(k)}}$ are the mean and covariance of $\theta|\mathcal{D}^{(k)} \sim p(\theta|\mathcal{D}^{(k)})$ in (6.3b).

Remark 6.3.3. *Note that for Model 6.2.1, the normality assumption of the posterior density is valid for the choice of uniform or normal prior density in (6.3b) (Bard, 1974).*

Now, if we consider a set of data $\mathcal{D}^{(k+1)} = \{\eta^{(k+1)}_{1:N}, y^{(k+1)}_{1:N}\}$ from experiment $j+1$, sampled independent of $\mathcal{D}^{(k)}$ then the posterior density in (6.3b) can be updated as

$$p(\theta|\mathcal{D}^{(k)}, \mathcal{D}^{(k+1)}) \propto p(y^{(k+1)}_{1:N}|\theta, \eta^{(k+1)}_{1:N}, \mathcal{D}^{(k)})p(\theta|\eta^{(k+1)}_{1:N}, \mathcal{D}^{(k)}) \tag{6.5a}$$

$$\propto p(y^{(k+1)}_{1:N}|\theta, \eta^{(k+1)}_{1:N})p(\theta|\mathcal{D}^{(k)}) \tag{6.5b}$$

Note that in sequential Bayesian design framework, the prior density $p(\theta|\mathcal{D}^{(k)})$ in (6.5b) is given by (6.4). Now for Model 6.2.1, the joint likelihood function in (6.5b) for independent and identically distributed observations $y^{(k+1)}_{1:N}$ is given by

$$p(y^{(k+1)}_{1:N}|\theta, \eta^{(k+1)}_{1:N}) \propto \exp\left(-\frac{1}{2}\sum_{t=1}^{N}[y^{(k+1)}_t - g(x^{(k+1)}_t, \theta)]^T R^{-1}[y^{(k+1)}_t - g(x^{(k+1)}_t, \theta)]\right), \tag{6.6}$$

where R^{-1} is the covariance of $W_t \sim \mathcal{N}(w_t|0, R)$, assumed to be constant across $k \in \mathbb{N}$. Substituting (6.4) and (6.6) into (6.5b), we obtain

$$p(\theta|\mathcal{D}^{(k)}, \mathcal{D}^{(k+1)}) \propto \exp\left(-\frac{1}{2}\sum_{t=1}^{N}[y^{(k+1)}_t - g(x^{(k+1)}_t, \theta)]^T R^{-1}[y^{(k+1)}_t - g(x^{(k+1)}_t, \theta)]\right.$$
$$\left. -\frac{1}{2}[\theta - \widehat{\theta}^{(k)}]^T \Sigma^{-1}_{\theta^{(k)}}[\theta - \widehat{\theta}^{(k)}]\right). \tag{6.7}$$

Let $\widehat{\theta}^{(k+1)}$ be the mean of $\theta|(\mathcal{D}^{(k)}, \mathcal{D}^{(k+1)}) \sim p(\theta|\mathcal{D}^{(k)}, \mathcal{D}^{(k+1)})$ computed using (6.7). Now linearizing $g(x_t^{(k+1)}, \theta)$ around $\widehat{\theta}^{(k+1)}$ using a first-order Taylor series, we have

$$g_i(x_t^{(k+1)}, \theta) \approx g_i(x_t^{(k+1)}, \widehat{\theta}^{(k+1)}) + [S_{t,i}^{(k+1)}]^T(\theta - \widehat{\theta}^{(k+1)}), \tag{6.8}$$

where $g_i(x_t^{(k+1)}, \theta)$ is the i sampling equation in Model 6.2.1; and

$$[S_{t,i}^{(k+1)}]^T = \frac{dg_i(x_t^{(k+1)}, \widehat{\theta}^{(k+1)})}{d\theta} \tag{6.9}$$

is a vector of derivatives of i sampling equation with respect to the model parameters θ. Note that $S_{t,i}^{(k+1)}$ in (6.9) can be calculated using the sensitivity equations given below

$$\frac{dx_{(k+1)}^{j+1}}{d\theta} = \frac{\partial f(x_t^{(k+1)}, u_t^{(k+1)}, \bar{u}, \theta, t)}{\partial x_t^{(k+1)}} \frac{dx_t^{(k+1)}}{d\theta} + \frac{\partial f(x_t^{(k+1)}, u_t^{(k+1)}, \bar{u}, \theta, t)}{\partial \theta}, \tag{6.10a}$$

$$\frac{dg_i(x_t^{(k+1)}, \theta)}{d\theta} = \frac{\partial g(x_t^{(k+1)}, \theta)}{\partial x_t^{(k+1)}} \frac{dx_t^{(k+1)}}{d\theta} + \frac{\partial g(x_t^{(k+1)}, \theta)}{\partial \theta}. \tag{6.10b}$$

Note that the sensitivity equations (6.10) can be augmented with (6.1a) in Model 6.2.1 and solved simultaneously to compute $[S_{t,i}^{(k+1)}]^T$. Now substituting (6.8) into (6.7), and based on rearrangements suggested by (Draper and Hunter, 1967*b*; Zullo, 1991), we obtain

$$p(\theta|\mathcal{D}^{(k)}, \mathcal{D}^{(k+1)}) \propto \exp\Big(-\frac{1}{2}[\theta - \widehat{\theta}^{(k+1)}]^T \sum_{a=1}^{m}\sum_{b=1}^{m}\frac{1}{\widehat{\sigma}_{ab}^2}[S_{1:N,a}^{(k+1)}]^T[S_{1:N,b}^{(k+1)}][\theta - \widehat{\theta}^{(k+1)}]^T$$
$$-\frac{1}{2}[\theta - \widehat{\theta}^{(k)}]^T\Sigma_{\theta^{(k)}}^{-1}[\theta - \widehat{\theta}^{(k)}]\Big), \tag{6.11}$$

where $\widehat{\sigma}_{ab}^2$ is the $R(a, b)$ element of the covariance matrix R computed as

$$(N - r)\widehat{\sigma}_{ab}^2 = \begin{cases} [y_{1:N,a}^{(k+1)} - \widehat{y}_{1:N,a}^{(k+1)}]^T[y_{1:N,a}^{(k+1)} - \widehat{y}_{1:N,a}^{(k+1)}] & a = b \\ [y_{1:N,a}^{(k+1)} - \widehat{y}_{1:N,a}^{(k+1)}]^T[y_{1:N,b}^{(k+1)} - \widehat{y}_{1:N,b}^{(k+1)}] & a \neq b \end{cases} \tag{6.12}$$

where $\widehat{y}_{1:N}^{(k+1)}$ is a model based predicted response corresponding to the design vector $\eta_{1:N}^{(k+1)}$ and estimates $\theta^{(k+1)}$. In sequential Bayesian design, $\widehat{\theta}^{(k+1)}$ is not known until experiment $k+1$ is actually implemented on the real process. Therefore, in (6.11), the unknown estimate $\widehat{\theta}^{(k+1)}$ can be replaced with $\widehat{\theta}^{(k)}$, available from experiment k, such that

$$p(\theta|\mathcal{D}^{(k)}, \mathcal{D}^{(k+1)}) \propto \exp\Big(-\frac{1}{2}[\theta - \widehat{\theta}^{(k)}]^T[\sum_{a=1}^{m}\sum_{b=1}^{m}\frac{1}{\widehat{\sigma}_{ab}^2}[S_{1:N,a}^{(k+1)}]^T[S_{1:N,b}^{(k+1)}] + \Sigma_{\theta(k)}^{-1}][\theta - \widehat{\theta}^{(k)}]\Big),$$
$$\tag{6.13}$$

where $S_{1:N,i}^{(k+1)}$ is a $N \times r$ matrix given by

$$
S_{1:N,a}^{(k+1)} = \begin{bmatrix}
\dfrac{\partial \widehat{y}_{1,a}^{(k+1)}}{\partial \widehat{\theta}_1^{(k)}} & \cdots & \dfrac{\partial \widehat{y}_{1,a}^{(k+1)}}{\partial \widehat{\theta}_r^{(k)}} \\[2ex]
\dfrac{\partial \widehat{y}_{2,a}^{(k+1)}}{\partial \widehat{\theta}_1^{(k)}} & \cdots & \dfrac{\partial \widehat{y}_{2,a}^{(k+1)}}{\partial \widehat{\theta}_r^{(k)}} \\[2ex]
\vdots & \vdots & \vdots \\[2ex]
\dfrac{\partial \widehat{y}_{N,a}^{(k+1)}}{\partial \widehat{\theta}_1^{(k)}} & \cdots & \dfrac{\partial \widehat{y}_{N,a}^{(k+1)}}{\partial \widehat{\theta}_r^{(k)}}
\end{bmatrix}. \tag{6.14}
$$

Note that (6.13) is a predicted parameter posterior density at experiment $k+1$, computed based on information available until experiment k. Now since (6.13) is a product of two normal densities, the covariance of $\theta|(\mathcal{D}^{(k)}, \mathcal{D}^{(k+1)}) \sim p(\theta|\mathcal{D}^{(k)}, \mathcal{D}^{(k+1)})$ is given by

$$
\Sigma_{\theta^{(k+1)}} = [M(\eta_{1:N}^{(k+1)}, \widehat{\theta}^{(k)})]^{-1}, \tag{6.15}
$$

where $M(\eta_{1:N}^{(k+1)}, \widehat{\theta}^{(k)})$ is the Bayesian information associated with $\eta_{1:N}^{(k+1)}$ and $\widehat{\theta}^{(k)}$, such that

$$
M(\eta_{1:N}^{(k+1)}, \widehat{\theta}^{(k)}) = \sum_{a=1}^{m} \sum_{b=1}^{m} \frac{1}{\widehat{\sigma}_{ab}^2} [S_{1:N,a}^{(k+1)}]^T [S_{1:N,b}^{(k+1)}] + \Sigma_{\theta^{(k)}}^{-1}. \tag{6.16}
$$

Remark 6.3.4. *The Bayesian information in (6.16) is derived under a Gaussian posterior density assumption. Note that this assumption is valid as long as: (i) the local linearization in (6.8) is reasonable; (ii) prior density $p(\theta|\mathcal{D}^{(k)})$ in (6.4) is selected according to Remark 6.3.3; and (ii) the measurement noise W_t in Model 6.2.1 is Gaussian.*

Using Eq.(6.15), a correlation matrix for experiment $k+1$ can also be obtained. (Pritchard and Bacon, 1978) proposed a scalar measure of the overall extent of correlation present among parameters through the use of correlation index

$$
C(\eta_{1:N}^{(k+1)}, \widehat{\theta}^{(k)}) = \left\{ \sum_{m=1}^{r} \sum_{m=1}^{r} \frac{\mathscr{C}^2(m,n)}{r^2 - r} \right\}^{1/2} \quad m \neq n, \tag{6.17}
$$

where $C(\eta_{1:N}^{(k+1)}, \widehat{\theta}^{(k)})$ is a scalar measure of correlation and $\mathscr{C}(m,n)$ is the (m,n) term of the correlation matrix. Note that (6.17) is general, and can be used to calculate overall correlation between parameters for any experiment, including the current design.

The Bayesian information matrix in (6.16) is a function of the estimate $\widehat{\theta}^{(k)}$. Therefore, to account for parameter uncertainties associated with $\widehat{\theta}^{(k)}$, Definition 6.3.1 requires taking expectation of (6.16) with respect to the prior density $p(\theta|\mathcal{D}^{(k)})$, computed in (6.4).

6.3.2   Evaluating expectation

The Bayesian ED-optimal input design in Definition 6.3.1 is based on expected Bayesian information matrix, where the expectation of the Bayesian information matrix is with respect to the prior parameter density $p(\theta|\mathcal{D}^{(k)})$. Unfortunately, for the model considered in Model 6.2.1, finding an analytical solution to expected Bayesian information matrix is non-trivial as it involves complex, multi-dimensional integrals of the form

$$\mathbb{E}_{p(\theta|\mathcal{D}^{(k)})}|M(\eta_{1:N}^{(k+1)},\theta)| = \int_{\Theta} |M(\eta_{1:N}^{(k+1)},\theta)|p(\theta|\mathcal{D}^{(k)})d\theta, \tag{6.18a}$$

$$\propto \int_{\theta_{1,LB}}^{\theta_{1,UB}} \cdots \int_{\theta_{r,LB}}^{\theta_{r,UB}} |M(\eta_{1:N}^{(k+1)},\theta)| \exp(-\frac{1}{2}[\theta - \widehat{\theta}^{(k)}]^T \Sigma_{\theta^{(k)}}^{-1} [\theta - \widehat{\theta}^{(k)}])d\theta_1 \ldots d\theta_r, \tag{6.18b}$$

where $\theta_{i,LB} \leq \theta_i \leq \theta_{i,UB}$ for all $1 \leq i \leq r$. Now considering the limitations of numerical techniques, such as the quadrature rule (see Section 6.1), we propose a perfect Monte Carlo (MC) sampling based method to approximate the complex, multi-dimensional integrals in (6.18b), such that with MC, (6.18b) can be approximated as follows:

$$\mathbb{E}_{p(\theta|\mathcal{D}^{(k)})}|M(\eta_{1:N}^{(k+1)},\theta)| \approx \frac{1}{N}\sum_{i=1}^{N} |M(\eta_{1:N}^{(k+1)},\theta^i)|, \tag{6.19}$$

where $\{\theta^i\}_{i=1}^N$ is a set of N random samples from the multi-variate Gaussian density $p(\theta|\mathcal{D}^{(k)})$. With (6.19), Definition 6.3.1 can now be approximated as

$$\eta_{1:N}^{(k+1)} = \underset{\eta_{1:N}^{(k+1)}\in\zeta}{\arg\max} \frac{1}{N}\sum_{i=1}^{N} |M(\eta_{1:N}^{(k+1)},\theta^i)|. \tag{6.20}$$

Note that the approximation in (6.20) can be made arbitrarily accurate for large values of N. From (6.20), it is also evident that the Bayesian ED-optimal input design depends on the choice of the prior density $p(\theta|\mathcal{D}^{(k)})$, whose design is discussed next.
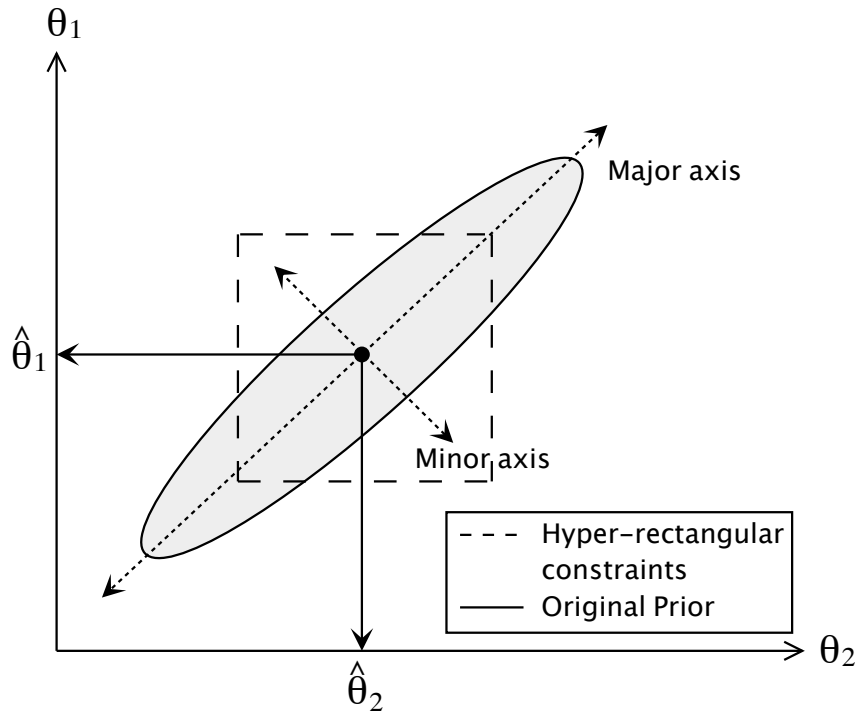
Figure 6.1: 95% joint confidence region for correlated parameters along with the hyper-rectangular constraints.

6.4   Projection based prior design

In this section, we discuss different methods to construct the prior density $p(\theta|\mathcal{D}^{(k)})$ used in Definition 6.3.1. First, for convenience, we define $p(\theta|\widehat{\theta}^{(k)}, \Sigma_{\theta^{(k)}}) \triangleq p(\theta|\mathcal{D}^{(k)})$. Now note that since $p(\theta|\widehat{\theta}^{(k)}, \Sigma_{\theta^{(k)}})$ is a multi-variate Gaussian density (see (6.4)), information in $p(\theta|\widehat{\theta}^{(k)}, \Sigma_{\theta^{(k)}})$ can be represented by a an ellipsoidal joint confidence region, as shown in Figure 6.1. The ellipsoid is centered at $\widehat{\theta}^{(k)}$, with axes length proportional to the uncertainties in the estimates. Note that the orientation of the ellipsoid in Figure 6.1 further reflects the information on degree of correlation between the estimates.

In presence of a hyper-rectangular constraints on the parameters of Model 6.2.1, a poor input design or poor parameter estimates may result in $\operatorname{supp} p(\theta|\widehat{\theta}^{(k)}, \Sigma_{\theta^{(k)}})$ stretching onto the infeasible parameter space, as illustrated in Figures 6.1 and 6.2(a). Problems related to sampling from infeasible density support are discussed in Section 6.1. To facilitate proper

(a) Original prior information

(b) Projected prior information
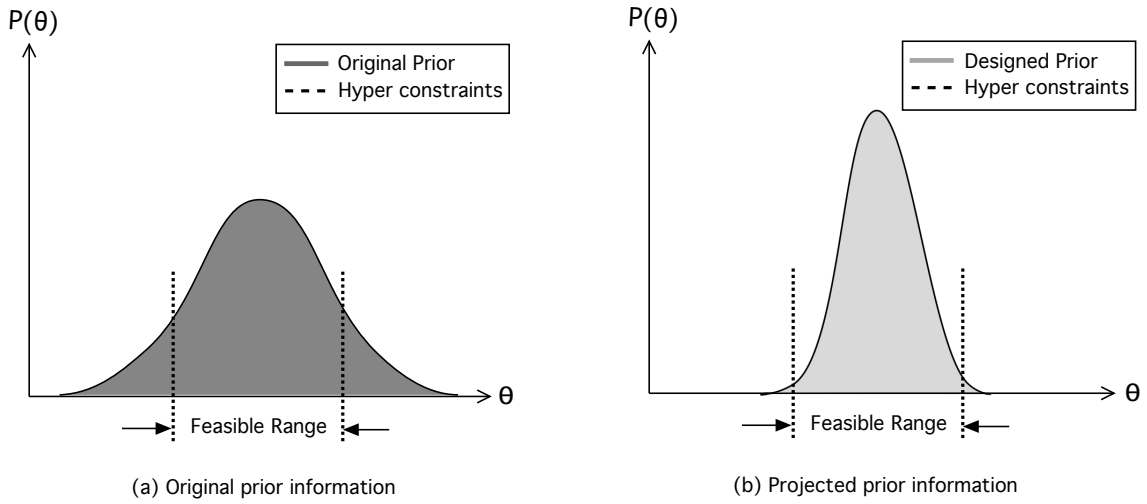
Figure 6.2: Illustration of the original prior distribution and the new constrained prior design based on the feasible parameter space.

organization of the prior information, we explore different design techniques, such that $p(\theta|\widehat{\theta}^{(k)}, \Sigma_{\theta^{(k)}})$ can be efficiently projected onto the feasible parameter space, as illustrated in Figure 6.2(b). In Figure 6.2, $p(\theta|\widehat{\theta}^{(k)}, \Sigma_{\theta^{(k)}})$ is projected onto another Gaussian density defined within the constrained parameter space; however, it is important to note that this is by no means the only mechanism to project $p(\theta|\widehat{\theta}^{(k)}, \Sigma_{\theta^{(k)}})$. The schematic in Figure 6.2 is presented, so that the reader can fully appreciate the problem being addressed in this chapter.

In this section, we develop and analyze the efficiency of three types of prior projections: circular, truncated and directional. Each of these prior designs project $p(\theta|\widehat{\theta}^{(k)}, \Sigma_{\theta^{(k)}})$ onto the constrained hyper-rectangular parameter space, thereby allowing appropriate sampling for Bayesian ED-optimal input design (see (6.20)).

6.4.1   Circular prior design

Circular prior design was proposed in (Asprey and Macchietto, 2002) for designing Bayesian ED-optimal input design. By construction, a circular prior design ignores information about $\widehat{\theta}^{(k)}$ and $\Sigma_{\theta^{(k)}}$ contained in $p(\theta|\widehat{\theta}^{(k)}, \Sigma_{\theta^{(k)}})$. Instead, a circular prior
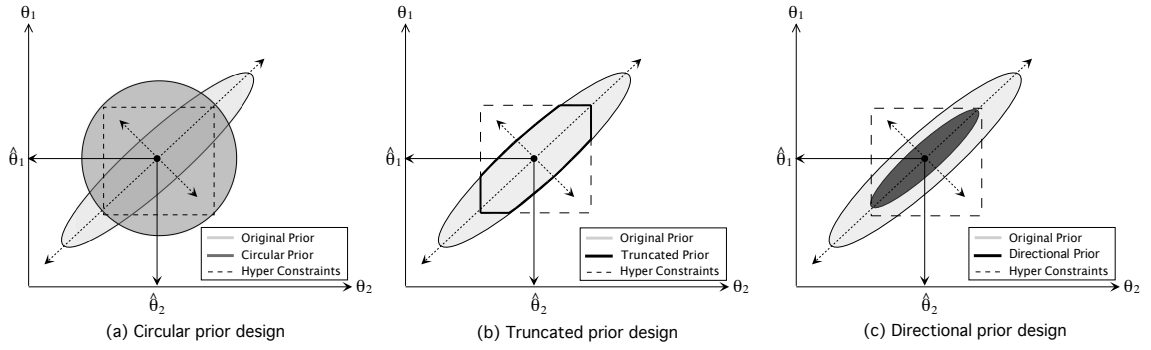
Figure 6.3: Schematic of various constraint based prior designs reproduced from the original prior distribution.

assumes an independent mean $\widehat{\theta}_{Cir}^{(k)}$ and covariance $\Sigma_{\theta^{(k)},Cir}$, such that the prior density can be represented as $p(\theta|\widehat{\theta}_{Cir}^{(k)}, \Sigma_{\theta^{(k)},Cir}) \sim \mathcal{N}(\theta|\widehat{\theta}_{Cir}^{(k)}, \Sigma_{\theta^{(k)},Cir})$. A schematic of a typical circular prior design is shown in Figure 6.3(a). Here, $\Sigma_{\theta^{(k)},Cir}$ is a $r \times r$ diagonal covariance matrix, whose entries are selected to make a high percentage of the joint confidence region of the circular prior circumscribe or inscribe the hyper-rectangular constraints, with center fixed at $\widehat{\theta}_{Cir}^{(k)}$. Note that this design further ignores the parameter correlation information in $p(\theta|\widehat{\theta}^{(k)}, \Sigma_{\theta^{(k)}})$, thereby resulting in a hyper-sphere around or inside the constrained space.

6.4.2   Truncated prior design

A truncated prior design is a new design approach developed in this chapter, which defines prior density at the intersection of $p(\theta|\widehat{\theta}^{(k)}, \Sigma_{\theta^{(k)}})$ and the hyper-rectangular constraints (see Figure 6.3(b)). The truncated prior density can be computed as given in the next theorem.

Theorem 6.4.1. *Let $p(\theta|\widehat{\theta}^{(k)}, \Sigma_{\theta^{(k)}})$ be the prior density given in (6.4), and let $\theta \in \Theta$ for $\theta_{LB} \leq \theta \leq \theta_{UB}$ be uniformly distributed, such that $\theta|\Theta \sim p(\theta|\Theta)$, then the truncated prior density defined at the intersection of $p(\theta|\widehat{\theta}^{(k)}, \Sigma_{\theta^{(k)}})$ and $p(\theta|\Theta)$ has a density function*

$$p(\theta|\widehat{\theta}^{(k)}, \Sigma_{\theta^{(k)}}, \Theta) \propto \begin{cases} zp(\theta|\widehat{\theta}^{(k)}, \Sigma_{\theta^{(k)}}) & \theta_{LB} \leq \theta \leq \theta_{UB}, \\ 0 & otherwise, \end{cases} \tag{6.21}$$

where $p(\theta|\widehat{\theta}^{(k)}, \Sigma_{\theta^{(k)}}, \Theta)$ is a truncated prior density and $z = (\theta_{UB} - \theta_{LB})^{-1}$ is a uniform density calculated based on $[\theta_{LB},\ \theta_{UB}]$.

Proof. Since $\theta \in \Theta$ for $\theta_{LB} \leq \theta \leq \theta_{UB}$ is uniformly distributed, its density $p(\theta|\Theta)$ is

$$p(\theta|\Theta) = \begin{cases} z & \theta_{LB} \leq \theta \leq \theta_{UB} \\ 0 & otherwise. \end{cases} \tag{6.22}$$

Now since a truncated prior is defined at the intersection of $p(\theta|\widehat{\theta}^{(k)}, \Sigma_{\theta^{(k)}})$ and $p(\theta|\Theta)$; it density, $p(\theta|\widehat{\theta}^{(k)}, \Sigma_{\theta^{(k)}}, \Theta)$ can be obtained using Bayes' rule, such that

$$p(\theta|\widehat{\theta}^{(k)}, \Sigma_{\theta^{(k)}}, \Theta) = \frac{p(\widehat{\theta}^{(k)}, \Sigma_{\theta^{(k)}}, \Theta|\theta)p(\theta)}{p(\widehat{\theta}^{(k)}, \Sigma_{\theta^{(k)}}, \Theta)}, \tag{6.23}$$

where $p(\theta)$ is a prior density on parameters even before knowing the hyper-constraints. Now by marginalizing $p(\widehat{\theta}^{(k)}, \Sigma_{\theta^{(k)}}, \Theta|\theta)$ in (6.23), we obtain

$$p(\theta|\widehat{\theta}^{(k)}, \Sigma_{\theta^{(k)}}, \Theta) = \frac{p(\widehat{\theta}^{(k)}, \Sigma_{\theta^{(k)}}|\theta)p(\Theta|\theta)p(\theta)}{p(\widehat{\theta}^{(k)}, \Sigma_{\theta^{(k)}})p(\Theta)}. \tag{6.24}$$

The result in (6.24) follows from the independent prior information assumption, i.e., $p(\widehat{\theta}^{(k)}, \Sigma_{\theta^{(k)}}, \Theta|\theta) = p(\widehat{\theta}^{(k)}, \Sigma_{\theta^{(k)}}|\theta)p(\Theta|\theta)$. Again applying Bayes' rule in (6.24), we get

$$p(\theta|\widehat{\theta}^{(k)}, \Sigma_{\theta^{(k)}}, \Theta) = \frac{p(\theta|\widehat{\theta}^{(k)}, \Sigma_{\theta^{(k)}})p(\widehat{\theta}^{(k)}, \Sigma_{\theta^{(k)}})p(\theta|\Theta)p(\Theta)p(\theta)}{p(\theta)p(\widehat{\theta}^{(k)}, \Sigma_{\theta^{(k)}})p(\Theta)p(\theta)}, \tag{6.25a}$$

$$= \frac{p(\theta|\widehat{\theta}^{j}, \Sigma_{\theta^{(k)}})p(\theta|\Theta)}{p(\theta)}. \tag{6.25b}$$

Substituting (6.22) into (6.25b), and ignoring the normalizing constant $p(\theta)$, we get (6.21), which completes the proof. □

From Theorem 6.4.1, it can be inferred that a truncated prior density maintains its center at $\widehat{\theta}^{(k)}$, available from experiment k. Furthermore, it also honours the hyper-rectangular constraints on the parameters by forcing the density to zero outside the feasible parameter space. Note that truncated prior design ensures sampling within the constrained space, and also preserves the overall orientation of $p(\theta|\widehat{\theta}^{(k)}, \Sigma_{\theta^{(k)}})$ within the constraint.

6.4.3   Directional prior design

Directional prior is another design approach, in which the original prior density $p(\theta|\widehat{\theta}^{(k)}, \Sigma_{\theta^{(k)}})$ is projected onto a parallel multi-variate Gaussian density defined inside the
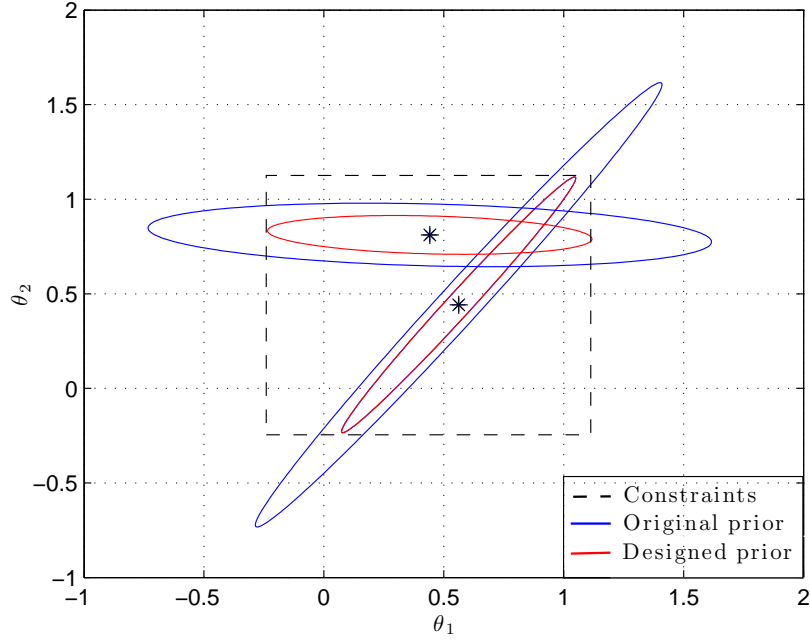
Figure 6.4: Projecting 95% joint confidence region onto the hyper-rectangular constraints using directional prior design scheme.

constrained space. Figure 6.3(c) shows a schematic of a typical directional prior density. Note that, since directional prior is also a Gaussian density, it can be represented as

$$p(\theta|\widehat{\theta}^{(k)}, \Sigma_{\theta^{(k)}, Dir}) \propto \exp(-\frac{1}{2}[\theta - \widehat{\theta}^{(k)}]^T \Sigma_{\theta^j, Dir}^{-1}[\theta - \widehat{\theta}^{(k)}], \tag{6.26}$$

where $\widehat{\theta}^{(k)}$ is from experiment k, and $\Sigma_{\theta^{(k)}, Dir}$ is defined to keep $p(\theta|\widehat{\theta}^{(k)}, \Sigma_{\theta^{(k)}, Dir})$ contained, and concentric to $p(\theta|\widehat{\theta}^{(k)}, \Sigma_{\theta^{(k)}})$. Figure 6.4 illustrates the directional prior design scheme by projecting 95% joint confidence region of the original prior density onto the constrained space. Important properties of directional prior design are discussed next.

Proposition 6.4.2. *Let* $p(\theta|\widehat{\theta}^{(k)}, \Sigma_{\theta^{(k)}})$ *in (6.4), and* $p(\theta|\widehat{\theta}^{(k)}, \Sigma_{\theta^{(k)}, Dir})$ *in (6.26) be the original and directional prior density, respectively, then* $p(\theta|\widehat{\theta}^{(k)}, \Sigma_{\theta^{(k)}})$ *and* $p(\theta|\widehat{\theta}^{(k)}, \Sigma_{\theta^{(k)}, Dir})$ *have concentric ellipsoids for*

$$\Sigma_{\theta^{(k)}, Dir} = \Psi \Lambda_{\theta^{(k)}, Dir} \Psi^T, \tag{6.27}$$

where Ψ is a $r \times r$ matrix, with columns as eigenvectors of $\Sigma_{\theta^{(k)}}$, and $\Lambda_{\theta^{(k)}, Dir}$ is a $r \times r$ diagonal matrix of eigenvalues of $\Sigma_{\theta^{(k)}, Dir}$.

Proof. Each ellipsoid of $p(\theta | \widehat{\theta}^{(k)}, \Sigma_{\theta^{(k)}})$ in Figure 6.3(c) represents a contour of constant probability density, which can be mathematically represented as

$$[\theta - \widehat{\theta}^{(k)}]^T \Sigma_{\theta j}^{-1} [\theta - \widehat{\theta}^{(k)}] = c^2, \tag{6.28}$$

where $c^2 \sim \chi^2_{\text{df}}(\alpha)$ and $\chi^2_{\text{df}}(\alpha)$ is the upper $(100\alpha)^{th}$ percentile of a χ^2 square distribution with df degrees of freedom. Note that the ellipsoid in (6.28) is centered at $\widehat{\theta}^{(k)}$, with axes along the direction of eigenvectors of $\Sigma_{\theta^{(k)}}$ and axial length proportional to the square-root of its eigenvalues, such that spectral decomposition of $\Sigma_{\theta^{(k)}}$ is given by

$$\Sigma_{\theta^{(k)}} = \Psi \Lambda_{\theta^{(k)}} \Psi^T \tag{6.29}$$

where Ψ and $\Lambda_{\theta^{(k)}}$ are both $r \times r$ matrix of eigenvectors and eigenvalues, respectively. Now, for the ellipsoids of $p(\theta | \widehat{\theta}^{(k)}, \Sigma_{\theta^{(k)}, Dir})$ to be concentric to (6.28), requires $\Sigma_{\theta^{(k)}, Dir}$ to have a spectral decomposition given by (6.27), which completes the proof. □

Remark 6.4.3. *Directional prior preserves the orientation of $p(\theta | \widehat{\theta}^{(k)}, \Sigma_{\theta^{(k)}})$. This property ensures that the information on parameter correlations, and overall orientation of $p(\theta | \widehat{\theta}^{(k)}, \Sigma_{\theta^{(k)}})$ is carried over the projection.*

Remark 6.4.4. *Note that in Proposition 6.4.2, $\Lambda_{\theta^{(k)}, Dir}$ is a diagonal matrix, with r degrees of freedom selected based on the hyper-rectangular parameter constraints.*

Remark 6.4.5. *From a practical stand point, for processes with strict constraints (e.g., viscosity of a fluid is strictly ≥ 0), projecting 99% of prior information onto the contained space is imperative to minimize the statistical risk of sampling from infeasible space.*

A mathematical mapping scheme for directional prior design is discussed next.

Proposition 6.4.6. *Let $p(\theta|\widehat{\theta}^{(k)}, \Sigma_{\theta^{(k)}})$ in (6.4), and $p(\theta|\widehat{\theta}^{(k)}, \Sigma_{\theta^{(k)},Dir})$ in (6.26) be the original and directional prior density, respectively, then $p(\theta|\widehat{\theta}^{(k)}, \Sigma_{\theta^{(k)}})$ and $p(\theta|\widehat{\theta}^{(k)}, \Sigma_{\theta^{(k)},Dir})$ satisfies the following equality:*

$$p(\theta|\widehat{\theta}^{(k)}, \Sigma_{\theta^{(k)},Dir}) = p_T(\theta|\widehat{\theta}^{(k)}, \Sigma_{\theta^{(k)},T}) p(\theta|\widehat{\theta}^{(k)}, \Sigma_{\theta^{(k)}}), \tag{6.30}$$

where:

$$p_T(\theta|\widehat{\theta}^{(k)}, \Sigma_{\theta^{(k)},T}) = \frac{1}{(2\pi)^{r/2}|\Sigma_{\theta^{(k)},T}|^{1/2}} \exp\left(-\frac{1}{2}(\theta - \widehat{\theta}^{(k)})^T \Sigma_{\theta^{(k)},T}^{-1}(\theta - \widehat{\theta}^{(k)})\right), \tag{6.31a}$$

$$\Sigma_{\theta^j,T} = \Psi[\Lambda_{\theta^{(k)},Dir}^{-1} - \Lambda_{\theta^{(k)}}^{-1}]^{-1}\Psi^T, \tag{6.31b}$$

also: $\Sigma_{\theta^{(k)}} = \Psi\Lambda_{\theta^{(k)}}\Psi^T$; *and* $\Sigma_{\theta^{(k)},Dir} = \Psi\Lambda_{\theta^{(k)},Dir}\Psi^T$.

Proof. Let the density transformation from $p(\theta|\widehat{\theta}^{(k)}, \Sigma_{\theta^{(k)}})$ to $p(\theta|\widehat{\theta}^{(k)}, \Sigma_{\theta^{(k)},Dir})$ be represented as

$$p(\theta|\widehat{\theta}^{(k)}, \Sigma_{\theta^{(k)}}) = J(\theta)p(\theta|\widehat{\theta}^{(k)}, \Sigma_{\theta^{(k)},Dir}), \tag{6.32}$$

where $J(\theta)$ is a function required for transforming density from $p(\theta|\widehat{\theta}^{(k)}, \Sigma_{\theta^{(k)}})$ to $p(\theta|\widehat{\theta}^{(k)}, \Sigma_{\theta^{(k)},Dir})$. Now substituting Eq.(6.29) into (6.4), we have

$$p(\theta|\widehat{\theta}^{(k)}, \Sigma_{\theta^{(k)}}) \propto \exp(-\frac{1}{2}[K^T\Lambda_{\theta^{(k)}}^{-1}K]), \tag{6.33}$$

where $K = \Psi^T[\theta - \widehat{\theta}^{(k)}]$. Now for any two random samples, θ^1 and θ^2 drawn from (6.33), we have

$$\frac{p(\theta^1|\widehat{\theta}^{(k)}, \Sigma_{\theta^{(k)}})}{p(\theta^2|\widehat{\theta}^{(k)}, \Sigma_{\theta^{(k)}})} = \exp(-\frac{1}{2}[K_1^T\Lambda_{\theta^{(k)}}^{-1}K_1 - K_2^T\Lambda_{\theta^{(k)}}^{-1}K_2]), \tag{6.34}$$

where $K_i = \Psi^T[\theta^i - \widehat{\theta}^{(k)}]$ for $i = \{1, 2\}$. Now, formulating a similar density ratio based on $p(\theta|\widehat{\theta}^{(k)}, \Sigma_{\theta^{(k)},Dir})$, using the same sampled point θ^1 and θ^2, we obtain

$$\frac{p(\theta^1|\widehat{\theta}^{(k)}, \Sigma_{\theta^{(k)},Dir})}{p(\theta^2|\widehat{\theta}^{(p)}, \Sigma_{\theta^{(p)},Dir})} = \exp(-\frac{1}{2}[K_1^T\Lambda_{\theta^{(k)},Dir}^{-1}K_1 - K_2^T\Lambda_{\theta,Dir}^{-1}K_2]). \tag{6.35}$$

Substituting (6.34) and (6.35) into (6.32), we have

$$\frac{J(\theta^1)}{J(\theta^2)} = \frac{\exp\left(-\frac{1}{2}\left[K_1^T[\Lambda_{\theta,Dir}^{-1} - \Lambda_{\theta}^{-1}]K_1\right]\right)}{\exp\left(-\frac{1}{2}\left[K_2^T[\Lambda_{\theta,Dir}^{-1} - \Lambda_{\theta}^{-1}]K_2\right]\right)} \triangleq \frac{p_T(\theta^1|\widehat{\theta}^{(k)}, \Sigma_{\theta^{(k)},T})}{p_T(\theta^2|\widehat{\theta}^{(k)}, \Sigma_{\theta^{(k)},T})}, \tag{6.36}$$

where $p_T(\theta|\widehat{\theta}^{(k)}, \Sigma_{\theta^{(k)},T})$ and $\Sigma_{\theta^{(k)},T}$ are given by (6.31a) and (6.31b), respectively, which completes the proof. $\square$

Remark 6.4.7. *From Proposition 6.4.6, it is evident that projection from the original to designed prior density is channeled through a multi-variate Gaussian density* $p_T(\theta|\widehat{\theta}^{(k)}, \Sigma_{\theta^{(k)},T})$, *whose covariance depends on the choice of* $\Lambda_{\theta^{(k)},Dir}$.

A procedure to select the eigenvalues of $\Sigma_{\theta^{(k)},Dir}$ is discussed next.

6.4.3.1   Selecting eigenvalues

Selecting appropriate eigenvalues of $\Sigma_{\theta^{(k)},Dir}$ is a key step in designing effective directional prior. In this chapter, we select the eigenvalues of $\Sigma_{\theta^{(k)},Dir}$ based on ellipsoid's axial lengths. For any hyper-rectangular constraints of the form $\theta_{LB} \le \theta \le \theta_{UB}$, the entries of $\Lambda_{\theta^j,Dir}$ can be chosen according to

$$\theta_{LB} \le \widehat{\theta}^{(k)} \pm c\Lambda_{\theta^{(k)},Dir}^{0.5} \le \theta_{UB}, \tag{6.37}$$

where $2c\Lambda_{\theta^{(k)},Dir}^{0.5}$ is a $r \times 1$ vector of axial lengths along each principle direction of the ellipsoid. The advantage of assigning eigenvalues using (6.37) is that axes length of directional prior density can be independently set along each principle direction.

6.5   Optimal control problem

The algorithm presented in Figure 6.5 shows encapsulation of Bayesian ED-optimal design criterion under the optimization framework. Once the design objective is set, the input design problem is formulated as an optimal control problem. Here, we adopt the optimal control strategy suggested by (Espie and Macchietto, 1989; Asprey and Macchietto, 2002) to include a variety of operational constraints on the design.

Note that designing a dynamic design sequence is an infinite dimensional optimization problem, which can be converted to non-linear programming (NLP) problem using control
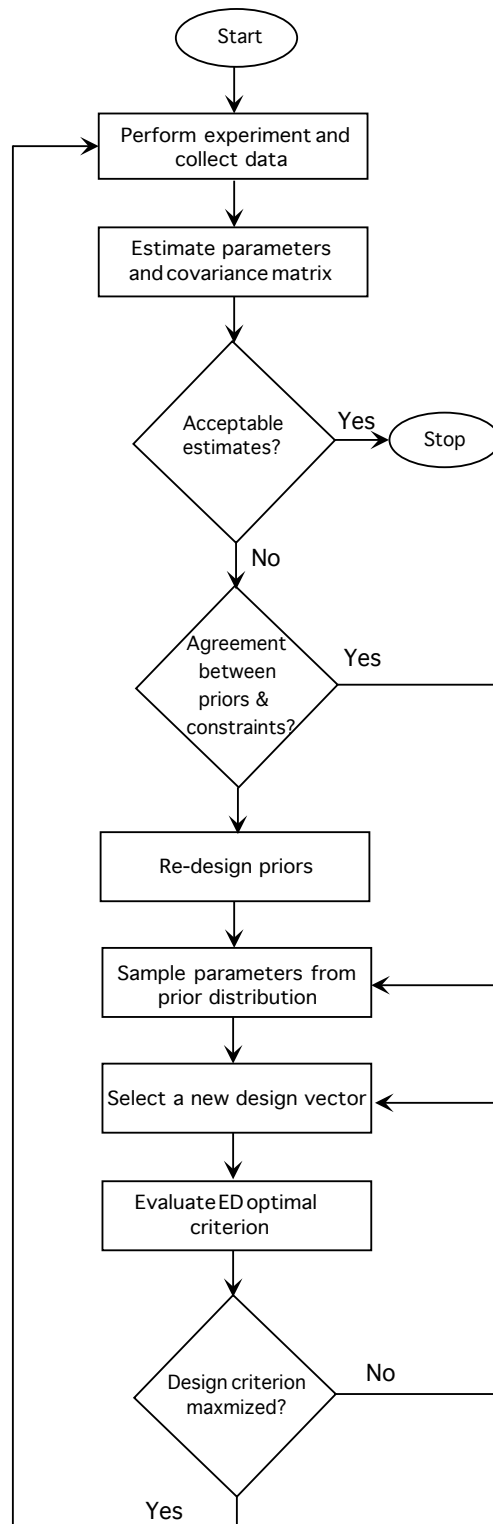
Figure 6.5: The proposed algorithm for sequential input design.
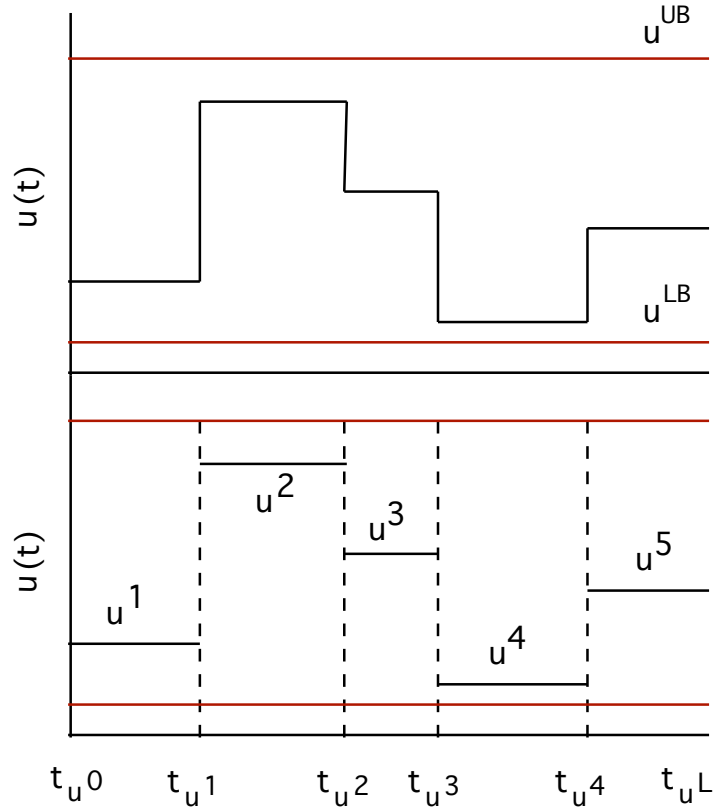
Figure 6.6: Control vector parametrization of design variable.

vector parametrization (CVP) technique (Kraft, 1985). CVP is a complete discretization approach, where continuous design space is discretized and approximated by simple parametric functions, as illustrated in Figure 6.6.

In this work, the p dimensional exogenous control variable is assumed to be piecewise constant in each discrete interval (l), such that $u_t = u^l$, where $1 \leq l \leq L$ and $1 \leq t \leq N$. Note that a piecewise constant input can be completely characterized by its magnitude, i.e., u^l, and duration of hold, calculated from the input switching time t_{u^l}. Here, t_{u^l} is a $p \times 1$ vector, representing switching time for the p control variables in the finite interval l. Mathematically, a discretized, piecewise constant input can be represented as

$$u_t = u^l, \qquad t_{u^{l-1}} \leq t \leq t_{u^l}, \qquad (6.38)$$

where $1 \leq l \leq L$ and $1 \leq \{t_{u^{l-1}}, t_{u^l}\} \leq N$. Other parametric representations such as

piecewise linear and piecewise quadratic can also be accommodated in the framework by including appropriate parametric functions. Finally, the discretized control variables u^l and switching time t_{u^l} for $1 \leq l \leq L$ and $1 \leq t_{u^l} \leq N$ can be augmented with the time-invariant control variables $\bar{u}$, and initial conditions x_0, such that the design variable $\eta_{1:N}^{(k)}$ at experiment k is given by

$$\eta_{1:N}^{(k)} = \begin{bmatrix} u^l, & t_{u^l}, & \bar{u}, & x_0 \end{bmatrix}, \tag{6.39}$$

where $1 \leq l \leq L$ and $1 \leq t_{u^l} \leq N$. Note that, in presence of other design variables, (6.39) can be appropriately expanded. The Bayesian ED-optimal design problem formulation proposed in this chapter is given next.

Formulation 6.5.1. *Discretizing the continuous design space ζ, using CVP method transforms the optimization problem in (6.20) into an NLP optimization problem, such that substituting (6.16) into (6.20), we have*

$$\eta_{1:N}^{(k+1)} = \arg\max_{\eta_{1:N}^{(k+1)} \in \zeta} \quad \frac{1}{N} \sum_{i=1}^{N} |M(\eta_{1:N}^{(k+1)}, \theta^i)|; \tag{6.40a}$$

$$s.t.$$

$$u^{LB} \leq u^l \leq u^{UB} \qquad\qquad 1 \leq l \leq L; \tag{6.40b}$$

$$\bar{u}^{LB} \leq \bar{u} \leq \bar{u}^{UB}; \tag{6.40c}$$

$$x_0^{LB} \leq x_0 \leq x_0^{UB}; \tag{6.40d}$$

$$t_u^{LB} \leq t_{u^l} - t_{u^{l-1}} \leq t_u^{UB} \qquad 1 \leq l \leq L; \tag{6.40e}$$

$$t_{u^L} \leq N, \tag{6.40f}$$

where $\{\bar{u}^{UB}, \bar{u}^{LB}\}$ and $\{x_0^{UB}, x_0^{LB}\}$ are the upper and lower bounds for $\bar{u}$ and x_0.

Remark 6.5.2. *Formulation 6.5.1 supports various equality and inequality constraints on the design variables, as shown in (6.40b) through (6.40f). As discussed in (Asprey and Macchietto, 2002), the mathematical singularities due to collapse of one or more control intervals can be avoided through a linear constraint (6.40e). Physically, (6.40e) constraint*
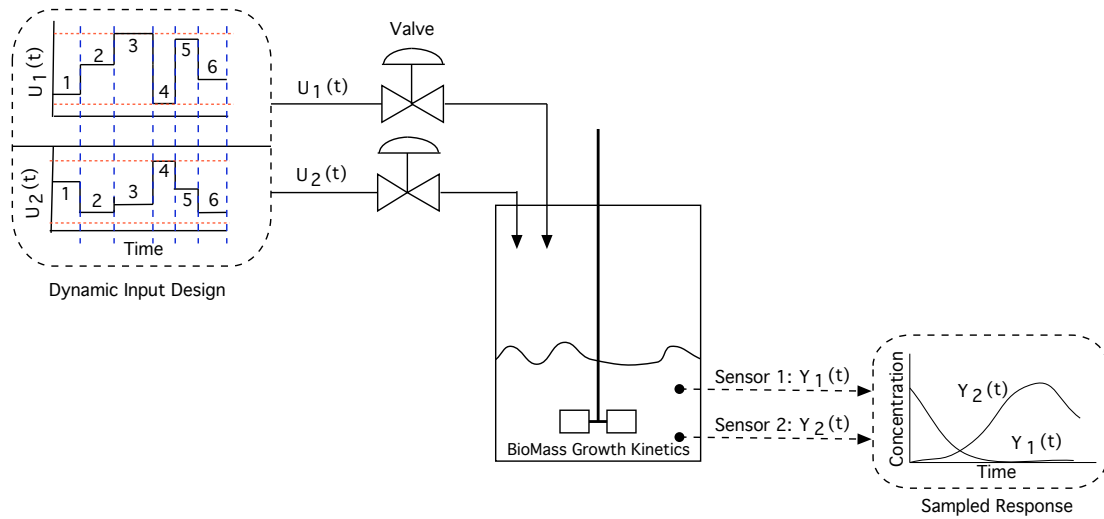
Figure 6.7: Schematic diagram of the Baker's yeast fermentation reactor

Table 6.1: Process design variables and constraints for the fermenter.

Process variables	Symbol	Constraints
Initial biomass concentration	$x_1(0)$	1-10 (g/L)
Initial substrate concentration	$x_2(0)$	0.1 (g/L)
Dilution factor	$u_1(t)$	0.05-0.20 (hr^{-1})
Substrate concentration in feed	$u_2(t)$	5-35 (g/L)
Control intervals	L	6
Switching time	t_{u^l}	0-40 (hr)
Time lapsed between intervals	$t_{u^l} - t_{u^{l-1}}$	4-20 (hr)
Experiment time	N	40 (hr)

the time lapse between two consecutive control moves. Also, the inequality (6.40f) prevents

implementing control actions beyond the final experimentation time N.

6.6   Numerical illustration

Effectiveness of different prior designs discussed in Section 6.4 is demonstrated on a Baker's yeast fermentation process (Espie and Macchietto, 1989).

6.6.1   Baker's yeast fermenter

Baker's fermenter is a semi-continuous batch reactor with two inputs and two outputs as shown in Figure 6.7. Assuming Monod kinetics for biomass growth and substrate

consumption, dynamics in the fermenter is given as (Asprey and Macchietto, 2000)

$$\frac{dx_1}{dt} = (\omega(t) - u_1(t) - \theta_4)x_1(t); \tag{6.41a}$$

$$\frac{dx_2}{dt} = -\frac{\omega(t)x_1(t)}{\theta_3} + u_1(t)(u_2(t) - x_2(t)); \tag{6.41b}$$

$$\omega(t) = \frac{\theta_1 x_2(t)}{\theta_2 + x_2(t)}, \tag{6.41c}$$

where x_1 and x_2 are the state variables representing biomass growth (g/L) and substrate consumption (g/L) as a function of time t, respectively. Manipulated variables u_1 and u_2 are the dilution factor (hr^{-1}) and substrate concentration in feed (g/L), respectively. Also there are four model parameters $\theta = \{\theta_1; \theta_2; \theta_3; \theta_4\}$ to be estimated using sampled input-output data. A priori information available on θ is the parameter constraint, where

$$0.01 \leq \theta_i \leq 1, \tag{6.42}$$

where $1 \leq i \leq 4$. For estimation purposes, θ is assumed to be equally probable in the space defined in (6.42). Note that in (6.41) there is no uncertainty in the model structure, and both x_1 and x_2 are measured through the measurement equation given below

$$Y_1(t) = x_1(t) + W_1(t), \tag{6.43a}$$

$$Y_2(t) = x_2(t) + W_2(t), \tag{6.43b}$$

where W_1 and W_2 are measurement noise sequences, such that $W_1 \sim \mathcal{N}(w_1|0, 0.04)$ and $W_2 \sim \mathcal{N}(w_2|0, 0.04)$. For this problem, the nominal values and ranges for both design and fixed process variables are given in Table 6.1. The number of control moves for both u_1 and u_2 are fixed, and their switching time assumed to be synchronized so that they change simultaneously (see Figure 6.7 for illustration). In total, there are 19 control variables in the design vector given below

$$\eta^j_{1:N} = \begin{bmatrix} x_1(0), & u^l_1, & u^l_2, & t_{u^l} \end{bmatrix}, \tag{6.44}$$

where $1 \leq l \leq 6$. The objective here is to use a priori information to design a series of Bayesian ED-optimal input designs for estimating θ.

Table 6.2: Process design variables for initial input design $(\eta_{1:N}^{(0)})$.

Process variable	Design value
$x_1(0)$	5.00
$u_1^l;\quad 1 \leq l \leq 6$	0.12; 0.12; 0.12; 0.12; 0.12; 0.12
$u_2^l;\quad 1 \leq l \leq 6$	15; 15; 15; 15; 15; 15
$t_{u^l};\quad 1 \leq l \leq 6$	0; 7; 14; 21; 28; 35

Table 6.3: Parameter estimates computed using initial input design $(\eta_{1:N}^{(0)})$.

θ	$\widehat{\theta}^{(0)}$	Covariance Matrix				Correlation Matrix			
		θ_1	θ_2	θ_3	θ_4	θ_1	θ_2	θ_3	θ_4
θ_1	0.5629	0.520	0.715	-0.010	-0.003	1.000	0.991	-0.098	-0.106
θ_2	0.4416		0.999	-0.031	-0.009		1.000	-0.219	-0.228
θ_3	0.8112			0.020	0.006			1.000	0.999
θ_4	0.1036				0.002				1.000
Measure		$\|M(\eta_{1:N}^{(0)}, \widehat{\theta}^{(0)})\| = 1.7654 \times 10^{10}$				$C(\eta_{1:N}^{(0)}, \widehat{\theta}^{(0)}) = 0.592$			

6.6.1.1   Initial input design

A zeroth experiment $(\eta_{1:N}^{(0)})$ is designed to obtain an initial estimate for the parameters. Lack of prior information on choice of $\eta_{1:N}^{(0)}$ suggests selecting a relatively simple design. Based on the design constraints (see Table 6.1) $\eta_{1:N}^{(0)}$ is selected as given in Table 6.2.

Parameter estimates and corresponding covariance and correlation matrices are presented in Table 6.3. Standard error for $\widehat{\theta}_1^{(0)}$ and $\widehat{\theta}_2^{(0)}$ are larger than the estimated values which suggests, poor estimation in statistical sense. The overall performance of the design is shown in Figure 6.8, where model predictions based on initial estimates ill-fit the dynamics of both biomass and substrate concentration. As discussed in Section 6.3.1, results from zeroth experiment can be summarized under $p(\theta|\widehat{\theta}^{(0)}, \Sigma_{\theta^{(0)}})$. Histograms generated from $p(\theta|\widehat{\theta}^{(0)}, \Sigma_{\theta^{(0)}})$ is presented in Figure 6.9 wherein, samples for θ_1, θ_2, θ_3, and θ_4^0 extend beyond the feasible parameter space defined in (6.42). The eigenvalues $\Lambda_{\theta^{(0)}} = [0.0266;\ 1.5085;\ 8.42 \times 10^{-4};\ 1.67 \times 10^{-6}]$ corresponds to axial length of ellipsoid generated based on the initial design. Next we implement the prior design discussed in Section 6.4 to project $p(\theta|\widehat{\theta}^{(0)}, \Sigma_{\theta^{(0)}})$ onto the constraints in (6.42).
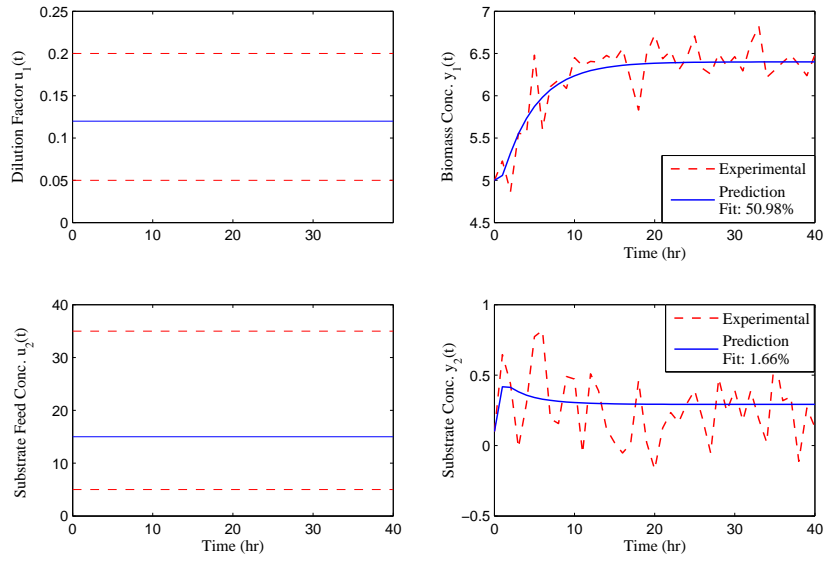
Figure 6.8: Infinite step ahead model predictions for initial input design.
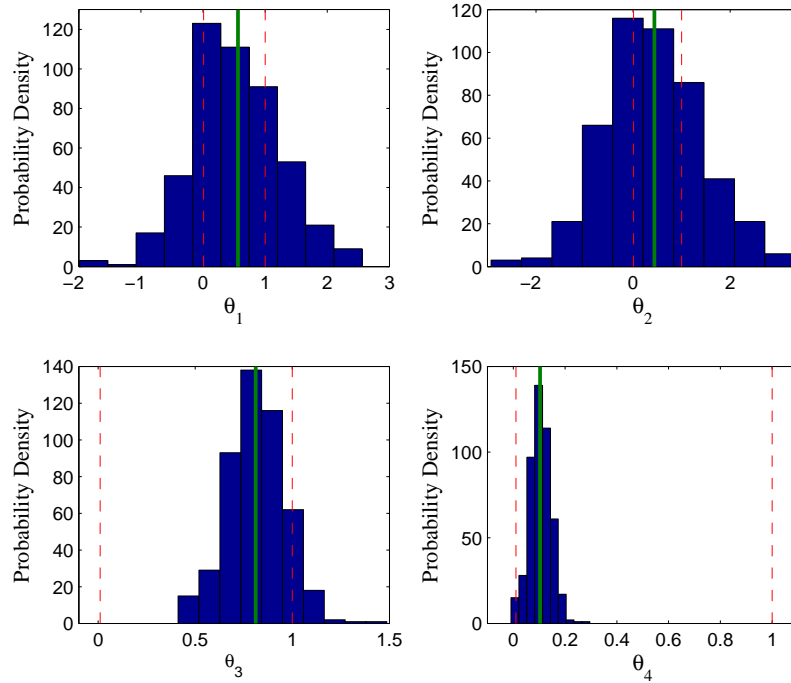
Figure 6.9: Histogram generated by sampling original prior distributions with initial estimates marked in green and constraints represented by broken red lines.

Table 6.4: Process design variables computed using circular prior.

Process variable	Design value					
$x_1(0)$	6.05					
u_1^l; $\quad 1 \le l \le 6$	0.19;	0.11;	0.05;	0.18;	0.05;	0.05
u_2^l; $\quad 1 \le l \le 6$	24.1;	10.4;	16.3;	19.4;	14.4;	16.4
t_{u^l}; $\quad 1 \le l \le 6$	0;	2.55;	6.95;	12.2;	16.4;	21.9

Table 6.5: Parameter estimates computed using circular prior.

θ	$\widehat{\theta}^{(1)}$	Covariance Matrix ($\times 10^{-5}$)				Correlation Matrix			
		θ_1	θ_2	θ_3	θ_4	θ_1	θ_2	θ_3	θ_4
θ_1	0.3365	15.38	75.25	3.086	0.516	1.000	0.917	0.280	0.224
θ_2	0.2638		440.0	-1.54	-1.04		1.000	-0.026	-0.085
θ_3	0.5279			7.866	1.583			1.000	0.962
θ_4	0.0267				0.344				1.000
Measure		$|M(\eta_{1:N}^{(1)}, \widehat{\theta}^{(1)})| = 8.4919 \times 10^{16}$				$C(\eta_{1:N}^{(1)}, \widehat{\theta}^{(1)}) = 0.6833$			

6.6.1.2   Circular prior design

As discussed in Section 6.4.1, circular prior design ignores all the information available from the zeroth run, and instead assumes a multi-variate Gaussian density around the hyper-rectangular constraints. Here, $\widehat{\theta}_{Cir}^{(0)} = [0.5;\ 0.5;\ 0.5;\ 0.5]$ is chosen as the center of $p(\theta|\widehat{\theta}_{Cir}^{(0)}, \Sigma_{\theta^{(0)},Cir})$, with $\Sigma_{\theta^{(0)},Cir}$ chosen as $\mathrm{diag}(0.06;\ 0.06;\ 0.06;\ 0.06)$ to contain 95% joint confidence region within the hyper-rectangular constraints. The histogram generated by sampling $p(\theta|\widehat{\theta}_{Cir}^{(0)}, \Sigma_{\theta^{(0)},Cir})$ is shown in Figure 6.11 in which about 4% of total sampled points ($N = 500$) are in the infeasible space. Table 6.4 gives the computed optimal design vector $(\eta_{1:N}^{(1)})$ using circular prior. Furthermore, parameter estimates obtained by implementing the optimal design is given in Table 6.5. Comparing it to the initial estimates (Table 6.3), there is an average reduction of about 95% in overall parameter uncertainty; however, the correlation index increases by 13.4% to 0.6833. This is because Bayesian ED-optimal criterion aims at reducing uncertainties in parameters alone, and does not include any quantifiable metric of correlation between parameters. Therefore, maximizing (6.20) could produce larger correlation between parameters as pointed by (Issanchou *et al.*, 2003).
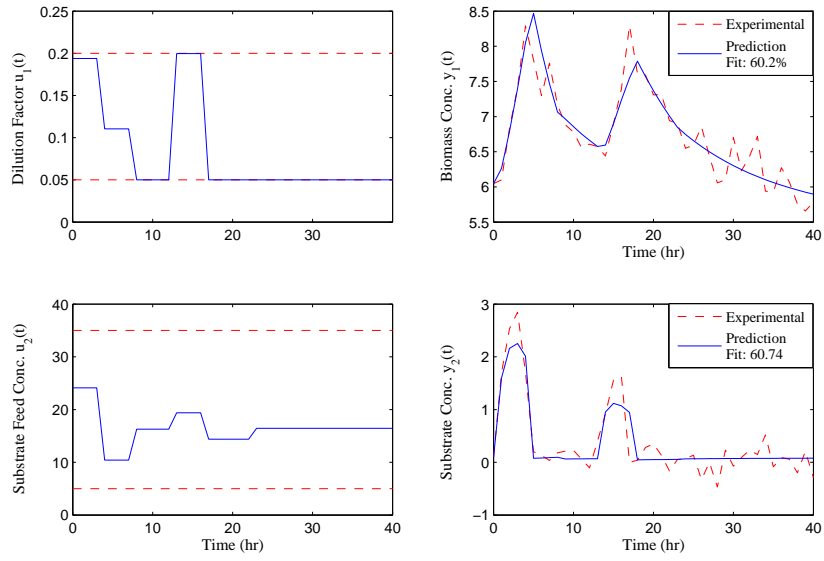
Figure 6.10: Infinite step ahead model predictions for circular prior based input design.
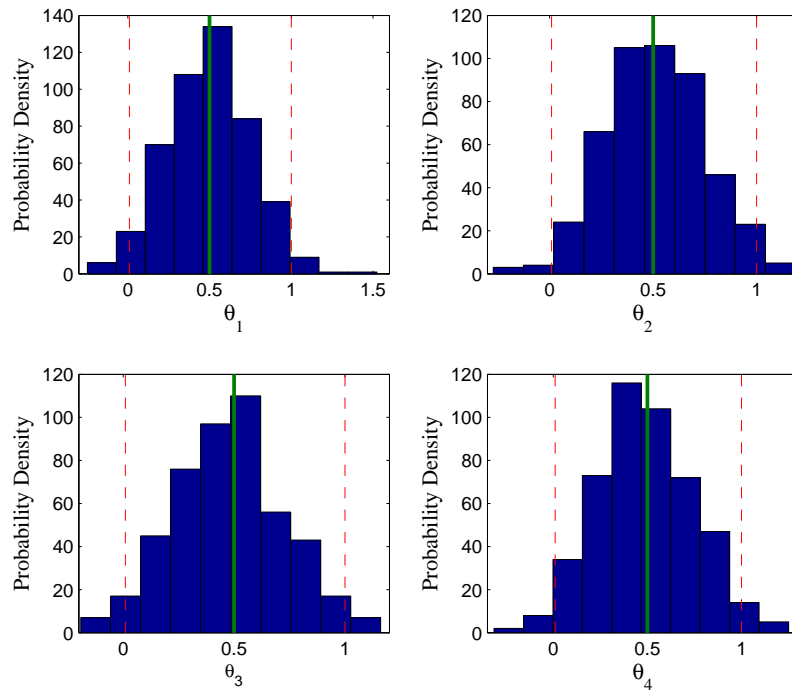
Figure 6.11: Histogram generated by sampling circular prior distributions with initial estimates marked in green and constraints represented by broken red lines.

Table 6.6: Process design variables computed using truncated prior.

Process variable		Design value					
$x_1(0)$		3.48					
u_1^l;	$1 \leq l \leq 6$	0.09;	0.07;	0.11;	0.11;	0.19;	0.06
u_2^l;	$1 \leq l \leq 6$	17.6;	6.05;	16.11;	5.00;	34.7;	18.3
t_{u^l};	$1 \leq l \leq 6$	0;	1.01;	7.59;	12.4;	17.16;	25.5

Table 6.7: Parameter estimates computed using truncated prior.

θ	$\widehat{\theta}^{(1)}$	Covariance Matrix ($\times 10^{-5}$)				Correlation Matrix			
		θ_1	θ_2	θ_3	θ_4	θ_1	θ_2	θ_3	θ_4
θ_1	0.3344	0.816	3.098	1.619	0.459	1.000	0.216	0.709	0.758
θ_2	0.3458		250.0	-17.7	-4.88		1.000	-0.44	-0.46
θ_3	0.5780			6.390	1.615			1.000	0.952
θ_4	0.0381				0.450				1.000
Measure		$|M(\eta_{1:N}^{(1)}, \widehat{\theta}^{(1)})| = 8.846 \times 10^{19}$				$C(\eta_{1:N}^{(1)}, \widehat{\theta}^{(1)}) = 0.6368$			

Often, there is a trade-off between reduction in parameter correlation, and increase in Bayesian information content in an experiment (Franceschini and Macchietto, 2008*b*). Figure 6.10 shows an infinite horizon predictions using estimates in Table 6.5.

6.6.1.3   Truncated prior design

Truncated prior design discussed in Section 6.4.2 allows sampling only in the feasible parameter space. The prior density in the infeasible region is forced to zero as shown in Figure 6.13. The optimal design vector $(\eta_{1:N}^{(1)})$ obtained using truncated prior is given in Table 6.6. Parameter estimates $(\widehat{\theta}^{(1)})$ along with covariance and correlation matrices are given in Table 6.7. On average there is reduction of about 96% in parameter uncertainty compared to the initial design with information index $|M(\eta_{1:N}^{(1)}, \widehat{\theta}^{(1)})|$ being 8.846×10^{19}. The difference between the information index for truncated and circular prior is of three orders of magnitude. Model predictions using truncated prior based input design is shown in Figure 6.12, suggesting a significant improvement in overall design quality.
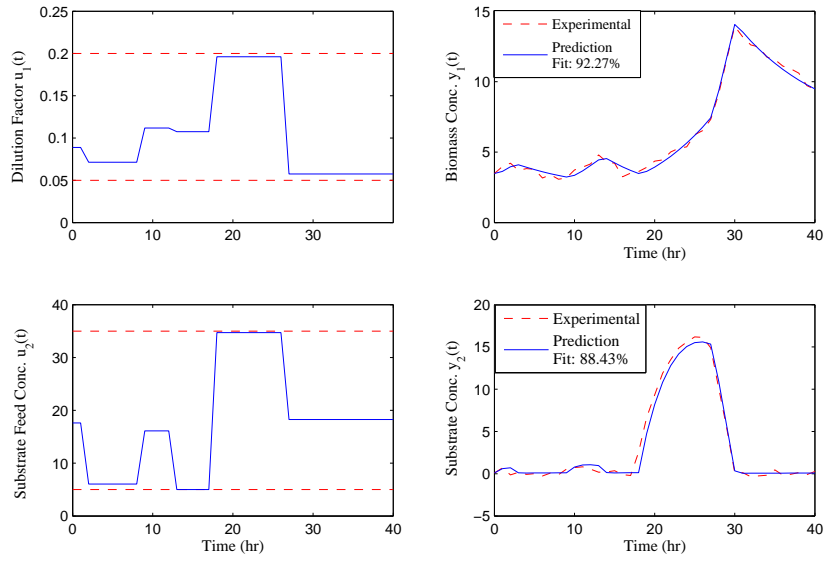
Figure 6.12: Infinite step ahead model predictions for truncated prior based input design.
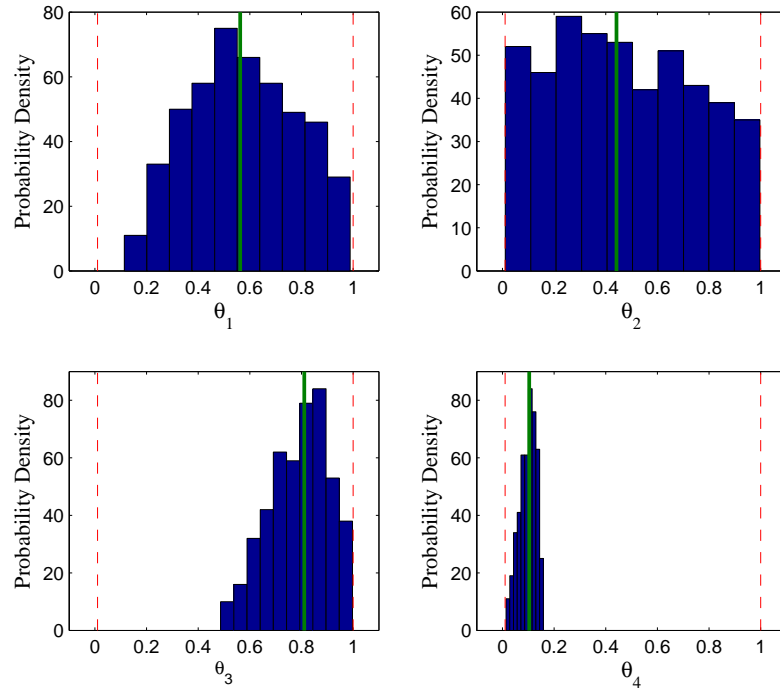
Figure 6.13: Histogram generated by sampling truncated prior distributions with initial estimates marked in green and constraints represented by broken red lines.

Table 6.8: Process design variables obtained using directional prior.

Process variable	Design value
$x_1(0)$	1.52
$u_1^l; \quad 1 \leq l \leq 6$	0.16; 0.19; 0.12; 0.05; 0.05; 0.19
$u_2^l; \quad 1 \leq l \leq 6$	20; 34.5; 33.7; 7.80; 13.6; 16.4
$t_{u^l}; \quad 1 \leq l \leq 6$	0; 1.14; 7.24; 12.6; 18.9; 26.2

Table 6.9: Parameter estimates computed using directional prior.

θ	$\widehat{\theta}^{(1)}$	Covariance Matrix $(\times 10^{-5})$				Correlation Matrix			
		θ_1	θ_2	θ_3	θ_4	θ_1	θ_2	θ_3	θ_4
θ_1	0.3172	0.470	0.850	1.180	0.350	1.000	0.174	0.902	0.898
θ_2	0.2573		50.1	-2.52	-0.97		1.000	-0.187	-0.24
θ_3	0.5497			3.640	1.030			1.000	0.951
θ_4	0.0308				0.320				1.000
Measure		$|M(\eta_{1:N}^{(1)}, \widehat{\theta}^{(1)})| = 1.816 \times 10^{21}$				$C(\eta_{1:N}^{(1)}, \widehat{\theta}^{(1)}) = 0.664$			

6.6.1.4   Directional prior design

In directional prior design, orientation of $p(\theta | \widehat{\theta}^{(0)}, \Sigma_{\theta^{(0)}})$ is preserved by keeping the eigenvectors of Σ_{θ^0} fixed as discussed in Section 6.4.3. The eigenvalues of $\Sigma_{\theta^0, Dir}$ are selected as $[0.0145; \ 0.0140; \ 8.42 \times 10^{-4}; \ 1.67 \times 10^{-6}]$ to contain the 95% joint confidence region for parameters within the feasible space. The eigenvalues corresponding to θ_3 and θ_4 are not altered since, more than 95% of the samples with respect to θ_3 and θ_4 are well within the hyper-rectangular constraints (see Figure 6.9). The histograms for θ_1 and θ_2 spread further into the infeasible parameter space, thereby requiring a significant reduction to their corresponding eigenvalues. The histogram for $p(\theta | \widehat{\theta}^{(0)}, \Sigma_{\theta^{(0)}, Dir})$ is shown in Figure 6.15 in which only about 2% of the sampled points fall in the infeasible space.

The optimal input design corresponding to the use of directional prior is given in Table 6.8. Also, the parameter estimates and its related covariance and correlation matrices are given in Table 6.9. It is important to note that the standard error for $\widehat{\theta}_2^{(1)}$ reduces significantly with the use of directional prior. On average there is 98% reduction in parameter uncertainty using directional prior based design. Compared to truncated prior (Table 6.7), the improvement with directional prior in terms of information index is of two
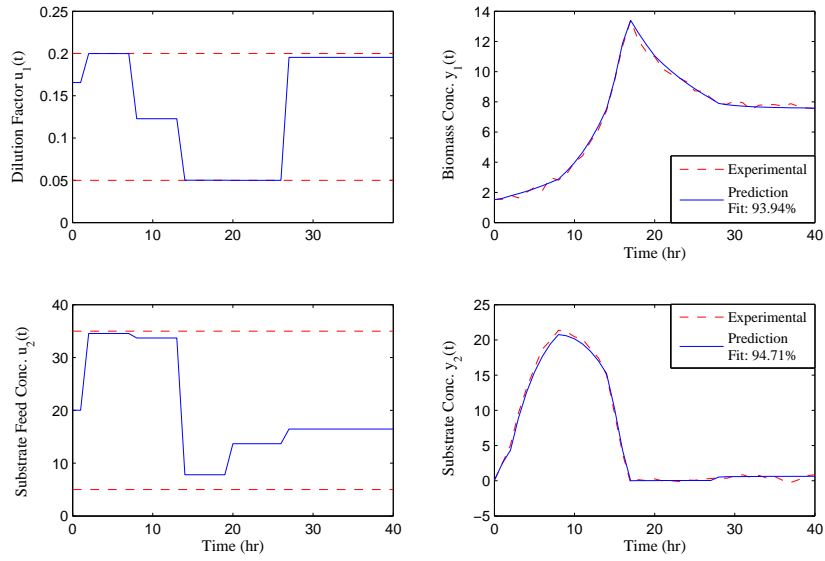
Figure 6.14: Infinite step ahead model predictions for directional prior based input design.
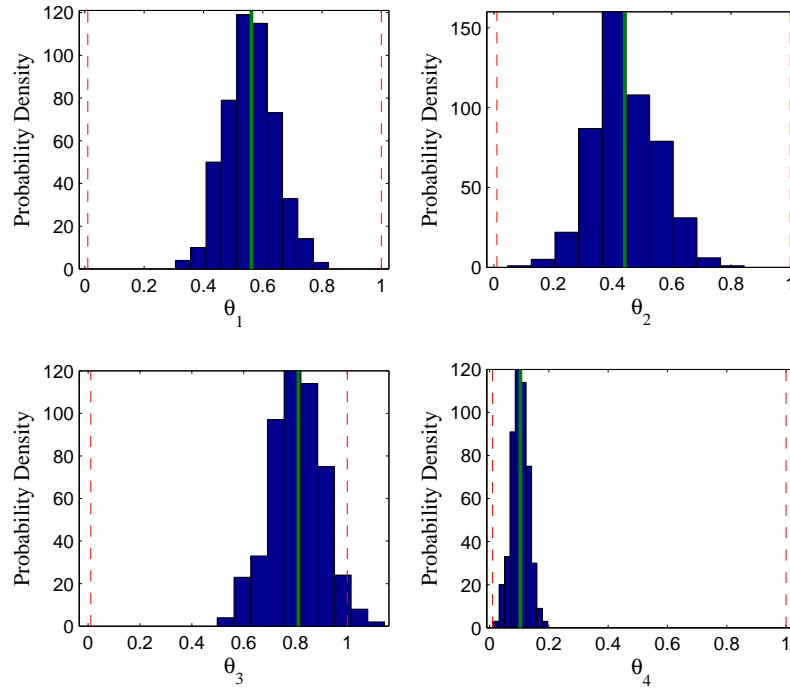

Figure 6.15: Histogram generated by sampling directional prior distributions with initial estimates marked in green and constraints represented by broken red lines.

orders of magnitude (Table 6.9). Furthermore, high percentage fit (over 94%) for both x_1 and x_2 in Figure 6.14 demonstrates the utility and efficacy of the directional prior design.

One may argue that one of the reasons for improvement using directional design may be attributed to a smaller prior region that results from the design. In fact, preservation of direction plays an important role in the improvement. To highlight the advantage of preserving orientation of $p(\theta|\widehat{\theta}^{(0)}, \Sigma_{\theta^{(0)}})$ in a prior design, a simulation exercise is conducted. Rotating $p(\theta|\widehat{\theta}^{(0)}, \Sigma_{\theta^{(0)},Dir})$ about any plane or axes changes its orientation, but keeps the volume of the ellipsoid, constant (Kay, 1993). In the simulation, we consider a prior density obtained by rotating $p(\theta|\widehat{\theta}^{(0)}, \Sigma_{\theta^{(0)},Dir})$ by 45° in counter-clock wise direction in the θ_3 and θ_4 plane. The rotated prior density is given by $p(\theta|A\widehat{\theta}^{(0)}, A\Sigma_{\theta^{(0)},Dir}A^T)$, where A is the required 4×4 rotation matrix. The information index computed using $p(\theta|A\widehat{\theta}^{(0)}, A\Sigma_{\theta^{(0)},Dir}A^T)$ as prior density is 8.372×10^{19}. The difference in information index for the two directional prior densities of the same volume, but different orientation is about two orders of magnitude. This demonstrates the advantage of preserving orientation, of the original prior distribution.

6.6.1.5   Classical D-optimal design

Results from classical non-robust D-optimal design are also provided here for comparison purposes. Adopting a similar approach, an optimal design vector is computed using the D-optimal criterion. Parameter estimates and its corresponding covariance and correlation matrices are calculated therefrom. Compared to the initial design, parameter uncertainty computed using D-optimal design reduce by 85% with information index $|M(\eta_{1:N}^{(1)}, \widehat{\theta}^{(1)})| = 3.6184 \times 10^{16}$ and correlation index $C(\eta_{1:N}^{(1)}, \widehat{\theta}^{(1)}) = 0.6545$. Certainly, ED-optimal design is more efficient than D-optimal design, in terms of achieving parameter estimates with reduced uncertainty. The same is summarized in Table 6.10. Furthermore, it is also evident from Table 6.10 that directional prior based Bayesian ED-optimal design outperforms the other two prior designs considered here.

Table 6.10: Summary of the results obtained using D and ED-optimal designs.

Parameters	True value	D-optimal $(\widehat{\theta}^{(1)})$	ED-optimal $(\widehat{\theta}^{(1)})$		
			Circular	Truncated	Directional
θ_1	0.31	0.352	0.336	0.334	0.317
θ_2	0.18	0.433	0.263	0.345	0.257
θ_3	0.55	0.569	0.527	0.578	0.549
θ_4	0.03	0.035	0.026	0.038	0.030
$M(\eta_{1:N}^{(1)}, \widehat{\theta^1})(\times 10^{17})$		0.361	0.849	884	18160

It is important to note that if desired, another sequential run can be similarly performed by selecting $p(\theta|\widehat{\theta}^{(1)}, \Sigma_{\theta^{(1)}})$ as a prior density, where $\widehat{\theta}^{(1)}$ and Σ_{θ^1} are the available parameter estimate, and its corresponding covariance matrix, respectively. For the simulation example considered here, the new prior distribution $p(\theta|\widehat{\theta}^{(1)}, \Sigma_{\theta^{(1)}})$ do not violate the hyper-rectangular constraints (6.42) anymore; therefore, it can be used directly without having to re-design it. Since, the algorithm for sequential input design (Figure 6.5) without prior design is routine, it is not considered here.

6.6.1.6   Robust design

As discussed earlier, Bayesian ED-optimal designs are optimal in the average sense, since they consider uncertainties associated with parameter estimates. To validate and compare the robust nature of Bayesian ED-optimal input with prior designs, another simulation experiment is performed. The optimal inputs computed based on different prior designs, along with a new set of model parameters (randomly selected from the feasible parameter space) are used, to generate model outputs using (6.41). The sampled input-output data sets are then used for estimating the new model parameters (see Table 6.11). Amongst the class of Bayesian ED-optimal designs, input design associated with directional prior is most successful in estimating the new model parameters. The simulation validates the robust nature of the directional prior based Bayesian ED-optimal experiment.

Table 6.11: Comparison of the robustness of D and ED-optimal designs

Parameters	True value	D-optimal $(\widehat{\theta}^{(1)})$	ED-optimal $(\widehat{\theta}^{(1)})$		
			Circular	Truncated	Directional
θ_1	0.79	0.906	0.599	0.873	0.795
θ_2	0.91	0.980	0.352	0.745	0.852
θ_3	0.90	0.915	0.857	0.943	0.922
θ_4	0.09	0.096	0.086	0.130	0.098
$M(\eta_{1:N}^{(1)}, \widehat{\theta}^{(1)})(\times 10^{14})$		0.74	2.47	6.95	372

6.7   Conclusions

The chapter focuses on the use of robust Bayesian input design in estimating parameters of non-linear processes. The proposed framework, makes use of a priori information amassed from previous input design to design informed future experiments. Different prior designs relating to organization and utilization of available information are discussed from a theoretical viewpoint. Development of these prior designs arise based on the need to project a priori parameter information onto the constrained space for achieving efficient integration of available process information with the input design algorithm.

Apart from the theoretical developments, performance of the prior designs are validated and compared on a Baker's yeast fermenter problem. In terms of minimum constraint violation, truncated prior design was the most effective; however, it fails to preserve a priori parameter correlation information. The advantage of preserving correlation information was also demonstrated through a separate simulation. Directional prior on the other hand, neatly projects complete a priori parameter information onto the contained space, including the correlation information. Amongst the class of proposed prior designs, directional prior based Bayesian ED-optimal input design, outperformed both circular and truncated prior based robust designs. Finally, the robust nature of the directional prior based Bayesian ED-optimal design in estimating new system parameters was also demonstrated.

Bibliography

Asprey, S.P. and S. Macchietto (2000). Statistical tool for optimal dynamic model building. *Computers and Chemical Engineering* **24**(2–7), 1261–1267.

Asprey, S.P. and S. Macchietto (2002). Designing robust optimal dynamic experiments. *Journal of Process Control* **12**(4), 545–556.

Bard, Y. (1974). *Non-linear Parameter Estimation*. Academic Press Inc., New York.

Box, G.E.P. and H.L. Lucas (1959). Design of experiments in non-linear situations. *Biometrika* **46**(1/2), 77–90.

Box, M.J. (1970). Some experiences with a non-linear experimental design criterion. *Technometrics* **12**(3), 569–589.

Chaloner, K. and I. Verdinelli (1995). Bayesian experimental design: a review. *Statistical Science* **10**(3), 273–304.

Draper, N.R. and W.G. Hunter (1966). Design of experiments for parameter estimation in multi-response situations. *Biometrika* **53**(3/4), 525–533.

Draper, N.R. and W.G. Hunter (1967*a*). The use of prior distribution in the design of experiments for parameter estimation in non-linear situations. *Biometrika* **54**(1/2), 147–153.

Draper, N.R. and W.G. Hunter (1967*b*). The use of prior distribution in the design of experiments for parameter estimation in non-linear situations: multi-response case. *Biometrika* **54**(3/4), 662–665.

Espie, D.M. and S. Macchietto (1989). The optimal design of dynamic experiments. *AIChE Journal* **35**(2), 223–229.

Fedorov, V.V. (1972). *Theory of Optimal Experiments*. Academic Press Inc., New York.

Fedorov, V.V. (1980). Convex design theory. *Series Statistics* **11**(3), 403–413.

Franceschini, G. and S. Macchietto (2008*a*). Model-based design of experiments for parameter precision: state of the art. *Chemical Engineering Sciences* **63**(19), 4846–4872.

Franceschini, G. and S. Macchietto (2008*b*). Novel anticorrelation criteria for model based experimental design: theory and formulations. *AIChE Journal* **54**(4), 1009–1024.

Geweke, J. (1996). *Handbook of Computational Economics*. Chap. Mont Carlo simulation and numerical integration. Elsevier Science, Amsterdam.

Goodwin, G.C and P.L. Payne (1977). *Dynamic System Identification: Experiment Design and Data Analysis*. Academic Press Inc., New York.

Hill, W.J. and W.G. Hunter (1974). Design of experiments for subsets of parameters. *Technometrics* **16**(3), 425–434.

Hill, W.J., W.G. Hunter and D.W. Wichern (1968). A joint design criterion for the dual problem of model discrimination and parameter estimation. *Technometrics* **10**(1), 145–160.

Hosten, L.H. and G. Emig (1975). Sequential design for precise parameter estimation in ordinary non-linear differential equations. *Chemical Engineering Sciences* **30**(11), 1357–1364.

Issanchou, S., P. Cognet and M. Cabassud (2003). Precise parameter estimation for chemical batch reactions in heterogeneous medium. *Chemical Engineering Science* **58**(9), 1805–1813.

Kay, S.M. (1993). *Fundamentals of Statistical Signal Processing: Estimation Theory*. Prentice Hall, New Jersey.

Kraft, D. (1985). *Computational Mathematical Programming*. Chap. On converting optimal control problems into non-linear programming problems. Springer, New York.

Mehra, R.K. (1974). Optimal input signals for parameter estimation in dynamic systems-survey and new results. *IEEE Transactions on Automatic Control* **19**(6), 753–768.

Ng, T.S. and G.C. Goodwin (1976). On optimal choice of sampling strategies for linear system identification. *International Journal of Control* **23**(4), 459–475.

Pritchard, D. and D.W. Bacon (1978). Prospects of reducing correlations among parameters estimates in kinetic models. *Chemical Engineering Science* **33**(11), 1539–1543.

Veach, E. (1977). Robust Monte Carlo methods for light transport simulation. PhD thesis. Stanford University, Stantord, USA.

Walter, E. and L. Pronzato (1990). Qualitative and quantitative experiment design for phenomenological modelsa survey. *Automatica* **26**(2), 195–213.

Zullo, L. (1991). Computer aided design of experiments- An engineering approach. PhD thesis. University of London, London, UK.

Chapter 7

A particle filter approach to approximate posterior Cramér-Rao lower bound: The case of hidden states

The posterior Cramér-Rao lower bound (PCRLB) derived in (Tichavský *et al.*, 1998) provides a bound on the mean square error (MSE) obtained with any non-linear state filter. Computing the PCRLB involves solving complex, multi-dimensional expectations, which do not lend themselves to an easy analytical solution. Furthermore, any attempt to approximate it using numerical or simulation based approaches requires a priori access to the true states, which may not be available, except in simulations or in carefully designed experiments. To allow recursive approximation of the PCRLB when the states are hidden or unmeasured, a new approach based on sequential Monte Carlo (SMC) or particle filters (PF) is proposed. The approach uses SMC methods to estimate the hidden states using a sequence of the available sensor measurements. The developed method is general and can be used to approximate the PCRLB in non-linear state-space models (SSMs) with non-Gaussian state and sensor noise. The efficacy of the developed method is illustrated on two simulation examples, including a ballistic target tracking problem at re-entry phase.

7.1   Introduction

Non-linear filtering is one of the most important Bayesian inferencing methods, with several key applications in: navigation (Gustafsson *et al.*, 2002), guidance (Gordon *et al.*, 1995), tracking (Chang and Tabaczynski, 1984), fault detection (Dearden *et al.*, 2004) and fault diagnosis (de Freitas *et al.*, 2004). Within the Bayesian framework, a filtering problem aims at constructing a posterior filter density (Doucet *et al.*, 2001).

In the last few decades, several tractable algorithms based on analytical and statistical approximation of the Bayesian filtering (e.g., extended Kalman filter (EKF) and unscented Kalman filter (UKF)) have been developed to allow tracking in non-linear SSMs (Arulampalam *et al.*, 2002). Although filters, such as EKF and UKF are efficient in tracking, their performance is often limited or affected by various numerical and statistical approximations. Despite the great practical interest in evaluating the non-linear filters, it still remains one of the most complex problems in estimation theory (Šimandl *et al.*, 2001).

The Cramér-Rao lower bound (CRLB) defined as an inverse of the Fisher information matrix (FIM) provides a theoretical lower bound on the second-order error (MSE) obtained with any maximum-likelihood (ML) based unbiased state or parameter estimator. An analogous extension of CRLB to the class of Bayesian estimators was derived by (Trees, 1968), which is commonly referred to as the PCRLB. The PCRLB is defined as the inverse of the posterior Fisher information matrix (PFIM) and provides a lower bound on the MSE obtained with any non-linear filter (Tichavský *et al.*, 1998). A full statistical characterization of any non-Gaussian posterior density requires all higher-order moments (Ristic *et al.*, 2004). As a result, the PCRLB does not fully characterize the accuracy of non-linear filters. Nonetheless, it is an important tool, as it only depends on: system dynamics; prior density of the states; and system noise characteristics (Bergman, 2001).

The PCRLB has been widely used as a benchmark for: (i) assessing the quality of different non-linear filters; (ii) comparing performances of non-linear filters against that

of an optimal filter; and (iii) determining whether the filter performance requirements are practical or not. Some of the key practical applications of the PCRLB include: comparison of several non-linear filters for ballistic target tracking (Farina *et al.*, 2002); terrain navigation (Bergman *et al.*, 1999); and design of systems with pre-specified performance bounds (Nehorai and Hawkes, 2000). The PCRLB is also widely used in several other areas related to: multi-sensor resource deployment (e.g., radar resource allocation (Glass and Smith, 2011), sonobuoy deployment in submarine tracking (Hernandez *et al.*, 2004)); sensor positioning (Farshidi *et al.*, 2006); and optimal observer trajectory for bearings-only tracking (Passerieux and Cappel, 1998; Helferty and Mudgett, 1993).

The original PCRLB formulation in (Trees, 1968) is based on batch data, which often renders its computation impractical for multi-dimensional non-linear SSMs. Alternatively, a recursive version of the PCRLB was proposed by (Bobrovsky and Zakai, 1975) for scalar non-linear SSMs with additive Gaussian noise. Its extension to deal with multi-dimensional case was developed much later in (Galdos, 1980; Doerschuk, 1995), where the authors compared the information matrix of a non-linear SSM with that of a suitable linear system with Gaussian noise. In the seminal paper (Tichavský *et al.*, 1998), the authors proposed an elegant approach to recursively compute the PCRLB for discrete-time, non-linear SSMs. Compared to (Galdos, 1980; Doerschuk, 1995), the PCRLB formulation in (Tichavský *et al.*, 1998) is more general as it is applicable to multi-dimensional non-linear SSMs with non-Gaussian state and sensor noise. An overview of the historical developments of the PCRLB, along with other critical discussions can be found in (Kerr, 1989).

The PCRLB in (Tichavský *et al.*, 1998) provides a recursive procedure to compute the lower bound for tracking in general non-linear SSMs, operating with the probability of detection $\mathrm{Pr}_d = 1$ and the probability of false alarm $\mathrm{Pr}_f = 0$. Since then, several modified versions of the PCRLB have also appeared, which allow tracking in situations, such as: measurement origin uncertainty ($\mathrm{Pr}_d = 1$ and $\mathrm{Pr}_f \geq 0$) (Hernandez *et al.*, 2002);

missed detection ($\Pr_d \leq 1$ and $\Pr_f = 0$) (Farina *et al.*, 2002*b*); and cluttered environments ($\Pr_d \leq 1$ and $\Pr_f \geq 0$) (Hernandez *et al.*, 2006). However, unlike the bound formulation given in (Tichavský *et al.*, 1998), the modified versions of the lower bound are mostly for a special class of non-linear SSMs with additive Gaussian state and sensor noise.

Notwithstanding a recursive procedure to compute the PCRLB in (Tichavský *et al.*, 1998), obtaining a closed form solution to it is non-trivial. This is due to the involved complex, multi-dimensional expectations with respect to the states and measurements, which do not lend themselves to an easy analytical solution, except in linear systems (Bergman, 2001), where the Kalman filter (KF) provides an exact solution to the PCRLB.

Several attempts have been made in the past to address the aforementioned issues. First, several authors considered approximating the PCRLB for systems with: (i) linear state dynamics with additive Gaussian noise and non-linear measurement model (Bergman, 2001; Hurtado *et al.*, 2008); (ii) linear and non-linear SSMs with additive Gaussian state and sensor noise (Šimandl *et al.*, 2001; Lei *et al.*, 2010); and (iii) linear SSMs with unknown measurement uncertainty (Zhang *et al.*, 2005). The special sub-class of non-linear SSMs with additive Gaussian noise allows reduction of the complex, multi-dimensional expectations to a lower dimension, which are relatively easier to approximate.

7.2   Motivation and contributions

To obtain a reasonable approximation to the PCRLB for general non-linear SSMs, several authors have considered using simulation based techniques, such as the Monte Carlo (MC) method. Although a MC method makes the lower bound computations off-line, nevertheless, it is a popular approach, since for many real-time applications in tracking and navigation, the design, selection and performance evaluation of different filtering algorithms are mostly done a priori or off-line. Furthermore, availability of huge amount of historical test-data, makes MC method a viable option. An MC based bound

approximation have appeared for several systems with: target generated measurements (Farina *et al.*, 2002; Hurtado *et al.*, 2008); measurement origin uncertainty (Hernandez *et al.*, 2002); cluttered environments (Hernandez *et al.*, 2006; Meng *et al.*, 2009); and Markovian models (Svensson, 2010; Bessell *et al.*, 2003). Although MC methods can be effectively used to approximate the involved expectations, with respect to the states and measurements, it requires an ensemble of the true states and measurements. While the sensor readings may be available from the historical test-data, the true states may not be available, except in simulations or in carefully designed experiments (Lei *et al.*, 2011).

To avoid having to use the true states, (Lei *et al.*, 2011) proposed an EKF and UKF based method to compute the PCRLB formulation in (Tichavský *et al.*, 1998). To approximate the bound, (Lei *et al.*, 2011) first assumes the densities associated with the expectations to be Gaussian, and then uses an EKF and UKF to approximate the Gaussian densities using an estimate of the mean and covariance. Even though the method proposed in (Lei *et al.*, 2011) is fast, since it only works with the first two statistical moments, there are several performance and applicability related issues with this numerical approach, such as: (i) relies on the linearisation of the underlying non-linear dynamics around the state estimates, which not only results in additional numerical errors, but also introduces bias in the PCRLB approximation; (ii) the method is applicable only for non-linear SSMs with additive Gaussian state and sensor noise; (iii) convergence of the numerical solution to the theoretical lower bound is not guaranteed; (iv) provides limited control for improving the quality of the resulting numerical solution; and (v) it involves long and tedious calculations of the first two moments of the assumed Gaussian densities.

Recently, (Zuo *et al.*, 2011) derived a conditional lower bound for general non-linear SSMs, and used an SMC based method to approximate it in absence of the true states. Unlike the unconditional PCRLB in (Tichavský *et al.*, 1998), the conditional PCRLB can be computed in real-time; however, as shown in (Zuo *et al.*, 2011), the bound in less optimistic

(or higher) compared to the unconditional PCRLB. This limits its use to applications, where real-time bound computation is far more important than obtaining a tighter limit on the tracking performance. However, in applications, such as filter design and selection, where the primary focus is on devising an efficient filtering strategy, the PCRLB in (Tichavský *et al.*, 1998) provides an optimistic measure of the filter performance.

To the authors' best knowledge, there are no known numerical method to approximate the unconditional PCRLB in (Tichavský *et al.*, 1998), when the true states are unavailable.

The following are the main contributions in this chapter: (i) an SMC based method is developed to numerically approximate the unconditional PCRLB in (Tichavský *et al.*, 1998), for a general stochastic non-linear SSMs operating with $\Pr_d = 1$ and $\Pr_f = 0$. The expectations defined originally with respect to the true states and measurements are reformulated to accommodate use of the available sensor readings. This is done by first conditioning the distribution of the true states over the sensor readings, and then using an SMC method to approximate it. (ii) Based on the above developments, a numerical method to compute the lower bound for a class of discrete-time, non-linear SSMs with additive Gaussian state and sensor noise is derived. This is required, since several practical problems, especially in tracking, navigation and sensor management, are often modelled as non-linear SSMs, with additive Gaussian noise. (iii) Convergence results for the SMC based PCRLB approximation is also provided. (iii) The quality of the SMC based PCRLB approximation is illustrated on two examples, which include a uni-variate, non-stationary growth model and a practical problem of ballistic target tracking at re-entry phase.

The proposed simulation based method is an off-line method, which can be used to deliver an efficient numerical approximation to the lower bound in (Tichavský *et al.*, 1998), based on the sensor readings alone. Compared to the EKF and UKF based PCRLB approximation method derived in (Lei *et al.*, 2011), the proposed SMC based method: (i) is far more general as it can approximate the PCRLB for a larger class of discrete-time, non-

linear SSMs with possibly non-Gaussian state and sensor noise; (ii) avoids numerical errors arising due to the use of dynamics linearisation methods; and (iii) provides a far greater control over the quality of the resulting approximation. Moreover, several theoretical results exist for the SMC methods, which can be used to suggest convergence of the SMC based PCRLB approximation to the actual lower bound. All these features of the proposed method are either validated theoretically or illustrated on simulation examples.

7.3   Problem formulation

In this chapter, we consider a model for a class of general stochastic non-linear systems.

Model 7.3.1. *Consider the following discrete-time, stochastic non-linear SSM*

$$X_{t+1} = f_t(X_t, u_t, \theta, V_t), \tag{7.1a}$$

$$Y_t = g_t(X_t, u_t, \theta, W_t), \tag{7.1b}$$

where: $X_t \in \mathcal{X} \subseteq \mathbb{R}^n$ and $Y_t \in \mathcal{Y} \subseteq \mathbb{R}^m$ are the state variables and sensor measurements, respectively; $u_t \in \mathcal{U} \subseteq \mathbb{R}^p$ is input variables and $\theta \in \Theta \subseteq \mathbb{R}^r$ are the model parameters. Also: the state and sensor noise are represented as $V_t \in \mathbb{R}^n$ and $W_t \in \mathbb{R}^m$, respectively. $f_t(\cdot)$ is an n-dimensional state mapping function and $g_t(\cdot)$ is a m-dimensional measurement mapping function, where each being possibly non-linear in its arguments.

Model 7.3.1 represents one of the most general classes of discrete-time, stochastic non-linear SSMs. For notational simplicity, explicit dependence on $u_t \in \mathcal{U}$ and $\theta \in \Theta$ are not shown in the rest of this article; however, all the derivations that appear in this chapter hold with u_t and θ included. Assumptions on Model 7.3.1 are discussed next.

Assumption 7.3.2. *The state and sensor dynamics are defined as $f_t := \mathcal{X} \times \mathbb{R}^n \to \mathbb{R}^n$ and $g_t := \mathcal{X} \times \mathbb{R}^m \to \mathbb{R}^m$, respectively, are at least twice differentiable with respect to $X_t \in \mathcal{X}$. Also, the parameters $\theta \in \Theta$ and inputs $u_t \in \mathcal{U}$ are assumed to be known a priori.*

Assumption 7.3.3. *Sensor measurements are target-originated, operating with probability of false alarm* $\Pr_f = 0$ *and probability of detection* $\Pr_d = 1$. *The target states* $X_t \in \mathcal{X}$ *are hidden Markov process, observed only through the measurement process* $Y_t \in \mathcal{Y}$.

Assumption 7.3.4. V_t, W_t *and* X_0 *are mutually independent sequences of independent random variables described by the probability density functions (pdfs)* $p(v_t)$, $p(w_t)$ *and* $p(x_0)$, *respectively. These pdfs are known in their classes (e.g., Gaussian; uniform) and are parametrized by a known and finite number of moments (e.g., mean; variance).*

Assumption 7.3.5. *For a random realization* $(x_{t+1}, x_t, v_t) \in \mathcal{X} \times \mathcal{X} \times \mathbb{R}^n$ *and* $(y_t, x_t, w_t) \in \mathcal{Y} \times \mathcal{X} \times \mathbb{R}^m$ *satisfying Model 7.3.1,* $\nabla_{v_t} f_t^T(x_t, v_t)$ *and* $\nabla_{w_t} g_t^T(x_t, w_t)$ *have rank* n *and* m, *such that using implicit function theorem,* $p(x_{t+1}|x_t) = p(V_t = \tilde{f}_t(x_t, x_{t+1}))$ *and* $p(y_t|x_t) = p(W_t = \tilde{g}_t(x_t, y_t))$ *do not involve Dirac delta functions.*

7.3.1   Posterior Cramér-Rao lower bound

The conventional CRLB provides a lower bound on the MSE of any ML based estimator. An analogous extension of the CRLB to the class of Bayesian estimators was derived by (Trees, 1968), and is referred to as the PCRLB inequality. Extension of the PCRLB to non-linear tracking was provided by (Tichavský *et al.*, 1998), and is given next.

Lemma 7.3.6. *Let* $\{Y_{1:t}\}_{t \in \mathbb{N}}$ *be a sequence from Model 7.3.1, then MSE of any tracking filter at* $t \in \mathbb{N}$ *is bounded from below by the following matrix inequality*

$$P_{t|t} \triangleq \mathbb{E}_{p(X_{0:t}, Y_{1:t})}[(X_t - \widehat{X}_{t|t})(X_t - \widehat{X}_{t|t})^T] \succcurlyeq J_t^{-1}, \tag{7.2}$$

where: $P_{t|t}$ *is a* $n \times n$ *matrix of MSE;* $\widehat{X}_{t|t} \triangleq \widehat{X}_t(Y_{1:t}) := \mathbb{R}^{tm} \to \mathbb{R}^n$ *is a point estimate of* $X_t \in \mathcal{X}$ *at time* $t \in \mathbb{N}$, *given the measurement sequence* $\{Y_{1:t} = y_{1:t}\} \triangleq \{y_1, \ldots, y_t\}$; J_t *is a* $n \times n$ *PFIM matrix;* J_t^{-1} *is a* $n \times n$ *PCRLB matrix;* $p(x_{0:t}, y_{1:t})$ *is a joint probability density of the states and measurements up until time* $t \in \mathbb{N}$; *the superscript* $(\cdot)^T$ *is the transpose operation; and* $\mathbb{E}_{p(\cdot)}[\cdot]$ *is the expectation operator with respect to the pdf* $p(\cdot)$.

Proof. See (Trees, 1968) for a detailed proof.   □

Inequality (7.2) implies that $P_{t|t} - J_t^{-1} \succcurlyeq 0$ is a positive semi-definite matrix for all $\widehat{X}_{t|t} \in \mathbb{R}^n$ and $t \in \mathbb{N}$. (7.2) can also be written in terms of a scalar MSE (SMSE) as

$$P_{t|t}^S \triangleq \mathbb{E}_{p(X_{0:t}, Y_{1:t})}[\|X_t - \widehat{X}_{t|t}\|^2] \geq \mathrm{Tr}[J_t^{-1}], \tag{7.3}$$

where $\mathrm{Tr}[\cdot]$ is the trace operator, and $\|\cdot\|$ is a 2-norm.

Lemma 7.3.7. *For a system represented by Model 7.3.1 and operating under Assumptions 7.3.2 through 7.3.5, the PFIM in Lemma 7.3.6 can be recursively computed as (Tichavský et al., 1998; Šimandl et al., 2001)*

$$J_{t+1} = D_t^{22} - [D_t^{12}]^T (J_t + D_t^{11})^{-1} D_t^{12}, \tag{7.4}$$

where:

$$D_t^{11} = \mathbb{E}_{p(X_{0:t+1}, Y_{1:t+1})}[-\Delta_{X_t}^{X_t} \log\ p(X_{t+1}|X_t)]; \tag{7.5a}$$

$$D_t^{12} = \mathbb{E}_{p(X_{0:t+1}, Y_{1:t+1})}[-\Delta_{X_t}^{X_{t+1}} \log\ p(X_{t+1}|X_t)]; \tag{7.5b}$$

$$D_t^{22} = \mathbb{E}_{p(X_{0:t+1}, Y_{1:t+1})}[-\Delta_{X_{t+1}}^{X_{t+1}} \log\ p(X_{t+1}|X_t) - \Delta_{X_{t+1}}^{X_{t+1}} \log\ p(Y_{t+1}|X_{t+1})]; \tag{7.5c}$$

and: Δ is a Laplacian operator such that $\Delta_X^Y \triangleq \nabla_X \nabla_Y^T$ with $\nabla_X \triangleq \left[\frac{\partial}{\partial X}\right]$ being a gradient operator, evaluated at the true states. Also, $J_0 = \mathbb{E}_{p(X_0)}[-\Delta_{X_0}^{X_0} \log\ p(X_0)]$.

Proof. See (Tichavský *et al.*, 1998) for a complete proof.   □

For Model 7.3.1, obtaining a closed-form solution to the PFIM or PCRLB is non-trivial. This is due to the complex integrals involved in (7.5), which do not lend themselves to an easy analytical solution. The main problem addressed in this chapter is discussed next.

Problem 7.3.8. *Compute a numerical solution to the PCRLB given in Lemma 7.3.6 for systems represented by Model 7.3.1 and operating under Assumptions 7.3.2 through 7.3.5.*

Use of simulation based methods in addressing Problem 7.3.8 is discussed next.

7.4   Approximating PCRLB

MC method is a popular approach, which can be used to approximate the PCRLB; however, as discussed in Section 7.2, MC method requires an ensemble of true states and sensor measurements. While sensor readings may be available from the historical test-data, the true states may not be available in practice. To allow the use of sensor readings in approximating the PCRLB, this chapter reformulates the integrals in (7.5) as given below.

Proposition 7.4.1. *The complex, multi-dimensional expectations in (7.5), with respect to the density $p(x_{0:t+1}, y_{1:t+1})$ can be reformulated, and written as follows:*

$$I_t^{11} = \mathbb{E}_{p(X_{0:t+1}|Y_{1:t+1})}[-\Delta_{X_t}^{X_t} \log \ p(X_{t+1}|X_t)]; \tag{7.6a}$$

$$I_t^{12} = \mathbb{E}_{p(X_{0:t+1}|Y_{1:t+1})}[-\Delta_{X_t}^{X_{t+1}} \log \ p(X_{t+1}|X_t)]; \tag{7.6b}$$

$$I_t^{22,a} = \mathbb{E}_{p(X_{0:t+1}|Y_{1:t+1})}[-\Delta_{X_{t+1}}^{X_{t+1}} \log \ p(X_{t+1}|X_t)]; \tag{7.6c}$$

$$I_t^{22,b} = \mathbb{E}_{p(X_{0:t+1}|Y_{1:t+1})}[-\Delta_{X_{t+1}}^{X_{t+1}} \log \ p(Y_{t+1}|X_{t+1})], \tag{7.6d}$$

where:

$$D_t^{11} = \mathbb{E}_{p(Y_{1:t+1})}[I_t^{11}]; \tag{7.6e}$$

$$D_t^{12} = \mathbb{E}_{p(Y_{1:t+1})}[I_t^{12}]; \tag{7.6f}$$

$$D_t^{22} = \mathbb{E}_{p(Y_{1:t+1})}[I_t^{22,a} + I_t^{22,b}]. \tag{7.6g}$$

Proof. The proof is based on decomposition of the pdf $p(x_{0:t+1}, y_{1:t+1})$ in (7.5), using the probability condition $p(x_{0:t+1}, y_{1:t+1}) = p(y_{1:t+1})p(x_{0:t+1}|y_{1:t+1})$. $\qquad\square$

Remark 7.4.2. *In Proposition 7.4.1 the integrals are with respect to $p(y_{1:t+1})$ and $p(x_{0:t+1}|y_{1:t+1})$. The advantage of representing (7.5) as (7.6) is evident: using historical test-data, expectations with respect to $p(y_{1:t+1})$ can be approximated using MC, while that defined with respect to $p(x_{0:t+1}|y_{1:t+1})$ can be approximated using an SMC method.*

7.4.1   SMC based PCRLB approximation

It is not our aim here to review SMC methods in details, but to simply highlight their role in approximating the multi-dimensional integrals in Proposition 7.4.1. For a detailed exposition on SMC methods, see (Doucet *et al.*, 2001; Ristic *et al.*, 2004). The essential idea behind SMC methods is to generate a large set of random particles (samples) from the target pdf, with respect to which the integrals are defined. The target pdf of interest in Proposition 7.4.1 is $p(x_{0:t}|y_{1:t})$. Using SMC methods, the target distribution, defined as $p(dx_{0:t+1}|y_{1:t+1}) \triangleq p(x_{0:t+1}|y_{1:t+1})dx_{0:t+1}$ can be approximated as given below.

$$\tilde{p}(dx_{0:t+1}|y_{1:t+1}) = \sum_{i=1}^{N} W_{0:t+1|t+1}^{i} \delta_{X_{0:t+1|t+1}^{i}}(dx_{0:t+1}), \tag{7.7}$$

where: $\tilde{p}(dx_{0:t+1}|y_{1:t+1})$ is an N-particle SMC approximation of the target distribution $p(dx_{0:t+1}|y_{1:t+1})$ and $\{X_{0:t+1|t+1}^{i}; W_{0:t+1|t+1}^{i}\}_{i=1}^{N}$ are the N pairs of particle realizations and their associated weights distributed according to $p(x_{0:t+1}|y_{1:t+1})$, such that $\sum_{i=1}^{N} W_{0:t|t}^{i} = 1$. Using (7.7), an SMC approximation of (7.6a), for example, can be computed as

$$\tilde{I}_{t}^{11} = \sum_{i=1}^{N} W_{0:t+1|t+1}^{i} [-\Delta_{X_t}^{X_t} \log\ p(X_{t+1|t+1}^{i}|X_{t|t+1}^{i})]. \tag{7.8}$$

where $\tilde{I}_{t}^{11}$ is an SMC estimate of I_{t}^{11} and the Laplacian is evaluated at $\{X_{t:t+1|t+1}^{i}\}_{i=1}^{N}$.

The convergence of (7.8) to (7.6a) depends on (7.7). Many sharp results on convergence of SMC methods are available (see (Crisan and Doucet, 2002) for a survey chapter and (Moral, 2004) for a book length review). A selection of these results highlighting the difficulties in approximating $p(dx_{0:t}|y_{1:t})$ with an SMC method are presented below.

Theorem 7.4.3. *For any bounded test function $\phi_t : \mathcal{X}^{t+1} \to \mathbb{R}$, there exists $C_{t,p} < \infty$, such that for any $p > 0$, $N \geq 1$ and $t \geq 1$, the following inequality holds*

$$\mathbb{E}\left[\left|\int_{\mathcal{X}^{t+1}} \phi_t(x_{0:t})\epsilon_t(dx_{0:t}|y_{1:t})\right|^p\right]^{\frac{1}{p}} \leq \frac{C_{t,p}\bar{\phi}_t}{N^{1/2}}, \tag{7.9}$$

where $\epsilon_t(dx_{0:t}|y_{1:t}) = \tilde{p}(dx_{0:t}|y_{1:t}) - p(dx_{0:t}|y_{1:t})$ is the N-particle approximation error, $\bar{\phi}_t = \sup_{x_{0:t} \in \mathcal{X}^{t+1}} |\phi_t(x_{0:t})|$, and the expectation is with respect to the particle realizations.

Proof. See Theorem 2 in (Moral and Doucet, 2003) for a detailed proof. □

Remark 7.4.4. *The result in Theorem 7.4.3 is weak, since $C_{t,p} \in \mathbb{R}$ being a function of $t \in \mathbb{N}$, grows exponentially/polynomially with time (Kantas et al., 2009). To guarantee a fixed precision of the approximation in (7.8), N has to increase with t. The result in Theorem 7.4.3 is not surprising, since (7.7) requires sampling from the pdf $p(x_{0:t}|y_{1:t})$, whose dimension increases as $n(t+1)$. In literature Theorem 7.4.3 is referred to as the sample path degeneracy problem. This is a fundamental limitation of SMC methods; wherein, for $N \in \mathbb{N}$, the quality of the approximation of $p(dx_{0:t}|y_{1:t})$ deteriorates with time.*

The motivation to use SMC methods to approximate the complex, multi-dimensional integrals in Proposition 7.4.1 is based on the fact that encouraging results can be obtained under the exponential forgetting assumption on Model 7.3.1. Since $\theta \in \Theta$ is assumed to be known (see Assumption 7.3.2), the forgetting property in Model 7.3.1 holds. With the forgetting property, it is possible to establish results of the form given in the next theorem.

Theorem 7.4.5. *For an integer $L > 0$, and any bounded test function $\phi_L : \mathcal{X}^L \to \mathbb{R}$, there exists $D_{L,p} < \infty$, such that for any $p > 0$, $N \geq 1$ and $t \geq 1$, the following inequality holds*

$$\mathbb{E}\left[\left|\int_{\mathcal{X}^L} \phi_L(x_{t-L+1:t})\epsilon_L(dx_{t-L+1:t}|y_{1:t})\right|^p\right]^{\frac{1}{p}} \leq \frac{D_{L,p}\bar{\phi}_L}{N^{1/2}}, \tag{7.10}$$

where $\epsilon_L(dx_{t-L+1:t}|y_{1:t}) = \int_{\mathcal{X}^{t-L+1}} \epsilon_t(dx_{0:t}|y_{1:t})$.

Proof. See Theorem 2 in (Moral and Doucet, 2003) for a detailed proof. □

Remark 7.4.6. *Since $D_{L,p} \in \mathbb{R}$ is independent of $t \in \mathbb{N}$, Theorem 7.4.5 suggests that an SMC based approximation of the most recent marginal posterior pdf $p(x_{t-L+1:t}|y_{1:t})$, over a fixed horizon $L > 0$ does not result in the error accumulation.*

For our purposes, to make the SMC based PCRLB approximation effective, the dimension of the integrals in Proposition 7.4.1 needs to be reduced. An SMC based approximation of the PCRLB over a reduced dimensional state-space is discussed next.

Lemma 7.4.7. *For a system represented by Model 7.3.1, using the Markov property of the target states in Assumptions 7.3.3, Proposition 7.4.1 can be written as follows:*

$$I_t^{11} = \mathbb{E}_{p(X_{t:t+1}|Y_{1:t+1})}[-\Delta_{X_t}^{X_t} \log\ p(X_{t+1}|X_t)]; \tag{7.11a}$$

$$I_t^{12} = \mathbb{E}_{p(X_{t:t+1}|Y_{1:t+1})}[-\Delta_{X_t}^{X_{t+1}} \log\ p(X_{t+1}|X_t)]; \tag{7.11b}$$

$$I_t^{22,a} = \mathbb{E}_{p(X_{t:t+1}|Y_{1:t+1})}[-\Delta_{X_{t+1}}^{X_{t+1}} \log\ p(X_{t+1}|X_t)]; \tag{7.11c}$$

$$I_t^{22,b} = \mathbb{E}_{p(X_{t+1}|Y_{1:t+1})}[-\Delta_{X_{t+1}}^{X_{t+1}} \log\ p(Y_{t+1}|X_{t+1})]. \tag{7.11d}$$

Proof. The proof is based on a straightforward use of the definition of expectation and Markov property of Model 7.3.1. For example, the integrals in (7.6a) can be written as

$$I_t^{11} = \int_{\mathcal{X}^{t+2}} [-\Delta_{x_t}^{x_t} \log\ p(x_{t+1}|x_t)] p(dx_{0:t+1}|y_{1:t+1}), \tag{7.12a}$$

$$= \int_{\mathcal{X}^2} [-\Delta_{x_t}^{x_t} \log\ p(x_{t+1}|x_t)] p(dx_{t:t+1}|y_{1:t+1}), \tag{7.12b}$$

$$= \mathbb{E}_{p(X_{t:t+1}|Y_{1:t+1})}[-\Delta_{X_t}^{X_t} \log\ p(X_{t+1}|X_t)], \tag{7.12c}$$

where $p(dx_{0:t+1}|y_{1:t+1}) \triangleq p(x_{0:t+1}|y_{1:t+1})dx_{0:t+1}$, and in (7.12c), since the integrand is independent of $x_{0:t-1} \in \mathcal{X}^t$, it is marginalized out of the integral. Equations (7.11b) through (7.11d) can be derived based on similar arguments, which completes the proof. □

Remark 7.4.8. *The dimension of the expectations in (7.6a) through (7.6c) reduces from $n(t+2)$ to $2n$; whereas, in (7.6d), it reduces from $n(t+2)$ to n for all $t \in \mathbb{N}$. Moreover, since expectations in Lemma 7.4.7 are with respect to $p(x_{t:t+1}|y_{1:t+1})$ and $p(x_{t+1}|y_{1:t+1})$, an SMC method can be effectively used with a finite number of particles (see Theorem 7.4.5).*

7.4.2   General non-linear SSMs

To approximate the multi-dimensional integrals in Lemma 7.4.7 for Model 7.3.1, a set of randomly generated samples from the target distribution $p(dx_{t:t+1}|y_{1:t+1})$ is required. First note that the target pdf $p(x_{t:t+1}|y_{1:t+1})$ can alternatively be written as given below.

Lemma 7.4.9. *The target pdf* $p(x_{t:t+1}|y_{1:t+1})$, *with respect to which the integrals in Lemma 7.4.7 are defined can be decomposed, and written as*

$$p(x_{t:t+1}|y_{1:t+1}) = \frac{p(x_{t+1}|x_t)p(x_t|y_{1:t})p(x_{t+1}|y_{1:t+1})}{\int_{\mathcal{X}} p(x_{t+1}|x_t)p(dx_t|y_{1:t})}. \tag{7.13}$$

Proof. First note that the target pdf $p(x_{t:t+1}|y_{1:t+1})$ can be written as

$$p(x_{t:t+1}|y_{1:t+1}) = p(x_t|x_{t+1}, y_{1:t}, y_{t+1})p(x_{t+1}|y_{1:t+1}). \tag{7.14}$$

From the Markov property of (7.1), and from the Bayes' theorem, (7.14) can be written as

$$p(x_{t:t+1}|y_{1:t+1}) = \frac{p(y_{t+1}|x_t, x_{t+1}, y_{1:t})p(x_t|x_{t+1}, y_{1:t})p(x_{t+1}|y_{1:t+1})}{p(y_{t+1}|x_{t+1}, y_{1:t})}, \tag{7.15a}$$

$$= \frac{p(y_{t+1}|x_{t+1}, y_{1:t})p(x_t|x_{t+1}, y_{1:t})p(x_{t+1}|y_{1:t+1})}{p(y_{t+1}|x_{t+1}, y_{1:t})}, \tag{7.15b}$$

$$= p(x_t|x_{t+1}, y_{1:t})p(x_{t+1}|y_{1:t+1}). \tag{7.15c}$$

Applying Bayes' theorem again in (7.15c) yields

$$p(x_{t:t+1}|y_{1:t+1}) = \frac{p(x_{t+1}|x_t, y_{1:t})p(x_t|y_{1:t})p(x_{t+1}|y_{1:t+1})}{p(x_{t+1}|y_{1:t})}, \tag{7.16a}$$

$$= \frac{p(x_{t+1}|x_t)p(x_t|y_{1:t})p(x_{t+1}|y_{1:t+1})}{\int_{\mathcal{X}} p(x_{t+1}|x_t)p(dx_t|y_{1:t})}, \tag{7.16b}$$

where in (7.16b), the Law of Total Probability is used, which completes the proof. □

Remark 7.4.10. *The procedure for generating random particles from densities, such as the uniform or Gaussian, is well described in literature; however, due to the multi-variate, and non-Gaussian nature of the target pdf, generating random particles from* $p(x_{t:t+1}|y_{1:t+1})$ *is a non-trivial problem. An alternative idea is to employ an importance sampling function (ISF), from which random particles are easier to generate (Doucet* et al.*, 2001).*

In this chapter, the product of two pdfs in (7.13) is selected as the ISF, such that

$$q(x_{t:t+1}|y_{1:t+1}) \triangleq p(x_t|y_{1:t})p(x_{t+1}|y_{1:t+1}), \tag{7.17}$$

Algorithm 7 SMC based posterior density approximation

Input: Given Model 7.3.1, satisfying Assumptions 7.3.2 through 7.3.5, assume a prior pdf on X_0, such that $X_0 \sim p(x_0)$. Also, select algorithm parameter N.

Output: Recursive SMC approximation of the posterior $p(dx_t|y_{1:t})$ for all $t \in \mathbb{N}$.

1: Generate N independent and identically distributed particles $\{X_{0|-1}^i\}_{i=1}^N \sim p(x_0)$ and set the associated weights to $\{W_{0|-1}^i = N^{-1}\}_{i=1}^N$. Set $t \leftarrow 1$.

2: Sample $\{X_{t|t-1}^i\}_{i=1}^N \sim p(x_t|y_{1:t-1})$. Set $\{W_{t|t-1}^i = N^{-1}\}_{i=1}^N$.

3: **while** $t \in \mathbb{N}$ **do**

4:   Use $\{Y_t = y_t\}$ and compute the importance weights $\{W_{t|t}^i\}_{i=1}^N$ using

$$W_{t|t}^i = \frac{W_{t|t-1}^i p(y_t|X_{t|t-1}^i)}{\sum_{j=1}^N W_{t|t-1}^j p(y_t|X_{t|t-1}^i)}. \tag{7.18}$$

5:   Resample the particle set $\{X_{t|t}^j\}_{j=1}^N$ with replacement from $\{X_{t|t-1}^i\}_{i=1}^N$, such that

$$\text{Pr}(X_{t|t}^j = X_{t|t-1}^i) = W_{t|t}^i, \tag{7.19}$$

  where $Pr(\cdot)$ is a probability measure. Set $\{W_{t|t}^i = N^{-1}\}_{i=1}^N$.

6:   Sample $\{X_{t+1|t}^i\}_{i=1}^N \sim p(x_{t+1}|y_{1:t})$ using (7.57). Set $\{W_{t+1|t}^i = N^{-1}\}_{i=1}^N$.

7:   Set $t \leftarrow t + 1$.

8: **end while**

---

where $q(x_{t:t+1}|y_{1:t+1})$ is a non-negative ISF on $\mathcal{X}^2$, such that $\text{supp}\, q(x_{t:t+1}|y_{1:t+1}) \supseteq \text{supp}\, p(x_{t:t+1}|y_{1:t+1})$. Choice of an ISF similar to (7.17) was also employed in (Tanizaki, 2001; Schön *et al.*, 2011) to develop a particle smoothing algorithm for discrete-time, non-linear SSMs. Thus to be able to generate random samples from (7.17), samples from the two posteriors $p(x_t|y_{1:t})$ and $p(x_{t+1}|y_{1:t+1})$ need to be generated first. Again, using the principles of ISF, particles from the posterior pdf can be generated using any advanced SMC methods (e.g., ASIR (Pitt and Shephard, 1999), resample-move algorithm (Gilks and Berzuini, 2002), block sampling strategy (Doucet *et al.*, 2006)) or for example, using the method in (Schön *et al.*, 2011; Gopaluni, 2008). The method described in (Schön *et al.*, 2011; Gopaluni, 2008) is outlined in Algorithm 7. It is important to note that in importance sampling, degeneracy is a common problem; wherein, after a few time instances, the density of the weights in (7.18) become skewed. The resampling step in

(7.18) is crucial in limiting the effects of degeneracy. Finally using Algorithm 7., the particle representation of $p(dx_t|y_{1:t})$ and $p(dx_{t+1}|y_{1:t+1})$ are given by

$$\tilde{p}(dx_t|y_{1:t}) = \frac{1}{N} \sum_{i=1}^{N} \delta_{X_{t|t}^i}(dx_t), \qquad (7.20a)$$

$$\tilde{p}(dx_{t+1}|y_{1:t+1}) = \frac{1}{N} \sum_{j=1}^{N} \delta_{X_{t+1|t+1}^j}(dx_{t+1}). \qquad (7.20b)$$

Here $\{X_{t|t}^i\}_{i=1}^N \sim \tilde{p}(x_t|y_{1:t})$ and $\{X_{t+1|t+1}^i\}_{i=1}^N \sim \tilde{p}(x_{t+1}|y_{1:t+1})$ are the N pairs of resampled i.i.d. samples from $\tilde{p}(x_t|y_{1:t})$ and $\tilde{p}(x_{t+1}|y_{1:t+1})$, respectively.

Remark 7.4.11. *Uniform convergence in time of (7.20) has been established by (Moral, 2004; Chopin, 2004). Although these results rely on strong mixing assumptions of Model 7.3.1, uniform convergence has been observed in numerical studies for a wide class of non-linear time-series models, where the mixing assumptions are not satisfied.*

Substituting (7.20) into (7.17), yields an SMC approximation of the ISF, i.e.,

$$\tilde{q}(dx_{t:t+1}|y_{1:t+1}) = \frac{1}{N^2} \sum_{j=1}^{N} \sum_{i=1}^{N} \delta_{X_{t|t}^i, X_{t+1|t+1}^j}(dx_{t:t+1}), \qquad (7.21)$$

where $\tilde{q}(dx_{t:t+1}|y_{1:t+1})$ is an N^2-particle SMC approximation of the ISF distribution $q(dx_{t:t+1}|y_{1:t+1})$ and $\{X_{t|t}^i; X_{t+1|t+1}^j\}_{i=1,j=1}^{N,N} \sim \tilde{q}(x_{t:t+1}|y_{1:t+1})$ are particles from the ISF.

Lemma 7.4.12. *An SMC approximation of the target distribution $p(dx_{t:t+1}|y_{1:t+1})$ can be computed using the SMC approximation of $q(dx_{t:t+1}|y_{1:t+1})$ given in (7.21), such that*

$$\tilde{p}(dx_{t:t+1}|y_{1:t+1}) = \sum_{i=1}^{N} W_{t|t,t+1|t+1}^i \delta_{X_{t|t}^i, X_{t+1|t+1}^i}(dx_{t:t+1}), \qquad (7.22)$$

where:

$$W_{t|t,t+1|t+1}^i \triangleq \frac{\zeta_{t|t,t+1|t+1}^i}{\sum_{j=1}^{N} \zeta_{t|t,t+1|t+1}^j}; \qquad (7.23a)$$

$$\zeta_{t|t,t+1|t+1}^i \triangleq \frac{p(X_{t+1|t+1}^i|X_{t|t}^i)}{N \sum_{m=1}^{N} p(X_{t+1|t+1}^i|X_{t|t}^m)}; \qquad (7.23b)$$

and $\tilde{p}(dx_{t:t+1}|y_{1:t+1})$ is an SMC approximation of the target distribution $p(dx_{t:t+1}|y_{1:t+1})$.

Proof. Substituting (7.21) into (7.13) followed by several algebraic manipulations yields an SMC approximation of $p(dx_{t:t+1}|y_{1:t+1})$, denoted by $\tilde{p}(dx_{t:t+1}|y_{1:t+1})$, such that

$$\tilde{p}(dx_{t:t+1}|y_{1:t+1}) = \frac{p(x_{t+1}|x_t)\tilde{q}(dx_{t:t+1}|y_{1:t+1})}{\int_{\mathcal{X}} p(x_{t+1}|x_t)\tilde{p}(dx_t|y_{1:t})}, \tag{7.24a}$$

$$= \frac{Np(x_{t+1}|x_t)\sum_{j=1}^{N}\sum_{i=1}^{N}\delta_{X_{t|t}^i,X_{t+1|t+1}^j}(dx_{t:t+1})}{N^2\int_{\mathcal{X}} p(x_{t+1}|x_t)\sum_{m=1}^{N}\delta_{X_{t|t}^i}(dx_t)}, \tag{7.24b}$$

$$= \frac{\sum_{j=1}^{N}\sum_{i=1}^{N}p(X_{t+1|t+1}^j|X_{t|t}^i)\delta_{X_{t|t}^i,X_{t+1|t+1}^j}(dx_{t:t+1})}{N\sum_{m=1}^{N}p(X_{t+1|t+1}^j|X_{t|t}^m)}, \tag{7.24c}$$

$$= \sum_{j=1}^{N}\sum_{i=1}^{N}W_{t|t,t+1|t+1}^{i,j}\delta_{X_{t|t}^i,X_{t+1|t+1}^j}(dx_{t:t+1}), \tag{7.24d}$$

where

$$W_{t|t,t+1|t+1}^{i,j} \triangleq \frac{p(X_{t+1|t+1}^j|X_{t|t}^i)}{N\sum_{m=1}^{N}p(X_{t+1|t+1}^j|X_{t|t}^m)}, \tag{7.25}$$

Equation (7.24d) is an SMC approximation of $p(dx_{t:t+1}|y_{1:t+1})$. The computational complexity of the weights in (7.25) is of the order $\mathcal{O}(N^2)$. As suggested in (Gopaluni, 2008), without significant loss in the quality of the approximation, the complexity can be reduced to the order $\mathcal{O}(N)$ by replacing (7.24d) with (7.22), which completes the proof. $\qquad \square$

The distribution of weights in (7.22) becomes skewed after a few time instances. To avoid this, the particles in (7.22) are resampled using systematic resampling, such that

$$\Pr(X_{t:t+1|t+1}^j = \{X_{t|t}^i; \ X_{t+1|t+1}^i\}) = W_{t|t,t+1|t+1}^i, \tag{7.26}$$

where $\{X_{t:t+1|t+1}^i\}_{i=1}^{N} \sim \tilde{p}(x_{t:t+1}|y_{1:t+1})$ are resampled i.i.d. particles. With resampling, the SMC approximation of the target distribution in (7.22) can be represented as

$$\tilde{p}(dx_{t:t+1}|y_{1:t+1}) = \frac{1}{N}\sum_{i=1}^{N}\delta_{X_{t:t+1|t+1}^i}(dx_{t:t+1}). \tag{7.27}$$

Expectation in Lemma 7.4.7, with respect to the marginalized pdf $p(x_t|y_{1:t+1})$ (see (7.11d)) can also be approximated using SMC methods as given in the next lemma.

Lemma 7.4.13. *Let* $\{X^i_{t:t+1|t+1}\}^N_{i=1}$ *in (7.27) be i.i.d. resampled particles distributed according to* $\tilde{p}(x_{t:t+1}|y_{1:t+1})$ *then an SMC approximation of* $p(dx_t|y_{1:t+1})$ *is given by*

$$\tilde{p}(dx_t|y_{1:t+1}) = \frac{1}{N} \sum_{i=1}^{N} \delta_{X^i_{t|t+1}}(dx_t), \tag{7.28}$$

where $\tilde{p}(dx_t|y_{1:t+1})$ *is an SMC approximation of* $p(dx_t|y_{1:t+1})$ *and* $\delta_{X^i_{t|t+1}}(\cdot)$ *is a marginalized Dirac delta function in* dx_t, *centred around the random particle* $X^i_{t|t+1}$.

Proof. See (Tulsyan *et al.*, 2013*b*) for the proof. $\qquad\qquad\qquad\qquad\qquad\square$

Lemma 7.4.13 gives a procedure for computing an SMC approximation of $p(dx_t|y_{1:t+1})$, using the particles from the SMC approximation of $p(dx_{t:t+1}|y_{1:t+1})$. Expectation with respect to $p(y_{1:t+1})$ in Proposition 7.4.1 can be approximated using MC method, such that

$$\tilde{p}(dy_{1:t+1}) = \frac{1}{M} \sum_{j=1}^{M} \delta_{Y^j_{1:t+1}}(dy_{1:t+1}), \tag{7.29}$$

where $\tilde{p}(dy_{1:t+1})$ is an MC approximation of $p(dy_{1:t+1})$, and M is the total number of i.i.d. measurement sequences obtained from the historical test-data. Note that the approximation in (7.29) is possible only under Assumption 7.3.2; however, in general, estimating the marginalized likelihood function $p(y_{1:t+1})$ is non-trivial (Kantas *et al.*, 2009).

Finally, an SMC approximation of the PCRLB for systems represented by Model 7.3.1 and operating under Assumptions 7.3.2 through 7.3.5 is summarized in the next lemma.

Lemma 7.4.14. *Let a general stochastic non-linear system be represented by Model 7.3.1, such that it satisfies Assumption 7.3.2 through 7.3.5. Let* $\{Y_{1:t} = y^j_{1:t}\}^M_{j=1}$ *be* $M \in \mathbb{N}$ *i.i.d. measurement sequences generated from Model 7.3.1, then the matrices (7.5a) through (7.5c) in Lemma 7.3.7 can be recursively approximated as follows:*

$$\tilde{D}^{11}_t = -\frac{1}{MN} \sum_{j=1}^{M} \sum_{i=1}^{N} [\Delta^{X_t}_{X_t} \log\, p(X^{i,j}_{t+1|t+1}|X^{i,j}_{t|t+1})]; \tag{7.30a}$$

$$\tilde{D}^{12}_t = -\frac{1}{MN} \sum_{j=1}^{M} \sum_{i=1}^{N} [\Delta^{X_{t+1}}_{X_t} \log\, p(X^{i,j}_{t+1|t+1}|X^{i,j}_{t|t+1})]; \tag{7.30b}$$

$$\tilde{D}_t^{22} = -\frac{1}{MN}\sum_{j=1}^{M}\sum_{i=1}^{N}[\Delta_{X_{t+1}}^{X_{t+1}}\log\ p(X_{t+1|t+1}^{i,j}|X_{t|t+1}^{i,j}) + \Delta_{X_{t+1}}^{X_{t+1}}\log\ p(Y_{t+1}^{j}|X_{t+1|t+1}^{i,j})];$$

$$(7.30c)$$

and $\{X_{t:t+1|t+1}^{i,j}\}_{i=1}^{N} \sim p(x_{t:t+1}|y_{1:t+1}^{j})$ is a set of N resampled particles from (7.27), distributed according to $p(x_{t:t+1}|y_{1:t+1}^{j})$ for all $\{Y_{1:t+1} = y_{1:t+1}^{j}\}_{j=1}^{M}$.

Proof. For a measurement sequence $\{Y_{1:t} = y_{1:t}^{j}\}$, an SMC approximation of the target distribution in (7.27) can be written as

$$\tilde{p}(dx_{t:t+1}|y_{1:t+1}^{j}) = \frac{1}{N}\sum_{i=1}^{N}\delta_{X_{t:t+1|t+1}^{i,j}}(dx_{t:t+1}),\tag{7.31}$$

where $X_{t:t+1|t+1}^{i,j} \sim p(x_{t:t+1}|y_{1:t+1}^{j})$ are resampled particles. Substituting (7.31) into Lemma 7.4.7, an SMC approximation of (7.11a) through (7.11d) can be obtained as follows:

$$\tilde{I}_t^{11} = \frac{1}{N}\sum_{i=1}^{N}-\Delta_{X_t}^{X_t}\log\ p(X_{t+1|t+1}^{i,j}|X_{t|t+1}^{i,j});\tag{7.32a}$$

$$\tilde{I}_t^{12} = \frac{1}{N}\sum_{i=1}^{N}-\Delta_{X_t}^{X_{t+1}}\log\ p(X_{t+1|t+1}^{i,j}|X_{t|t+1}^{i,j});\tag{7.32b}$$

$$\tilde{I}_t^{22,a} = \frac{1}{N}\sum_{i=1}^{N}-\Delta_{X_{t+1}}^{X_{t+1}}\log\ p(X_{t+1|t+1}^{i,j}|X_{t|t+1}^{i,j});\tag{7.32c}$$

$$\tilde{I}_t^{22,b} = \frac{1}{N}\sum_{i=1}^{N}-\Delta_{X_{t+1}}^{X_{t+1}}\log\ p(Y_{t+1}^{j}|X_{t+1|t+1}^{i,j}),\tag{7.32d}$$

where $\tilde{I}_t$ is an SMC approximation of I_t. Substituting (7.32) and (7.29) into (7.6e) through (7.6g) yields (7.30a) through (7.30c), which completes the proof. □

Lemma 7.4.14 gives an SMC based numerical method to approximate the complex, multi-dimensional integrals in Lemma 7.3.7. Note that since Lemma 7.4.14 is valid for a general non-linear SSMs, the derivatives of the logarithms of the pdfs in (7.30a) through (7.30c) are left in its original form, but can be computed for a given system.

Building on the developments in this section, an SMC approximation of the PCRLB for a class of non-linear SSMs with additive Gaussian noise is presented next.

7.4.3   Non-linear SSMs with additive Gaussian noise

Many practical applications in tracking (e.g., ballistic target tracking (Farina *et al.*, 2002), bearings-only tracking (Cadre and Trémois, 1998), range-only tracking (Song, 1999), multi-sensor resource deployment (Hernandez *et al.*, 2004) and other navigation problems (Karlsson *et al.*, 2003)) can be described by non-linear SSMs with additive Gaussian noise. Since the class of practical problems with additive Gaussian noise is extensive, especially in tracking, navigation and sensor management, an SMC based numerical method for approximating the PCRLB for such class of non-linear systems is presented.

Model 7.4.15. *Consider the class of non-linear SSMs with additive Gaussian noise*

$$X_{t+1} = f_t(X_t) + V_t, \tag{7.33a}$$

$$Y_t = g_t(X_t) + W_t, \tag{7.33b}$$

where $V_t \in \mathbb{R}^n$ and $W_t \in \mathbb{R}^m$ are mutually independent sequences from the Gaussian distribution, such that $V_t \sim \mathcal{N}(v_t|0, Q_t)$ and $W_t \sim \mathcal{N}(w_t|0, R_t)$.

Note that Model 7.4.15 can also be represented as

$$\log[p(X_{t+1}|X_t)] = c_1 - \frac{1}{2}[X_{t+1} - f_t(X_t)]^T Q_t^{-1}[X_{t+1} - f_t(X_t)], \tag{7.34a}$$

$$\log[p(Y_{t+1}|X_{t+1})] = c_2 - \frac{1}{2}[Y_{t+1} - g_{t+1}(X_{t+1})]^T R_{t+1}^{-1}[Y_{t+1} - g_{t+1}(X_{t+1})], \tag{7.34b}$$

where $c_1 \in \mathbb{R}_+$ and $c_2 \in \mathbb{R}_+$ are normalizing constant and $\mathbb{R}_+ := [0, \infty)$.

Result 7.4.16. *The first and second order partial derivative of (7.34a) is given by*

$$\nabla_{X_t} \log[p(X_{t+1}|X_t)] = [\nabla_{X_t} f_t^T(X_t)] Q_t^{-1}[X_{t+1} - f_t(X_t)], \tag{7.35a}$$

$$\Delta_{X_t}^{X_t} \log[p(X_{t+1}|X_t)] = -[\nabla_{X_t} f_t^T(X_t)] Q_t^{-1}[\nabla_{X_t} f_t(X_t)] + [\Delta_{X_t}^{X_t} f_t^T(X_t)] \Lambda_{X_t}^{-1} \Psi_{X_t}, \tag{7.35b}$$

and the first with respect to $X_{t+1} \in \mathcal{X}$ and the second with respect to $X_t \in \mathcal{X}$ is given by

$$\Delta_{X_t}^{X_{t+1}} \log[p(X_{t+1}|X_t)] = [\nabla_{X_t} f_t^T(X_t)] Q_t^{-1}, \tag{7.35c}$$

where: $\Lambda_{X_t}^{-1} = Q_t^{-1} I_{n^2 \times n^2}$; $\Psi_{X_t} = [X_{t+1} - f_t(X_t)] I_{n^2 \times n}$; $I_{n^2 \times n^2}$, *and* $I_{n^2 \times n}$ *are* $n^2 \times n^2$

and $n^2 \times n$ *identity matrix, respectively. Also:* $[\nabla_{X_t} f_t^T(X_t)]$ *and* $[\Delta_{X_t}^{X_t} f_t^T(X_t)]$ *are*

$$[\nabla_{X_t} f_t^T(X_t)] \triangleq [\nabla_{X_t} f_t^{(1)}(X_t), \cdots, \nabla_{X_t} f_t^{(n)}(X_t)]_{n \times n}, \tag{7.36a}$$

$$[\Delta_{X_t}^{X_t} f_t^T(x_t)] \triangleq [\Delta_{X_t}^{X_t} f_t^{(1)}(X_t), \cdots, \Delta_{X_t}^{X_t} f_t^{(n)}(X_t)]_{n \times n^2}, \tag{7.36b}$$

where $f_t(X_t) \triangleq [f_t^{(1)}(X_t), \cdots, f_t^{(n)}(X_t)]^T$ *is a* $n \times 1$ *vector valued function in (7.33a).*

Result 7.4.17. *The second order partial derivative of (7.34a) and (7.34b) is given by*

$$\Delta_{X_{t+1}}^{X_{t+1}} \log[p(X_{t+1}|X_t)] = -Q_t^{-1} \tag{7.37a}$$

$$\Delta_{X_{t+1}}^{X_{t+1}} \log[p(Y_{t+1}|X_{t+1})] = [\Delta_{X_{t+1}}^{X_{t+1}} g_{t+1}^T(X_{t+1})] \Lambda_{Y_{t+1}}^{-1} \Psi_{Y_{t+1}} - [\nabla_{X_{t+1}} g_{t+1}^T(X_{t+1})] R_{t+1}^{-1}$$

$$\times [\nabla_{X_{t+1}} g_{t+1}(X_{t+1})] \tag{7.37b}$$

where: $\Lambda_{Y_{t+1}}^{-1} = R_{t+1}^{-1} I_{n^2 \times n^2}$; $\Psi_{Y_{t+1}} = [Y_{t+1} - g_{t+1}(X_{t+1})] I_{n^2 \times n}$; $I_{n^2 \times n^2}$, *and* $I_{n^2 \times n}$ *are*

$n^2 \times n^2$ *and* $n^2 \times n$ *identity matrix. Also:* $[\nabla_{X_{t+1}} g_{t+1}(X_{t+1})]$ *and* $[\Delta_{X_{t+1}}^{X_{t+1}} g_{t+1}(X_{t+1})]$ *are*

$$[\nabla_{X_{t+1}} g_{t+1}^T(X_{t+1})] = [\nabla_{X_{t+1}} g_{t+1}^{(1)}(X_{t+1}), \dots, \nabla_{X_{t+1}} g_{t+1}^{(m)}(X_{t+1})]_{m \times m}; \tag{7.38a}$$

$$[\Delta_{X_{t+1}}^{X_{t+1}} g_{t+1}^T(X_{t+1})] = [\Delta_{X_{t+1}}^{X_{t+1}} g_{t+1}^{(1)}(X_{t+1}), \dots, \Delta_{X_{t+1}}^{X_{t+1}} g_{t+1}^{(m)}(X_{t+1})]_{m \times m^2}; \tag{7.38b}$$

where $g_{t+1}(X_{t+1}) \triangleq [g_{t+1}^{(1)}(X_{t+1}), \cdots, g_{t+1}^{(n)}(X_{t+1})]^T$ *is a* $m \times 1$ *vector function in (7.33b).*

Lemma 7.4.18. *For a system given by Model 7.4.15, under Assumptions 7.3.2 through 7.3.5 the matrices (7.11a) through (7.11d) in Lemma 7.4.7 can be written as:*

$$I_t^{11} = \mathbb{E}_{p(X_t|Y_{1:t+1})} [\nabla_{X_t} f_t^T(X_t)] Q_t^{-1} [\nabla_{X_t} f_t(X_t)]; \tag{7.39a}$$

$$I_t^{12} = \mathbb{E}_{p(X_t|Y_{1:t+1})} [-\nabla_{X_t} f_t^T(X_t)] Q_t^{-1}; \tag{7.39b}$$

$$I_t^{22,a} = Q_t^{-1}; \tag{7.39c}$$

$$I_t^{22,b} = \mathbb{E}_{\frac{p(Y_{1:t})}{p(Y_{1:t+1})}} \mathbb{E}_{p(X_{t+1}|Y_{1:t})} [\nabla_{X_{t+1}} g_{t+1}^T(X_{t+1})] R_{t+1}^{-1} [\nabla_{X_{t+1}} g_{t+1}^T(X_{t+1})]. \tag{7.39d}$$

Proof. (7.39a): Substituting (7.35b) into (7.11a) yields

$$I_t^{11} = \mathbb{E}_{p(X_{t:t+1}|Y_{1:t+1})}\left[[\nabla_{X_t}f_t^T(X_t)]Q_t^{-1}[\nabla_{X_t}f_t(X_t)] - [\Delta_{X_t}^{X_t}f_t^T(x_t)]\Lambda_{X_t}^{-1}\Psi_{X_t}\right], \quad (7.40a)$$

$$= \mathbb{E}_{p(X_t|Y_{1:t+1})}\mathbb{E}_{p(X_{t+1}|X_t,Y_{1:t+1})}\left[[\nabla_{X_t}f_t^T(X_t)]Q_t^{-1}[\nabla_{X_t}f_t(X_t)] - [\Delta_{X_t}^{X_t}f_t^T(X_t)]\Lambda_{X_t}^{-1}\Psi_{X_t}\right], \quad (7.40b)$$

where (7.40b) is obtained by substituting the probability relation $p(x_{t:t+1}|y_{1:t+1}) = p(x_{t+1}|x_t, y_{1:t+1})p(x_t|y_{1:t+1})$ into (7.40a). Finally, by noting the following two conditions

$$\mathbb{E}_{p(X_{t+1}|X_t,Y_{1:t+1})}[\nabla_{X_t}f_t^T(X_t)]Q_t^{-1}[\nabla_{X_t}f_t(X_t)] = [\nabla_{X_t}f_t^T(X_t)]Q_t^{-1}[\nabla_{X_t}f_t(X_t)], \quad (7.41)$$

$$\mathbb{E}_{p(X_{t+1}|X_t,Y_{1:t+1})}[\Delta_{X_t}^{X_t}f_t^T(X_t)]\Lambda_{X_t}^{-1}\Psi_{X_t} = [\Delta_{X_t}^{X_t}f_t^T(X_t)]\Lambda_{X_t}^{-1}\mathbb{E}_{p(X_{t+1}|X_t,Y_{1:t+1})}[\Psi_{x_t}] = 0, \quad (7.42)$$

and substituting (7.41) and (7.42) into (7.40b) yields (7.39a).

(7.39b): Substituting (7.35c) into (7.11b) yields

$$I_t^{12} = \mathbb{E}_{p(X_{t:t+1}|Y_{1:t+1})}[-[\nabla_{X_t}f_t^T(X_t)]Q_t^{-1}]. \quad (7.43)$$

Substituting the probability relation $p(x_{t:t+1}|y_{1:t+1}) = p(x_{t+1}|x_t, y_{1:t+1})p(x_t|y_{1:t+1})$ into (7.43), followed by taking independent terms out of the integral yields (7.39b).

(7.39c): Substituting (7.37a) into (7.11c) yields (7.39c).

(7.39d): Using Bayes' rule, the expectation in (7.11d) can be rewritten as

$$I_t^{22,b} = \mathbb{E}_{\frac{p(X_{t+1},Y_{1:t+1})}{p(Y_{1:t+1})}}[-\Delta_{X_{t+1}}^{X_{t+1}}\log\ p(Y_{t+1}|X_{t+1})]. \quad (7.44)$$

Now using the probability condition $p(x_{t+1}, y_{1:t+1}) = p(y_{t+1}|x_{t+1})p(x_{t+1}|y_{1:t})p(y_{1:t})$, the expectation in (7.44) can further be decomposed and written as

$$I_t^{22,b} = \mathbb{E}_{\frac{p(Y_{1:t})}{p(Y_{1:t+1})}}\mathbb{E}_{p(X_{t+1}|Y_{1:t})}\mathbb{E}_{p(Y_{t+1}|X_{t+1})}[-\Delta_{X_{t+1}}^{X_{t+1}}\log\ p(Y_{t+1}|X_{t+1})]. \quad (7.45)$$

Substituting (7.37b) into (7.45) yields

$$I_t^{22,b} = \mathbb{E}_{\frac{p(Y_{1:t})}{p(Y_{1:t+1})}}\mathbb{E}_{p(X_{t+1}|Y_{1:t})}\mathbb{E}_{p(Y_{t+1}|X_{t+1})}\left[[-\Delta_{X_{t+1}}^{X_{t+1}}g_{t+1}^T(X_{t+1})]\Lambda_{Y_{t+1}}^{-1}\Psi_{Y_{t+1}}\right.$$
$$\left. +[\nabla_{X_{t+1}}g_{t+1}^T(X_{t+1})]R_{t+1}^{-1}[\nabla_{X_{t+1}}g_{t+1}(X_{t+1})]\right]. \quad (7.46)$$

Noting the following two conditions

$$\mathbb{E}_{p(Y_{t+1}|X_{t+1})}[\nabla_{X_{t+1}}g_{t+1}^T(X_{t+1})]R_{t+1}^{-1}[\nabla_{X_{t+1}}g_{t+1}(X_{t+1})]$$

$$= [\nabla_{X_{t+1}}g_{t+1}^T(X_{t+1})]R_{t+1}^{-1}[\nabla_{X_{t+1}}g_{t+1}(X_{t+1})], \qquad (7.47)$$

$$\mathbb{E}_{p(Y_{t+1}|X_{t+1})}[\Delta_{X_{t+1}}^{X_{t+1}}g_{t+1}^T(X_{t+1})]\Lambda_{Y_{t+1}}^{-1}\Psi_{Y_{t+1}}]$$

$$= \Delta_{X_{t+1}}^{X_{t+1}}g_{t+1}^T(X_{t+1})\Lambda_{Y_{t+1}}^{-1}\mathbb{E}_{p(Y_{t+1}|X_{t+1})}[\Psi_{Y_{t+1}}] = 0, \qquad (7.48)$$

and substituting (7.47) and (7.48) into (7.46) yields (7.39d), which completes the proof.   □

Using the results of Lemma 7.4.18, an SMC approximation of the PCRLB for Model 7.4.15 can be subsequently computed, as discussed in the next lemma.

Lemma 7.4.19. *Let a stochastic non-linear system with additive Gaussian state and sensor noise be represented by Model 7.4.15, such that it satisfies Assumption 7.3.2 through 7.3.5. Let $\{Y_{1:t} = y_{1:t}^j\}_{j=1}^M$ be $M \in \mathbb{N}$ i.i.d. measurement sequences generated from Model 7.4.15, then (7.5a) through (7.5c) in Lemma 7.3.7 can be recursively approximated as follows:*

$$\tilde{D}_t^{11} = \frac{1}{MN}\sum_{j=1}^M\sum_{i=1}^N[\nabla_{X_t}f_t^T(X_{t|t+1}^{i,j})]Q_t^{-1}[\nabla_{X_t}f_t(X_{t|t+1}^{i,j})]; \qquad (7.49a)$$

$$\tilde{D}_t^{12} = \frac{1}{MN}\sum_{j=1}^M\sum_{i=1}^N -[\nabla_{X_t}f_t^T(X_{t|t+1}^{i,j})]Q_t^{-1}; \qquad (7.49b)$$

$$\tilde{D}_t^{22} = Q_t^{-1} + \frac{1}{MN}\sum_{j=1}^M\sum_{i=1}^N[\nabla_{X_{t+1}}g_{t+1}^T(X_{t+1|t}^{i,j})]R_{t+1}^{-1}[\nabla_{X_{t+1}}g_{t+1}^T(X_{t+1|t}^{i,j})]; \qquad (7.49c)$$

and $\{X_{t|t+1}^{i,j}\}_{i=1}^N \sim p(x_t|y_{1:t+1}^j)$ and $\{X_{t+1|t}^{i,j}\}_{i=1}^N \sim p(x_{t+1}|y_{1:t}^j)$ are sets of N resampled particles from Lemma 7.4.13 and Algorithm 7, respectively, for all $\{Y_{1:t+1} = y_{1:t+1}^j\}_{j=1}^M$.

Proof. For $\{Y_{1:t} = y_{1:t}^j\}$, the SMC approximation in (7.28) can be written as

$$\tilde{p}(dx_t|y_{1:t+1}^j) = \frac{1}{N}\sum_{i=1}^N \delta_{X_{t|t+1}^{i,j}}(dx_t), \qquad (7.50)$$

where $X_{t|t+1}^{i,j} \sim p(x_t|y_{1:t+1}^j)$. Substituting (7.50) into (7.39a) and (7.39b) yields

$$\tilde{I}_t^{11} = \frac{1}{N} \sum_{i=1}^{N} [\nabla_{X_t} f_t^T(X_{t|t+1}^{i,j})] Q_t^{-1} [\nabla_{X_t} f_t(X_{t|t+1}^{i,j})], \tag{7.51a}$$

$$\tilde{I}_t^{12} = -\frac{1}{N} \sum_{i=1}^{N} [\nabla_{X_t} f_t^T(X_{t|t+1}^{i,j})] Q_t^{-1}, \tag{7.51b}$$

where $\tilde{I}_t$ is an SMC approximations of I_t. Substituting (7.51) and (7.29) into (7.6e) and (7.6f) yields (7.49a) and (7.49b), respectively. Computing an SMC approximation of D_t^{22} in (7.6g) for Model 7.4.15 requires a slightly different approach. Substituting (7.39c) and (7.39d) into (7.6g) yields

$$D_t^{22} = \mathbb{E}_{p(Y_{1:t+1})}[Q_t^{-1} + \mathbb{E}_{\frac{p(Y_{1:t})}{p(Y_{1:t+1})}} \mathbb{E}_{p(X_{t+1}|Y_{1:t})}[\nabla_{X_{t+1}} g_{t+1}^T(X_{t+1})] R_{t+1}^{-1} [\nabla_{X_{t+1}} g_{t+1}^T(X_{t+1})]], \tag{7.52a}$$

$$= Q_t^{-1} + \mathbb{E}_{p(Y_{1:t})} \mathbb{E}_{p(X_{t+1}|Y_{1:t})} [\nabla_{X_{t+1}} g_{t+1}^T(X_{t+1})] R_{t+1}^{-1} [\nabla_{X_{t+1}} g_{t+1}^T(X_{t+1})], \tag{7.52b}$$

where Q_t^{-1} is independent of the measurement sequence. Also, $\mathbb{E}_{p(Y_{1:t+1})} \mathbb{E}_{\frac{p(Y_{1:t})}{p(Y_{1:t+1})}}[\cdot] = \mathbb{E}_{p(Y_{1:t})}[\cdot]$. For $\{Y_{1:t} = y_{1:t}^j\}$, random samples $\{X_{t+1|t}^{i,j}\}_{i=1}^{N} \sim p(x_{t+1}|y_{1:t}^j)$ from Algorithm 7 delivers an SMC approximation of $p(dx_{t+1}|y_{1:t}^j)$ represented as

$$\tilde{p}(dx_{t+1}|y_{1:t}^j) = \frac{1}{N} \sum_{i=1}^{N} \delta_{X_{t+1|t}^{i,j}}(dx_{t+1}) \tag{7.53}$$

where $\tilde{p}(dx_{t+1}|y_{1:t}^j)$ is an SMC approximation of $p(dx_{t+1}|y_{1:t}^j)$. Substituting (7.53) and (7.29) into (7.52b) yields (7.49c), which completes the proof. $\square$

Result 7.4.20. *An SMC approximation of the PFIM for Model 7.4.15 is obtained by substituting (7.49a) through (7.49c) in Lemma 7.4.19 into (7.4) in Lemma 7.3.7, such that*

$$\tilde{J}_{t+1} = \tilde{D}_t^{22} - [\tilde{D}_t^{12}]^T (\tilde{J}_t + \tilde{D}_t^{11})^{-1} \tilde{D}_t^{12}, \tag{7.54}$$

where $\tilde{J}_{t+1}$ is an SMC approximation of J_{t+1}. Applying matrix inversion lemma (Horn and Johnson, 1985) in (7.54) gives an SMC approximation of the PCRLB, such that

$$\tilde{J}_{t+1}^{-1} = [\tilde{D}_t^{22}]^{-1} - [\tilde{D}_t^{22}]^{-1} [\tilde{D}_t^{12}]^T \left[\tilde{D}_t^{12} [\tilde{D}_t^{22}]^{-1} [\tilde{D}_t^{12}]^T - (\tilde{J}_t + \tilde{D}_t^{11}) \right]^{-1} \tilde{D}_t^{12} [\tilde{D}_t^{22}]^{-1}, \tag{7.55}$$

where $\tilde{J}_{t+1}^{-1}$ is an SMC approximation of J_{t+1}^{-1} in (7.2) in Lemma 7.3.6.

7.5   Final Algorithm

Algorithms 8 and 9 give the procedure for computing an SMC approximation of the PCRLB for Models 7.3.1 and 7.4.15, respectively.

Remark 7.5.1. *In practice, an ensemble of M measurement sequences $\{Y_{1:T} = y_{1:T}^j\}_{j=1}^M$ required by Algorithms 8 and 9 are obtained from historical process data; however, in simulations, it can be generated by simulating Models 7.3.1 and 7.4.15, M times starting at i.i.d. initial states drawn from $X_0 \sim p(x_0)$. Note that this procedure also requires simulation of the true states; however, true states are not used in Algorithms 8 and 9.*

For illustrative purposes, to assess the numerical reliability of Algorithms 8 and 9, a quality measure is defined as follows

$$\Lambda_J = \frac{1}{T} \sum_{t=1}^{T} [J_t^{-1} - \tilde{J}_t^{-1}] \circ [J_t^{-1} - \tilde{J}_t^{-1}], \tag{7.56}$$

where Λ_J is the average sum of square of errors in approximating the PCRLB and $\circ$ is the Hadamard product. Λ_J is a $n \times n$ matrix, with diagonal element $\Lambda_J(j, j)$ as the average sum of square of errors accumulated in approximating the PCRLB for state j, where $1 \leq j \leq n$.

7.6   Convergence

Computing the PCRLB in Lemma 7.3.6 involves solving the complex, multi-dimensional integrals; however, as stated earlier, for Models 7.3.1 and 7.4.15 the PCRLB cannot be solved in closed form. Algorithms 8 and 9 gives a N particle and M simulation based SMC approximation of the PCRLB for Models 7.3.1 and 7.4.15, respectively. It is therefore natural to question the convergence properties of the proposed numerical method. In this regard, results such as Theorem 7.4.5 and Remark 7.4.11 are important as it ensures that the proposed numerical solution does not result in accumulation of errors. It is emphasized that although Theorem 7.4.5 and Remark 7.4.11 not necessarily imply convergence of the

---

Algorithm 8 SMC based PCRLB approximation for Model 7.3.1

    Input: Given Model 7.3.1, satisfying Assumptions 7.3.2 through 7.3.5, assume a prior pdf on X_0, such that $X_0 \sim p(x_0)$. Also, select algorithm parameters- T, N and M.
    Output: SMC approximation of the PCRLB for Model 7.3.1.

1: Generate and store M i.i.d. sequences $\{Y_{1:T}^j\}_{j=1}^M \sim p(y_{1:T})$ of length T, by simulating Model 7.3.1, M times starting at M i.i.d. initial states $\{X_{0|-1}^i\}_{j=1}^M \sim p(x_0)$.

2: **for** $j = 1$ to M **do**

3:     **for** $t = 1$ to T **do**

4:         Store resampled particles $\{X_{t|t}^{i,j}\}_{i=1}^N \sim p(x_t|y_{1:t}^j)$ using Algorithm 7.

5:         Store resampled particles $\{X_{t-1:t|t}^{i,j}\}_{i=1}^N \sim p(x_{t-1:t}|y_{1:t}^j)$ using Lemma 7.4.12.

6:     **end for**

7: **end for**

8: Compute PFIM J_0 at $t = 0$ based on the initial target state pdf $X_0 \sim p(x_0)$. If $X_0 \sim \mathcal{N}(x_0|C_{x_0}, P_{0|0})$ then from Lemma 7.3.7, $J_0 = P_{0|0}^{-1}$.

9: **for** $t = 0$ to $T - 1$ **do**

10:     Compute an SMC estimate (7.30a) through (7.30c) in Lemma 7.4.14.

11:     Compute PCRLB $\tilde{J}_{t+1}^{-1}$ by substituting (7.30a) through (7.30c) into (7.55).

12: **end for**

Algorithm 9 SMC based PCRLB approximation for Model 7.4.15

    Input: Given Model 7.4.15, satisfying Assumptions 7.3.2 through 7.3.5, assume a prior on X_0, such that $X_0 \sim p(x_0)$. Also, select algorithm parameters- T, N and M.
    Output: SMC approximation of the PCRLB for Model 7.4.15.

1: Generate and store M i.i.d. sequences $\{Y_{1:T}^j\}_{j=1}^M \sim p(y_{1:T})$ of length T, by simulating Model 7.4.15, M times starting at M i.i.d. initial states $\{X_{0|-1}^i\}_{j=1}^M \sim p(x_0)$.

2: **for** $j = 1$ to M **do**

3:     **for** $t = 1$ to T **do**

4:         Store predicted particles $\{X_{t|t-1}^{i,j}\}_{i=1}^N \sim p(x_t|y_{1:t-1}^j)$ using Algorithm 7.

5:         Store resampled particles $\{X_{t|t}^{i,j}\}_{i=1}^N \sim p(x_t|y_{1:t}^j)$ using Algorithm 7.

6:         Store resampled particles $\{X_{t-1|t}^{i,j}\}_{i=1}^N \sim p(x_{t-1:t}|y_{1:t}^j)$ using Lemma 7.4.13.

7:     **end for**

8: **end for**

9: Compute PFIM J_0 at $t = 0$ based on the initial target state pdf $X_0 \sim p(x_0)$. If $X_0 \sim \mathcal{N}(x_0|C_{x_0}, P_{0|0})$ then from Lemma 7.3.7, $J_0 = P_{0|0}^{-1}$.

10: **for** $t = 0$ to $T - 1$ **do**

11:     Compute an SMC estimate (7.49a) through (7.49c) in Lemma 7.4.19.

12:     Compute PCRLB $\tilde{J}_{t+1}^{-1}$ by substituting (7.49a) through (7.49c) into using (7.55).

13: **end for**

SMC based PCRLB and MSE to its theoretical values, nevertheless, it provides a strong

theoretical basis for the numerous approximations used in Algorithms 8 and 9.

From an application perspective, it is instructive to highlight that the numerical quality of the SMC based PCRLB approximation in Algorithms 8 and 9 can be made accurate by simply increasing the number of particles (N) and the MC simulations (M). The choice of N and M are user defined, which can be selected based on the required numerical accuracy, and available computing speed. It is important to emphasize that due to the multiple approximations involved in deriving a tractable solution, for practical purposes, with a finite N and M, the condition $P_{t|t} - \tilde{J}_t^{-1} \succcurlyeq 0$ is not guaranteed to hold for all $t \in \mathbb{N}$.

The quality of the SMC based PCRLB solution is validated next via simulation.

7.7   Numerical illustrations

In this section, two simulation examples are presented to demonstrate the utility and performance of the proposed SMC based PCRLB solution. The first example is a ballistic target tracking problem at re-entry phase. The aim of this study is three fold: first to demonstrate the performance and utility of the proposed method on a practical problem; second, to demonstrate the quality of the bound approximation for a range of target state and sensor noise variances; and third, to study the sensitivity of the involved SMC approximations to the number of particles used.

The performance of the SMC based PCRLB solution on a second example involving a uni-variate, non-stationary growth model, which is a standard non-linear, and bimodal benchmark model is then illustrated. This example is profiled to demonstrate the accuracy of the SMC based PCRLB solution for highly non-linear SSMs with non-Gaussian noise.

7.7.1   Example 1: Ballistic target tracking at re-entry

In Section 7.4.3, an SMC based method for approximating the PCRLB was presented for non-linear SSMs with additive Gaussian state and sensor noise (See Algorithm 9). In this section, the quality of Algorithm 9 is validated on a practical problem of ballistic target

tracking at re-entry phase. This particular problem has attracted a lot of attention from researchers for both theoretical and practical reasons. See (Li and Jilkov, 2001*a*) and the references cited therein for a detailed survey on the ballistic target tracking.

7.7.1.1   Model setup

Consider a target launched along a ballistic flight whose kinematics are described in a 2D Cartesian coordinate system. This particular description of the kinematics assumes that the only forces acting on the target at any given time are the forces due to gravity and drag. All other forces such as: centrifugal acceleration, Coriolis acceleration, wind, lift force and spinning motion are assumed to have a small effect on the target trajectory. With the position and the velocity of the target at time $t \in \mathbb{N}$ described in 2D Cartesian coordinate system as (X_t, H_t) and $(\dot{X}_t, \dot{H}_t)$, respectively, its motion in the re-entry phase can be described by the following discrete-time non-linear SSM (Farina *et al.*, 2002)

$$X_{t+1} = AX_t + GF_t(X_t) + G.\begin{bmatrix} 0 \\ -g \end{bmatrix} + V_t, \tag{7.57}$$

where the states $X_t \triangleq [X_t \quad \dot{X}_t \quad H_t \quad \dot{H}_t]^T$. Also, the matrices A and G are as follows

$$A \triangleq \begin{bmatrix} 1 & \Delta T & 0 & 0 \\ 0 & 1 & 0 & 0 \\ 0 & 0 & 1 & \Delta T \\ 0 & 0 & 0 & 1 \end{bmatrix}, \quad G \triangleq \begin{bmatrix} \dfrac{\Delta T^2}{2} & 0 \\ \Delta T & 0 \\ 0 & \dfrac{\Delta T^2}{2} \\ 0 & \Delta T \end{bmatrix}, \tag{7.58}$$

where ΔT is the time interval between two consecutive radar measurements.

In (7.57) $F_t(X_t)$ models the drag force, which acts in a direction opposite to the target velocity. In terms of the states, $F_t(X_t)$ can be modelled as

$$F_t(X_t) = -\frac{g\rho(H_t)}{2\beta}\sqrt{\dot{X}_t^2 + \dot{H}_t^2}\begin{bmatrix} \dot{X}_t \\ \dot{H}_t \end{bmatrix}, \tag{7.59}$$

where: g is the acceleration due to gravity; β is the ballistic coefficient whose value depends on the shape, mass and the cross sectional area of the target (Ristic *et al.*, 2004); and $\rho(H_t)$

is the density of the air, defined as an exponentially decaying function of H_t, such that

$$\rho(H_t) = \alpha_1 e^{(-\alpha_2 H_t)} \tag{7.60}$$

where: $\alpha_1 = 1.227$ kg·m^{-3}, $\alpha_2 = 1.09310 \times 10^{-4}$m^{-1} for $H_t < 9144$m; and $\alpha_1 = 1.754$ kg·m^{-3}, $\alpha_2 = 1.4910 \times 10^{-4}$m^{-1} for $H_t \geq 9144$m. Note that the drag force, $F_t(X_t)$ is the only non-linear term in the state equation. In (7.57) the state noise $V_t \in \mathbb{R}^4$ is a i.i.d. sequence of multi-variate Gaussian random vector represented as $V_t \sim \mathcal{N}(v_t|0, Q_t)$, with zero mean and covariance matrix Q_t given as

$$Q_t = \gamma I_{2\times2} \otimes \Theta, \quad \Theta = \begin{bmatrix} \dfrac{\Delta T^3}{3} & \dfrac{\Delta T^2}{2} \\ \dfrac{\Delta T^2}{2} & \Delta T \end{bmatrix}, \tag{7.61}$$

where: $\gamma \in \mathbb{R}_+$; $I_{2\times2}$ is a 2×2 identity matrix; and $\otimes$ is the Kronecker product. The intensity of the state noise, determined by γ, accounts for all the forces neglected in (7.57), including any deviations arising due to system-model mismatch. The target measurements are collected by a conventional radar (e.g., dish radar) assumed to be stationed at the origin. The sensor readings are measured in the natural sensor coordinate system, which include range (R_t) and elevation (E_t) of the target. The radar measurements $Y_t = [R_t \quad E_t]^T$ are related to the states X_t through a non-linear observation model given below.

$$Y_t = \begin{bmatrix} \sqrt{X_t^2 + H_t^2} \\ \arctan\left(\dfrac{H_t}{X_t}\right) \end{bmatrix} + W_t. \tag{7.62}$$

In (7.62) $W_t \in \mathbb{R}^2$ is an i.i.d. sequence of multi-variate Gaussian random vector represented as $W_t \sim \mathcal{N}(w_t|0, R_t)$, with zero mean and non-singular covariance matrix R_t given as

$$R_t = \begin{bmatrix} \sigma_r^2 & 0 \\ 0 & \sigma_e^2 \end{bmatrix}, \tag{7.63}$$

where $\sigma_r \in \mathbb{R}_+$ and $\sigma_e \in \mathbb{R}_+$ are the standard deviation associated with range and elevation measurements. In (7.62), it is assumed that the true target elevation angle lies between 0 and $\pi/2$ radians; otherwise, it suffices to add π radians to the arctan term in (7.62).

Remark 7.7.1. *To avoid use of a non-linear sensor model, some authors (Farina et al., 2002; Lei et al., 2011) considered transforming the radar measurements in (7.62) into the Cartesian coordinate system, wherein the sensor dynamics manifest themselves into a linear model. Even though this strategy eliminates the need to handle non-linearity in sensor measurements, tracking in Cartesian coordinates couples the sensor noise across two coordinate systems and makes the noise non-Gaussian and state dependent (Li and Jilkov, 2001b). Since the proposed method can deal with strong state and sensor non-linearities, the radar readings are monitored in natural sensor coordinates alone.*

7.7.1.2 Simulation setup

For simulation, the model parameters are selected as given in Table 7.1. The aim of this study is to evaluate the quality of the SMC based PCRLB solution for a range of target state and sensor noise variances. This allows full investigation of the quality of the SMC based approximation for a range of noise characteristics. The cases considered here are given in Table 7.2. From Assumption 7.3.2, β is assumed to be fixed and known a priori.

Table 7.1: Parameter values used in Example 1.

Process variables	Symbol	values
accel. due to gravity	g	9.8 m/s^2
ballistic coefficient	β	40000 kg.m$^{-1} \cdot$ s^{-2}
radar sampling time	ΔT	2 s
total tracking time	T	120 s
state noise	V_t	$V_t \sim \mathcal{N}(v_t\|0, Q_t)$
sensor noise	W_t	$W_t \sim \mathcal{N}(w_t\|0, R_t)$
noise parameters	$\gamma,\ \sigma_r,\ \sigma_e$	see Table 7.2
initial states	$X_0^\star$	$\begin{bmatrix} 232 \text{ km} \\ 2.290 \cos(190^0) \text{ km/s} \\ 88 \text{ km} \\ 2.290 \sin(190^o) \text{ km/s} \end{bmatrix}$
probability of detection	$\Pr_d$	1
probability of false alarm	$\Pr_f$	0

Figure 7.1 shows a sample trajectory of the target in the $X - H$ plane along with its velocity map as a function of time, generated using Case 1 (see Table 7.2).

Table 7.2: Cases considered for Example 1.

Case	γ	σ_r	σ_ϵ
1	1.0	100m	0.017rad
2	5.0	100m	0.017rad
3	1.0	500m	0.085rad
4	5.0	500m	0.085rad
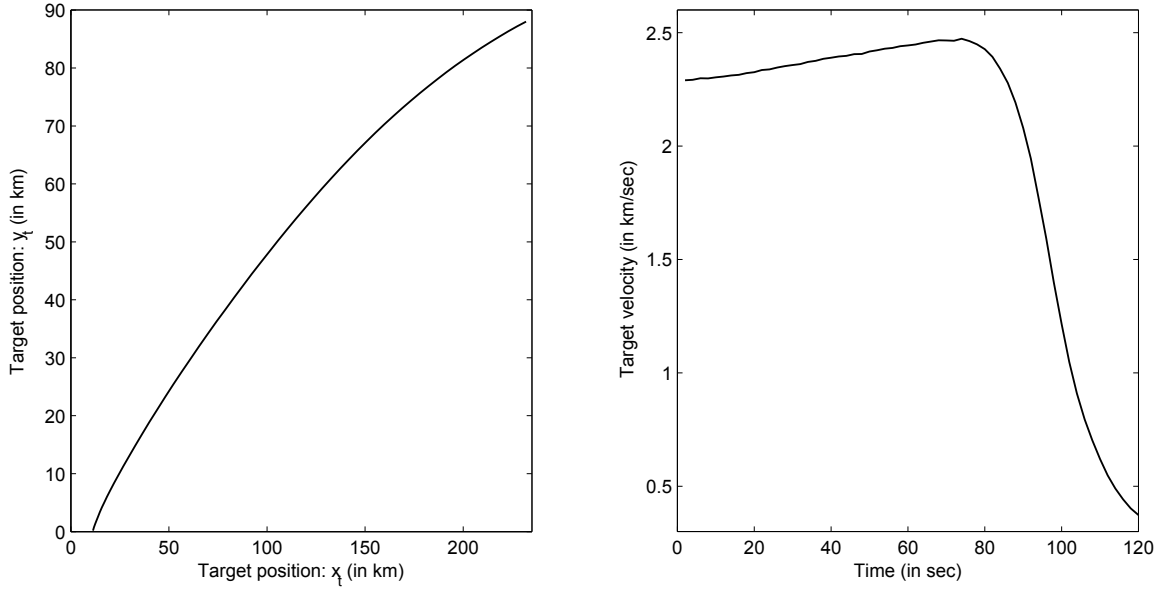
Figure 7.1: Sample trajectory showing position and velocity of the target at re-entry phase.

Table 7.3: Variable values used in Example 1.

Process variables	Symbol	values
state noise	V_t	$V_t \sim \mathcal{N}(v_t|0, Q_t)$
sensor noise	W_t	$W_t \sim \mathcal{N}(w_t|0, R_t)$
noise parameters	$\gamma,\ \sigma_r,\ \sigma_e$	see Table 7.2
initial states	X_0	$X_0 \sim \mathcal{N}(x_0|C_{x_0}, P_{0|0})$
	C_{x_0}	$\begin{bmatrix} 232 \text{ km} \\ 2.290\cos\left(190^0\right) \text{ km/s} \\ 88 \text{ km} \\ 2.290\sin(190^o) \text{ km/s} \end{bmatrix}$
	$[P_{0|0}]^{1/2}$	$\begin{bmatrix} 1\text{km} & 0 & 0 & 0 \\ 0 & 20\text{m/s} & 0 & 0 \\ 0 & 0 & 1\text{km} & 0 \\ 0 & 0 & 0 & 20\text{m/s} \end{bmatrix}$
Number of particles	N	1000
MC simulations	M	200

7.7.1.3   Results

The kinematics of the ballistic target consist of non-linear state and sensor models with additive Gaussian noise, for which the PCRLB can be approximated using Algorithm 9. First, the state and sensor models in (7.57) and (7.62), respectively, are defined as

$$f_t(X_t) = AX_t + GF_t(X_t) + G.\begin{bmatrix} 0 \\ -g \end{bmatrix}, \tag{7.64a}$$

$$g_{t+1}(X_{t+1}) = \begin{bmatrix} \sqrt{X_{t+1}^2 + H_{t+1}^2} \\ \arctan\left(\dfrac{H_{t+1}}{X_{t+1}}\right) \end{bmatrix}. \tag{7.64b}$$

To compute the required gradients $\nabla_{X_t} f_t(X_t)$ and $\nabla_{X_{t+1}} g_{t+1}(X_{t+1})$, differentiating (7.57) with respect to X_t, and (7.62) with respect to X_{t+1}, yields

$$\nabla_{X_t} f_t(X_t) = A + GM_t(X_t), \tag{7.65a}$$

$$\nabla_{X_{t+1}} g_{t+1}(X_{t+1}) = N_{t+1}(X_{t+1}), \tag{7.65b}$$

where: $M_t(X_t)$ and $N_{t+1}(X_{t+1})$ in (7.65a) and (7.65b), respectively, are 2×4 matrices, whose entries are:

$$M_t(X_t)[1,1] = 0, \tag{7.66a}$$

$$M_t(X_t)[2,1] = 0, \tag{7.66b}$$

$$M_t(X_t)[1,2] = -\frac{g}{2\beta}\rho(H_t)\left[\frac{2\dot{X}_t^2 + \dot{H}_t^2}{\sqrt{\dot{X}_t^2 + \dot{H}_t^2}}\right], \tag{7.66c}$$

$$M_t(X_t)[2,2] = -\frac{g}{2\beta}\rho(H_t)\left[\frac{\dot{X}_t\dot{H}_t}{\sqrt{\dot{X}_t^2 + \dot{H}_t^2}}\right], \tag{7.66d}$$

$$M_t(X_t)[1,3] = \frac{g\alpha_2}{2\beta}\rho(H_t)\left[\sqrt{\dot{X}_t^2 + \dot{H}_t^2}\right]\dot{X}_t, \tag{7.66e}$$

$$M_t(X_t)[2,3] = \frac{g\alpha_2}{2\beta}\rho(H_t)\left[\sqrt{\dot{X}_t^2 + \dot{H}_t^2}\right]\dot{H}_t, \tag{7.66f}$$

$$M_t(X_t)[1,4] = M_t(X_t)[2,2], \tag{7.66g}$$

$$M_t(X_t)[2,4] = -\frac{g}{2\beta}\rho(H_t)\left[\frac{\dot{X}_t^2 + 2\dot{H}_t^2}{\sqrt{\dot{X}_t^2 + \dot{H}_t^2}}\right]; \tag{7.66h}$$

and:

$$N_{t+1}(X_{t+1})[1, 1] = \frac{\mathrm{X}_{t+1}}{\sqrt{\dot{\mathrm{X}}_{t+1}^2 + \dot{\mathrm{H}}_{t+1}^2}}, \tag{7.67a}$$

$$N_{t+1}(X_{t+1})[2, 1] = \frac{\mathrm{H}_{t+1}}{\dot{\mathrm{X}}_{t+1}^2 + \dot{\mathrm{H}}_{t+1}^2}, \tag{7.67b}$$

$$N_{t+1}(X_{t+1})[1, 2] = 0, \tag{7.67c}$$

$$N_{t+1}(X_{t+1})[2, 2] = 0, \tag{7.67d}$$

$$N_{t+1}(X_{t+1})[1, 3] = \frac{\mathrm{H}_{t+1}}{\sqrt{\dot{\mathrm{X}}_{t+1}^2 + \dot{\mathrm{H}}_{t+1}^2}}, \tag{7.67e}$$

$$N_{t+1}(X_{t+1})[2, 3] = \frac{\mathrm{X}_{t+1}}{\dot{\mathrm{X}}_{t+1}^2 + \dot{\mathrm{H}}_{t+1}^2}, \tag{7.67f}$$

$$N_{t+1}(X_{t+1})[1, 4] = 0, \tag{7.67g}$$

$$N_{t+1}(X_{t+1})[2, 4] = 0. \tag{7.67h}$$

To evaluate the numerical quality of Algorithm 1, we compare the SMC based PCRLB solution against the theoretical values. The theoretical bound is computed using an ensemble of the true state trajectories, simulated using (7.57) (see (Farina *et al.*, 2002; Ristic *et al.*, 2004) for further details). Here we compare the square root of the diagonal elements of the theoretical PCRLB matrix J_t^{-1} and its approximation $\tilde{J}_t^{-1}$ for all $t \in [0, T]$. The results are summarized next for the cases given in Table 7.2. For fair comparison of all the cases, the parameters required by Algorithm 9 are specified as given in Table 7.3.

Case 1: Figure 7.2 compares the square root of the SMC based approximate bound against the theoretical PCRLB. Clearly, the approximate bound for both the position and velocity of the target in both X and H coordinates accurately follows the theoretical bound at all tracking time instants. Note that the high values of the PCRLB in Figure7.2 highlights tracking difficulties as the target approaches the ground.

Case 2: In this case the state noise intensity is increased five fold and the sensor noise is kept at a small value (see Table 7.2). Notwithstanding the increased noise variance, the PCRLB approximation is almost exact at all tracking time instants. The results for
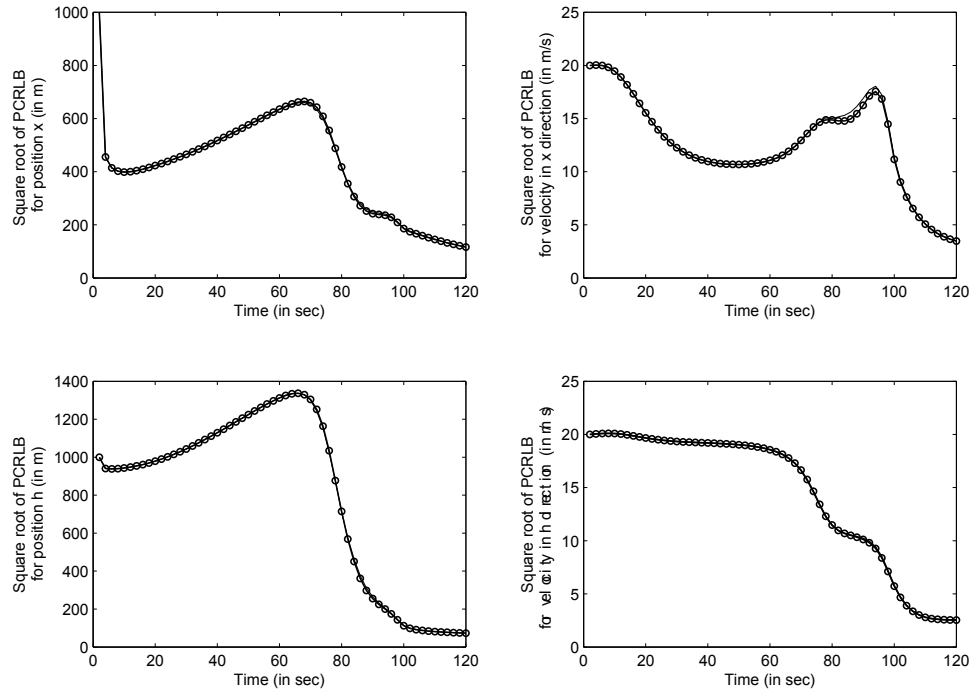
Figure 7.2: Comparing the square root of the theoretical (solid line with marker) and approximate PCRLB (solid line) for all the target states under Case 1.
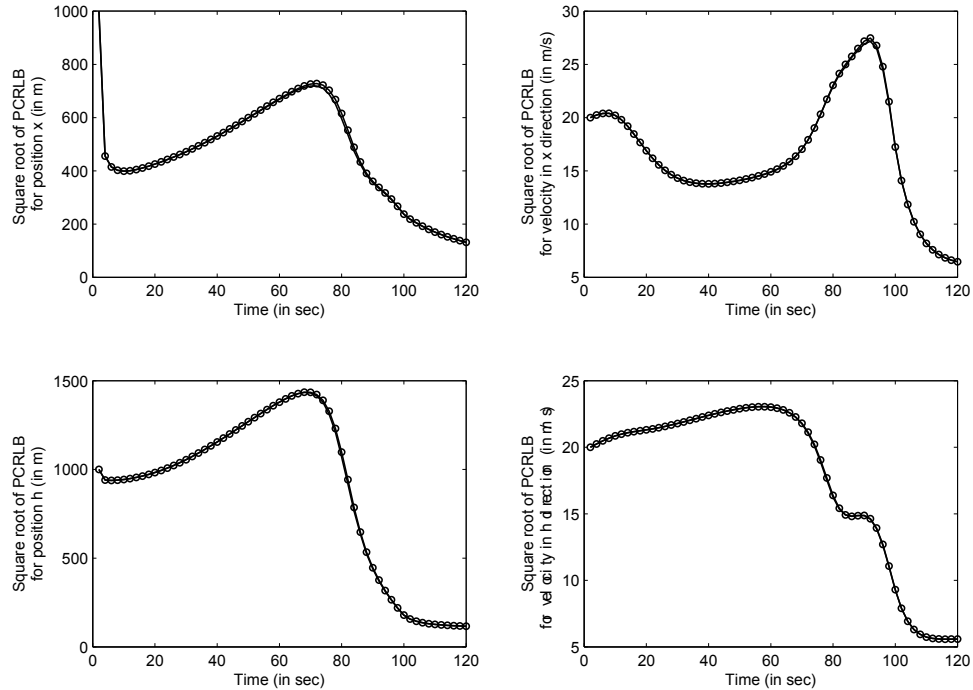
Figure 7.3: Comparing the square root of the theoretical (solid line with marker) and approximate PCRLB (solid line) for all the target states under Case 2.

Table 7.4: Average sum of square of errors in approximating the PCRLB for the states in Example 1, under the cases in Table 7.2.

Λ_J values	Case 1	Case 2	Case 3	Case 4
$\Lambda_J(1,1)\ (\times 10^{-6})$	9.30	50.7	5.87	130
$\Lambda_J(2,2)\ (\times 10^{-11})$	4.50	2.06	7.08	46.2
$\Lambda_J(3,3)\ (\times 10^{-5})$	3.56	23.1	2.96	100
$\Lambda_J(4,4)\ (\times 10^{-13})$	8.63	24.8	19.6	122

Case 2 are shown in Figure 7.3. Table 7.4 compares the Λ_J values for Case 2 computed using (7.56). Based on Table 7.4, the results from Cases 1 and 2 closely compare in terms of the order of the Λ_J values. To allow further comparison with Case 1, the square root of the approximate PCRLBs for Cases 1 and 2 are compared in Figure 7.6. In terms of the magnitude, the PCRLB for Case 2 is higher than that for Case 1, suggesting tracking difficulties with larger noise intensity.

Case 3: Again for Case 3, performance similar to Figure 7.2 is obtained as given in Figure 7.4. The same is evident from Table 7.4, where the average sum of square of error in approximating the PCRLB for Cases 1 and 3 are of the same order.

Case 4: Results for Case 4 is given in Figure 7.5. Higher values of the PCRLB for Case 4 in Figure 7.6 reaffirms the estimation issues associated with larger noise variances. Similar conclusions can be drawn based on Table 7.4, where the Λ_J values for Case 4 are the highest compared to the previous cases. Nevertheless, the errors are bounded and within a few orders of the Λ_J values reported for Case 1.

All the above case studies suggest that the proposed approach is accurate in approximating the theoretical PCRLB under large state and sensor noise variances.

Remark 7.7.2. *Note that in (Lei* et al.*, 2011), a similar ballistic target tracking problem at re-entry phase was considered to illustrate the use of an EKF and UKF based method in approximating the theoretical PCRLB. Unlike the non-linear sensor model considered here (see (7.62)), (Lei* et al.*, 2011) used the change of coordinates method to obtain a linear sensor model representation. It is important to highlight that even with a linear*
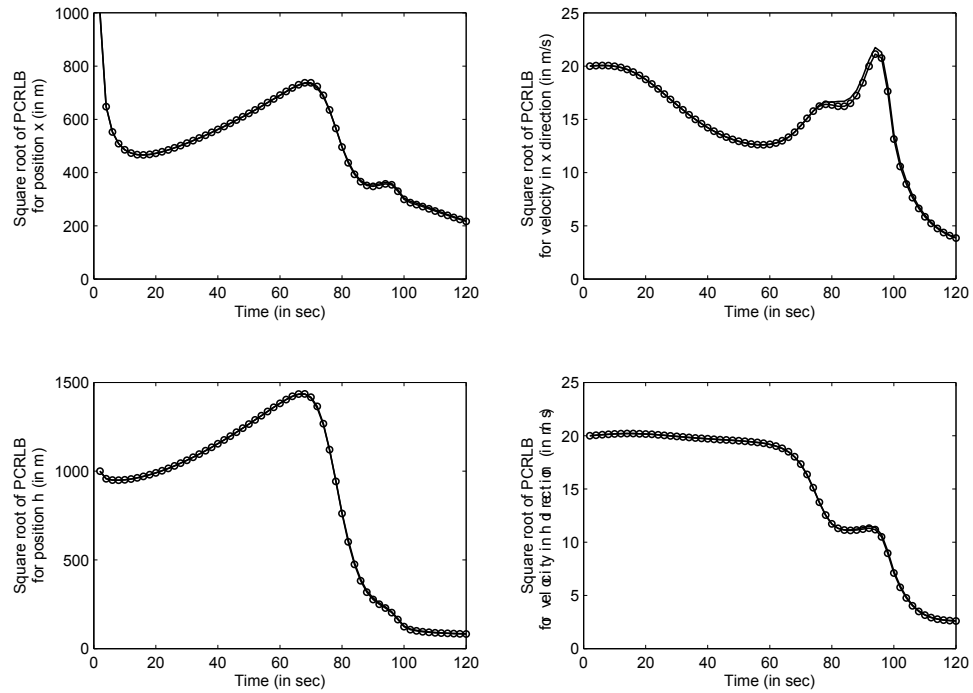
Figure 7.4: Comparing the square root of the theoretical (solid line with marker) and approximate PCRLB (solid line) for all the target states under Case 3.
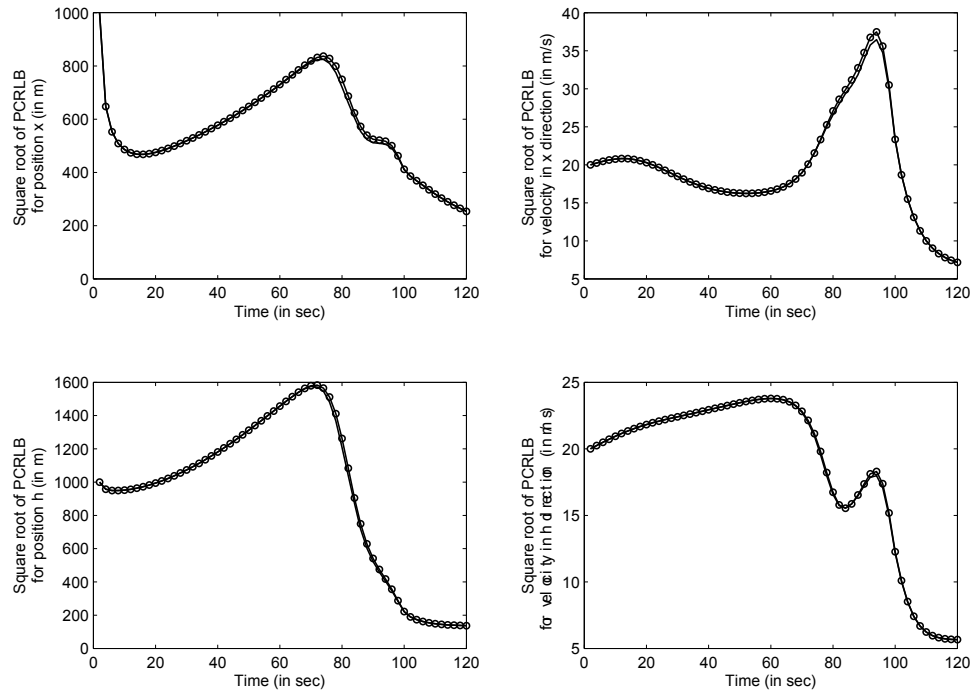
Figure 7.5: Comparing the square root of the theoretical (solid line with marker) and approximate PCRLB (solid line) for all the target states under Case 4.
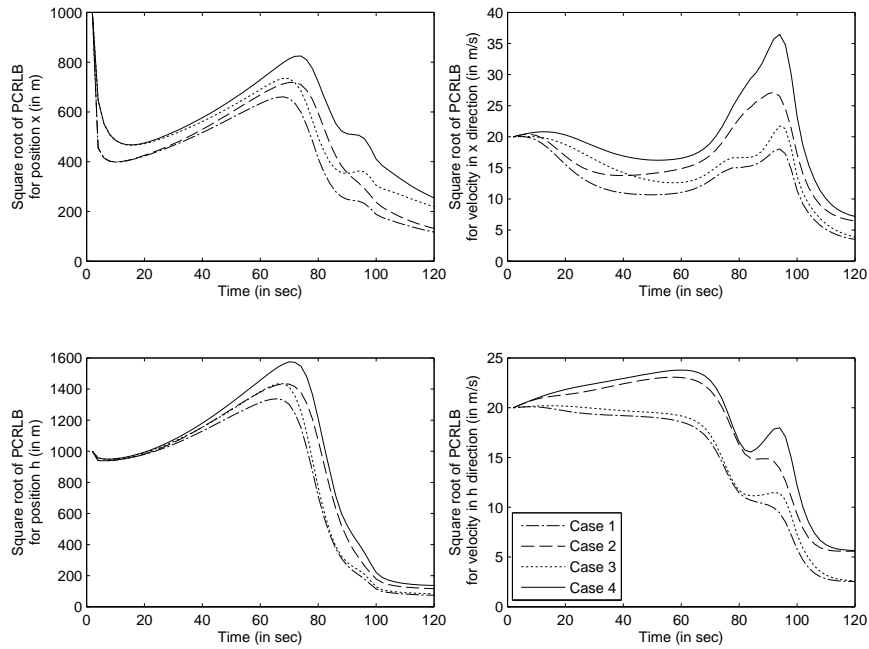
Figure 7.6: Comparing the square root of the approximate PCRLBs for the target states under the cases listed in Table 7.2.
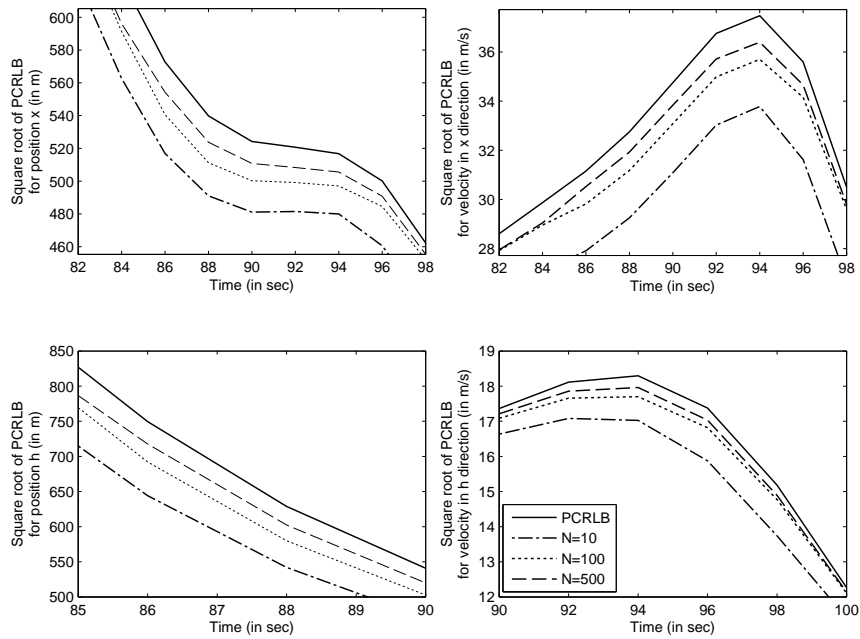
Figure 7.7: Comparing the square root of the theoretical and approximate PCRLBs for different values of N in Example 1, Case 4. Note that all the sub-figures have been appropriately scaled up allow clear illustration of the effect of N on the quality of approximation.

sensor model, the EKF and UKF based method yields a biased estimate of the PCRLB for the target states (see Figures 4 through 7 in (Lei et al., 2011)). Whereas, under a more challenging situation, as one considered here, the SMC based method yields an unbiased estimate of the PCRLB (see Figures 7.2 through 7.5, and Table 7.4). This highlights the advantages of the SMC based method (both in terms of the accuracy and applicability) over the EKF and UKF based PCRLB in presence of strong system or sensor non-linearities.

Next we study the sensitivity of the involved SMC approximations to the number of particles used. In Figure 7.7, approximate PCRLB bounds are compared against the theoretical PCRLB for different values of N. The results are obtained by varying N in Algorithm 1. From Figure 7.7, it is clear that by simply increasing N, which is a tuning parameter in Algorithm 1, the quality of the SMC approximations can be significantly improved. For all the simulation cases, the number of Monte Carlo simulations was selected as $M = 200$ (see Table 7.3). Computation of a single Monte Carlo simulation took 0.69 seconds on a 3.33 GHz Intel Core i5 processor running on Windows 7. Note that the reported absolute execution time is solely for instructive purposes and is not intended to reflect on the true computational complexity of the proposed algorithm. Collectively, from Figures 7.2 through 7.7, it is evident that the SMC based method is accurate in approximating the theoretical PCRLB for a range of target state and sensor noise variances.

7.7.2   Example 2: A non-linear and non-Gaussian system

The aim of this study is to demonstrate the effectiveness of the proposed SMC based method in approximating the PCRLB in presence of a non-Gaussian noise.

7.7.2.1   Model setup

A more challenging situation is considered in this section that involves the following discrete-time, uni-variate non-stationary growth model

$$X_{t+1} = \frac{X_t}{2} + \frac{25X_t}{1 + X_t^2} + 8\cos{(1.2t)} + V_t, \tag{7.68a}$$

$$Y_t = \frac{X_t^2}{20} + W_t, \tag{7.68b}$$

where $V_t \in \mathbb{R}$ is an i.i.d. sequence following a Gaussian distribution, such that $V_t \sim \mathcal{N}(v_t|0, Q_t)$. The noise variance is defined as $Q_t = 5 \times 10^{-3} \; \forall t \in [1, T]$, where T is 30 seconds. Also, the initial state is modelled as $X_0 \sim \mathcal{N}(x_0|0, 0.01)$. This example has been profiled due to it being acknowledged as a benchmark problem in non-linear state estimation in several previous studies (Doucet *et al.*, 2001; Hernandez *et al.*, 2004).

7.7.2.2   Simulation setup

To compute the SMC based approximate PCRLB solution, two different sensor noise models are considered in (7.68b). For Case 1, $W_t \in \mathbb{R}$ is an i.i.d. sequence following a Gaussian distribution, such that $W_t \sim \mathcal{N}(w_t|0, R_t)$, while for Case 2, $W_t \in \mathbb{R}$ is again an i.i.d sequence, but follows a Rayleigh distribution, such that $W_t \sim \mathcal{R}(w_t|R_t)$. For both the cases, the sensor noise variance $R_t = 1 \times 10^{-3} \; \forall t \in [1, T]$ is considered. Here Case 2 represents a much more challenging situation, where estimation is considered under a non-Gaussian sensor noise. For fair comparison, $M = 200$ and $N = 100$ are selected.

7.7.2.3   Results

Case 1: Comparison of the approximate and the theoretical PCRLB for the Gaussian sensor noise case is given in Figure 7.8. The results suggest that for the chosen N, the approximate PCRLB almost exactly follows the theoretical PCRLB at all filtering time instants. The same is reflected in the error value computed using (7.56), which is $\Lambda_J = 4.19 \times 10^{-9}$.
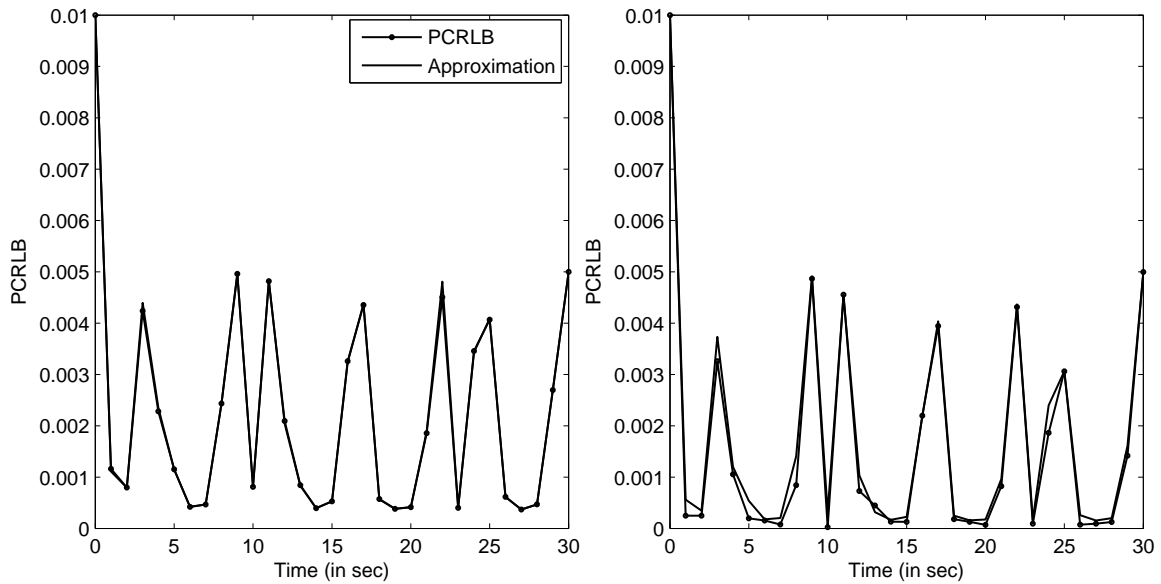
Figure 7.8: Comparing the approximate PCRLB against the theoretical PCRLB in Example 2 under Gaussian (left) and Rayleigh (right) sensor noise distributions.

Case 2: Figure 7.8 compares the approximate PCRLB solution against the theoretical PCRLB for the Rayleigh sensor noise case. Although the approximation almost exactly follows the theoretical solution, compared to Case 1, the approximation is relatively coarser at certain time instants. This highlights the issues associated with estimation under non-Gaussian noise with limited N. Finally, the Λ_J value for Case 2 is 4.62×10^{-8}, which is within an order of the value reported for Case 1.

The simulation study clearly illustrates the efficacy of the proposed method in approximating the PCRLB for non-linear SSMs with non-Gaussian noise.

7.8   Discussions

The simulation results in Section 7.7 demonstrate the utility and performance of the SMC based PCRLB approximation method developed in this chapter. It is important to highlight that despite of the many convergence results discussed in Section 7.6, the choice of an SMC method plays a crucial role in determining the quality of the PCRLB approximation. Here,

the use of a sequential-importance-resampling (SIR) filter of (Gopaluni, 2008; Schön *et al.*, 2011) is motivated by the fact that it is relatively less sensitive to large state noise and is computationally less expensive. Furthermore, the importance weights are easily evaluated and the importance functions can be easily sampled (Ristic *et al.*, 2004); however, other algorithms such as Auxiliary-SIR (ASIR) (Pitt and Shephard, 1999) or Regularized PF (RPF) (Musso *et al.*, 2001) algorithm can also be used in place of SIR, as long as they are consistent with the approach developed herein.

An appropriate choice of the resampling method in Algorithm 7 is also crucial as it can substantially improve the quality of the approximations. The choice of the systematic resampling is supported by an easy implementation procedure and the low-order of computational complexity $\mathcal{O}(N)$ (Doucet *et al.*, 2001). Other resampling schemes such as stratified sampling (Kitagawa, 1996) and residual sampling (Liu and Chen, 1998) can also be used as an alternative to systematic resampling in the proposed framework.

In summary, with the aforementioned options, coupled with the user-defined choice of the parameters N and M, an SMC based PCRLB approximation approach provides an efficient control over the numerical quality of the solution.

7.9   Conclusions

In this chapter a numerical method to recursively approximate the PCRLB in (Tichavský *et al.*, 1998) for a general discrete-time, non-linear SSMs operating with $\mathrm{Pr}_d = 1$ and $\mathrm{Pr}_f = 0$ is presented. The presented method is effective in approximating the PCRLB, when the true states are hidden or unavailable. This has practical relevance in situations; wherein, the test-data consist of only sensor readings. The proposed approach makes use of the sensor readings to estimate the hidden true states, using an SMC method. The method is general and can be used to compute the lower bound for non-linear dynamical systems, with non-Gaussian state and sensor noise. The quality and utility of the SMC based PCRLB

approximation was validated on two simulation examples, including a practical problem of ballistic target tracking at re-entry phase. The analysis of the numerical quality of the SMC based PCRLB approximation was investigated for a range of target state and sensor noise variances, and with different number of particles. The proposed method exhibited acceptable and consistent performance in all the simulations. Increasing the number of particles was in particular, found to be effective in reducing the errors in the PCRLB estimates. Finally, some of the strategies for improving the quality of the SMC based approximations were also discussed.

The current chapter assumes the model parameters to be known a priori; however, for certain applications, this assumption might be a little restrictive. Future work will focus on extending the results of this work to handle such situations. Furthermore, use of SMC method in approximating the modified versions of the PCRLB, which allow tracking in situations, such as: target generated measurements; measurement origin uncertainty; cluttered environments; and Markovian models will also be considered.

Bibliography

Arulampalam, M.S., S. Maskell, N. Gordon and T. Clapp (2002). A tutorial on particle filters for online non-linear/non-Gaussian Bayesian tracking. *IEEE Transactions on Signal Processing* **50**(2), 174–188.

Bergman, N. (2001). *Sequential Monte Carlo Methods in Practice*. Chap. Posterior Cramér-Rao bounds for sequential estimation. Springer–Verlag, New York.

Bergman, N., L. Ljung and F. Gustafsson (1999). Terrain navigation using Bayesian statistics. *IEEE Control Systems Magazine* **19**(3), 33–40.

Bessell, A., B. Ristic, A. Farina, X. Wang and M.S. Arulampalam (2003). Error performance bounds for tracking a manoeuvring target. In: *Proccedings of the 6th International Conference of Information Fusion*. Queensland, Australia. pp. 903–910.

Bobrovsky, B.Z. and M. Zakai (1975). A lower bound on the estimation error for Markov processes. *IEEE Transactions on Automatic Control* **20**(62), 785–788.

Cadre, J. and O. Trémois (1998). Bearings-only tracking for maneuvering sources. *IEEE Transactions on Aerospace and Electronic Systems* **34**(1), 179–193.

Chang, C.B. and J. Tabaczynski (1984). Application of state estimation to target tracking. *IEEE Transactions on Automatic Control* **29**(2), 98–109.

Chopin, N. (2004). Central limit theorem for sequential Monte Carlo methods and its application to Bayesian inference. *The Annals of Statistics* **32**(6), 2385–2411.

Crisan, D. and A. Doucet (2002). A survey of convergence results on particle filtering methods for practitioners. *IEEE Transactions on Signal Processing* **50**(3), 736–746.

de Freitas, N., R. Dearden, F. Hutter, R.M. Menendez, J. Mutch and D. Poole (2004). Diagnosis by a waiter and a Mars explorer. *Proceedings of the IEEE* **92**(3), 455–468.

Dearden, R., T. Willeke, R. Simmons, V. Verma, F. Hutter and S. Thrun (2004). Real-time fault detection and situational awareness for rovers: report on the Mars technology program task. In: *Proceedings of the IEEE Aerospace Conference*. Montana, USA. pp. 826–840.

Doerschuk, P.C. (1995). A Cramér-Rao bound for discrete-time non-linear filtering problems. *IEEE Transactions on Automatic Control* **40**(8), 1465–1469.

Doucet, A., M. Briers and S. Sénécal (2006). Efficient block sampling strategies for sequential Monte Carlo methods. *Journal of Computational and Graphical Statistics* **15**(3), 693–711.

Doucet, A., N. de Freitas and N. Gordon (2001). *Sequential Monte Carlo Methods in Practice*. Chap. On sequential Monte Carlo methods. Springer–Verlag, New York.

Farina, A., B. Ristic and D. Benvenuti (2002*a*). Tracking a ballistic target: comparison of several non-linear filters. *IEEE Transactions on Aerospace and Electronic Systems* **38**(3), 854–867.

Farina, A., B. Ristic and L. Timmoneri (2002*b*). Cramér-Rao bounds for non-linear filtering with $P_d < 1$ and its application to target tracking. *IEEE Transactions on Signal Processing* **50**(8), 1916–1924.

Farshidi, F., S. Sirouspour and T. Kirubarajan (2006). Optimal positioning of multiple cameras for object recognition using Cramér-Rao lower bound. In: *Proceedings of the*

IEEE International Conference on Robotics and Automation. Orlando, USA. pp. 934–939.

Galdos, J.I. (1980). A Cramér-Rao bound for multi-dimensional discrete-time dynamical systems. *IEEE Transactions on Automatic Control* **25**(1), 117–119.

Gilks, W.R. and C. Berzuini (2002). Following a moving target–Monte Carlo inference for dynamic Bayesian models. *Journal of the Royal Statistical Society: Series B* **63**(1), 127–146.

Glass, J.D. and L.D. Smith (2011). MIMO radar resource allocation using posterior Cramér-Rao lower bounds. In: *Proceedings of the IEEE Aerospace Conference*. Montana, USA. pp. 1–9.

Gopaluni, R.B. (2008). A particle filter approach to identification of non-linear processes under missing observations. *The Canadian Journal of Chemical Engineering* **86**(6), 1081–1092.

Gordon, N., D. Salmond and C. Ewing (1995). Bayesian state estimation for tracking and guidance using the bootstrap filter. *Journal of Guidance, Control and Dynamics* **18**(6), 1434–1443.

Gustafsson, F., F. Gunnarsson, N. Bergman, U. Forssell, J. Jansson, R. Karlsson and P.J. Nordlund (2002). Particle filters for positioning, navigation, and tracking. *IEEE Transactions on Signal Processing* **50**(2), 425–437.

Helferty, J.P. and D.R. Mudgett (1993). Optimal observer trajectories for bearings only tracking by minimizing the trace of the Cramér-Rao lower bound. In: *Proceedings of the IEEE Conference on Decision and Control*. San Antonio, USA. pp. 936–939.

Hernandez, M.L., A.D. Marrs, N.J. Gordon, S. Maskell and C.M. Reed (2002). Cramér-Rao bounds for non-linear filtering with measurement origin uncertainty. In: *Proceedings*

of the 5th International Conference on Information Fusion. Maryland, USA. pp. 18–15.

Hernandez, M.L., T. Kirubarajan and Y. Bar-Shalom (2004). Multisensor resource deployment using posterior Cramér-Rao bounds. *IEEE Transactions on Aerospace and Electronic Systems* **40**(2), 399–416.

Hernandez, M.L., T. Kirubarajan and Y. Bar-Shalom (2006). PCRLB for tracking in cluttered environments: measurement sequence conditioning approach. *IEEE Transactions on Aerospace and Electronic Systems* **42**(2), 680–704.

Horn, R.A. and C.R. Johnson (1985). *Matrix Analysis*. Cambridge University Press, New York.

Hurtado, M., T. Zhao and A. Nehorai (2008). Adaptive polarized waveform design for target tracking based on sequential Bayesian inference. *IEEE Transactions on Signal Processing* **56**(3), 1120–1133.

Kantas, N., A. Doucet, S.S. Singh and J. Maciejowski (2009). An overview of sequential Monte Carlo methods for parameter estimation in general state-space models. In: *Proceedings of the 15th IFAC Symposium on System Identification*. Saint-Malo, France. pp. 774–785.

Karlsson, R., F. Gusfafsson and T. Karlsson (2003). Particle filtering and Cramér-Rao lower bound for underwater navigation. In: *Proceedings of the IEEE International Conference on Acoustics, Speech and Signal Processing*. Hong Kong. pp. 65–68.

Kerr, T.H. (1989). Status of CR like bounds for non-linear filtering. *IEEE Transactions on Aerospace and Electronic Systems* **25**(5), 590–601.

Kitagawa, G. (1996). Monte Carlo filter and smoother for non-Gaussian non-linear state-space models. *Journal of Computational and Graphical Statistics* **5**(1), 1–25.

Lei, M., B. J. Van Wyk and Q. Yong (2011). Online estimation of the approximate posterior Cramér-Rao lower bound for discrete-time non-linear filtering. *IEEE Transactions on Aerospace and Electronic Systems* **47**(1), 37–57.

Lei, M., P. Del Moral and C. Baehr (2010). Error analysis of approximated PCRLBs for non-linear dynamics. In: *Proceedings of the 8th IEEE International Conference on Control and Automation*. Xiamen, China. pp. 1988–1993.

Li, X.R. and V.P. Jilkov (2001*a*). A survey of maneuvering target tracking–Part II: Ballistic target models. In: *Proceedings of the SPIE Conference on Signal and Data Processing of Small Targets*. San Diego, USA. pp. 559–581.

Li, X.R. and V.P. Jilkov (2001*b*). A survey of maneuvering target tracking–Part III: Measurement models. In: *Proceedings of the SPIE Conference on Signal and Data Processing of Small Targets*. San Diego, USA. pp. 423–446.

Liu, J.S. and R. Chen (1998). Sequential Monte Carlo methods for dynamics systems. *Journal of the American Statistical Association* **93**(443), 1032–1044.

Meng, H., M.L. Hernandez, Y. Liu and X. Wang (2009). Computationally efficient PCRLB for tracking in cluttered environments: measurement existence conditioning approach. *IET Signal Processing* **3**(2), 133–149.

Moral, P. Del (2004). *Feynman-Kac Formulae: Genealogical and Interacting Particle Systems with Applications*. Springer–Verlag, New York.

Moral, P. Del and A. Doucet (2003). *Séminaire de Probabilités XXXVII*. Chap. On a Class of genealogical and interacting Metropolis models. Springer, Berlin Heidelberg.

Musso, C., N. Oudjane and F. LeGland (2001). *Sequential Monte Carlo Methods in Practice*. Chap. Improving regularized particle filters. Springer–Verlag, New York.

Nehorai, A. and M. Hawkes (2000). Performance bounds for estimating vector systems. *IEEE Transactions on Signal Processing* **48**(6), 1737–1749.

Passerieux, J.M. and D. Van Cappel (1998). Optimal observer maneuver for bearings-only tracking. *IEEE Transactions on Aerospace and Electronic Systems* **34**(3), 777–788.

Pitt, M.K. and N. Shephard (1999). Filtering via simulation: auxiliary particle filters. *Journal of the American Statistical Association* **94**(446), 590–599.

Ristic, B., M.S. Arulampalam and N. Gordon (2004). *Beyond the Kalman Filter: Particle Filters for Tracking Applications*. Chap. Suboptimal non-linear filters. Artech House, Boston.

Schön, T.B., A. Wills and B. Ninness (2011). System identification of non-linear state-space models. *Automatica* **47**(1), 39–49.

Song, T.L. (1999). Observability of target tracking with range-only measurements. *IEEE Journal of Oceanic Engineering* **24**(3), 383–387.

Svensson, L. (2010). On the Bayesian Cramér-Rao bound for Markovian switching systems. *IEEE Transactions on Signal Processing* **58**(9), 4507–4516.

Tanizaki, H. (2001). Non-linear and non-Gaussian state-space modeling using sampling techniques. *Annals of the Institute of Statistical Mathematics* **53**(1), 63–81.

Tichavský, P., C. Muravchik and A. Nehorai (1998). Posterior Cramér-Rao bounds for discrete-time non-linear filtering. *IEEE Transactions on Signal Processing* **46**(5), 1386–1396.

Trees, H.L.V. (1968). *Detection, Estimation and Modulation Theory–Part I*. Chap. Classical detection and estimation theory. Wiley, New York.

Tulsyan, A., B. Huang, R.B. Gopaluni and J.F. Forbes (2013). On simultaneous state and parameter estimation in non-linear state-space models. *Journal of Process Control* **23**(4), 516–526.

Šimandl, M., J. Královec and P. Tichavský (2001). Filtering, predictive, and smoothing Cramér-Rao bounds for discrete-time non-linear dynamic systems. *Automatica* **37**(11), 1703–1716.

Zhang, X., P. Willett and Y. Bar-Shalom (2005). Dynamic Cramér-Rao bound for target tracking in clutter. *IEEE Transactions on Aerospace and Electronic Systems* **41**(4), 1154–1167.

Zuo, L., R. Niu and P.K. Varshney (2011). Conditional posterior Cramér–Rao lower bounds for non-linear sequential Bayesian estimation. *IEEE Transactions on Signal Processing* **59**(1), 1–14.

Chapter 8

Assessment, diagnosis, and optimal selection of non-linear state filters

Non-linear state filters of different approximations and capabilities allow for real-time estimation of unmeasured states in non-linear stochastic processes. It is well known that the performance of these non-linear filters depends on the numerical and statistical approximations used in their design. Despite the practical interest in evaluating the performance of different non-linear filtering methods, it remains one of the most complex problems in the area of non-linear state estimation. We propose the use of posterior Cramér-Rao lower bound (PCRLB) or mean square error (MSE) inequality as a filtering performance benchmark. Using the PCRLB inequality, an assessment and diagnosis tool is developed for monitoring and evaluating the performance of different non-linear filters. Based on the developed tool, a minimum MSE non-linear filter switching strategy is proposed to maintain high filtering performance under various operating conditions. The complex, high dimensional integrals involved in the computation of the PCRLB inequality are approximated using sequential Monte Carlo (SMC) methods. The approach is illustrated through a numerical example.

8.1   Introduction

Recent advances in high speed computing technology have enabled the process and manufacturing industries to use complex, high-fidelity non-linear dynamical models, such as in: fermentation bioreactor (Chitralekha *et al.*, 2010); polymerization (Achilias and Kiparissides, 1992); and petroleum reservoirs (Evensen, 2007). The implementation of advanced control and monitoring strategies on such complex systems requires measurement of key state variables; however, in most processes many important state variables are often unmeasured. These unmeasured states can be estimated within the Bayesian framework by solving a filtering problem; wherein, a posterior density for the unmeasured states is constructed at each sampling-time (Doucet *et al.*, 2001). In linear filtering, the posterior density can be exactly represented by Kalman filter (KF), using a finite number of moments (e.g., mean, variance); whereas, in non-linear filtering, at least in theory, infinite number of moments are required for the exact representation of the density (Ristic *et al.*, 2004). Thus, with finite computing capabilities, an optimal non-linear filter is not realizable.

Over the years several filtering methods based on statistical and analytical approximations of the optimal non-linear filter have been developed for state estimation in non-linear systems (Sorenson, 1974; Maybeck, 1982). Most of these non-linear filters can be classified as either Kalman based filters (e.g., extended KF (EKF); unscented KF (UKF); ensemble KF (EnKF)) or SMC based filters (e.g., sequential importance resampling (SIR) filter; auxiliary SIR (ASIR) filter; Rao-Blackwellized particle filter (RBPF)). Although Kalman and SMC based filters can be used for state estimation in general or specific type of non-linear systems, their performance (compared to the optimal non-linear filter) is often constrained by the underlying numerical and statistical approximations. A detailed exposition of these filtering methods and related approximations is not included here but can be found in the handbook of non-linear filtering (Crisan and Rozovskii, 2011).

A recent surge of interest in developing advanced methods for state estimation in

non-linear systems has left researchers and practitioners inundated with a large number of filtering methods to choose from. To allow researchers to develop efficient filtering methods, and practitioners to select right filtering strategy for their process, several authors have considered comparing and analysing the performance of different filtering methods on general non-linear systems (Kandepu *et al.*, 2008; Arulampalam *et al.*, 2002; Merwe and Wan, 2001). Many application specific comparisons of non-linear filters have also been established for systems in: chemical industries (Romanenko and Castro, 2004; Mesbah *et al.*, 2011; Shenoy *et al.*, 2012); aerospace (Farina *et al.*, 2002; Cui *et al.*, 2005); and communications (Caffery and Stuber, 2000; Wang *et al.*, 2008).

Notwithstanding the elaborate but empirical comparative studies, optimal selection of a filtering strategy for a given non-linear system is still an open problem. The problems associated with non-linear filter selection are highlighted in several recent studies. For instance, (Mesbah *et al.*, 2011) reported that EKF and UKF performed better than EnKF in a batch crystallizer and (Pacharu *et al.*, 2012) reported better EnKF performance compared to EKF and UKF on a packed bed reactor. Similarly, (Shao *et al.*, 2010) reported that SIR outperformed UKF in estimating the states of a gas phase reaction in a continuous stirred tank reactor, but (Shenoy *et al.*, 2012) showed that UKF outperformed SIR on a polymer reactor. Similar inconclusive results have also been observed with other pairs of filtering methods, such as EnKF and SIR (see (Merwe and Wan, 2001; LaViola, 2003)), and SIR and ASIR (see (Pitt and Shephard, 1999; Johansen and Doucet, 2008)). Apart from these results, a recent study done on a stochastic Lorenz system suggests that it is possible for two filters to outperform each other in different operating regions. (Kivman, 2003) showed that the performance of EnKF is better than that of SIR and vice versa depending on the operation region. This highlights the sensitivity of the performance of a non-linear filter to the process dynamics, the filter approximation, and the process operating conditions.

These elaborate empirical studies indicate that there is no single non-linear filter that

provides the best estimates for any process. It is not even possible to choose a non-linear filter that retains high filtering performance on a given process under all operating conditions. A practitioner is thus left with no clear substitute for the optimal non-linear filter. An approach to resolve this dilemma is to start with a family of non-linear filters and switch between them as and when required so as to maintain high filtering performance. Naturally, this approach has to depend on a performance measure of non-linear filters that is independent of the process conditions. Contributions of this work are discussed next.

8.2   Motivation and contributions

The performance of a non-linear filter is a function of the process dynamics and operating conditions- two properties over which a user has limited leverage. A systematic and careful assessment of non-linear filters will help in: (i) assessing the quality of the numerical approximations; (ii) comparing their performance against that of an optimal non-linear filter; and (iii) devising an effective filtering strategy for a given process. Despite the strong practical interest in evaluating the performance of non-linear filters, it remains one of the most complex problems in non-linear estimation theory (Šimandl *et al.*, 2001).

Several authors proposed using the normalized estimation error squared (NEES) as a measure of non-linear filter performance (Farina *et al.*, 2002; Li *et al.*, 2001; Bar-Shalom and Li, 1993). When the state estimation error for a non-linear filter is approximately Gaussian, it can be shown that the NEES follows a Chi-square distribution with certain degrees of freedom (Li *et al.*, 2001). The performance of a filter is then judged based on the hypothesis test-based confidence levels constructed using the NEES values. Despite its simplicity, the NEES computations require a priori knowledge of the true states. The true states are generally not available, except in computer simulations or in carefully conducted experiments (Lei *et al.*, 2011). (Bar-Shalom *et al.*, 2001) proposed replacing the NEES with normalized innovation square (NIS); however, the measure is not meaningful for multi-

modal measurement models. Moreover, since the NIS is based on the measurements and not the states, inference based on the NIS value alone is not reliable (Jones *et al.*, 2011). (Bates and Watts, 1988) proposed a non-linearity measure based on the magnitudes of first and second-order terms in a Taylor series approximation of a non-linear process. This measure was exploited by (Mallick *et al.*, 2005; Mallick and Scala, 2006) in assessing the performance of various non-linear state filters.

The NEES, NIS and non-linearity measures provide a convenient and quick way to qualitatively assess the performance of non-linear filters in real-time; however, there are limitations of these measures as summarized in (Li *et al.*, 2001; Niu *et al.*, 2008): (i) fail to provide any quantitative measure of filter performance; (ii) not useful in comparing multiple filters; (iii) computation requires a priori access to the true states; (iv) can be constructed and computed only for certain classes of non-linear systems; (v) depend on the input-output data; (vi) require the state estimation error and innovation sequence to have a Gaussian distribution; and (vii) provide limited insights for improving filter performance.

A performance measure that improves on the above weaknesses is therefore crucial for developing an efficient assessment procedure for non-linear filters. The conventional Cramér-Rao lower bound (CRLB) provides a theoretical lower bound on the mean square error (MSE) of any maximum-likelihood (ML) based unbiased state or parameter estimator. An analogous extension of the CRLB to the Bayesian estimators was derived by (Trees, 1968) and is called the PCRLB inequality. The PCRLB is general and provides a lower bound on the MSE of any non-linear filter (Trees, 1968) and for any non-linear system (Tichavský *et al.*, 1998) and thus, provides a reliable performance measure.

Unlike other measures, the PCRLB can only be computed off-line. Nevertheless, for many real-time applications of state estimation (e.g., in control and process monitoring), the design, performance evaluation and selection of filters are mostly done a priori or off-line, thereby making the PCRLB an attractive option. Moreover, the PCRLB is an

important measure that depends only on the fundamental properties of the process, such as the process dynamics and noise characteristics (Bergman, 2001). The PCRLB is in fact independent of the choice of a filtering method or any particular realization of the input-output data. Some recently reported important practical applications of the PCRLB inequality are: comparison of several non-linear filters for ballistic target tracking (Farina *et al.*, 2002), terrain navigation (Bergman *et al.*, 1999), and design of systems with pre-specified performance bounds (Nehorai and Hawkes, 2000).

Computing the PCRLB inequality involves solving complex high dimensional integral that does not have an analytical solution for the general non-linear systems (Bergman, 2001). Several authors - (Tichavský *et al.*, 1998; Bergman, 2001; Bergman *et al.*, 1999; Šimandl *et al.*, 2001) - have used simulation based techniques, such as the perfect Monte Carlo (MC) method to approximate the PCRLB inequality. Despite the convergence results showing MC based PCRLB inequality converges to the true inequality (Bergman, 2001), the MC based method requires access to the true states and measurements. Since, the true states are rarely available in practical settings, no practical method of approximation should use true states in the approximation of the PCRLB inequality.

Authors in (Lei *et al.*, 2011) highlighted the problem with MC method, and proposed using EKF and UKF to approximate the PCRLB inequality. Although the method proposed in (Lei *et al.*, 2011) is fast, there are several performance and applicability related issues with this approach: (i) relies on the linearization of the underlying non-linear dynamics around the state estimates and introduces bias in the approximation; (ii) cannot be used to approximate the MSE of a non-linear filter; (iii) applicable only to a special class of non-linear system; (iv) convergence of the PCRLB approximation to the true PCRLB is not guaranteed; (v) provides limited control for improving the quality of the approximation.

The following are the main contributions in this article: (i) A PCRLB inequality based performance measure is proposed for off-line assessment of multiple non-linear filters.

(ii) A PCRLB inequality based procedure for diagnosis of non-linear filter performance is developed. (iii) A switching filter strategy is proposed for state estimation in general non-linear state-space models (SSMs). According to this strategy, at each sampling-time, the performance of a pre-determined bank of Kalman and SMC based non-linear filters is first assessed using the developed measure, and then the filter with highest performance measure is selected for delivering the state estimate. (iv) A sequential MC (SMC) based method is proposed to approximate the PCRLB inequality. This idea has been partially reported by the authors in two earlier publications (Tulsyan *et al.*, 2013*a*; Tulsyan *et al.*, 2012); wherein, an SMC based method is used to approximate the PCRLB. In this work, we revisit those methods and extend it to approximate the MSE of a non-linear filter. Convergence results for the proposed SMC based PCRB inequality method is also provided. (v) Finally, the procedure for assessing and diagnosing the performance of non-linear state filters and its use in designing an optimal state estimation strategy is illustrated on discrete-time, univariate and non-stationary non-linear SSM. The notation used in this chapter are given next.

Notation: $\mathbb{N} := \{0, 1, 2, \dots\}$; $\mathbb{R}_+ := [0, \infty)$; $\mathbb{R}^{n \times n}$ is the set of real valued $n \times n$ matrices; $\mathcal{S}^n \subset \mathbb{R}^{n \times n}$ is the space of symmetric matrices; $I_{n \times n}$ is a $n \times n$ identity matrix; $\mathcal{S}^n_+$ is the cone of symmetric positive semi-definite matrices in $\mathcal{S}^n$; and $\mathcal{S}^n_{++}$ is its interior, i.e., the positive definite matrices. The partial order on $\mathcal{S}^n$ induced by $\mathcal{S}^n_+$ and $\mathcal{S}^n_{++}$ are denoted by $\succeq$ and $\succ$, respectively. Let $A = A(i, j)$ and $B = B(i, j)$ be two matrices in $\mathbb{R}^{n \times n}$ then the Hadamard product of A and B is $A \circ B = A(i, j)B(i, j)$ and the Hadamard inverse of A is $A^{\circ -1} = 1/A(i, j)$, where $1 \leq i, j \leq n$, if and only if $A(i, j) \neq 0$ for all $1 \leq i, j \leq n$. $(A)^T$ and $\mathrm{Tr}[A]$ are the transpose and trace of matrix A. $\| \cdot \|$ is a 2-norm operator and $|\cdot|$ is the absolute value. If x, y and z are three vectors in $\mathbb{R}^n$ then $z \leq x \leq y$ implies element-wise inequality. $\nabla_X \triangleq \left[\frac{\partial}{\partial X} \right]$ is the gradient operator and $\Delta^Y_X \triangleq \nabla_X \nabla^T_Y$ is the Laplacian operator. $\mathcal{C}^k(\mathbb{R})$ is a class of continuous function in $\mathbb{R}$ with k-order derivative in $\mathbb{R}$. $\mathrm{Pr}(\cdot)$ is

a probability measure and $\mathbb{E}_{p(\cdot)}[\cdot]$ is expectation with respect to the probability density $p(\cdot)$.

8.3   Problem formulation

Let $X_t \in \mathcal{X} \subseteq \mathbb{R}^n$ be a discrete-time, unobserved Markov state process characterized by its initial density $p(x_0)$ and a Markov transition density $p_\theta(x_{t+1}|x_t, u_t)$. Here, $u_t \in \mathcal{U} \subseteq \mathbb{R}^p$ and $\theta \in \Theta \subseteq \mathbb{R}^r$ are the control variables and model parameters, respectively. The process $X_t \in \mathcal{X}$ is hidden, but observed through a measurement process $Y_t \in \mathcal{Y} \subseteq \mathbb{R}^m$. $Y_t \in \mathcal{Y}$ at $t \in \mathbb{N}$ is conditionally independent given $X_t \in \mathcal{X}$ and $u_t \in \mathcal{U}$, and is characterized by the conditional marginal density $p_\theta(y_t|x_t, u_t)$. To summarize, we have the following model:

$$X_0 \sim p(x_0); \tag{8.1a}$$

$$X_{t+1}|(X_t, u_t) \sim p_\theta(x_{t+1}|x_t, u_t); \tag{8.1b}$$

$$Y_t|(X_t, u_t) \sim p_\theta(y_t|x_t, u_t). \tag{8.1c}$$

Although the representation in (8.1) includes a wide class of discrete-time, stochastic non-linear time-series models, the class of model structure considered here is given below.

Model 8.3.1. Non-linear SSM with non-Gaussian noise

$$X_{t+1} = f_t(X_t, u_t, \theta, V_t), \tag{8.2a}$$

$$Y_t = g_t(X_t, u_t, \theta, W_t), \tag{8.2b}$$

where: the state and measurement noise sequences are represented as $V_t \in \mathbb{R}^n$ and $W_t \in \mathbb{R}^m$; $f_t(\cdot)$ is an n-dimensional non-linear state transition function; and $g_t(\cdot)$ is an m-dimensional non-linear measurement mapping function.

Other standard models used throughout this chapter for illustration purposes are given below.

Model 8.3.2. Non-linear SSM with additive Gaussian noise

$$X_{t+1} = f_t(X_t) + V_t, \tag{8.3a}$$

$$Y_t = g_t(X_t) + W_t, \tag{8.3b}$$

where $V_t \sim \mathcal{N}(v_t|0, Q_t)$ and $W_t \sim \mathcal{N}(w_t|0, R_t)$ are mutually independent sequences of independent Gaussian random variables with zero mean and finite variance.

Model 8.3.3. Linear SSM with additive Gaussian noise

$$X_{t+1} = A_t X_t + V_t, \tag{8.4a}$$

$$Y_t = C_t X_t + W_t, \tag{8.4b}$$

where $A_t \in \mathbb{R}^{n \times n}$ and $C_t \in \mathbb{R}^{m \times n}$ are known system matrices and $V_t \in \mathbb{R}^n$ and $W_t \in \mathbb{R}^m$ are zero mean, finite variance Gaussian noise sequences, as defined in Model 8.3.2.

Model 8.3.1 represents a general class of discrete-time, non-linear SSMs. Next we discuss the assumptions on Model 8.3.1.

Assumption 8.3.4. *The true model with parameter set $\theta^\star \in \Theta$ is same as Model 8.3.1 with $\theta = \theta^\star$ known a priori. This ensures there is no process-model mismatch.*

Assumption 8.3.5. *$V_t \in \mathbb{R}^n$ and $W_t \in \mathbb{R}^m$ are the mutually independent sequences of independent random variables described by the probability density functions (pdfs) $p(v_t)$ and $p(w_t)$, respectively. $X_0 \in \mathcal{X}$ is also an independent random variable, such that $X_0 \sim p(x_0)$. These pdfs are known in their classes (e.g., Gaussian; Rayleigh) and are parametrized by a known and finite number of moments (e.g., mean; variance). This ensures the densities in (8.1) are known and computable.*

Assumption 8.3.6. *Ignoring $\theta \in \Theta$ and $u_t \in \mathcal{U}$, the process and measurement models defined as $f_t := \mathcal{X} \times \mathbb{R}^n \to \mathbb{R}^n$ and $g_t := \mathcal{X} \times \mathbb{R}^m \to \mathbb{R}^m$, respectively, are such that on the open set $\mathcal{X}$, f_t is $\mathcal{C}^k(\mathcal{X})$ and g_t is $\mathcal{C}^k(\mathcal{X})$, where $k \geq 2$. This ensures (8.1) is at least twice differentiable with respect to the states $X_t \in \mathcal{X}$.*

Assumption 8.3.7. *For a random realization* $(x_{t+1}, x_t, v_t) \in \mathcal{X} \times \mathcal{X} \times \mathbb{R}^n$ *and* $(y_t, x_t, w_t) \in$ $\mathcal{Y} \times \mathcal{X} \times \mathbb{R}^m$ *satisfying Model 8.3.1,* $\nabla_{v_t} f_t^T(x_t, v_t)$ *and* $\nabla_{w_t} g_t^T(x_t, w_t)$ *have rank* n *and* m*, such that using implicit function theorem,* $p(x_{t+1}|x_t) = p(V_t = \tilde{f}_t(x_t, x_{t+1}))$ *and* $p(y_t|x_t) = p(W_t = \tilde{g}_t(x_t, y_t))$*. This ensures (8.1) does not involve any delta functions.*

Remark 8.3.8. *Since* $\theta \in \Theta$ *and* $u_t \in \mathcal{U}$ *are known a priori (see Assumption 8.3.4), explicit dependency of (8.1) on* $\theta \in \Theta$ *and* $u_t \in \mathcal{U}$ *will not be considered unless warranted.*

The problem of state estimation in Model 8.3.1 is an active area of research (Arulampalam *et al.*, 2002; Andrieu *et al.*, 2004). The Bayesian idea for solving the state estimation problem is to construct the posterior pdf $p(x_t|y_{1:t})$ at $t \in \mathbb{N}$. Here, $p(x_t|y_{1:t})$ is a probabilistic representation of available statistical information on the hidden state X_t conditioned on the measurement sequence $Y_{1:t} = \{y_{1:t}\} \triangleq \{y_1, \ldots, y_t\}$. From the Markov property of Model 8.3.1 and Bayes' theorem-

$$p(x_t|y_{1:t}) \propto p(y_t|x_t)p(x_t|y_{1:t-1}), \tag{8.5a}$$

$$p(x_t|y_{1:t-1}) = \int_{\mathcal{X}} p(x_t|x_{t-1})p(dx_{t-1}|y_{1:t-1}), \tag{8.5b}$$

where $p(dx_{t-1}|y_{1:t-1}) \triangleq p(x_{t-1}|y_{1:t-1})dx_{t-1}$. In principle, (8.5) provides a recursive approach to compute $p(x_t|y_{1:t}) \; \forall t \in \mathbb{N}$.

Remark 8.3.9. *Except for Model 8.3.3, or when* $\mathcal{X}$ *is a finite set, with finite computing capabilities, (8.5) cannot be solved in closed form. In other words, an optimal non-linear filter, which solves (8.5) exactly, is not realizable for Model 8.3.1.*

Over the years, many advanced filtering methods have developed to approximate the optimal filter. Unfortunately, the quality of the state estimates obtained with these non-linear filters depends on the underlying numerical and statistical approximation techniques used in their design. The main problems addressed in this chapter are stated next.

Problem 8.3.10. *Develop a measure for performance assessment of non-linear state filters.*

Problem 8.3.11. *Develop a method for performance diagnosis of non-linear state filters.*

Problem 8.3.12. *Develop an optimal filtering strategy for state estimation in Model 8.3.1.*

The solutions to Problems 8.3.10 through 8.3.12 are discussed in the following sections.

8.4   Posterior Cramér-Rao lower bound for non-linear state estimation

The central idea to solve Problems 8.3.10 through 8.3.12 is to use a performance benchmark. As discussed in Section 8.2, the PCRLB inequality will be used as a benchmark for assessment and diagnosis of non-linear state filters. The PCRLB provides a lower bound on the MSE of a non-linear state filter, such that the following result holds.

Lemma 8.4.1. *Let a non-linear system be represented by Model 8.3.1 and let $Y_{1:t} \in \mathcal{Y}^t$ be a random measurement sequence generated from Model 8.3.1, then the MSE of any non-linear state filter, involved in estimation of the state process $X_t \in \mathcal{X}$ at $t \in \mathbb{N}$, given $Y_{1:t} \in \mathcal{Y}^t$ is bounded by the following matrix inequality*

$$P_{t|t} \triangleq \mathbb{E}_{p(X_{0:t}, Y_{1:t})}[(X_t - \widehat{X}_{t|t})(X_t - \widehat{X}_{t|t})^T] \succcurlyeq J_t^{-1}, \qquad (8.6)$$

where: $P_{t|t} \in \mathcal{S}_{++}^n$ is the MSE of a non-linear filter; $\widehat{X}_{t|t} \triangleq \widehat{X}_t(Y_{1:t}) := \mathbb{R}^{tm} \to \mathbb{R}^n$ is the state estimate computed by a non-linear filter; $J_t \in \mathcal{S}_{++}^n$ is the posterior FIM (PFIM); $J_t^{-1} \in \mathcal{S}_{++}^n$ is the lower bound or PCRLB; and $p(x_{0:t}, y_{1:t})$ is a density.

Proof. See (Trees, 1968) for a detailed proof. □

The inequality (8.6) guarantees $P_{t|t} - J_t^{-1} \in \mathcal{S}_+^n$ for all $\widehat{X}_{t|t} \in \mathbb{R}^n$ and $t \in \mathbb{N}$. In scalar form, (8.6) can be represented as

$$P_{t|t}^S \triangleq \mathbb{E}_{p(X_{0:t}, Y_{1:t})}[\|X_t - \widehat{X}_{t|t}\|^2] \geq \text{Tr}[J_t^{-1}], \qquad (8.7)$$

where: $P_{t|t}^S = \text{Tr}[P_{t|t}]$. For $n = 1$, $P_{t|t}^S = P_{t|t}$. A recursive approach to compute the PFIM or PCRLB in Lemma 8.4.1 can be derived for Model 8.3.1; however, for the sake of brevity, only the results are presented in this chapter.

Lemma 8.4.2. *For Model 8.3.1 operating under Assumptions 8.3.4 through 8.3.7, and represented by (8.1), the PFIM in Lemma 8.4.1 can be recursively computed as follows:*

$$J_{t+1} = D_t^{22} - [D_t^{12}]^T (J_t + D_t^{11})^{-1} D_t^{12}, \tag{8.8}$$

where:

$$D_t^{11} = \mathbb{E}_{p(X_{0:t+1}, Y_{1:t+1})}[-\Delta_{X_t}^{X_t} \log\ p(X_{t+1}|X_t)]; \tag{8.9a}$$

$$D_t^{12} = \mathbb{E}_{p(X_{0:t+1}, Y_{1:t+1})}[-\Delta_{X_t}^{X_{t+1}} \log\ p(X_{t+1}|X_t)]; \tag{8.9b}$$

$$D_t^{22} = \mathbb{E}_{p(X_{0:t+1}, Y_{1:t+1})}[-\Delta_{X_{t+1}}^{X_{t+1}} \log\ p(X_{t+1}|X_t) - \Delta_{X_{t+1}}^{X_{t+1}} \log\ p(Y_{t+1}|X_{t+1})]; \tag{8.9c}$$

and the PFIM at $t = 0$ is given by $J_0 = \mathbb{E}_{p(X_0)}[-\Delta_{X_0}^{X_0} \log\ p(X_0)]$.

Proof. See (Šimandl *et al.*, 2001; Tichavský *et al.*, 1998) for a detailed proof.   □

Remark 8.4.3. *Assumptions 8.3.4 through 8.3.7 are the regulatory conditions for the densities $p(x_0)$, $p(x_{t+1}|x_t)$ and $p(y_{t+1}|x_{t+1})$ in (8.9), which ensures $J_{t+1} \in \mathcal{S}_{++}^n$ or $J_{t+1}^{-1} \in \mathcal{S}_{++}^n$ exists.*

Remark 8.4.4. *Authors in (Ristic et al., 2004; Lei et al., 2011) define expectations in (8.9a) and (8.9b), and in (8.9c), with respect to the density $p(x_{t:t+1})$ and $p(x_{t:t+1}, y_{t+1})$, respectively. This is because (8.9a) and (8.9b) can be simplified as the integrand is independent of $(x_{0:t-1}, y_{1:t+1}) \in \mathcal{X}^t \times \mathcal{Y}^{t+1}$. Similarly, since (8.9c) is independent of $(x_{0:t-1}, y_{1:t}) \in \mathcal{X}^t \times \mathcal{Y}^t$, the joint density can be marginalized. (8.9) facilitates the developments of the later sections.*

Remark 8.4.5. *Expectation in (8.9) with respect to the density $p(x_{0:t+1}, y_{1:t+1}, u_{1:t+1})$ makes the lower bound independent of random realizations $(x_{0:t+1}, y_{1:t+1}, u_{1:t+1}) \in \mathcal{X}^{t+2} \times$*

$\mathcal{Y}^{t+1} \times \mathcal{U}^{t+1}$; *however, the lower bound does depend on the sets themselves. Note that for Model 8.3.1, $\mathcal{X}^{t+2}$ and $\mathcal{Y}^{t+1}$ depends on the choice of $\mathcal{U}^{t+1}$. Thus the lower bound in Lemma 8.4.1 only depends on: the process dynamics described in Model 8.3.1; the noise pdfs $p(v_t)$ and $p(w_t)$; and the choice of $p(x_0)$ and $\mathcal{U}^t$.*

Remark 8.4.5 highlights the PCRLB as a system property, which is independent of the choice of a filtering method or any specific realization of the states, measurements or inputs.

Result 8.4.6. *For Model 8.3.2 satisfying Assumptions 8.3.4 through 8.3.7, the matrices (8.9) can be simplified and written as*

$$D_t^{11} = \mathbb{E}_{p(X_t, Y_{1:t+1})}[\nabla_{X_t} f_t^T(X_t)]Q_t^{-1}[\nabla_{X_t} f_t^T(X_t)]^T; \tag{8.10a}$$

$$D_t^{12} = \mathbb{E}_{p(X_t, Y_{1:t+1})}[-\nabla_{X_t} f_t^T(X_t)]Q_t^{-1}; \tag{8.10b}$$

$$D_t^{22} = \mathbb{E}_{p(X_{t+1}, Y_{1:t})}[\nabla_{X_{t+1}} g_t^T(X_{t+1})]R_{t+1}^{-1}[\nabla_{X_{t+1}} g_{t+1}^T(X_{t+1})]^T + Q_t^{-1}. \tag{8.10c}$$

Proof. See (Tichavský *et al.*, 1998) for a detailed proof of this result. □

Result 8.4.7. *For Model 8.3.3 satisfying Assumptions 8.3.4 through 8.3.7, the matrices (8.9) can be simplified and written as*

$$D_t^{11} = A_t^T Q_t^{-1} A_t^T; \tag{8.11a}$$

$$D_t^{12} = - A_t^T Q_t^{-1}; \tag{8.11b}$$

$$D_t^{22} = C_{t+1}^T R_{t+1}^{-1} C_{t+1}^T + Q_t^{-1}. \tag{8.11c}$$

Proof. Defining Model 8.3.2 as $f_t(X_t) = A_t X_t$ and $g_t(X_t) = C_t X_t$, and substituting $[\nabla_{X_t} f_t^T(X_t)] = A_t^T$ and $[\nabla_{X_{t+1}} g_t^T(X_{t+1})] = C_{t+1}^T$ into Result 8.4.6 yields the result. □

Performance assessment of non-linear state filters are discussed in the next section.

8.4.1   Performance assessment of non-linear state filters

This section deals with Problem 8.3.10 in Section 8.3. For Model 8.3.1, even though an optimal non-linear filter, which solves the state estimation problem formulated in (8.5)

exactly, may not be realisable, the PCRLB can be regarded as a measure of its performance. Thus, using Lemma 8.4.1, the MSE of any tractable non-linear filter can be compared against that of an optimal non-linear filter. Despite this, the PCRLB inequality in Lemma 8.4.1 is not convenient to use in the given form. This is because assessment of a non-linear filter using Lemma 8.4.1 requires simultaneous monitoring of the MSE and PCRLB. To avoid this, a performance measure is defined, as given next.

Definition 8.4.8. *Let $P_{t|t} \in \mathcal{S}_{++}^n$ be the MSE obtained with a non-linear state filter, and let $J_t^{-1} \in \mathcal{S}_{++}^n$ be the PCRLB for Model 8.3.1, both computed at $t \in \mathbb{N}$ and satisfying the inequality in Lemma 8.4.1, then the non-linear state filter performance is*

$$\Phi_t = J_t^{-1} \circ P_{t|t}^{\circ -1} \tag{8.12}$$

where: Φ_t is the filter performance assessment measure at $t \in \mathbb{N}$; $P_{t|t}^{\circ -1}$ is the Hadamard inverse of $P_{t|t}$; and $J_t^{-1} \circ P_{t|t}^{\circ -1}$ is the Hadamard product of J_t^{-1} and $P_{t|t}^{\circ -1}$.

The properties of Φ_t in Definition 8.4.8 are given next.

Theorem 8.4.9. *Let $J_t^{-1} \in \mathcal{S}_{++}^n$ and $P_{t|t} \in \mathcal{S}_{++}^n$ be such that they satisfy (8.6) then Φ_t at $t \in \mathbb{N}$ in Definition 8.4.8 satisfies the inequality $0 < \Phi_t(i,i) \le 1$ for $1 \le i \le n$ and is such that: (a) $\Phi_t \in \mathcal{S}^n$; and (b) $\Phi_t \in \mathcal{S}_{++}^n$ if and only if $P_{t|t}^{\circ -1} \in \mathcal{S}_{++}^n$.*

Proof. (a) $P_{t|t} \in \mathcal{S}_{++}^n$ implies $P_{t|t}^{\circ -1} \in \mathcal{S}^n$, which with $J_t^{-1} \in \mathcal{S}_{++}^n$ implies $\Phi_t = J_t^{-1} \circ P_{t|t}^{\circ -1} \in \mathcal{S}^n$. Now, since $P_{t|t}(i,i) > 0$ and $J_t^{-1}(i,i) > 0$, we have $\Phi_t(i,i) = J_t^{-1}(i,i)[P_t(i,i)]^{-1} > 0$ for $1 \le i \le n$. Also, note that since $J_t^{-1} \in \mathcal{S}_{++}^n$ and $P_{t|t} \in \mathcal{S}_{++}^n$ satisfies the PCRLB inequality (8.6), i.e., $P_{t|t} - J_t^{-1} \succcurlyeq 0$, we have $P_{t|t}(i,i) \ge J_t^{-1}(i,i)$, which implies $\Phi_t(i,i) = J_t^{-1}(i,i)[P_t(i,i)]^{-1} \le 1$ for $1 \le i \le n$. Thus combining the two results, we have $0 < \Phi_t(i,i) \le 1$ for $1 \le i \le n$. (b) If $P_{t|t} \in \mathcal{S}_{++}^n$ have positive off-diagonal entries and just one positive eigenvalue then from Corollary 2.8 in (Reams, 1999), we have $P_{t|t}^{\circ -1} \in \mathcal{S}_{++}^n$. Using Schur Product Theorem (Bapat and Raghavan, 1997), $\Phi_t \in \mathcal{S}_{++}^n$, which completes the proof. $\square$

Theorem 8.4.9 shows that the performance measure in Definition 8.4.8 is bounded with $0 < \Phi_t(i, i) \leq 1$ for $1 \leq i \leq n$. Using Theorem 8.4.9, filter efficiency is defined next.

Definition 8.4.10. *A state filter at $t \in \mathbb{N}$ is efficient for state $1 \leq i \leq n$, if $\Phi_t(i, i) = 1$ (i.e., $P_{t|t}(i, i) - J_t^{-1}(i, i) = 0$) or efficient for all the states, if $\mathrm{Tr}[\Phi_t] = n$ (i.e., $\mathrm{Tr}[P_{t|t} - J_t^{-1}] = 0$).*

Remark 8.4.11. *Another measure of non-linear state filter performance can be defined as $\Phi_t' := J_t^{-1} P_{t|t}^{-1} \preccurlyeq I_{n \times n}$, with $\Phi_t' = I_{n \times n}$ indicating efficiency; however, note that with Φ_t', defining filter efficiency for individual states is not easy. This is because by inverting $P_{t|t}$, the diagonal elements of $P_{t|t}$ get coupled.*

The choice of the state estimate $\widehat{X}_{t|t} \in \mathbb{R}^n$ for which $\mathrm{Tr}[\Phi_t]$ at $t \in \mathbb{N}$ is maximized is discussed next.

Result 8.4.12. *To compute the state estimate $\widehat{X}_{t|t} \in \mathbb{R}^n$ at $t \in \mathbb{N}$, a common approach is to minimize $P_{t|t}^S$. This ensures $P_{t|t}^S - \mathrm{Tr}[J_t^{-1}] \geq 0$ in (8.7) is minimized. The optimal point estimate that minimizes $P_{t|t}^S$ is referred to as the minimum MSE (MMSE) estimate, and is the conditional mean of $X_t | (Y_{1:t} = y_{1:t}) \sim p(x_t | y_{1:t})$, i.e., $\widehat{X}_{t|t} = X_{t|t}^\star \triangleq \mathbb{E}_{p(X_t | Y_{1:t})}[X_t]$.*

Proof. Proof of the MMSE estimates can be found in (Trees, 1968). □

Theorem 8.4.13. *Let $J_t^{-1} \in \mathcal{S}_{++}^n$ and $P_{t|t} \in \mathcal{S}_{++}^n$ be such that they satisfy (8.6) then the MMSE estimate $\widehat{X}_{t|t} \in \mathbb{R}^n$ minimizing $\mathrm{Tr}[P_{t|t}]$ also maximizes $\mathrm{Tr}[\Phi_t]$, such that*

$$\widehat{X}_{t|t} = \underset{\widehat{X}_{t|t} \in \mathbb{R}^n}{\arg\min} \mathrm{Tr}[P_{t|t}] = \underset{\widehat{X}_{t|t} \in \mathbb{R}^n}{\arg\max} \mathrm{Tr}[\Phi_t]. \tag{8.13}$$

Proof. The MMSE estimate $\widehat{X}_{t|t} \in \mathbb{R}^n$ is computed by solving the optimization problem:

$$\widehat{X}_{t|t} = \underset{\widehat{X}_{t|t} \in \mathbb{R}^n}{\arg\min} \operatorname{Tr}[P_{t|t}], \tag{8.14a}$$

$$= \underset{\widehat{X}_{t|t} \in \mathbb{R}^n}{\arg\min} \operatorname{Tr}[P_{t|t} - J_t^{-1}], \tag{8.14b}$$

$$= \underset{\widehat{X}_{t|t} \in \mathbb{R}^n}{\arg\min} \sum_{i=1}^{n} [P_{t|t}(i,i) - J_t^{-1}(i,i)], \tag{8.14c}$$

$$= \underset{\widehat{X}_{t|t} \in \mathbb{R}^n}{\arg\min} \sum_{i=1}^{n} [\Phi_t(i,i)]^{-1} - 1] J_t^{-1}(i,i), \tag{8.14d}$$

$$= \underset{\widehat{X}_{t|t} \in \mathbb{R}^n}{\arg\min} \sum_{i=1}^{n} [\Phi_t(i,i)]^{-1} J_t^{-1}(i,i), \tag{8.14e}$$

$$= \sum_{i=1}^{n} \underset{\widehat{X}_{t|t} \in \mathbb{R}^n}{\arg\min} [\Phi_t(i,i)]^{-1} J_t^{-1}(i,i), \tag{8.14f}$$

$$= \sum_{i=1}^{n} J_t^{-1}(i,i) \underset{\widehat{X}_{t|t} \in \mathbb{R}^n}{\arg\min} [\Phi_t(i,i)]^{-1}, \tag{8.14g}$$

$$= \sum_{i=1}^{n} \underset{\widehat{X}_{t|t} \in \mathbb{R}^n}{\arg\max} [\Phi_t(i,i)], \tag{8.14h}$$

$$= \underset{\widehat{X}_{t|t} \in \mathbb{R}^n}{\arg\max} \sum_{i=1}^{n} [\Phi_t(i,i)] = \underset{\widehat{X}_{t|t} \in \mathbb{R}^n}{\arg\max} \operatorname{Tr}[\Phi_t], \tag{8.14i}$$

where (8.14a) to (8.14b) follows from Result 8.4.12; (8.14e) to (8.14f) follows from the fact that $[\Phi_t(i,i)]^{-1} J_t^{-1}(i,i) > 0$, this is because $0 < \Phi_t(i,i) \leq 1$ (from Theorem 8.4.9) and $J_t^{-1}(i,i) > 0$ (since $J_t^{-1} \in \mathcal{S}_{++}^n$) for $1 \leq i \leq n$; and (8.14h) to (8.14i) again follows from Theorem 8.4.9, which completes the proof. $\square$

Remark 8.4.14. *Theorem 8.4.13 shows that the performance of a filter in terms of Definition 8.4.8 can be maximized for the choice of an MMSE estimate. Since, calculating the MMSE estimate in Remark 8.4.12 requires computation of (8.5), except for Model 8.3.3, or when $\mathcal{X}$ is a finite set, exact MMSE state estimates cannot be computed in closed form.*

Remark 8.4.15. *For Model 8.3.1, non-linear state filters only provide an approximation to the posterior density in (8.5) thus in practice, the estimate delivered by non-linear filters*

is not an MMSE estimate, i.e., $\widehat{X}_{t|t} \triangleq \mathbb{E}_{\tilde{p}(X_t|Y_{1:t})}[X_t] \neq X_{t|t}^{\star}$ almost surely, where $\widehat{X}_{t|t}$ is the mean of $\tilde{p}(x_t|y_{1:t})$ and $\tilde{p}(x_t|y_{1:t})$ is an approximation of $p(x_t|y_{1:t})$ computed by the filter.

Note that since Φ_t at $t \in \mathbb{N}$ in Definition 8.4.8 is a function of the state estimate $\widehat{X}_{t|t} \in \mathbb{R}^n$, non-linear filters of different approximations and capabilities have different Φ_t matrices. Thus by monitoring Φ_t, or some scalar metric of Φ_t (e.g., trace), performance of multiple filters can be simultaneously monitored for all $t \in \mathbb{N}$. While comparing filters, ideally, the best performing filter is the one which is efficient (see Definition 8.4.10); however, for non-linear filters, efficiency is rarely achieved (See Remark 8.4.15). For practical purposes, filter with highest $\text{Tr}[\Phi_t]$ value is the the best performing filter at $t \in \mathbb{N}$.

Although Definition 8.4.8 provides a vital tool for assessment of non-linear state filters, it provides limited insight in diagnosing those performance. This is because of the use of an overall second-order error or MSE in Definition 8.4.8. The PCRLB inequality based filter performance diagnosis is presented next.

8.4.2   Performance diagnosis of non-linear state filters

This section deals with Problem 8.3.11 in Section 8.3. For researchers designing improved non-linear filtering methods, it is often in their interest to understand why the performance of existing filters is low or in which all ways can the overall filtering performance be improved. This is particularly important for non-linear filters; wherein, the state estimates are often not the MMSE estimates (see Remark 8.4.15). To answer these performance related questions, the PCRLB inequality based performance diagnosis tool is presented in this section. Note that the second-order error associated with a filter is completely characterized by its MSE. A thorough diagnosis of filter performance, therefore requires clear understanding of the second-order error. The next theorem shows how MSE of a filter can be decomposed into its separate sources of errors.

Theorem 8.4.16. *Let $X_{t|t}^{\star}$ and $V_{t|t}^{\star}$ be the true conditional mean and covariance of*

$X_t|(Y_{1:t} = y_{1:t}) \sim p(x_t|y_{1:t})$, *respectively. Let $\widehat{X}_{t|t}$ and $\widehat{V}_{t|t}$ be the conditional mean and covariance of $X_t|(Y_{1:t} = y_{1:t}) \sim \tilde{p}(x_t|y_{1:t})$, respectively, as computed by a non-linear filter then for $\widehat{X}_{t|t} \neq X_{t|t}^\star$ almost surely, and $\widehat{V}_{t|t} \neq V_{t|t}^\star$ almost surely, the MSE for the filter, $P_{t|t}$ at $t \in \mathbb{N}$ can be written as*

$$P_{t|t} = \mathbb{E}_{p(Y_{1:t})}[\widehat{V}_{t|t}] + \mathbb{E}_{p(Y_{1:t})}[B_{V_{t|t}}^\star] + \mathbb{E}_{p(Y_{1:t})}[B_{X_{t|t}}^\star[B_{X_{t|t}}^\star]^T], \tag{8.15}$$

where $\widehat{X}_{t|t}$ is an estimate, and $B_{V_{t|t}}^\star \triangleq [V_{t|t}^\star - \widehat{V}_{t|t}] \in \mathcal{S}^n$ and $B_{X_{t|t}}^\star \triangleq [X_{t|t}^\star - \widehat{X}_{t|t}] \in \mathbb{R}^n$ are the conditional bias in estimating the mean and covariance of $X_t|(Y_{1:t} = y_{1:t}) \sim p(x_t|y_{1:t})$.

Proof. Using the Law of Total Probability, the expectation in the MSE, with respect to $p(x_{0:t}, y_{1:t})$ can be written as

$$P_{t|t} = \mathbb{E}_{p(Y_{1:t})}\mathbb{E}_{p(X_{0:t}|Y_{1:t})}[(X_t - \widehat{X}_{t|t})(X_t - \widehat{X}_{t|t})^T], \tag{8.16}$$

where $p(x_{0:t}, y_{1:t}) = p(x_{0:t}|y_{1:t})p(y_{1:t})$ is used. Now since $[(X_t - \widehat{X}_{t|t})(X_t - \widehat{X}_{t|t})^T]$ at time $t \in \mathbb{N}$ is independent of the state trajectory $(x_{0:t-1}) \in \mathcal{X}^t$, (8.16) can be simplified as

$$P_{t|t} = \mathbb{E}_{p(Y_{1:t})}\mathbb{E}_{p(X_t|Y_{1:t})}[(X_t - \widehat{X}_{t|t})(X_t - \widehat{X}_{t|t})^T]. \tag{8.17}$$

Adding and subtracting $X_{t|t}^\star = \mathbb{E}_{p(X_t|Y_{1:t})}[X_t]$ in (8.17) yields

$$P_{t|t} = \mathbb{E}_{p(Y_{1:t})}\mathbb{E}_{p(X_t|Y_{1:t})}[(X_t - X_{t|t}^\star + X_{t|t}^\star - \widehat{X}_{t|t})(X_t - X_{t|t}^\star + X_{t|t}^\star - \widehat{X}_{t|t})^T]. \tag{8.18}$$

Several algebraic manipulations in (8.18) yield the following

$$P_{t|t} = \mathbb{E}_{p(Y_{1:t})}\mathbb{E}_{p(X_t|Y_{1:t})}[K_{X_{t|t}}^\star + L_{X_{t|t}}^\star + [L_{x_{t|t}}^\star]^T + B_{X_{t|t}}^\star[B_{X_{t|t}}^\star]^T], \tag{8.19}$$

where: $K_{X_{t|t}}^\star = [X_t - X_{t|t}^\star][X_t - X_{t|t}^\star]^T; L_{X_{t|t}}^\star = [X_t - X_{t|t}^\star][X_{t|t}^\star - \widehat{X}_{t|t}]^T; B_{X_{t|t}}^\star = [X_{t|t}^\star - \widehat{X}_{t|t}]$. Now while evaluating the inner expectation in (8.19), note that $\mathbb{E}_{p(X_t|Y_{1:t})}[K_{X_{t|t}}^\star] = V_{t|t}^\star$. Also $\mathbb{E}_{p(X_t|Y_{1:t})}[L_{X_{t|t}}^\star] = \mathbb{E}_{p(X_t|Y_{1:t})}[L_{X_{t|t}}^\star]^T = 0$, since $\mathbb{E}_{p(X_t|Y_{1:t})}[X_t - X_{t|t}^\star] = 0$; and $\mathbb{E}_{p(X_t|Y_{1:t})}[B_{X_{t|t}}^\star][B_{X_{t|t}}^\star]^T = B_{X_{t|t}}^\star[B_{X_{t|t}}^\star]^T$, since $B_{X_{t|t}}^\star[B_{X_{t|t}}^\star]^T$

is conditionally independent of $(x_t) \in \mathcal{X}$ given a measurement sequence $(y_{1:t}) \in \mathcal{Y}^t$. Substituting these simplifying expressions into (8.19) we get

$$P_{t|t} = \mathbb{E}_{p(Y_{1:t})}[V_{t|t}^\star + B_{X_{t|t}}^\star [B_{X_{t|t}}^\star]^T]. \tag{8.20}$$

Again adding and subtracting $\widehat{V}_{t|t}$ in (8.20) and substituting $B_{V_{t|t}}^\star = [V_{t|t}^\star - \widehat{V}_{t|t}]$ yields (8.15), which completes the proof. $\square$

Remark 8.4.17. *(8.15) can be simplified by substituting $\widehat{V}_{t|t} + B_{V_{t|t}}^\star = V_{t|t}^\star$. Nonetheless, we use the representation in (8.15) for reasons which will become apparent later on.*

Using Theorem 8.4.16, non-linear filter bias is defined next.

Definition 8.4.18. *A filter is conditionally unbiased in mean if $B_{X_{t|t}}^\star = 0$ almost surely, and unconditionally unbiased in mean if $\mathbb{E}_{p(Y_{1:t})}[B_{X_{t|t}}^\star] = 0$. A filter which is both conditionally and unconditionally unbiased in mean is said to be unbiased in mean. Bias in mean can be similarly defined.*

Definition 8.4.19. *A filter is conditionally unbiased in covariance if $B_{V_{t|t}}^\star = 0$ almost surely, and unconditionally unbiased if $\mathbb{E}_{p(Y_{1:t})}[B_{V_{t|t}}^\star] = 0$. A filter which is both conditionally and unconditionally unbiased in covariance is said to be unbiased in covariance. Bias in covariance can be similarly defined.*

The conditions under which a non-linear filter is unbiased in mean and covariance are discussed in the next theorem.

Theorem 8.4.20. *Let $B_{V_{t|t}}^\star \in \mathcal{S}^n$ and $B_{X_{t|t}}^\star \in \mathbb{R}^n$ be the conditional bias in the mean and covariance, respectively, then: (a) $B_{V_{t|t}}^\star = 0$ and $B_{X_{t|t}}^\star = 0$ almost surely are the necessary conditions for $\mathbb{E}_{p(Y_{1:t})}[B_{V_{t|t}}^\star] = 0$ and $\mathbb{E}_{p(Y_{1:t})}[B_{X_{t|t}}^\star] = 0$, respectively; and (b) $B_{X_{t|t}}^\star = 0$ almost surely is the necessary and sufficient condition for $\mathbb{E}_{p(Y_{1:t})}[B_{X_{t|t}}^\star[B_{X_{t|t}}^\star]^T] = 0$.*

Proof. (a) First note that $B_{V_{t|t}}^\star \in \mathcal{S}^n$ is a positive or negative definite matrix depending on the measurement sequence $(y_{1:t}) \in \mathcal{Y}^t$. This implies that $\mathbb{E}_{p(Y_{1:t})}[B_{V_{t|t}}^\star] \in \mathcal{S}^n$ is an

indefinite matrix, which in turn implies that $B^\star_{V_{t|t}} = 0$ almost surely is only a necessary condition for $\mathbb{E}_{p(Y_{1:t})}[B^\star_{V_{t|t}}] = 0$. Now from Theorem 15.2 in (Billingsley, 1995), we can show that $B^\star_{X_{t|t}} = 0$ almost surely is a necessary condition for $\mathbb{E}_{p(Y_{1:t})}[B^\star_{X_{t|t}}] = 0$. (b) Since for $B^\star_{X_{t|t}} \in \mathbb{R}^n$, $\mathbb{E}_{p(Y_{1:t})}[B^\star_{X_{t|t}}[B^\star_{X_{t|t}}]^T] \in \mathcal{S}^n$ with positive diagonal elements, which implies that $B^\star_{X_{t|t}} = 0$ almost surely is both necessary and sufficient condition for $\mathbb{E}_{p(Y_{1:t})}[B^\star_{X_{t|t}}[B^\star_{X_{t|t}}]^T] = 0$, which completes the proof. □

Remark 8.4.21. *Theorem 8.4.20 shows that if a non-linear filter is unbiased in mean or variance, it does not imply that it is conditionally unbiased as well.*

The MSE of an unbiased non-linear filter is given next.

Corollary 8.4.22. *Let $\widehat{X}_{t|t}$ and $\widehat{V}_{t|t}$ be the first and second moment of $X_t|(Y_{1:t} = y_{1:t}) \sim \tilde{p}(x_t|y_{1:t})$ computed by a non-linear filter, such that it satisfies $B^\star_{X_{t|t}} = 0$ almost surely then the MSE of the non-linear filter is given by*

$$P_{t|t} = \mathbb{E}_{p(Y_{1:t})}[V^\star_{t|t}] \tag{8.21}$$

Proof. Substituting $B^\star_{X_{t|t}} = 0$ into (8.15), and using the fact that $\widehat{V}_{t|t} + B^\star_{V_{t|t}} = V^\star_{t|t}$ yields (8.21), which completes the proof. □

Remark 8.4.23. *Since $P_{t|t} = \mathbb{E}_{p(Y_{1:t})}[V^\star_{t|t}]$ is only a function of the true conditional covariance of the posterior, the MSE cannot be reduced any further. In fact the MSE is independent of the choice of the filtering method. Thus, a non-linear filter which satisfies $B^\star_{X_{t|t}} = 0$ almost surely is efficient.*

Remark 8.4.24. *In Definition 8.4.10, filter efficiency at time $t \in \mathbb{N}$ is defined based on Φ_t; whereas, in Remark 8.4.23 it is defined based on $P_{t|t}$. Note that the two definitions of efficiency are equivalent, since Φ_t and $P_{t|t}$ are related by Theorem 8.4.13.*

Theorem 8.4.16 provides a procedure to decompose $P_{t|t}$ into its sources of errors, thereby providing a means to diagnose non-linear filter performance. The PCRLB inequality based diagnosis results are summarized in the theorem given below.

Theorem 8.4.25. *Let $X_{t|t}^\star$ and $V_{t|t}^\star$ be the true conditional mean and covariance of $X_t|(Y_{1:t} = y_{1:t}) \sim p(x_t|y_{1:t})$, respectively. Let $\widehat{X}_{t|t}$ and $\widehat{V}_{t|t}$ be the conditional mean and covariance of $X_t|(Y_{1:t} = y_{1:t}) \sim \tilde{p}(x_t|y_{1:t})$, respectively, computed using a non-linear filter, such that $\widehat{X}_{t|t}$ is also the state estimate then from Lemma 8.4.1 and Theorems 8.4.16 and 8.4.20 we have*

(a) If $B_{V_{t|t}}^\star = 0$ almost surely and $B_{X_{t|t}}^\star = 0$ almost surely then the PCRLB inequality (8.6) is given by

$$P_{t|t} = \mathbb{E}_{p(Y_{1:t})}[V_{t|t}^\star] = J_t^{-1}, \tag{8.22a}$$

which implies the non-linear filter is efficient, unbiased in mean and covariance and yields an MMSE estimate.

(b) If $B_{V_{t|t}}^\star = 0$ almost surely and $B_{X_{t|t}}^\star \neq 0$ almost surely then the PCRLB inequality (8.6) is given by

$$P_{t|t} = \mathbb{E}_{p(Y_{1:t})}[V_{t|t}^\star] + \mathbb{E}_{p(Y_{1:t})}[B_{X_{t|t}}^\star [B_{X_{t|t}}^\star]^T] \succcurlyeq J_t^{-1}, \tag{8.22b}$$

which implies the non-linear filter is not efficient, conditionally biased in mean (or biased in mean if $\mathbb{E}_{p(Y_{1:t})}[B_{X_{t|t}}^\star] \neq 0$), but unbiased in covariance and fails to yield an MMSE estimate.

(c) If $B_{V_{t|t}}^\star \neq 0$ almost surely and $B_{X_{t|t}}^\star = 0$ almost surely then the PCRLB inequality (8.6) is given by

$$P_{t|t} = \mathbb{E}_{p(Y_{1:t})}[\widehat{V}_{X_{t|t}}] + \mathbb{E}_{p(Y_{1:t})}[B_{V_{t|t}}^\star] = \mathbb{E}_{p(y_{1:t})}[V_{t|t}^\star] = J_t^{-1}, \tag{8.22c}$$

which implies the non-linear filter is efficient, unbiased in mean, but conditionally biased in covariance (or biased in covariance if $\mathbb{E}_{p(Y_{1:t})}[B_{V_{t|t}}^\star] \neq 0$) and yields an MMSE estimate.

(d) If $B_{V_{t|t}}^\star \neq 0$ almost surely and $B_{X_{t|t}}^\star \neq 0$ almost surely then the PCRLB inequality (8.6) is given by

$$P_{t|t} = \mathbb{E}_{p(Y_{1:t})}[\widehat{V}_{t|t}] + \mathbb{E}_{p(Y_{1:t})}[B_{V_{t|t}}^\star] + \mathbb{E}_{p(Y_{1:t})}[B_{X_{t|t}}^\star [B_{X_{t|t}}^\star]^T] \succcurlyeq J_t^{-1}, \tag{8.22d}$$

which implies the non-linear filter is not efficient, conditionally biased in mean and covariance (or biased in mean and covariance if $\mathbb{E}_{p(Y_{1:t})}[B^{\star}_{X_{t|t}}] \neq 0$ and $\mathbb{E}_{p(Y_{1:t})}[B^{\star}_{V_{t|t}}] \neq 0$, respectively), and fails to yield an MMSE estimate.

Proof. (a) Since the filter satisfies $B^{\star}_{V_{t|t}} = 0$ almost surely; Corollary 8.4.22 and Remark 8.4.23 imply that the filter is efficient. From Theorem 8.4.20, the conditions $B^{\star}_{V_{t|t}} = 0$ almost surely and $B^{\star}_{X_{t|t}} = 0$ almost surely are also the necessary conditions for the filter to be unbiased in mean and covariance. Also, since the filter is conditionally unbiased in mean, Result 8.4.12 implies that the filter yields an MMSE estimate. Proofs for (b) through (d) are similar and omitted here for the sake of brevity. $\square$

Remark 8.4.26. *From Theorems 8.4.25(a) and (c) it is clear that $B^{\star}_{X_{t|t}} = 0$ almost surely is the necessary and sufficient condition for filter efficiency. Nevertheless Theorem 8.4.25(a), which require the filter to satisfy the conditions $B^{\star}_{X_{t|t}} = 0$ and $B^{\star}_{V_{t|t}} = 0$ almost surely, not only guarantees filter efficiency, but also ensures that the filter is unbiased with respect to the mean and covariance of the true posterior density.*

Remark 8.4.27. *To exactly solve the state estimation problem for Model 8.3.1, infinitely many moments of the approximate posterior density should exactly match with that of the true posterior density. With finite computing capabilities, since this is not possible to achieve, the representation of MSE in Theorem 8.4.16 and the results in Theorem 8.4.25, at least ensure that diagnosis of a non-linear filter is performed based on the first two moments of the approximate posterior density.*

Result 8.4.28. *For Model 8.3.3, the KF is efficient, unbiased in mean and covariance, and yields an MMSE estimate. The MSE of the KF at $t \in \mathbb{N}$ is given by*

$$P_{t|t} = J_t^{-1}, \tag{8.23}$$

where $J_t^{-1} \in \mathcal{S}^n_{++}$ can be computed from Result 8.4.7.
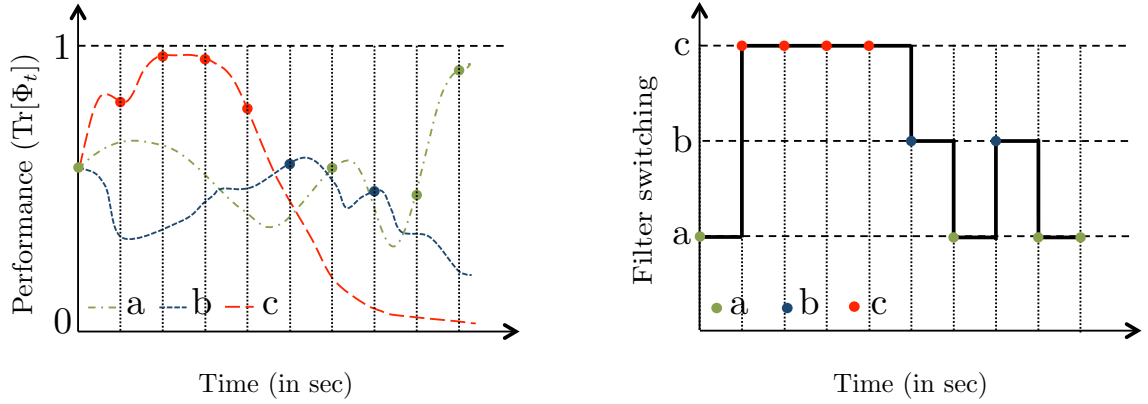
Figure 8.1: [Left] sample performance trajectories of three tractable non-linear filters (referred to as filters: a, b, and c) computed using (8.12). Note that the $\Phi_t \; \forall t \in [0,9]$ values for all three filters are in between 0 and 1; [Right] an optimal switching map based on the performance of three filters. The idea is to always switch to the filter, which has the highest $\Phi_t \; \forall t \in [0,9]$ value.

Proof. It is well known that KF yields conditionally unbiased estimates of $X^\star_{t|t}$ and $V^\star_{t|t}$ (Ristic *et al.*, 2004), such that $B^\star_{V_{t|t}} = 0$ almost surely and $B^\star_{X_{t|t}} = 0$ almost surely. Since KF satisfies the conditions of Theorem 8.4.25(a), the result follows.   □

It is important to highlight that the MSE of the KF in (8.23) is equivalent to its covariance update step at time $t \in \mathbb{N}$ (Ristic *et al.*, 2004; Tichavský *et al.*, 1998).

Remark 8.4.29. *Theorem 8.4.25 serves as guidelines to assess and diagnose performance of different non-linear filters. Furthermore, it also provides a better resolution to the researchers by allowing them to focus their non-linear filter design on either the bias reduction in the mean or covariance, or both. This is to promote an overall improvement in the performance and efficiency of non-linear filters.*

The PCRLB inequality based optimal filtering strategy for non-linear state estimation is discussed next.

8.4.3   Optimal filtering strategy for non-linear state estimation

This section deals with Problem 8.3.12 in Section 8.3. For state estimation in processes described by Model 8.3.1, a PCRLB inequality based filter switching strategy is proposed in this chapter. This strategy is motivated by the fact that there is no one single non-linear filter, which is guaranteed to perform well for all non-linear systems, and at all operating conditions. In such situations, the idea is to start with a set of multiple non-linear filters, and switch between them based on their performance.

In the proposed filter switching strategy, the performance of a pre-determined bank of Kalman and SMC based filters is first assessed using $\text{Tr}[\Phi_t]$ values and then the non-linear filter with highest $\text{Tr}[\Phi_t]$ value is selected for delivering the state estimate at $t \in \mathbb{N}$. Figure 8.1 illustrates the procedure for devising the filter switching strategy using the performance measure in Definition 8.4.8. Formally, the filter switching strategy proposed in this chapter can be represented as given next.

Definition 8.4.30. *Let $\mathcal{B}$ be a bank of non-linear filters, such that $i \in \mathcal{F}$ is the filter identity in $\mathcal{B}$, where $\mathcal{F} = \{1, 2, \ldots, F\}$ and $F \in \mathbb{N}$. Also, let Φ_t^i and $\widehat{X}_{t|t}^i$ be the performance measure and state estimate of the non-linear filter $i \in \mathcal{F}$ then*

$$i_t^\star = \arg\max_{i \in \mathcal{F}} \text{Tr}[\Phi_t^i], \tag{8.24}$$

where $i_t^\star \in \mathcal{F}$ is the filter in $\mathcal{B}$ to be switched to at $t \in \mathbb{N}$ and $\widehat{X}_{t|t}^{i_t^\star}$ being the state estimate to be selected at $t \in \mathbb{N}$.

Theorem 8.4.31. *Let $F \in \mathbb{N}$ be the number of non-linear filters in an arbitrarily chosen filter bank $\mathcal{B}$ then with respect to the bank $\mathcal{B}$, state estimation in Model 8.3.1 according to Definition 8.4.30 gives an optimal minimum MMSE estimation strategy.*

Proof. The very construction of (8.24) based on Lemma 8.4.1 makes Definition 8.4.30 an average-optimal MMSE state estimation strategy for Model 8.3.1, with respect to the filter bank $\mathcal{B}$. This completes the proof.   □

Remark 8.4.32. *Theorem 8.4.31 highlights that given a set of non-linear filters, performing state estimation in Model 8.3.1 according to Definition 8.4.30 yields the lowest MSE.*

Remark 8.4.33. *The filter switching strategy given in Definition 8.4.30 is based on average performance of the filter in estimating all the states of Model 8.3.1; however, if required, the switching strategy can also be implemented for individual states. This would result in an n-dimensional switching map.*

8.4.4   An integrated filter assessment and diagnosis approach

It is possible to integrate the performance assessment, diagnosis tools developed in Sections 8.4.1 and 8.4.2, respectively, for devising an optimal switching strategy for state estimation in Model 8.3.1 (see Figure 8.2). The first step of this integrated procedure requires the operating region for Model 8.3.1 to be specified (see Remark 8.4.5). In the second and third step, a bank of non-linear filters is selected and its performance is assessed using Definition 8.4.8. If the non-linear filter performance is low, diagnosis is performed using Theorem 8.4.25. Based on the diagnosis results, the filters are redesigned and reassessed for its performance using Definition 8.4.8. Once the overall performance of the filters in the bank over the entire operating region is satisfactory, the optimal switching strategy can be devised using Definition 8.4.30. Finally, state estimation in Model 8.3.1 over the selected operating region can be performed according to the developed filter switching map. All the steps in Figure 8.2 are illustrated on a simulation example in Section 8.6.3.

Remark 8.4.34. *Note that the filter redesign step in Figure 8.2 is a non-trivial exercise. Designing non-linear filters with specific properties (e.g., low bias in mean or variance) not only requires a thorough understanding of the underlying statistical and numerical approximations, it also requires a comprehensive knowledge of non-linear filtering theory. Since, filter design is not included in the scope of this work, it will not be pursued.*
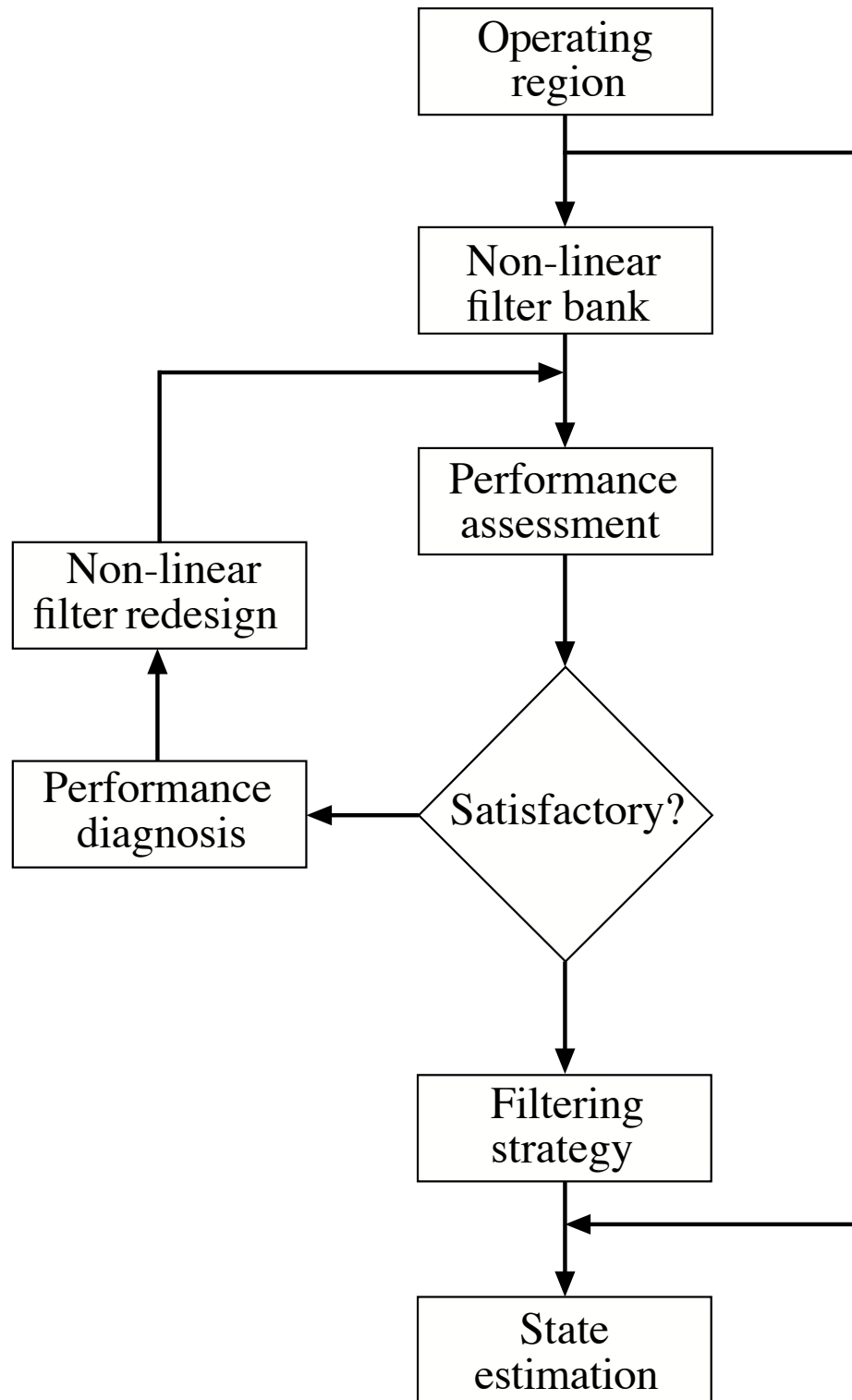
Figure 8.2: Flowchart for the PCRLB inequality based performance assessment, diagnosis and optimal selection of non-linear filtering strategy for state estimation in Model 8.3.1.

8.5   PCRLB inequality approximation

The PCRLB inequality based tools developed in Section 8.4 allow for performance assessment, diagnosis and optimal selection of a filtering strategy for state estimation in Model 8.3.1; however, obtaining a closed form solution to (8.6) is a non-trivial problem. This is because the complex, multi-dimensional integrals in the PCRLB and MSE cannot be solved analytically. The use of numerical methods to compute (8.6) is discussed next.

8.5.1   Perfect MC sampling based approximation

The idea of perfect MC sampling is to numerically solve complex, multi-dimensional integrals of the form $S_t = \mathbb{E}_{p(X_{0:t}, Y_{1:t})} [h_t(X_{0:t}, Y_{1:t})]$, where $h_t : \mathcal{X}^{t+1} \times \mathcal{Y}^t \to \mathbb{R}$. Using M i.i.d. random trajectories $\{X_{1:t}^{\star j}, Y_{1:t}^j\}_{j=1}^M \sim p(x_{0:t}, y_{1:t})$ distributed according to $p(x_{0:t}, y_{1:t})$, the distribution $p(x_{0:t}, y_{1:t})dx_{0:t}dy_{1:t} \triangleq p(dx_{0:t}, dy_{1:t})$ can be approximated as

$$\tilde{p}(dx_{0:t}, dy_{1:t}) = \frac{1}{M} \sum_{j=1}^M \delta_{X_{0:t}^{\star j}, Y_{1:t}^j}(dx_{0:t}, dy_{1:t}), \tag{8.25}$$

where $\tilde{p}(dx_{0:t}, dy_{1:t})$ is an MC approximation of $p(dx_{0:t}, dy_{1:t})$ and $\delta_{X_0}(dx)$ is the Dirac delta mass located at random sample X_0. Using (8.25), a MC estimate of S_t is given by

$$\tilde{S}_t = \int_{\mathcal{X}^{t+1}} \int_{\mathcal{Y}^t} h_t(x_{0:t}, y_{1:t})\tilde{p}(dx_{0:t}, dy_{1:t}), \tag{8.26a}$$

$$= \frac{1}{M} \sum_{j=1}^M h_t(X_{0:t}^{\star j}, Y_{1:t}^j), \tag{8.26b}$$

where $\tilde{S}_t$ is a MC estimate of S_t. Since (8.26b) is based on a perfect MC sampling, using the strong law of large numbers (SLLN), asymptotic convergence results, such as $\tilde{S}_t \xrightarrow{a.s.} S_t$, as $M \to +\infty$, where $\xrightarrow{a.s.}$ denotes almost sure convergence can be established. The procedure to approximate the PCRLB inequality using a MC method is given next.

Result 8.5.1. *Simulating M i.i.d. sample paths $\{X_{0:t}^{\star j}, Y_{1:t}^j\}_{j=1}^M \sim p(x_{0:t}, y_{1:t})$ using Model 8.3.1, starting at M i.i.d. initial positions $\{X_0^j\}_{j=1}^M \sim p(x_0)$ and computing the state*

estimates $\{\widehat{X}^j_{t|t}\}^M_{j=1}$, *the MSE of a non-linear filter at* $t \in \mathbb{N}$ *can be approximated as*

$$\tilde{P}_{t|t} = \frac{1}{M} \sum_{j=1}^M (X^{\star j}_t - \widehat{X}^j_{t|t})(X^{\star j}_t - \widehat{X}^j_{t|t})^T, \tag{8.27}$$

where $\tilde{P}_{t|t}$ *is a MC estimate of* $P_{t|t}$ *based on* M *simulations.*

Proof. Substituting (8.25) into the definition of MSE given in Lemma 8.4.1 yields (8.27), which completes the proof. □

Result 8.5.2. *Simulating* M *i.i.d. sample paths* $\{X^{\star j}_{0:t}, Y^j_{1:t}\}^M_{j=1} \sim p(x_{0:t}, y_{1:t})$ *using Model 8.3.2, starting at* M *i.i.d. initial positions* $\{X^j_0\}^M_{j=1} \sim p(x_0)$, *an MC estimate of (8.10a) through (8.10c) in Result 8.4.6 is given as follows:*

$$\tilde{D}^{11}_t = \frac{1}{M} \sum_{j=1}^M [\nabla_{X^{\star j}_t} f^T_t(X^{\star j}_t)] Q^{-1}_t [\nabla_{X_t} f^T_t(X^{\star j}_t)]^T; \tag{8.28a}$$

$$\tilde{D}^{12}_t = \frac{1}{M} \sum_{j=1}^M -[\nabla_{X_t} f^T_t(X^{\star j}_t)] Q^{-1}_t; \tag{8.28b}$$

$$\tilde{D}^{22}_t = \frac{1}{M} \sum_{j=1}^M [\nabla_{X_{t+1}} g^T_t(X^{\star j}_{t+1})] R^{-1}_{t+1} [\nabla_{X_{t+1}} g^T_{t+1}(X^{\star j}_{t+1})]^T + Q^{-1}_t, \tag{8.28c}$$

where $\tilde{D}_t$ *is a MC estimate of* D_t.

Proof. Substituting (8.25) into (8.10) yields (8.28), which completes the proof. □

Substituting (8.28) into (8.8), a MC estimate of the PFIM J_{t+1} at $t \in \mathbb{N}$ can be obtained.

Remark 8.5.3. *Though convergence results, such as* $\tilde{P}_{t|t} \xrightarrow{a.s.} P_{t|t}$ *and* $\tilde{J}_{t+1} \xrightarrow{a.s.} J_{t+1}$ *can be established as* $M \to \infty$, *the approximation in Results 8.5.1 and 8.5.2 require an ensemble of the true states and measurements. While measurements may be available from the historical process data, the true states may not be available, except in simulations or in carefully conducted experiments. Thus, no practical numerical method should use true states in the computation of the PCRLB inequality.*

An SMC based PCRLB inequality is discussed next.

8.5.2   SMC based approximation

The central idea to use SMC based methods in approximating the PCRLB inequality in Lemma 8.4.1 is to allow use of available measurements. To do this, the expectations in the MSE and PFIM are reformulated and written as given next.

Proposition 8.5.4. *The complex, multi-dimensional expectations in (8.9), with respect to the density $p(x_{0:t+1}, y_{1:t+1})$ can be reformulated, and written as follows:*

$$I_t^{11} = \mathbb{E}_{p(X_{0:t+1}|Y_{1:t+1})}[-\Delta_{X_t}^{X_t} \log\ p(X_{t+1}|X_t)]; \tag{8.29a}$$

$$I_t^{12} = \mathbb{E}_{p(X_{0:t+1}|Y_{1:t+1})}[-\Delta_{X_t}^{X_{t+1}} \log\ p(X_{t+1}|X_t)]; \tag{8.29b}$$

$$I_t^{22,a} = \mathbb{E}_{p(X_{0:t+1}|Y_{1:t+1})}[-\Delta_{X_{t+1}}^{X_{t+1}} \log\ p(X_{t+1}|X_t)]; \tag{8.29c}$$

$$I_t^{22,b} = \mathbb{E}_{p(X_{0:t+1}|Y_{1:t+1})}[-\Delta_{X_{t+1}}^{X_{t+1}} \log\ p(Y_{t+1}|X_{t+1})], \tag{8.29d}$$

such that:

$$D_t^{11} = \mathbb{E}_{p(Y_{1:t+1})}[I_t^{11}]; \tag{8.29e}$$

$$D_t^{12} = \mathbb{E}_{p(Y_{1:t+1})}[I_t^{12}]; \tag{8.29f}$$

$$D_t^{22} = \mathbb{E}_{p(Y_{1:t+1})}[I_t^{22,a} + I_t^{22,b}]. \tag{8.29g}$$

Also, the expectation in the MSE in (8.6) can be written as

$$P_{t|t} = \mathbb{E}_{p(Y_{1:t})}\mathbb{E}_{p(X_{0:t}|Y_{1:t})}[(X_t - \widehat{X}_{t|t})(X_t - \widehat{X}_{t|t})^T]. \tag{8.30}$$

Proof. Rewriting   the   integrals   using   the   probability   condition $p(x_{0:t+1}, y_{1:t+1}) = p(y_{1:t+1})p(x_{0:t+1}|y_{1:t+1})$ yields the result.   □

Remark 8.5.5. *The integrals in (8.29) and (8.30) are with respect to $p(y_{1:t+1})$ and $p(x_{0:t+1}|y_{1:t+1})$.   The advantage of this representation is evident: using historical data, the integrals with respect to $p(y_{1:t+1})$ can be approximated using a perfect MC method discussed in Section 8.5.1, while integrals with respect to $p(x_{0:t+1}|y_{1:t+1})$ can be approximated using an SMC method.*

It is not our aim here to review SMC methods in detail, but to highlight their role in approximating the PCRLB inequality. For a detailed exposition, see (Doucet *et al.*, 2001; Arulampalam *et al.*, 2002), for example. The essential idea behind SMC methods is to generate a set of random particles and their weights from the target pdf, with respect to which integrals are defined. The target pdf in (8.29) and (8.30) is $p(x_{0:t}|y_{1:t})$. Using SMC methods $p(x_{0:t+1}|y_{1:t+1})dx_{0:t+1} \triangleq p(dx_{0:t+1}|y_{1:t+1})$ can be approximated as

$$\tilde{p}(dx_{0:t+1}|y_{1:t+1}) = \sum_{i=1}^{N} W_{0:t+1|t+1}^{i} \delta_{X_{0:t+1|t+1}^{i}}(dx_{0:t+1}), \tag{8.31}$$

where: $\tilde{p}(dx_{0:t+1}|y_{1:t+1})$ is an approximation of $p(dx_{0:t+1}|y_{1:t+1})$ and $\{X_{0:t+1}^{i};\ W_{0:t+1|t+1}^{i}\}_{i=1}^{N}$ are the N pairs of particle realizations and their associated weights distributed according to $p(x_{0:t+1}|y_{1:t+1})$, such that $\sum_{i=1}^{N} W_{0:t+1|t+1}^{i} = 1$. Using (8.31), an SMC approximation of (8.29a), for example, is given as

$$\tilde{I}_t^{11} = \sum_{i=1}^{N} W_{0:t+1|t+1}^{i}[-\Delta_{X_t}^{X_t} \log\ p(X_{t+1|t+1}^{i}|X_{t|t+1}^{i})], \tag{8.32}$$

where $\tilde{I}_t^{11}$ is an SMC estimate of I_t^{11}, with the Laplacian evaluated at the random particle $\{X_{t:t+1|t+1}^{i}\}_{i=1}^{N}$.

Convergence of (8.32) to (8.29a) depends on the numerical quality of the estimate in (8.31). Many sharp results on convergence of SMC methods are available (see (Crisan and Doucet, 2002) for a survey paper and (Moral, 2004) for a book length review). A selection of these results highlighting the difficulties in approximating $p(dx_{0:t}|y_{1:t})$ in (8.31) with an SMC method are presented below.

Theorem 8.5.6. *For any bounded test function $\phi_t : \mathcal{X}^{t+1} \to \mathbb{R}$, there exists $C_{t,p} < \infty$, such that for any $p > 0$, $N \geq 1$ and $t \geq 1$, the following inequality holds*

$$\mathbb{E}\left[\left|\int_{\mathcal{X}^{t+1}} \phi_t(x_{0:t})\epsilon_t(dx_{0:t}|y_{1:t})\right|^p\right]^{\frac{1}{p}} \leq \frac{C_{t,p}\bar{\phi}_t}{N^{1/2}}, \tag{8.33}$$

where $\epsilon_t(dx_{0:t}|y_{1:t}) = \tilde{p}(dx_{0:t}|y_{1:t}) - p(dx_{0:t}|y_{1:t})$ is the approximation error, $\bar{\phi}_t = \sup_{x_{0:t} \in \mathcal{X}^{t+1}} |\phi_t(x_{0:t})|$, and the expectation is with respect to the particle realizations.

Proof. See Theorem 2 in (Moral and Doucet, 2003) for a detailed proof. □

The result in Theorem 8.5.6 is weak, since $C_{t,p}$ being a function of t, grows exponentially or polynomially with time (Kantas *et al.*, 2009). Hence to guarantee a fixed precision of (8.31), N has to increase with t. The result in (8.33) is not surprising, since the approximation in (8.31) requires sampling from the pdf $p(x_{0:t}|y_{1:t})$, whose dimension increases as $n(t+1)$. It is referred to as the path degeneracy problem. This is a fundamental limitation of the SMC method; wherein, for a fixed N, the quality of the approximation of $p(dx_{0:t}|y_{1:t})$ deteriorates with time.

Remark 8.5.7. *The motivation to use SMC methods to approximate the integrals in (8.29) and (8.30) is based on the fact that encouraging results can be obtained under the exponential forgetting assumption on Model 8.3.1. Since $\theta \in \Theta$ is known (see Assumption 8.3.4), the forgetting property in Model 8.3.1 holds.*

For Model 8.3.1, it is possible to establish the following result.

Theorem 8.5.8. *For an integer $L > 0$, and any bounded test function $\phi_L : \mathcal{X}^L \to \mathbb{R}$, there exists $D_{L,p} < \infty$, such that for any $p > 0$, $N \geq 1$ and $t \geq 1$, the following inequality holds*

$$\mathbb{E}\left[\left|\left|\int_{\mathcal{X}^L} \phi_L(x_{t-L+1:t})\epsilon_L(dx_{t-L+1:t}|y_{1:t})\right|\right|^p\right]^{\frac{1}{p}} \leq \frac{D_{L,p}\bar{\phi}_L}{N^{1/2}}, \tag{8.34}$$

where $\epsilon_L(dx_{t-L+1:t}|y_{1:t}) = \int_{\mathcal{X}^{t-L+1}} \epsilon_t(dx_{0:t}|y_{1:t})$.

Proof. See Theorem 2 in (Moral and Doucet, 2003) for a detailed proof. □

Remark 8.5.9. *Since $D_{L,p}$ is independent of $t \in \mathbb{N}$, Theorem 8.5.8 suggests that an SMC based approximation of the most recent marginal posterior pdf $p(x_{t-L+1:t}|y_{1:t})$, over a fixed horizon $L > 0$ does not result in the error accumulation (Kantas* et al., *2009).*

To make the SMC based PCRLB approximation effective, the dimension of the integrals in Proposition 8.5.4 needs to be reduced. An SMC based approximation of the PCRLB over a reduced dimensional state-space is discussed next.

8.5.2.1   SMC based PCRLB approximation

In this section we present an SMC based approximation of the PFIM and the PCRLB for Model 8.3.1. The developments of this section have been reported by the authors in two earlier publications (Tulsyan *et al.*, 2013*a*; Tulsyan *et al.*, 2012). The results are presented here for the sake of completeness and are important for the development of the later sections. Reduction of the complex, multi-dimensional integrals in (8.29) to a lower dimension is given next.

Lemma 8.5.10. *For a system represented by Model 8.3.1, using Markov property of the state process in (8.2), the complex, multi-dimensional integrals in (8.29) can be written as:*

$$I_t^{11} = \mathbb{E}_{p(X_{t:t+1}|Y_{1:t+1})}[-\Delta_{X_t}^{X_t} \log p(X_{t+1}|X_t)]; \tag{8.35a}$$

$$I_t^{12} = \mathbb{E}_{p(X_{t:t+1}|Y_{1:t+1})}[-\Delta_{X_t}^{X_{t+1}} \log p(X_{t+1}|X_t)]; \tag{8.35b}$$

$$I_t^{22,a} = \mathbb{E}_{p(X_{t:t+1}|Y_{1:t+1})}[-\Delta_{X_{t+1}}^{X_{t+1}} \log p(X_{t+1}|X_t)]; \tag{8.35c}$$

$$I_t^{22,b} = \mathbb{E}_{p(X_{t+1}|Y_{1:t+1})}[-\Delta_{X_{t+1}}^{X_{t+1}} \log p(Y_{t+1}|X_{t+1})]. \tag{8.35d}$$

Proof. The proof uses the definition of expectation and Markov property of Model 8.3.1. See (Tulsyan *et al.*, 2013*a*) for a detailed proof. □

Remark 8.5.11. *Note that the dimension of the expectation in (8.29a) through (8.29c) reduces from $n(t + 2)$ to $2n$; whereas, in (8.29d), it reduces from $n(t + 2)$ to n for all $t \in \mathbb{N}$. Moreover, since expectations in Lemma 8.5.10 are with respect to $p(x_{t:t+1}|y_{1:t+1})$ and $p(x_{t+1}|y_{1:t+1})$, an SMC method can effectively approximate it using finite number of particles (see Theorem 8.5.8).*

Lemma 8.5.12. *The target pdf $p(x_{t:t+1}|y_{1:t+1})$, with respect to which the integrals in Lemma 8.5.10 are defined can be alternatively written as follows*

$$p(x_{t:t+1}|y_{1:t+1}) = \frac{p(x_{t+1}|x_t)p(x_t|y_{1:t})p(x_{t+1}|y_{1:t+1})}{\int_{\mathcal{X}} p(x_{t+1}|x_t)p(dx_t|y_{1:t})}. \tag{8.36}$$

Proof. The proof is based on the use of Bayes' theorem. See (Tulsyan *et al.*, 2013a; Tulsyan *et al.*, 2012) for a detailed derivation. □

Remark 8.5.13. *Generating samples from densities, such as the uniform or Gaussian are well known; however, due to the multi-variate, and non-Gaussian nature of $p(x_{t:t+1}|y_{1:t+1})$, generating random samples from it is non-trivial. An alternative idea is to employ an importance sampling function (ISF) from which random particles are relatively easier to generate (Robert and Casella, 2004).*

The two posteriors in (8.36) are selected as the ISF, such that

$$q(x_{t:t+1}|y_{1:t+1}) \triangleq p(x_t|y_{1:t})p(x_{t+1}|y_{1:t+1}), \tag{8.37}$$

where $q(x_{t:t+1}|y_{1:t+1})$ is a non-negative ISF on $\mathcal{X}^2$, such that $\operatorname{supp} q(x_{t:t+1}|y_{1:t+1}) \supseteq \operatorname{supp} p(x_{t:t+1}|y_{1:t+1})$. Choice of an ISF similar to (8.37) was also employed in (Tanizaki, 2001; Schön *et al.*, 2011) to develop a particle smoothing algorithm for discrete-time non-linear systems. Thus to be able to generate random samples from (8.37), samples from the two posteriors $p(x_t|y_{1:t})$ and $p(x_{t+1}|y_{1:t+1})$ need to be generated first. Again, using the principles of importance sampling, particles from the posterior pdf can be generated using any advanced SMC methods (e.g., ASIR (Pitt and Shephard, 1999), resample-move algorithm (Gilks and Berzuini, 2002), block sampling strategy (Doucet *et al.*, 2006)) or for example, using the method in (Gopaluni, 2008; Schön *et al.*, 2011). The method described in (Gopaluni, 2008; Schön *et al.*, 2011) is outlined in Algorithm 10. It is important to note that in importance sampling, degeneracy is a common problem; wherein, after a few time instances, the density of the weights in (8.38) become skewed. The resampling step in (8.39) is crucial in limiting the effects of degeneracy. Finally, particle approximation of

---

Algorithm 10 SMC based posterior density approximation

Input: Given Model 8.3.1, satisfying Assumptions 8.3.4 through 8.3.7, assume a prior pdf on X_0, such that $X_0 \sim p(x_0)$. Also, select algorithm parameter N.

Output: Recursive SMC approximation of the posterior $p(dx_t|y_{1:t})$ for all $t \in \mathbb{N}$.

1: Generate N independent and identically distributed particles $\{X_{0|-1}^i\}_{i=1}^N \sim p(x_0)$ and set the associated weights to $\{W_{0|-1}^i = N^{-1}\}_{i=1}^N$. Set $t \leftarrow 1$.

2: Sample $\{X_{t|t-1}^i\}_{i=1}^N \sim p(x_t|y_{1:t-1})$.

3: **while** $t \in \mathbb{N}$ **do**

4:    Use $\{Y_t = y_t\}$ and compute $\{W_{t|t}^i\}_{i=1}^N$ using

$$W_{t|t}^i = \frac{p(y_t|X_{t|t-1}^i)}{\sum_{i=1}^N p(y_t|X_{t|t-1}^i)}. \tag{8.38}$$

5:    Resample $\{X_{t|t}^i\}_{j=1}^N$ according to

$$\Pr(X_{t|t}^i = X_{t|t-1}^i) = W_{t|t}^i. \tag{8.39}$$

Set $\{W_{t|t}^i = N^{-1}\}_{i=1}^N$.

6:    Sample $\{X_{t+1|t}^i\}_{i=1}^N \sim p(x_{t+1}|y_{1:t})$.

7:    Set $t \leftarrow t + 1$.

8: **end while**

$p(dx_t|y_{1:t})$ and $p(dx_{t+1}|y_{1:t+1})$ are given by

$$\tilde{p}(dx_t|y_{1:t}) = \frac{1}{N} \sum_{i=1}^N \delta_{X_{t|t}^i}(dx_t); \tag{8.40a}$$

$$\tilde{p}(dx_{t+1}|y_{1:t+1}) = \frac{1}{N} \sum_{j=1}^N \delta_{X_{t+1|t+1}^j}(dx_{t+1}). \tag{8.40b}$$

Here $\{X_{t|t}^i\}_{i=1}^N \sim \tilde{p}(x_t|y_{1:t})$ and $\{X_{t+1|t+1}^i\}_{i=1}^N \sim \tilde{p}(x_{t+1}|y_{1:t+1})$ are the N pairs of resampled i.i.d. samples from $\tilde{p}(x_t|y_{1:t})$ and $\tilde{p}(x_{t+1}|y_{1:t+1})$, respectively. See (Gopaluni, 2008; Schön *et al.*, 2011) for further details.

Remark 8.5.14. *Uniform convergence in time of (8.40) has been established by (Moral, 2004; Chopin, 2004). Although these results rely on strong mixing assumptions of Model 8.3.1, uniform convergence has been observed in numerical studies for a wide class of models, where the mixing assumptions are not satisfied.*

Remark 8.5.15. *The SMC method in Algorithm 10 provides a procedure to generate samples from $p(x_t|y_{1:t})$. Based on this one can argue that any non-linear filter can as well be used in place of the method in Algorithm 10. In (Lei et al., 2011), the authors used EKF and UKF to approximate $p(x_t|y_{1:t})$. Limitations of EKF and UKF based approximations are discussed in Section 8.2. Note that since the PCRLB computation is off-line, use of Algorithm 10 or any advanced SMC methods (e.g., ASIR (Pitt and Shephard, 1999), resample-move algorithm (Gilks and Berzuini, 2002), block sampling strategy (Doucet et al., 2006)) would deliver a numerically more efficient estimate of $p(x_t|y_{1:t})$. Compared to thefilters we are interested in monitoring (e.g., EKF, UKF, EnKF), advanced SMC methods are computationally intensive, and are rarely used for on-line estimation.*

Substituting (8.40) into (8.37) yields

$$\tilde{q}(dx_{t:t+1}|y_{1:t+1}) = \frac{1}{N^2} \sum_{j=1}^{N} \sum_{i=1}^{N} \delta_{X_{t|t}^i, X_{t+1|t+1}^j}(dx_{t:t+1}), \qquad (8.41)$$

where $\tilde{q}(dx_{t:t+1}|y_{1:t+1})$ is an N^2-particle SMC approximation of the ISF distribution $q(dx_{t:t+1}|y_{1:t+1})$ and $\{X_{t|t}^i; \; X_{t+1|t+1}^j\}_{i=1,j=1}^{N,N} \sim \tilde{q}(x_{t:t+1}|y_{1:t+1})$ are particles from the ISF.

Lemma 8.5.16. *An SMC approximation of the target distribution $p(dx_{t:t+1}|y_{1:t+1})$ can be computed using the SMC approximation of $q(dx_{t:t+1}|y_{1:t+1})$ given in (8.41), such that*

$$\tilde{p}(dx_{t:t+1}|y_{1:t+1}) = \sum_{i=1}^{N} W_{t|t,t+1|t+1}^i \delta_{X_{t|t}^i, X_{t+1|t+1}^i}(dx_{t:t+1}), \qquad (8.42)$$

where:

$$W_{t|t,t+1|t+1}^i \triangleq \frac{\zeta_{t|t,t+1|t+1}^i}{\sum_{j=1}^{N} \zeta_{t|t,t+1|t+1}^j}; \qquad (8.43a)$$

$$\zeta_{t|t,t+1|t+1}^i \triangleq \frac{p(X_{t+1|t+1}^i|X_{t|t}^i)}{N \sum_{m=1}^{N} p(X_{t+1|t+1}^i|X_{t|t}^m)}; \qquad (8.43b)$$

and $\tilde{p}(dx_{t:t+1}|y_{1:t+1})$ is an SMC approximation of the target distribution $p(dx_{t:t+1}|y_{1:t+1})$.

Proof. See (Tulsyan *et al.*, 2013a; Tulsyan *et al.*, 2012) for a detailed proof.   □

As in (8.38), the distribution of the weights in (8.43a) becomes skewed after a few time instances. To avoid this, particles in (8.42) are resampled according to the following equality

$$Pr(X_{t:t+1|t+1}^i = \{X_{t|t}^i;\ X_{t+1|t+1}^i\}) = W_{t|t,t+1|t+1}^i, \tag{8.44}$$

where $\{X_{t:t+1|t+1}^i\}_{i=1}^N \sim \tilde{p}(x_{t:t+1}|y_{1:t+1})$ are the N resampled particles. With resampling, (8.42) can be represented as

$$\tilde{p}(dx_{t:t+1}|y_{1:t+1}) = \frac{1}{N} \sum_{i=1}^N \delta_{X_{t:t+1|t+1}^i}(dx_{t:t+1}). \tag{8.45}$$

As discussed in Remark 8.5.5, the integrals in (8.29e) through (8.29g), with respect to the pdf $p(y_{1:t+1})$ can be approximated using a perfect MC sampling method, such that

$$\tilde{p}(dy_{1:t+1}) = \frac{1}{M} \sum_{j=1}^M \delta_{Y_{1:t+1}^j}(dy_{1:t+1}), \tag{8.46}$$

where $\tilde{p}(dy_{1:t+1})$ is an MC approximation of $p(dy_{1:t+1})$, and M is the total number of i.i.d. measurement sequences obtained from the historical test-data.

Remark 8.5.17. *The approximation in (8.46) is possible only under Assumption 8.3.4. In general, the marginalized likelihood function $p(y_{1:t+1})$ does not have a closed form solution, and approximating it using numerical methods is non-trivial (Kantas et al., 2009).*

An SMC approximation of (8.9) is given in the next lemma.

Lemma 8.5.18. *Let $\{Y_{1:t} = y_{1:t}^j\}_{j=1}^M$ be $M \in \mathbb{N}$ i.i.d. measurement sequences generated from Model 8.3.1, satisfying Assumptions 8.3.4 through 8.3.7, then the matrices (8.9a)*

through (8.9c) in Lemma 8.4.2 can be recursively approximated as follows:

$$\tilde{D}_t^{11} = -\frac{1}{MN}\sum_{j=1}^{M}\sum_{i=1}^{N}[\Delta_{X_t}^{X_t}\log\ p(X_{t+1|t+1}^{i,j}|X_{t|t+1}^{i,j})];$$ (8.47a)

$$\tilde{D}_t^{12} = -\frac{1}{MN}\sum_{j=1}^{M}\sum_{i=1}^{N}[\Delta_{X_t}^{X_{t+1}}\log\ p(X_{t+1|t+1}^{i,j}|X_{t|t+1}^{i,j})];$$ (8.47b)

$$\tilde{D}_t^{22} = -\frac{1}{MN}\sum_{j=1}^{M}\sum_{i=1}^{N}[\Delta_{X_{t+1}}^{X_{t+1}}\log\ p(X_{t+1|t+1}^{i,j}|X_{t|t+1}^{i,j}) + \Delta_{X_{t+1}}^{X_{t+1}}\log\ p(Y_{t+1}^{j}|X_{t+1|t+1}^{i,j})];$$

(8.47c)

and $\{X_{t:t+1|t+1}^{i,j}\}_{i=1}^{N}\sim p(x_{t:t+1}|y_{1:t+1}^{j})$ is a set of N resampled particles from (8.45) for all $\{Y_{1:t+1} = y_{1:t+1}^{j}\}_{j=1}^{M}$.

Proof. See (Tulsyan *et al.*, 2013a; Tulsyan *et al.*, 2012) for a detailed proof. □

Now substituting (8.47) into (8.8) yields

$$\tilde{J}_{t+1} = \tilde{D}_t^{22} - [\tilde{D}_t^{12}]^T(\tilde{J}_t + \tilde{D}_t^{11})^{-1}\tilde{D}_t^{12},$$ (8.48)

where $\tilde{J}_{t+1}$ is an SMC approximation of J_{t+1}. Applying the matrix inversion lemma (Horn and Johnson, 1985) in (8.48) yields

$$\tilde{J}_{t+1}^{-1} = [\tilde{D}_t^{22}]^{-1} - [\tilde{D}_t^{22}]^{-1}[\tilde{D}_t^{12}]^T\left[\tilde{D}_t^{12}[\tilde{D}_t^{22}]^{-1}[\tilde{D}_t^{12}]^T - (\tilde{J}_t + \tilde{D}_t^{11})\right]^{-1}\tilde{D}_t^{12}[\tilde{D}_t^{22}]^{-1},$$

(8.49)

where $\tilde{J}_{t+1}^{-1}$ is an SMC approximation of J_{t+1}^{-1}. Finally, (8.49) gives an SMC based solution to compute the theoretical PCRLB in (8.6). Note that the numerical solution in (8.49) is general, and is valid for stochastic processes described by Model 8.3.1.

Lemma 8.5.19. *Let $\{Y_{1:t} = y_{1:t}^{j}\}_{j=1}^{M}$ be $M \in \mathbb{N}$ i.i.d. measurement sequences generated from Model 8.3.2, satisfying Assumptions 8.3.4 through 8.3.7, then the matrices (8.9a)*

through (8.9c) in Lemma 8.4.2 can be recursively approximated as follows:

$$\tilde{D}_t^{11} = \frac{1}{MN} \sum_{j=1}^{M} \sum_{i=1}^{N} [\nabla_{X_t} f_t^T (X_{t|t+1}^{i,j})] Q_t^{-1} [\nabla_{X_t} f_t (X_{t|t+1}^{i,j})]; \tag{8.50a}$$

$$\tilde{D}_t^{12} = \frac{1}{MN} \sum_{j=1}^{M} \sum_{i=1}^{N} -[\nabla_{X_t} f_t^T (X_{t|t+1}^{i,j})] Q_t^{-1}; \tag{8.50b}$$

$$\tilde{D}_t^{22} = Q_t^{-1} + \frac{1}{MN} \sum_{j=1}^{M} \sum_{i=1}^{N} [\nabla_{X_{t+1}} g_{t+1}^T (X_{t+1|t}^{i,j})] R_{t+1}^{-1} [\nabla_{X_{t+1}} g_{t+1}^T (X_{t+1|t}^{i,j})]; \tag{8.50c}$$

and $\{X_{t|t+1}^{i,j}\}_{i=1}^{N} \sim p(x_t|y_{1:t+1}^j)$ and $\{X_{t+1|t}^{i,j}\}_{i=1}^{N} \sim p(x_{t+1}|y_{1:t}^j)$ are sets of N resampled particles from (8.45) and Algorithm 10, respectively, for all $\{Y_{1:t+1} = y_{1:t+1}^j\}_{j=1}^{M}$.

Proof. See (Tulsyan *et al.*, 2013*a*) for the detailed proof of this result. □

An SMC based approximation of the MSE is discussed next.

8.5.2.2   SMC based MSE approximation

An SMC based approximation of the MSE representation in (8.30) and (8.15) is discussed in this section. Note that to evaluate the inner expectation in (8.30), a set of random particles from $p(x_{0:t}|y_{1:t})$ are required. Use of an SMC method to generate random particles from $p(x_{0:t}|y_{1:t})$ is ineffective, as it suffers from the path degeneracy problem (see Theorem 8.5.6). To allow an effective use of SMC methods, (8.30) can be written as

$$P_{t|t} = \mathbb{E}_{p(Y_{1:t})} \mathbb{E}_{p(X_t|Y_{1:t})} [(X_t - \widehat{X}_{t|t})(X_t - \widehat{X}_{t|t})^T]. \tag{8.51}$$

In (8.51), since the integrand is independent of $(x_{0:t-1}) \in \mathcal{X}^t$, it is marginalized out of the integral. Now since the inner expectation in (8.51) is with respect to the density $p(x_t|y_{1:t})$, an SMC method can be readily used (see Theorem 8.5.8). Substituting resampled particles from (8.40a) into (8.51) yields an estimate of the MSE, denoted by $\tilde{P}_{t|t}$, such that

$$\tilde{P}_{t|t} = \mathbb{E}_{p(Y_{1:t})} \left[\frac{1}{N} \sum_{i=1}^{N} (X_{t|t}^i - \widehat{X}_{t|t})(X_{t|t}^i - \widehat{X}_{t|t})^T \right], \tag{8.52}$$

where $\{X_{t|t}^i\}_{i=1}^N \sim p(x_t|y_{1:t})$ is a set of random particles. Note that the state estimate $\widehat{X}_{t|t}$ being a function of $Y_{1:t}$ alone does not have any running index. Now to evaluate (8.52) with respect to $p(dy_{1:t})$, substituting (8.46) into (8.52) yields

$$\tilde{P}_{t|t} = \frac{1}{MN} \sum_{j=1}^M \sum_{i=1}^N (X_{t|t}^{i,j} - \widehat{X}_{t|t}^j)(X_{t|t}^{i,j} - \widehat{X}_{t|t}^j)^T, \tag{8.53}$$

where $\{X_{t|t}^{i,j}\}_{i=1,j=1}^{N,M}$ and $\{\widehat{X}_{t|t}^j\}_{j=1}^M$ are computed using (8.40a) and a non-linear filter, respectively. SMC methods can also be used to approximate the MSE representation in (8.15). To do this, note that the true conditional posterior mean and covariance of $X_t|(Y_{1:t} = y_{1:t}) \sim p(x_t|y_{1:t})$ (see Theorem 8.4.16) need to be approximated first. The next lemma discusses an SMC based approximation of the required moments.

Lemma 8.5.20. *Let $X_{t|t}^\star$ and $V_{t|t}^\star$ be the conditional mean and covariance of $X_t|(Y_{1:t} = y_{1:t}) \sim p(x_t|y_{1:t})$, then using SMC methods, the two moments can be approximated as*

$$\tilde{X}_{t|t}^\star = \frac{1}{N} \sum_{i=1}^N X_{t|t}^i, \tag{8.54a}$$

$$\tilde{V}_{t|t}^\star = \frac{1}{N} \sum_{i=1}^N (X_{t|t}^i - \tilde{X}_{t|t}^\star)(X_{t|t}^i - \tilde{X}_{t|t}^\star)^T, \tag{8.54b}$$

where $\tilde{X}_{t|t}^\star$ and $\tilde{V}_{t|t}^\star$ are the SMC estimates of $X_{t|t}^\star$ and $V_{t|t}^\star$, respectively, and $\{X_{t|t}^i\}_{i=1}^N \sim p(x_t|y_{1:t})$ is a set of N resampled particles generated using (8.40a).

Proof. Substituting (8.40a) into the definition of $X_{t|t}^\star$ yields $\tilde{X}_{t|t}^\star = \int_\mathcal{X} x_t \tilde{p}(dx_t|y_{1:t}) = \frac{1}{N} \sum_{i=1}^N X_{t|t}^i$, and substituting (8.40a) and $\tilde{X}_{t|t}^\star$ into the definition of $V_{t|t}^\star$ yields $\tilde{V}_{t|t}^\star = \int_\mathcal{X} (x_t - \tilde{x}_{t|t}^\star)(x_t - \tilde{x}_{t|t}^\star)^T \tilde{p}(dx_t|y_{1:t}) = \frac{1}{N} \sum_{i=1}^N (X_{t|t}^i - \tilde{X}_{t|t}^\star)(X_{t|t}^i - \tilde{X}_{t|t}^\star)^T.$ $\square$

Corollary 8.5.21. *Let $B_{X_{t|t}}^{\star j}$ and $B_{V_{t|t}}^{\star j}$ be the conditional bias in estimating the mean and covariance of $X_t|(Y_{1:t} = y_{1:t}^j) \sim p(x_t|y_{1:t}^j)$, then an SMC estimate of the MSE in (8.15) is*

$$\tilde{P}_{t|t} = \frac{1}{M} \sum_{j=1}^M \widehat{V}_{t|t}^j + \frac{1}{M} \sum_{j=1}^M \tilde{B}_{V_{t|t}}^{\star j} + \frac{1}{M} \sum_{j=1}^M \tilde{B}_{X_{t|t}}^{\star j} [\tilde{B}_{X_{t|t}}^{\star j}]^T, \tag{8.55}$$

where $\tilde{B}_{X_{t|t}}^{\star j} = [\tilde{X}_{t|t}^{\star j} - \widehat{X}_{t|t}^j]$ and $\tilde{B}_{V_{t|t}}^{\star j} = [\tilde{V}_{t|t}^{\star j} - \widehat{V}_{t|t}^j]$ are an SMC estimate of the conditional bias in estimating the true conditional mean and covariance, respectively.

Proof. Substituting (8.54), (8.46) into (8.15) yields (8.55).   □

Remark 8.5.22. *The SMC estimate of the MSE in (8.55) can also be computed starting from (8.53). As in Theorem 8.4.16, adding and subtracting $\tilde{X}_{t|t}^{\star j}$ in (8.53), and following the steps and arguments presented in Theorem 8.4.16, (8.55) can be obtained.*

8.5.2.3   SMC based assessment, diagnosis and filter switching

The SMC based approximation of the measure in Definition 8.4.8 can be computed using the SMC based PCRLB and MSEcomputed in Sections 8.5.2.1 and 8.5.2.2, respectively. This is done by substituting (8.49) and (8.53) into (8.12), such that

$$\tilde{\Phi}_t = \tilde{J}_t^{-1} \circ \tilde{P}_{t|t}^{\circ -1}, \tag{8.56}$$

where $\tilde{\Phi}_t$ is an SMC based performance measure at $t \in \mathbb{N}$. Similarly, an SMC based non-linear filter diagnosis can be performed by replacing the true bias terms and true MSE in Theorem 8.4.25 with their SMC estimates given in Corollary 8.5.21.

Remark 8.5.23. *Satisfying $\tilde{B}_{V_{t|t}}^\star = 0$ almost surely and $\tilde{B}_{X_{t|t}}^\star = 0$ almost surely may not be possible in practice. For practical purposes, the diagnosis results in Theorem 8.4.25 can be selected based on $|\tilde{B}_{V_{t|t}}^\star| \preccurlyeq \epsilon_1$ and $|\tilde{B}_{X_{t|t}}^\star| \leq \epsilon_2$, where $\epsilon_1 \in \mathcal{S}_+^n$ and $\epsilon_2 \in \mathbb{R}_+^n$ are the user defined threshold values.*

Finally, substituting (8.56) into (8.24), an SMC based filter switching strategy can be represented as follows

$$i_t^\star = \arg\max_{i \in \mathcal{F}} \mathrm{Tr}[\tilde{\Phi}_t^i]. \tag{8.57}$$

SMC based PCRLB inequality algorithm is discussed next.

8.5.3   Final algorithm

Algorithms 11 and 12 give the procedure for computing the SMC based PCRLB inequality for Models 8.3.1 and 8.3.2, respectively, while Algorithm 14 outlines a procedure

to perform SMC based performance assessment, diagnosis, and non-linear state filter selection.

Remark 8.5.24. *M measurement sequences $\{Y_{1:T} = y_{1:T}^j\}_{j=1}^M$ required by Algorithms 11 and 12 are obtained from historical data; however, in simulations, it can be generated by simulating the process model, M times starting at i.i.d. initial states drawn from $p(x_0)$. Note that this procedure also requires simulation of the true states; however, is not used in any form to develop the SMC based PCRLB inequality approximation procedure discussed in Algorithms 11 and 12.*

For illustrative purposes, to assess the numerical quality of Algorithms 11 and 12, the following two measures are defined

$$\Lambda_J = \frac{1}{T} \sum_{t=1}^{T} \mathrm{Tr} \left[[J_t^{-1} - \tilde{J}_t^{-1}] \circ [J_t^{-1}]^{\circ -1} \right], \tag{8.58a}$$

$$\Lambda_P = \frac{1}{T} \sum_{t=1}^{T} \mathrm{Tr} \left[[P_{t|t} - \tilde{P}_{t|t}] \circ [P_{t|t}^{\circ -1}] \right], \tag{8.58b}$$

where Λ_J and Λ_P are the average sum of relative errors in approximating the PCRLB and MSE, respectively.

8.5.4   Convergence

Computing the PCRLB inequality involves solving complex integrals; however, as stated earlier, for Models 8.3.1 and 8.3.2 the PCRLB and MSE cannot be solved in closed form. Algorithms 11 and 12 gives a N particle and M simulation based SMC approximation of the PCRLB and MSE for Models 8.3.1 and 8.3.2, respectively. It is therefore natural to question the convergence properties of the proposed numerical method. In this regard, results such as Theorem 8.5.8 and Remark 8.5.14 are important as it ensures that the proposed numerical solution does not result in accumulation of errors. It is emphasized that although Theorem 8.5.8 and Remark 8.5.14 not necessarily imply convergence of the

---

Algorithm 11 SMC based PCRLB and MSE approximation for Model 8.3.1

Module 1: SMC based PCRLB approximation for Model 8.3.1

Input: Given Model 8.3.1, satisfying Assumptions 8.3.4 through 8.3.7, assume a prior pdf on X_0, such that $X_0 \sim p(x_0)$. Also, select algorithm parameters- T, N and M.

Output: SMC approximation of the PCRLB for Model 8.3.1.

1: Generate and store M i.i.d. sequences $\{Y_{1:T}^j\}_{j=1}^M \sim p(y_{1:T})$ of length T, by simulating Model 8.3.1, M times starting at M i.i.d. initial states $\{X_{0|-1}^i\}_{j=1}^M \sim p(x_0)$.

2: **for** $j = 1$ to M **do**

3:      **for** $t = 1$ to T **do**

4:          Store resampled particles $\{X_{t|t}^{i,j}\}_{i=1}^N \sim p(x_t|y_{1:t}^j)$ using (8.40a).

5:          Store resampled particles $\{X_{t-1:t|t}^{i,j}\}_{i=1}^N \sim p(x_{t-1:t}|y_{1:t}^j)$ using (8.45).

6:          Store the true conditional mean $\tilde{X}_{t|t}^{\star j}$ using (8.54a).

7:          Store the true conditional covariance $\tilde{V}_{t|t}^{\star j}$ using (8.54b).

8:      **end for**

9: **end for**

10: Compute PFIM J_0 at $t = 0$ based on the initial target state pdf $X_0 \sim p(x_0)$. If $X_0 \sim \mathcal{N}(x_0|C_{x_0}, P_{0|0})$ then from Lemma 8.4.2, $J_0 = P_{0|0}^{-1}$.

11: **for** $t = 0$ to $T - 1$ **do**

12:      Compute an SMC estimate (8.47a) through (8.47c) in Lemma 8.5.18.

13:      Compute PCRLB $\tilde{J}_{t+1}^{-1}$ by substituting (8.47a) through (8.47c) into (8.49).

14: **end for**

Module 2: SMC based MSE approximation for Model 8.3.1

Input: A non-linear filter for state estimation in Model 8.3.1.

Output: SMC approximation of the MSE for the non-linear filter.

15: **for** $j = 1$ to M **do**

16:      **for** $t = 1$ to T **do**

17:          Store the conditional mean estimate $\widehat{X}_{t|t}^j$.

18:          Store the conditional covariance estimate $\widehat{V}_{t|t}^j$.

19:          Store the bias in conditional mean estimate $\tilde{B}_{X_{t|t}}^{\star j}$.

20:          Store the bias in conditional covariance estimate $\tilde{B}_{V_{t|t}}^{\star j}$.

21:      **end for**

22: **end for**

23: Compute MSE $P_{0|0}$ at $t = 0$ based on the initial target state pdf $X_0 \sim p(x_0)$. If $X_0 \sim \mathcal{N}(x_0|C_{x_0}, P_{0|0})$ then $P_{0|0}$ is the covariance of X_0.

24: **for** $t = 1$ to T **do**

25:      Compute MSE estimate $\tilde{P}_{t|t}$ using (8.53).

26: **end for**

---

approximate PCRLB and MSE to its theoretical values, nevertheless, it provides a strong theoretical basis for the numerous approximations used in Algorithms 11 and 12.

Algorithm 12 SMC based PCRLB and MSE approximation for Model 8.3.2

Module 1: SMC based PCRLB approximation for Model 8.3.2

Input: Given Model 8.3.2, satisfying Assumptions 8.3.4 through 8.3.7, assume a prior pdf on X_0, such that $X_0 \sim p(x_0)$. Also, select algorithm parameters- T, N and M.

Output: SMC approximation of the PCRLB for Model 8.3.2.

1: Generate and store M i.i.d. sequences $\{Y_{1:T}^j\}_{j=1}^M \sim p(y_{1:T})$ of length T, by simulating Model 8.3.1, M times starting at M i.i.d. initial states $\{X_{0|-1}^i\}_{j=1}^M \sim p(x_0)$.

2: **for** $j = 1$ to M **do**

3:     **for** $t = 1$ to T **do**

4:         Store predicted particles $\{X_{t|t-1}^{i,j}\}_{i=1}^N \sim p(x_t|y_{1:t-1}^j)$ using Algorithm 10.

5:         Store resampled particles $\{X_{t|t}^{i,j}\}_{i=1}^N \sim p(x_t|y_{1:t}^j)$ using (8.40a).

6:         Store resampled particles $\{X_{t-1:t|t}^{i,j}\}_{i=1}^N \sim p(x_{t-1:t}|y_{1:t}^j)$ using (8.45).

7:         Store the true conditional mean $\tilde{X}_{t|t}^{\star j}$ using (8.54a).

8:         Store the true conditional covariance $\tilde{V}_{t|t}^{\star j}$ using (8.54b).

9:     **end for**

10: **end for**

11: Compute PFIM J_0 at $t = 0$ based on the initial target state pdf $X_0 \sim p(x_0)$. If $X_0 \sim \mathcal{N}(x_0|C_{x_0}, P_{0|0})$ then from Lemma 8.4.2, $J_0 = P_{0|0}^{-1}$.

12: **for** $t = 0$ to $T - 1$ **do**

13:     Compute an SMC estimate (8.50a) through (8.50c) in Result 8.5.19.

14:     Compute PCRLB $\tilde{J}_{t+1}^{-1}$ by substituting (8.50a) through (8.50c) into (8.49).

15: **end for**

Module 2: SMC based MSE approximation for Model 8.3.2

Input: A non-linear filter for state estimation in Model 8.3.2.

Output: SMC approximation of the MSE for the non-linear filter.

16: **for** $j = 1$ to M **do**

17:     **for** $t = 1$ to T **do**

18:         Store the conditional mean estimate $\widehat{X}_{t|t}^j$.

19:         Store the conditional covariance estimate $\widehat{V}_{t|t}^j$.

20:         Store the bias in conditional mean estimate $\tilde{B}_{X_{t|t}}^{\star j}$.

21:         Store the bias in conditional covariance estimate $\tilde{B}_{V_{t|t}}^{\star j}$.

22:     **end for**

23: **end for**

24: Compute MSE $P_{0|0}$ at $t = 0$ based on the initial target state pdf $X_0 \sim p(x_0)$. If $X_0 \sim \mathcal{N}(x_0|C_{x_0}, P_{0|0})$ then $P_{0|0}$ is the covariance of X_0.

25: **for** $t = 1$ to T **do**

26:     Compute MSE estimate $\tilde{P}_{t|t}$ using (8.53).

27: **end for**

Algorithm 13 SMC based performance assessment, diagnosis and non-linear filter selection

---

    Input: Given Model 8.3.1 or 8.3.2, satisfying Assumptions 8.3.4 through 8.3.7, assume a prior $X_0 \sim p(x_0)$. Select an operating trajectory, and a bank with $\mathcal{F} = \{1, 2, \ldots, F\}$ non-linear state filters. Also, select algorithm parameters- T, N and M.

    Output: An optimal non-linear state estimation strategy for Model 8.3.1 or 8.3.2.

        Module 1: Performance assessment of non-linear state filters

1: **for** $t = 1$ to T **do**
2:    Compute $\tilde{J}_t$ using Module 1 of Algorithms 11 or 12.
3: **end for**
4: **for** $i = 1$ to F **do**
5:    **for** $t = 1$ to T **do**
6:       Compute $\tilde{P}_{t|t}$ for filter $i \in \mathcal{F}$ using Module 2 of Algorithms 11 or 12.
7:       Compute $\tilde{\Phi}_t$ for filter $i \in \mathcal{F}$ using (8.56).
8:    **end for**
9: **end for**

        Module 2: Performance diagnosis and redesign of non-linear state filters

10: **while** (performance is unsatisfactory) **do**
11:    **for** $i = 1$ to F **do**
12:       **for** $t = 1$ to T **do**
13:          **for** $j = 1$ to M **do**
14:             Compute $\tilde{B}^{\star j}_{X_{t|t}}$ and $\tilde{B}^{\star j}_{V_{t|t}}$ for filter $i \in \mathcal{F}$ using Corollary 8.5.21.
15:          **end for**
16:          Use Theorem 8.4.25 to perform non-linear filter diagnosis.
17:       **end for**
18:    **end for**
19:    Redesign non-linear filters and update the filter bank $\mathcal{B}$.
20:    **for** $i = 1$ to F **do**
21:       **for** $t = 1$ to T **do**
22:          Compute $\tilde{P}_{t|t}$ for filter $i \in \mathcal{F}$ using Module 2 of Algorithms 11 or 12.
23:          Compute $\tilde{\Phi}_t$ for filter $i \in \mathcal{F}$ using (8.56).
24:       **end for**
25:    **end for**
26: **end while**

        Module 3: Non-linear filtering strategy for state estimation

27: **for** $t = 1$ to T **do**
28:    Compute the non-linear filter switching strategy using (8.57).
29: **end for**

From an application perspective, it is instructive to highlight that the numerical quality of the SMC based PCRLB inequality in Algorithms 11 and 12 can be made accurate by

simply increasing the number of particles (N) and the MC simulations (M). The choice of N and M are user defined, which can be selected based on the required numerical accuracy, and available computing speed. It is important to emphasize that due to the multiple approximations involved in deriving a tractable solution, for practical purposes, with a finite N and M, the condition $\tilde{P}_{t|t} - \tilde{J}_t^{-1} \succcurlyeq 0$ is not guaranteed to hold for all $t \in \mathbb{N}$.

8.6   Numerical illustration

In this section, we present a simulation example to demonstrate the utility of the PCRLB inequality based filter assessment and diagnosis tools in devising an optimal filtering strategy for state estimation in non-linear systems. Consider a process described by a discrete-time, uni-variate, and non-stationary SSM (Tulsyan *et al.*, 2013*b*)

$$X_{t+1} = \frac{X_t}{2} + \frac{X_t}{1 + X_t^2} u_t + 8\cos(1.2t) + V_t, \tag{8.59a}$$

$$Y_t = \frac{X_t^2}{20} + W_t, \tag{8.59b}$$

where: $V_t \in \mathbb{R}$ and $W_t \in \mathbb{R}$ are mutually independent sequences of independent random variables following a Gaussian distribution, such that $V_t \sim \mathcal{N}(v_t|0, Q_t)$ and $W_t \sim \mathcal{N}(w_t|0, R_t)$; X_0 is the initial state, which follows an independent Gaussian distribution, such that $X_0 \sim \mathcal{N}(x_0|0, 0.5)$; and $u_t \in \mathbb{R}$ is the scheduling variable, such that $u_t \in \mathcal{U} \ \forall t \in [0, T]$, where $\mathcal{U} = \{0, \ 25, \ 35\}$ and $T = 19$ seconds.

Remark 8.6.1. *In general, as long as a process variable exerts significant influence on the process dynamics, it can be treated as a scheduling variable. In (8.59) u_t controls the degree of non-linearity in the state process. Note that for large values of u_t, the state dynamics in (8.59a) is highly non-linear.*

Remark 8.6.2. *In unit operations, scheduling variables help in operating the process in a certain orderly way, which is normally referred to as the operating trajectory (Xu* et

---

Algorithm 14 SMC based performance assessment, diagnosis and non-linear filter selection

---

Input: Given Model 8.3.1 or 8.3.2, satisfying Assumptions 8.3.4 through 8.3.7, assume a prior $X_0 \sim p(x_0)$. Select an operating trajectory, and a bank $\mathcal{B}$ with F non-linear state filters. Also, select algorithm parameters- T, N and M.
Output: State estimation strategy for Model 8.3.1 or 8.3.2.

Module 1: Performance assessment

1: **for** $t = 1$ to T **do**
2:    Compute $\tilde{J}_t$ using Algorithms 11 or 12.
3: **end for**
4: **for** $i = 1$ to F **do**
5:    **for** $t = 1$ to T **do**
6:       Compute $\tilde{P}_{t|t}$ for $i \in \mathcal{F}$ using Algorithms 11 or 12.
7:       Compute $\tilde{\Phi}_t^i$ for $i \in \mathcal{F}$ using (8.56).
8:    **end for**
9: **end for**

Module 2: Performance diagnosis and redesign

10: **while** (performance is unsatisfactory) **do**
11:    **for** $i = 1$ to F **do**
12:       **for** $t = 1$ to T **do**
13:          **for** $j = 1$ to M **do**
14:             Compute $\tilde{B}^{\star j}_{X_{t|t}}$ and $\tilde{B}^{\star j}_{V_{t|t}}$ using Corollary 8.5.21.
15:          **end for**
16:       Use Theorem 8.4.25 to perform diagnosis.
17:       **end for**
18:    **end for**
19:    Redesign filters and update bank $\mathcal{B}$.
20:    **for** $i = 1$ to F **do**
21:       **for** $t = 1$ to T **do**
22:          Compute $\tilde{P}_{t|t}$ for $i \in \mathcal{F}$ using Algorithms 11 or 12.
23:          Compute $\tilde{\Phi}_t$ for $i \in \mathcal{F}$ using (8.56).
24:       **end for**
25:    **end for**
26: **end while**

Module 3: Filtering strategy for state estimation

27: **for** $t = 1$ to T **do**
28:    Compute filter switching map using (8.57).
29: **end for**

---

al., 2009). The operating trajectory is composed of several pre-designed operating points,

through which different production objectives can be met. Examples for the operating

Table 8.1: Average sum of relative errors in approximating the PCRLB for a range of operating conditions and noise variances.

Case	Process noise	Measurement noise	Average sum of relative errors (Λ_J)		
	Q_t	R_t	$u_t = 0$	$u_t = 25$	$u_t = 35$
	$\forall t \in [0, T]$	$\forall t \in [0, T]$	$\forall t \in [0, T]$	$\forall t \in [0, T]$	$\forall t \in [0, T]$
1	0.1	0.1	4.0×10^{-3}	1.9×10^{-2}	1.2×10^{-2}
2	0.1	1.0	6.5×10^{-4}	3.6×10^{-3}	2.9×10^{-3}
3	1.0	0.1	2.9×10^{-2}	7.9×10^{-2}	5.3×10^{-2}
4	1.0	1.0	1.3×10^{-2}	4.2×10^{-2}	3.4×10^{-2}

points, include: different loads of a power plant; and steam quality in a boiler.

The aim of this study is three fold: (i) to evaluate the efficiency of the SMC based PCRLB constructed for (8.59); (ii) to evaluate the efficiency of the SMC method in approximating the MSE for a non-linear filter used in estimating the states in (8.59); and (iii) to demonstrate the utility of the PCRLB inequality based performance assessment and diagnosis tool in devising an optimal filter switching strategy for state estimation in (8.59).

8.6.1   Experiment 1: SMC based PCRLB approximation

In this experiment we: (i) evaluate the efficiency of the proposed SMC method in approximating the PCRLB computed for (8.59); (ii) study the quality of the SMC based PCRLB for a range of operating trajectories and noise variances; and (iii) assess the sensitivity of SMC approximations to the number of MC simulations (M) and particles (N) used. Note that, since (8.59) has the same structure as Model 8.3.2, the true and SMC based PCRLB for (8.59) can be computed using Result 8.5.2 and Algorithm 12, respectively. To compute the PCRLB, we first simulate (8.59) to generate an ensemble of the true state and measurement sequences of size $M = 200$, starting at M i.i.d. initial states drawn from $X_0 \sim \mathcal{N}(x_0|0, 0.5)$. An ensemble of true states is required for computing the true PCRLB (see Remark 8.5.24). To allow full investigation of the SMC based PCRLB, wide range of operating trajectories and noise variances are considered (see Table 8.1).

Figure 8.3 gives the results for $u_t = 25 \ \forall t \in [0, T]$. Figures 8.3(a) and (b) compare
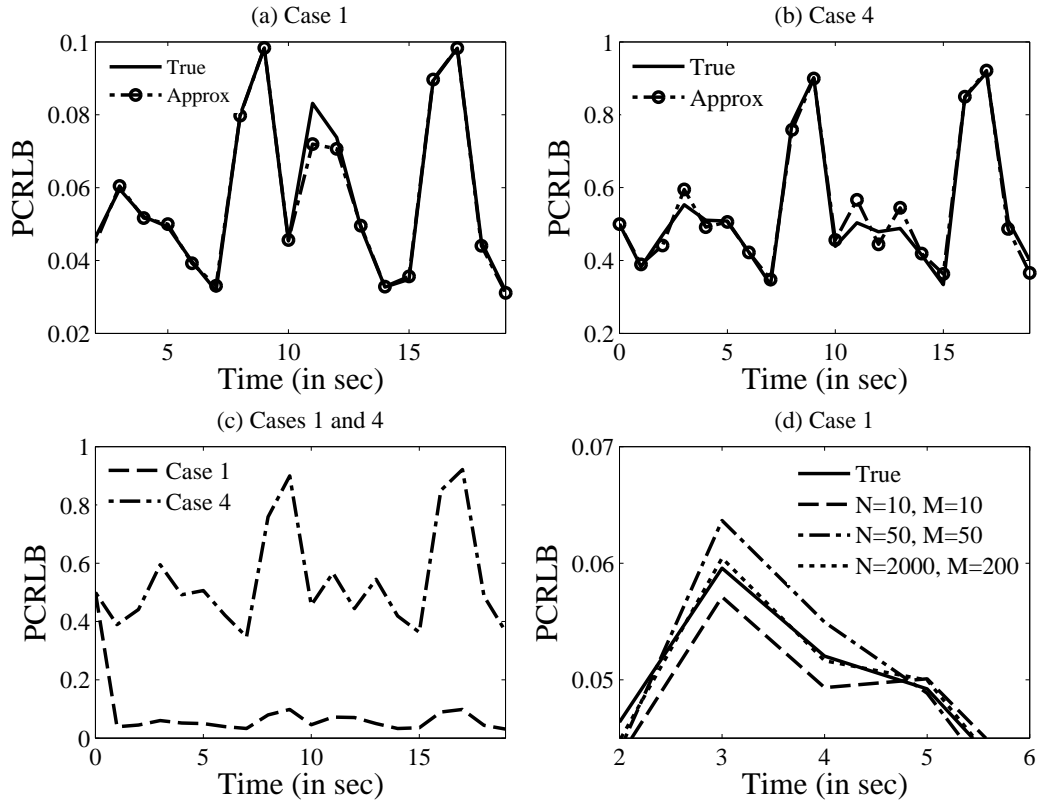
Figure 8.3: (a) and (b) compare the SMC based PCRLB against the true PCRLB for Cases 1 and 4, respectively. Here (a) and (b) are computed based on $N = 2000$ and $M = 200$. (c) juxtaposes the SMC based PCRLBs obtained in (a) and (b) for comparison. (d) compares the true PCRLB for Case 1 against the SMC based PCRLBs obtained with different N and M values. Here (d) has been appropriately scaled up to illustrate the effects of N and M on the SMC based PCRLB. The results are all based on (8.59) operating at $u_t = 25 \, \forall t \in [0, T]$.

the SMC based PCRLB against the true PCRLB for Cases 1 and 4, respectively. The approximate PCRLB solution in Figure 8.3(a) accurately follows the true PCRLB. Even for the increased noise variance case (see Figure 8.3(b)), the SMC based PCRLB is almost exact at all sampling-time instants. The approximate PCRLBs for Cases 1 and 4 are compared in Figure 8.3(c). In Figure 8.3(c), the PCRLB for Case 4 is higher than that for Case 1, suggesting estimation difficulties with larger noise intensity. Note that this claim is further validated in Section 8.6.2. In Figure 8.3(d), the approximate PCRLB bounds for Case 1, with different values of N and M are compared against the true PCRLB. The results are obtained by varying N and M in Algorithm 12. Figure 8.3(d), suggests that by

Table 8.2: Average sum of relative errors in approximating the MSE for a range of operating conditions and noise variances.

Case	Process noise Q_t $\forall t \in [0, T]$	Measurement noise R_t $\forall t \in [0, T]$	Average sum of relative errors (Λ_P)		
			$u_t = 0$ $\forall t \in [0, T]$	$u_t = 25$ $\forall t \in [0, T]$	$u_t = 35$ $\forall t \in [0, T]$
1	0.1	0.1	5.4×10^{-2}	4.3×10^{-2}	2.0×10^{-2}
2	0.1	1.0	3.8×10^{-2}	5.5×10^{-2}	2.3×10^{-2}
3	1.0	0.1	2.6×10^{-2}	5.9×10^{-2}	2.9×10^{-2}
4	1.0	1.0	4.6×10^{-2}	10×10^{-2}	3.8×10^{-2}

simply increasing N and M, which are a tuning parameters in Algorithm 12, the quality of the SMC approximations can be significantly improved. Similar conclusions were drawn for other operating trajectories.

Table 8.1 summarizes the results of this section in term of the average sum of relative errors Λ_J (see (8.58a)). Based on Table 8.1, the Λ_J values for Cases 1 and 2 closely compare across all operating conditions; whereas, for Cases 3 and 4, the Λ_J values are relatively higher, but comparable and bounded. Note that the order of magnitude of Λ_J is approximately 10^{-3}, which demonstrates the numerical reliability of the SMC based PCRLB for a range of operating trajectories and noise variances.

8.6.2   Experiment 2: SMC based MSE approximation

The aim of this study is same as Section 8.6.1, except we focus on approximating the MSE of a non-linear filter. For illustrative purposes, we consider an EKF for state estimation in (8.59). Using the data from Section 8.6.1, the true and SMC based MSE are computed using Result 8.5.1 and Algorithm 12, respectively.

Figure 8.4 gives the results for $u_t = 25 \ \forall t \in [0, T]$. Figure 8.4(a) and (b) compare the SMC based MSE against the true MSE for Cases 1 and 4, respectively. The approximate MSEs of Cases 1 and 4 accurately follow the true MSEs at all filtering time instants. In Figure 8.4(c), relatively higher MSE for Case 4, especially in the intervals $t \in [9, 14]$ and $t \in [17, 18]$ validates the claim made in Section 8.6.1 about estimation difficulties at higher
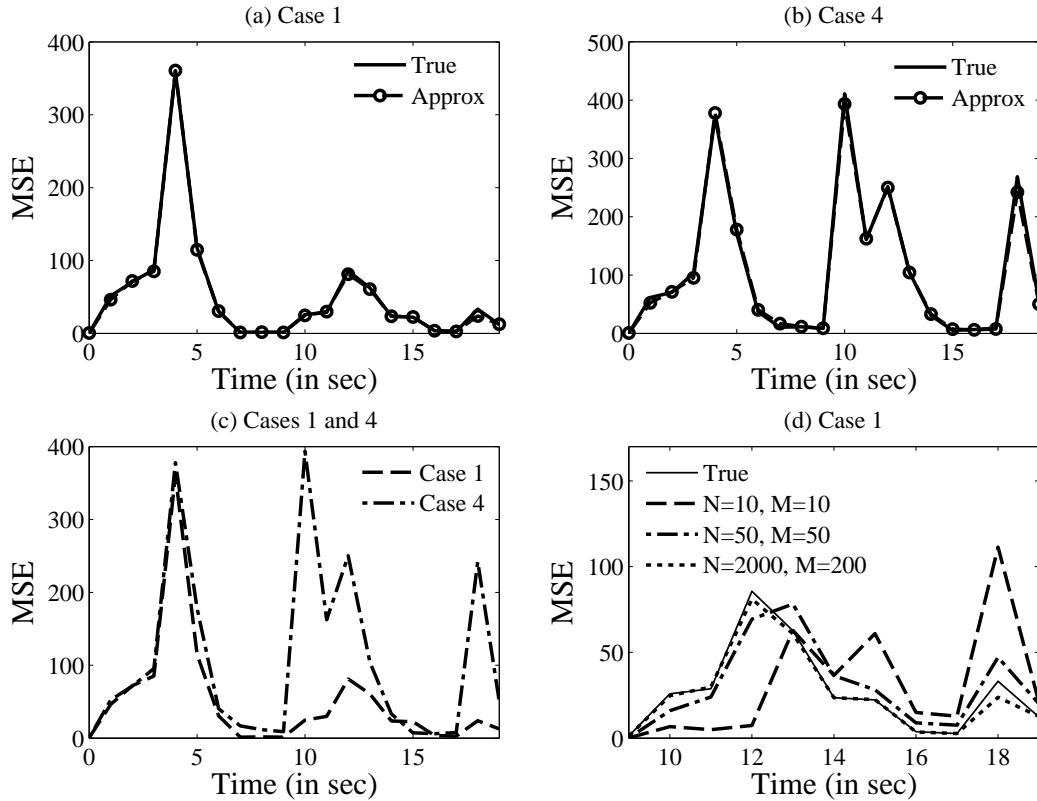
Figure 8.4: (a) and (b) compare the SMC based MSE against the true MSE for Cases 1 and 4, respectively. Here (a) and (b) are computed based on $N = 2000$ and $M = 200$. (c) juxtaposes the SMC based MSEs obtained in (a) and (b) for comparison. (d) compares the true MSE for Case 1 against the SMC based MSEs obtained with different N and M values. Here (d) has been appropriately scaled up to illustrate the effects of N and M on the SMC based MSE. Note that all the MSEs are for the EKF, and are based on (8.59) operating at $u_t = 25 \ \forall t \in [0, T]$.

noise intensities. Figure 8.4(d) shows improvement in the approximations with increase in

N and M. Comparing Figures 8.3(d) and 8.4(d) suggest that the quality of the SMC based

MSE is relatively more sensitive to the choice of N and M.

Table 8.2 summarizes the result of this section in terms of the average sum of relative

errors Λ_P (see (8.58b)). The Λ_P values for Cases 1 though 4 across all operating conditions

are of the order 10^{-2}. A close comparison of Λ_J and Λ_P in Tables 8.1 and 8.2, respectively,

can be explained, since the same particle set is used for approximating the PCRLB and the

MSE (see Algorithm 12). Repeating the experiment with other non-linear filters, such as

UKF, SIR and ASIR yielded similar conclusions.

In summary, the results in Sections 8.6.1 and 8.6.2: (i) suggest that for (8.59), the SMC method is accurate in approximating the true PCRLB inequality for a range of operating trajectories and process and measurement noise variances; and (ii) highlight the importance of carefully tuning N and M for an overall improvement in the quality of the SMC approximations.

8.6.3   Experiment 3: Optimal non-linear filter switching strategy

In this section, we demonstrate the utility of PCRLB inequality based assessment and diagnosis tool in devising an optimal filter switching strategy for state estimation in (8.59). A step-by-step procedure outlined in Algorithm 14 or Figure 8.2 is presented next.

8.6.3.1   Step 1: Selecting an operating trajectory

As discussed in Section 8.4.4, devising an optimal filter switching strategy for a process requires a priori knowledge of the process operating conditions. The aim of this step is to define an operating trajectory for (8.59), such that $u_t \in \mathcal{U}$, where $\mathcal{U} = \{0, \ 25, \ 35\}$ and $t \in [0, T]$. Figure 8.5(a) shows a randomly generated operating trajectory, and Figures 8.5(b) and (c) give an ensemble of i.i.d. measurement sequences generated therefrom. Here, Figure 8.5(b) is the training set, which will be used for assessment, diagnosis and for devising a filter switching strategy; whereas, Figure 8.5(c) is the validation set, which will be used evaluating the quality of the developed filtering strategy. Note that for the operating trajectory given in Figure 8.5(a), (8.59a) is linear in state for $t \in [0, 9]$ and non-linear for $t \in [11, 19]$.

Remark 8.6.3. *Transition from one operating point to another is a common phenomenon in batch processes; wherein, the product grade decides the process dynamics.*
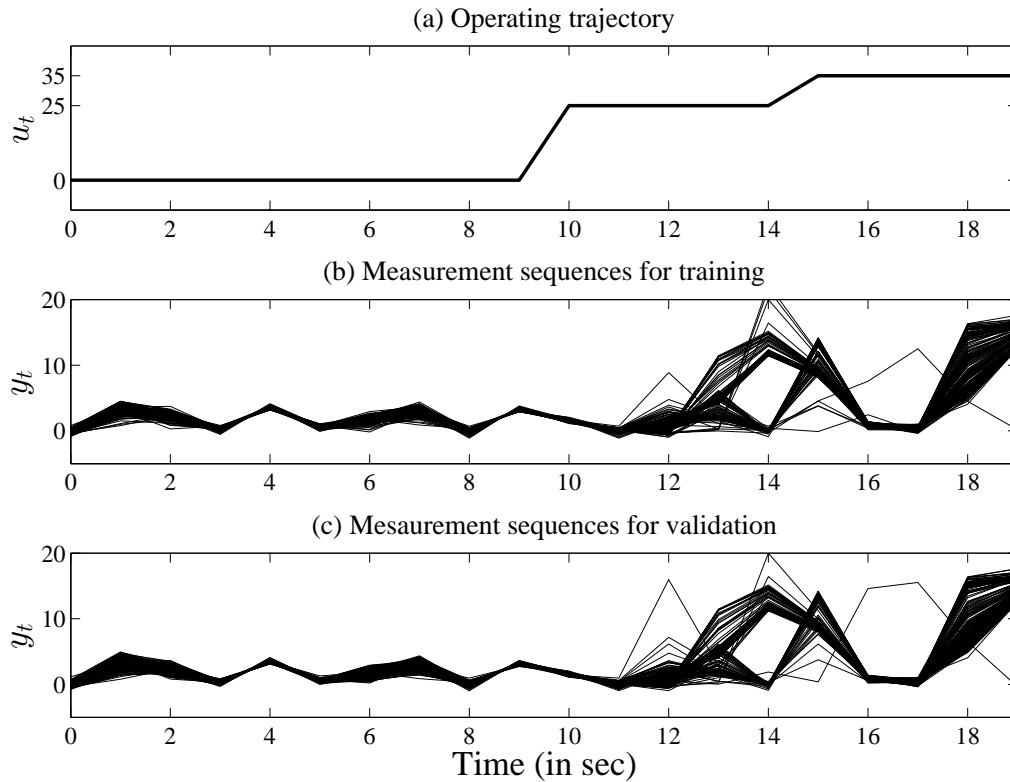
Figure 8.5: (a) shows a randomly generated operation profile for $u_t \, \forall t \in [0, T]$, such that $u_t \in \mathcal{U}$, where $\mathcal{U} = \{0, \ 25, \ 35\}$. (b) and (c) are independently generated $M = 200$ measurement sequences, obtained by simulating the model in (8.59) starting at M i.i.d. initial states drawn from $X_0 \sim \mathcal{N}(x_0|0, 0.05)$ using the operating trajectory in (a). Here, the noise variances are selected as $Q_t = R_t = 0.1 \, \forall t \in [0, T]$. Note that (b) and (c) are the training and validation set, respectively.

8.6.3.2   Step 2: Bank of non-linear filters

The second step in devising an optimal filter switching strategy for the operating trajectory

in Figure 8.5(a) is to select a bank of non-linear filters (see Figure 8.2). To illustrate this

step, we consider a bank $\mathcal{B}$ with four non-linear filters- EKF, UKF, SIR and ASIR. Here,

the EKF and UKF are the standard Kalman based filters; whereas, the SIR and ASIR are

the SMC based filters using an ensemble of 50 particles and a systematic resampling step.

Note that for the sake of brevity, the pseudo-codes for the filters are not provided here, but

can be found in any standard textbook. See (Ristic *et al.*, 2004) for example. All the non-

linear filters in the bank $\mathcal{B}$ are initialized with $X_0 \sim \mathcal{N}(x_0|0, 0.5)$, $V_t \sim \mathcal{N}(v_t|0, Q_t = 0.1)$,
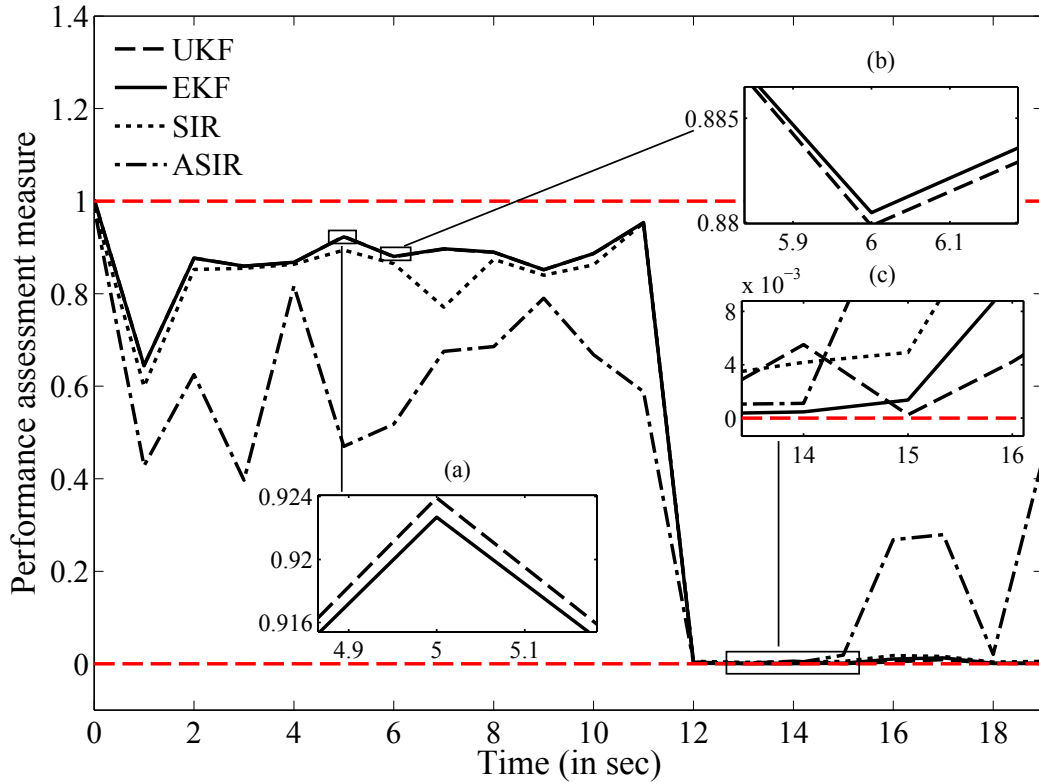
Figure 8.6: The SMC based performance assessment measure, $\tilde{\Phi}_t \; \forall t \in [0, T]$ computed for the filter bank. Here $\tilde{\Phi}_t$ is computed using (8.56). Appropriate magnification of the key regions of the main figure are provided as insets. The broken red horizontal lines are the upper and lower bound for $\tilde{\Phi}_t \; \forall t \in [0, T]$.

and $W_t \sim \mathcal{N}(w_t | 0, R_t = 0.1)$. This allows for a fair assessment of the filters, and ensure there is no process-model mismatch (see Assumption 8.3.4). For all the filters, the state estimate $\widehat{X}_{t|t} \; \forall t \in [0, T]$ is the conditional mean of the approximate posterior density.

8.6.3.3   Step 3: Filter performance assessment

In this step we assess the performance of the non-linear filters, using the PCRLB inequality based assessment measure developed in Section 8.4.1.   Using the ensemble of the measurement sequences from Step 1 (see Figure 8.5(b)), we compute the SMC based PCRLB and the SMC based MSE for all the filters. This step uses a similar procedure as in Sections 8.6.1 and 8.6.2. Figure 8.6 gives the SMC based assessment measure $\tilde{\Phi}_t$ for the filters, computed using Module 1 of Algorithm 14.

Remark 8.6.4. *In Section 8.5.3, it was pointed that due to multiple approximations involved in deriving an SMC based PCRLB inequality, with a finite N, the positive semi definite condition on $\tilde{P}_{t|t} - \tilde{J}_t^{-1}$ is not guaranteed to hold for all $t \in [0, T]$; however, in this numerical simulation, since $\tilde{\Phi}_t \ \forall t \in [0, T]$ values for all the filters are in between 0 and 1 (See Figure 8.6), we can conclude that $\tilde{P}_{t|t} - \tilde{J}_t^{-1} \succcurlyeq 0 \ \forall t \in [0, T]$ for all the filters.*

Comparing $\tilde{\Phi}_t \ \forall t \in [0, T]$ values in Figure 8.6, it is evident that the EKF, UKF and SIR maintain a high performance over the interval $t \in [0, 11]$, but plummets on $t \in [12, 19]$; whereas, the ASIR shows a relatively lower performance on the interval $t \in [0, 14]$, but improves over $t \in [15, 19]$. Note that on the interval $t \in [0, 9]$ (see Figure 8.6), the EKF and UKF outperforms each other at multiple sampling-time points. An instance of this can be seen in the insets (a) and (b) provided in Figure 8.6. Finally, insets (c) in Figure 8.6 shows the low, but competitive performance of all the filters on the interval $t \in [12, 15]$.

In summary, the results of Step 3: (i) establish the numerical reliability of the SMC based PCRLB inequality under multiple operating points; (ii) reaffirm the popular belief that filters perform well in the regions of the state-space, where the dynamics is either linear or can be efficiently linearised; and (ii) highlight the sensitivity of filter performance to the process dynamics, filter approximation and process conditions.

8.6.3.4   Step 4: Filter performance diagnosis

The diagnosis and filter redesign steps in Figure 8.2 are optional; wherein, the decision to perform them is based on the assessment results. From Figure 8.6, it is evident that none of the filters in the bank are efficient, i.e., $\tilde{\Phi}_t \neq 1 \ \forall t \in [0, T]$ (see Definition 8.4.10). Moreover, low $\tilde{\Phi}_t$ values in the interval $t \in [12, 19]$ suggest huge scope for improvement. Note that since performance in the interval $t \in [0, 9]$ is satisfactory, we only focus on $t \in [10, 19]$. To perform filter diagnosis, we compute the conditional bias in the mean and variance for all the filters (see Theorem 8.4.25). This is done using Module 2 of Algorithm 14.
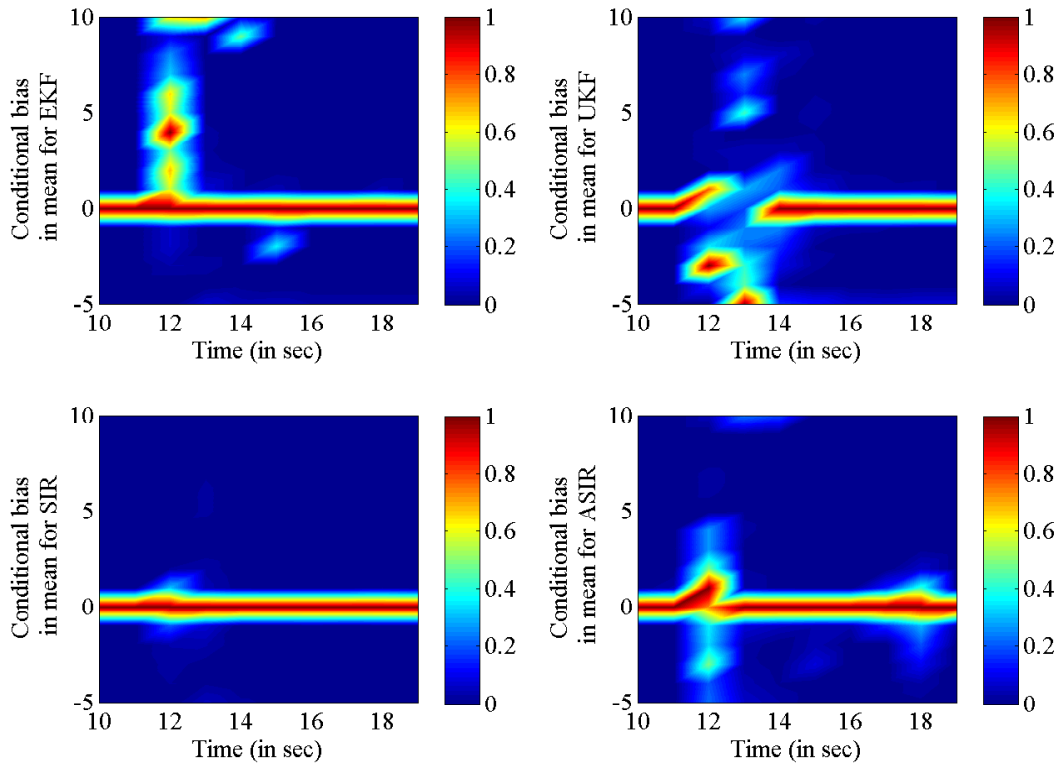
Figure 8.7: SMC estimate of the conditional bias in the mean computed for the non-linear filters in the filter bank. The results are based on $M = 200$ simulations and the color bar denotes the concentration (in %) of the bias values. The axis has been rescaled to the operating region of interest.

Figures 8.7 and 8.8 give an SMC estimate of the conditional bias in mean and variance for all the filters. From Figures 8.7 and 8.8 it is evident that the conditional bias in mean and variance are non-zero almost surely. This explains why the performance of all the filters in the interval $t \in [10, 19]$ drop (see Figure 8.6). In fact, other than SIR filter, the conditional bias in mean and variance for EKF, UKF and ASIR blow-up in the interval $t \in [11, 14]$. This suggest that compared to other filters in the bank, the true posterior density approximation with respect to the first two moment is relatively better with SIR filter.

Figure 8.9 gives SMC estimate of the unconditional bias in mean and variance for the filters in the interval $t \in [10, 19]$. From Figure 8.9 it is clear that unconditional bias in mean and variance for all the filters are also non-zero. It is instructive to highlight that on
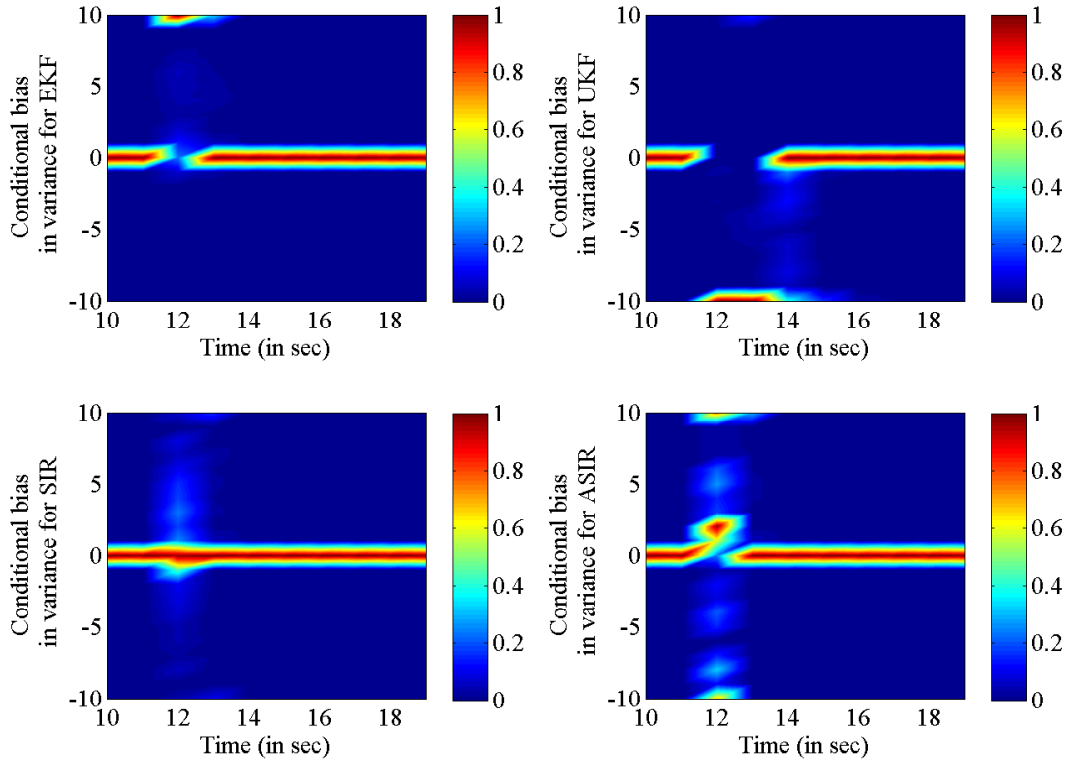
Figure 8.8: SMC estimate of the conditional bias in the variance computed for the non-linear filters in the filter bank. The results are based on $M = 200$ simulations and the color bar denotes the concentration (in %) of the bias values. The axis has been rescaled to the operating region of interest.

the interval $t \in [11, 14]$, unconditional bias in mean for SIR filter is the least; whereas, on $t \in [14, 19]$, ASIR has the lowest unconditional bias in mean (see Figure 8.9(a)). Figure 8.9 suggest that on an average sense, compared to the EKF; UKF better approximates the mean of the true posterior, but yields a poor estimate of the posterior variance. Also, in comparison with the Kalman based filters; SMC based filters yield relatively better estimates of the mean and variance.

In summary, since the conditional and unconditional bias in mean and variance are non-zero in the interval $t \in [10, 19]$, diagnosis results in Theorem 8.4.25(d) applies: (i) the filters are not efficient; (ii) yield biased estimates of mean and variance; and (iii) filters fail to yield an MMSE estimate. Moreover, relatively large values of conditional and unconditional bias in mean and variance in the interval $t \in [11, 14]$ suggest serious problems with filter
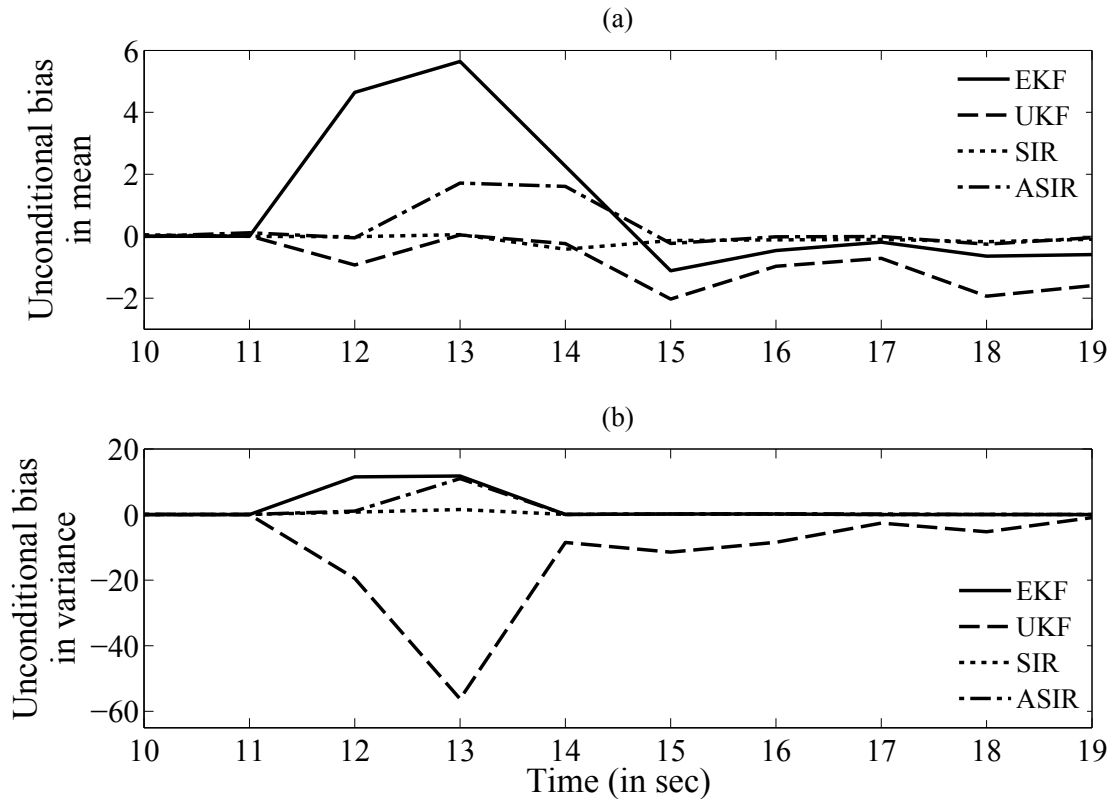
Figure 8.9: (a) compares SMC estimate of unconditional bias in the mean for the non-linear filters in the filter bank. (b) compares SMC estimate of unconditional bias in variance for the non-linear filters in the filter bank. Note that the minimum values in (a) for EKF, UKF, SIR and ASIR are: -1.11; -2.03; -0.42; and -0.25, respectively; whereas, the minimum values in (b) are: 1.2×10^{-2}; -56.2; -4.1×10^{-3}; and 1.9×10^{-2}, respectively.

performance in that interval.

Remark 8.6.5. *Note that for illustration purposes, the diagnosis result is based on filter satisfying the strict conditions on the bias in Theorem 8.4.25; however, for all practical purposes, the diagnosis should be performed as in Remark 8.5.23.*

8.6.3.5   Step 5: Filter redesign and performance assessment

From Step 4, it is clear that there is a huge scope for improving the performance of non-linear filters. Now to achieve an overall improvement in the filtering performance, we can either re-start the assessment procedure with a bank of new filters and hope the performance to improve, or more formally, improve the design of the existing filters. For
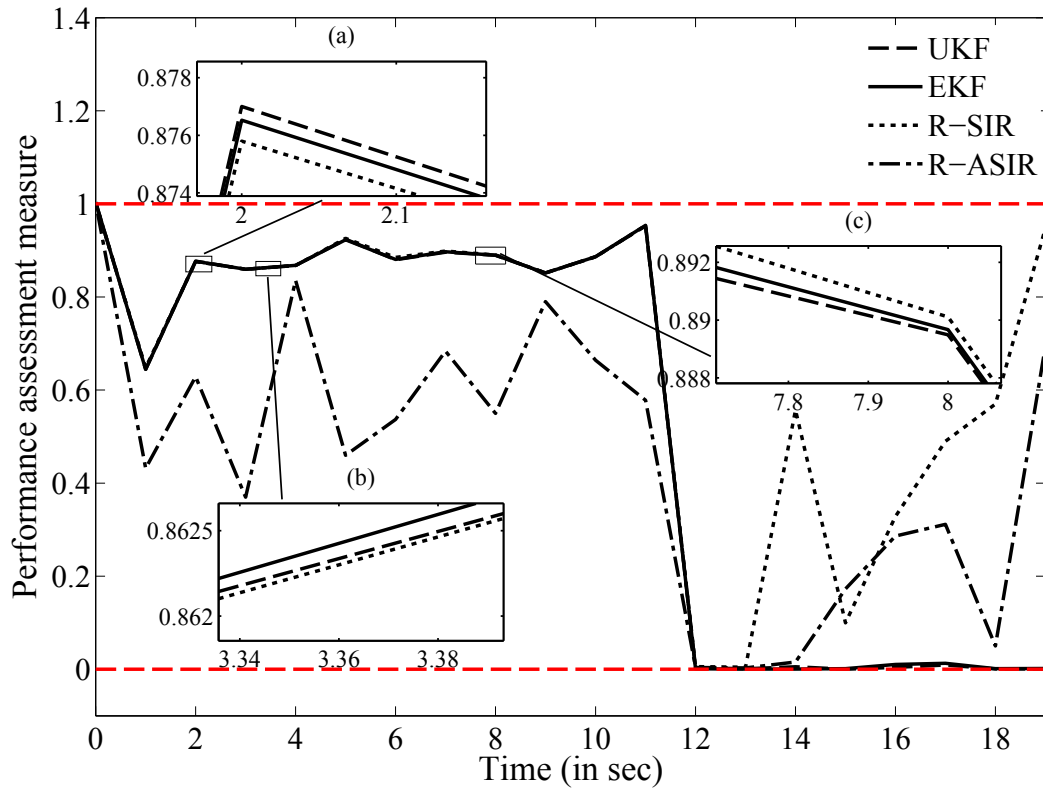
Figure 8.10: The SMC based performance assessment measure, $\tilde{\Phi}_t \; \forall t \in [0, T]$ computed for the bank with redesigned filters. Appropriate magnification of the key regions of the main figure are provided as insets. The broken red horizontal lines are the upper and lower bound for $\tilde{\Phi}_t \; \forall t \in [0, T]$.

the latter option, the assessment and diagnosis results, such as Figures 8.6 through 8.9 provide a means to improve the filter design. Note that designing filters with specific properties is non-trivial (see Remark 8.4.34), and is not included in the scope of this work. Nevertheless, for illustration purposes, we present results with simple design changes to the filters selected in Step 2.

Note that the standard EKF and UKF in the bank do not have any filter tuning parameters; however, for the SIR and ASIR, we can change the particle size and the resampling strategy. Considering the on-line implementability issues with SMC based filters (see Remark 8.5.15), we consider three options for the particle size- 50, 500, and 1000, and four options for the resampling strategy- systematic, stratified, residual, and multinomial. Using

the procedure in Step 3, the performance of the SIR and ASIR are assessed for different combinations of the particle size and resampling strategy. Of the 12 possible combinations, the SIR with 1000 particles and multinomial resampling, and ASIR with 1000 particles and residual resampling were found to have the highest performance in terms of $\tilde{\Phi}_t \ \forall t \in [0, T]$ values. Identifying the redesigned SIR and ASIR with R-SIR and R-ASIR, respectively, the bank of redesigned non-linear filters, include: EKF; UKF; R-SIR; and R-ASIR.

Figure 8.10 gives the $\tilde{\Phi}_t \ \forall t \in [0, T]$ values for the bank of redesigned non-linear filters. Comparing Figure 8.6 with Figure 8.10, the improvement with the R-SIR and R-ASIR over the interval $t \in [12, 19]$ is evident. Although the performance of the R-ASIR on $t \in [0, 11]$ is still low (compared to Figure 8.6); the performance of the R-SIR increases significantly. Note that on the interval $t \in [0, 11]$ the EKF, UKF and R-SIR outperforms each other multiple times (see the insets in Figure 8.10).

In summary, the results of Step 5 illustrates the use of the filter assessment and diagnosis results in designing filters with better performance. Note that Steps 3 through 5 can be iterated, until the user defined performance requirements are met.

8.6.3.6   Step 6: Filter switching strategy and state estimation

In this step we: (i) design and evaluate the quality of the optimal filter switching strategy for state estimation in (8.59) under the operating trajectory in Figure 8.5(a); and (ii) demonstrate the performance benefits with Steps 4 and 5.

Non-linear filter switching strategy is devised using Module 3 of Algorithm 14. Figure 8.11(a) gives the switching strategy for the bank with filters- EKF, UKF, SIR and ASIR (see Step 2); whereas, Figure 8.11(b) gives the strategy for the bank with filters- EKF, UKF, R-SIR and R-ASIR (see Step 5). Here, Figures 8.11(a) and (b) are constructed using the $\tilde{\Phi}_t \ \forall t \in [0, T]$ values computed previously in Figures 8.6 and 8.10, respectively. It is important to highlight that the strategies in Figures 8.11(a) and (b) are both optimal, with respect to the choice of the filter bank (see Theorem 8.4.31). Finally, to evaluate the

(a) Switching strategy with Step 3


(b) Switching strategy with Step 5
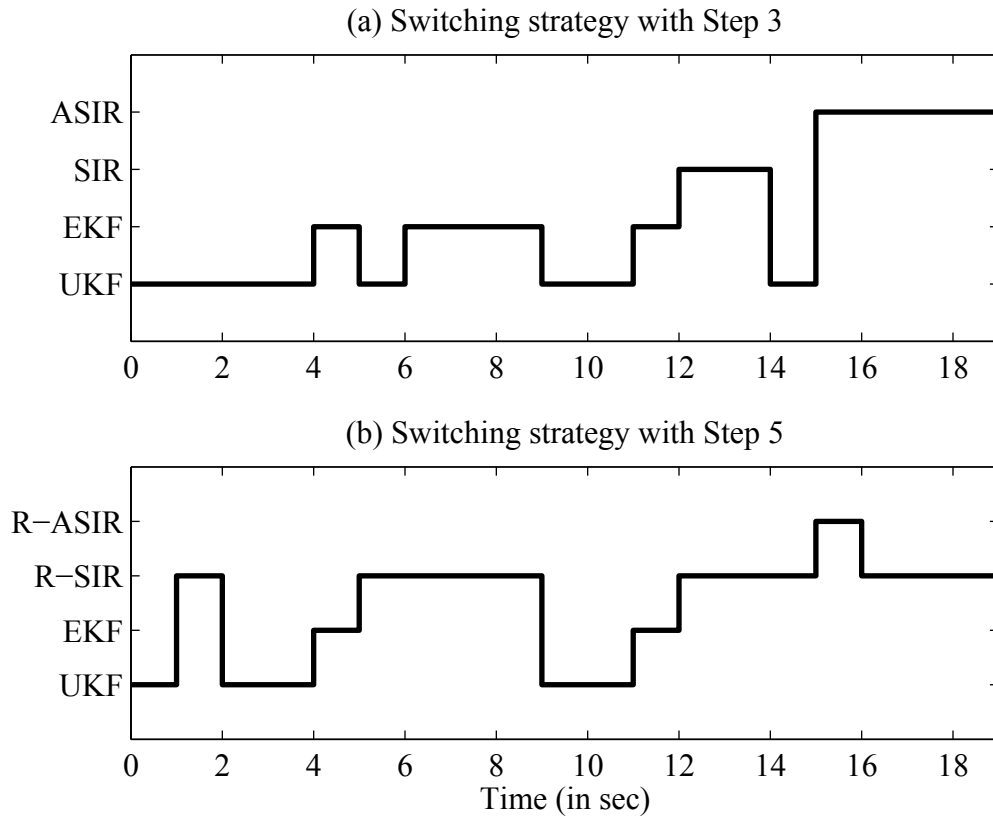
Figure 8.11: (a) the optimal filter switching map without the filter diagnosis and redesign step. (b) the optimal filter switching map with the filter diagnosis and redesign step.

efficiency of the developed strategies, we perform state estimation in (8.59), according to Figures 8.11(a) and (b). For comparison purposes, we also consider use of EKF, UKF, SIR and ASIR as a single-filter-use strategy. Table 8.3 compares six different strategies in terms of their total MSE, i.e., $\sum_{t=1}^{T} \tilde{P}_{t|t}$. Here, the total MSEs for the two sets are computed using Result 8.5.1.

From Table 8.3, it is clear that compared to the single-filter-use strategy, the filter switching strategy yields smaller total MSE for training and validation sets. In summary, the results of this step: (i) illustrates that for non-linear systems, the filter switching strategy is the optimal state estimation strategy; (ii) highlight the importance of performing filter diagnosis and redesign steps before devising the filter switching map.

Table 8.3: Total MSE in estimating the states of (8.59) with different filtering strategies using the training and validation data sets.

Measurement set	Filtering strategy					
	UKF	EKF	SIR	ASIR	Figure 8.11(a)	Figure 8.11(b)
Training (Figure8.5(b))	356.24	396.43	73.31	129.79	43.52	28.60
Validation (Figure8.5(c))	405.28	355.77	65.31	161.05	56.37	28.53

8.7   Conclusions

In this chapter we propose the use of a PCRLB inequality as a performance benchmark for non-linear state filters. Using PCRLB inequality, an assessment measure is developed to monitor and evaluate the MSE performance of multiple non-linear state filters. A diagnosis procedure based on second-order filter error decomposition is also developed to improve non-linear filtering performance. Using the assessment and diagnosis tool, a minimum MSE non-linear filter switching strategy is proposed for state estimation in general non-linear SSMs. According to the proposed strategy, at each sampling-time, the performance of a pre-determined bank of Kalman and SMC based non-linear filters is first assessed using the PCRLB based measure, and then the filter with highest performance measure is selected for delivering the state estimate. The complex, multi-dimensional integrals involved in the computation of the PCRLB inequality and the tools developed therefrom are approximated using SMC methods. The utility and efficiency of the SMC based filter assessment and diagnosis tool in devising an optimal filter switching strategy was illustrated on an example.

The current work assumes the model parameters to be known a priori; however, for certain applications, this assumption might be a little restrictive. Future work will focus on extending the results of this work to handle such situations.

Bibliography

Achilias, D.S. and C. Kiparissides (1992). Development of a general mathematical framework for modeling diffusion controlled free-radical polymerization reactions. *Macromolecules* **25**(14), 3739–3750.

Andrieu, C., A. Doucet, S.S. Singh and V. B. Tadic (2004). Particle methods for change detection, system identification, and control. *Proceedings of IEEE* **92**(3), 423–438.

Arulampalam, M.S., S. Maskell, N. Gordon and T. Clapp (2002). A tutorial on particle filters for online non-linear/non-Gaussian Bayesian tracking. *IEEE Transactions on Signal Processing* **50**(2), 174–188.

Bapat, R.B. and T.E.S. Raghavan (1997). *Nonnegative Matrices and Applications*. Cambridge University Press, New York.

Bar-Shalom, Y. and X.R. Li (1993). *Estimation and Tracking: Principles, Techniques and Software*. Artech House, Dedham.

Bar-Shalom, Y., X.R. Li and T. Kirubarajan (2001). *Estimation with Applications to Tracking and Navigation*. Wiley, New York.

Bates, D.M. and D.G. Watts (1988). *Non-linear Regression Analysis and Its Applications*. Chap. Curvature measures of non-linearity. Wiley, New York.

Bergman, N. (2001). *Sequential Monte Carlo Methods in Practice*. Chap. Posterior Cramér-Rao bounds for sequential estimation. Springer–Verlag, New York.

Bergman, N., L. Ljung and F. Gustafsson (1999). Terrain navigation using Bayesian statistics. *IEEE Control Systems Magazine* **19**(3), 33–40.

Billingsley, P. (1995). *Probability and Measure*. Chap. The integral. Wiley, New York.

Caffery, J. and G.L. Stuber (2000). Non-linear multi-user parameter estimation and tracking in CDMA systems. *IEEE Transactions on Communications* **48**(12), 2053–2063.

Chitralekha, S.B., J. Prakash, H. Raghavan, R.B. Gopaluni and S.L. Shah (2010). A comparison of simultaneous state and parameter estimation schemes for a continuous fermentor reactor. *Journal of Process Control* **20**(8), 934–943.

Chopin, N. (2004). Central limit theorem for sequential Monte Carlo methods and its application to Bayesian inference. *The Annals of Statistics* **32**(6), 2385–2411.

Crisan, D. and A. Doucet (2002). A survey of convergence results on particle filtering methods for practitioners. *IEEE Transactions on Signal Processing* **50**(3), 736–746.

Crisan, D. and B. Rozovskii (2011). *The Oxford Handbook of Non-linear Filtering*. Oxford University Press, Oxford.

Cui, N., L. Hong and J.R. Layne (2005). A comparison of non-linear filtering approaches with an application to ground target tracking. *Signal Processing* **85**(8), 1469 –1492.

Doucet, A., M. Briers and S. Sénécal (2006). Efficient block sampling strategies for sequential Monte Carlo methods. *Journal of Computational and Graphical Statistics* **15**(3), 693–711.

Doucet, A., N. de Freitas and N. Gordon (2001). *Sequential Monte Carlo Methods in Practice*. Chap. On sequential Monte Carlo methods. Springer–Verlag, New York.

Evensen, G. (2007). *Data Assimilation: The Ensemble Kalman Filter*. Chap. Estimation in an oil reservoir simulator. Springer, Berlin/Heidelberg.

Farina, A., B. Ristic and D. Benvenuti (2002). Tracking a ballistic target: comparison of several non-linear filters. *IEEE Transactions on Aerospace and Electronic Systems* **38**(3), 854–867.

Gilks, W.R. and C. Berzuini (2002). Following a moving target-Monte Carlo inference for dynamic Bayesian models. *Journal of the Royal Statistical Society: Series B* **63**(1), 127–146.

Gopaluni, R.B. (2008). A particle filter approach to identification of non-linear processes under missing observations. *The Canadian Journal of Chemical Engineering* **86**(6), 1081–1092.

Horn, R.A. and C.R. Johnson (1985). *Matrix Analysis*. Cambridge University Press, New York.

Johansen, A.M. and A. Doucet (2008). A note on the auxiliary particle filter. *Statistics and Probability Letters* **78**(12), 1498–1504.

Jones, E., M. Scalzo, A. Bubalo, M. Alford and B. Arthur (2011). Measures of non-linearity for single target tracking problems. In: *Proceedings of the SPIE Signal Processing, Sensor Fusion and Target Recognition XX*. Orlando, USA. pp. 1–14.

Kandepu, R., B. Foss and L. Imsland (2008). Applying the unscented Kalman filter for non-linear state estimation. *Journal of Process Control* **18**(7–8), 753–768.

Kantas, N., A. Doucet, S.S. Singh and J. Maciejowski (2009). An overview of sequential Monte Carlo methods for parameter estimation in general state-space models. In: *Proceedings of the 15th IFAC Symposium on System Identification*. Saint-Malo, France. pp. 774–785.

Kivman, G.A. (2003). Sequential parameter estimation for stochastic systems. *Non-linear Processes in Geophysics* **10**(3), 253–259.

LaViola, J.J. (2003). A comparison of unscented and extended Kalman filtering for estimating quaternion motion. In: *Proccedings of the American Control Conference*. Colorado, USA. pp. 2435–2440.

Lei, M., B.J. Van Wyk and Q. Yong (2011). Online estimation of the approximate posterior Cramér-Rao lower bound for discrete-time non-linear filtering. *IEEE Transactions on Aerospace and Electronic Systems* **47**(1), 37–57.

Li, X.R., Z. Zhao and V.P. Jilkov (2001). Practical measures and test for credibility of an estimator. In: *Proceedings of the Workshop on Estimation, Tracking and Fusion*. Monterey, USA. pp. 481–495.

Mallick, M. and B.F. La Scala (2006). Differential geometry measures of non-linearity for the video tracking problem. In: *Proceedings of the SPIE Signal Processing, Sensor Fusion and Target Recognition XV*. Orlando, USA. pp. 1–13.

Mallick, M., B.F. La Scala and M.S. Arulampalam (2005). Differential geometry measures of non-linearity for the bearing-only tracking problem. In: *Proceedings of the SPIE Signal Processing, Sensor Fusion and Target Recognition XIV*. Bellingham, USA. pp. 288–300.

Maybeck, P.S. (1982). *Stochastic Models, Estimation and Control*. Vol. 2. Academic Press, New York.

Merwe, R.V.D. and E.A. Wan (2001). The square-root unscented Kalman filter for state and parameter-estimation. In: *Proccedings of the IEEE International Conference on Acoustics, Speech, and Signal Processing*. Utah, USA. pp. 3461–3464.

Mesbah, A., A.E.M. Huesman, H.J.M. Kramer and P.M.J. Van den Hof (2011). A comparison of non-linear observers for output feedback model-based control of seeded batch crystallization processes. *Journal of Process Control* **21**(4), 652–666.

Moral, P. Del (2004). *Feynman-Kac Formulae: Genealogical and Interacting Particle Systems with Applications*. Springer–Verlag, New York.

Moral, P. Del and A. Doucet (2003). *Séminaire de Probabilités XXXVII*. Chap. On a class of genealogical and interacting Metropolis models. Springer, Berlin/Heidelberg.

Nehorai, A. and M. Hawkes (2000). Performance bounds for estimating vector systems. *IEEE Transactions on Signal Processing* **48**(6), 1737–1749.

Niu, R., P.K. Varshney, M. Alford, A. Bubalo, E. Jones and M. Scalzo (2008). Curvature non-linearity measure and filter divergence detector for non-linear tracking problems. In: *Proceedings of the 11th International Conference on Information Fusion*. Cologne, Germany. pp. 1–8.

Pacharu, S.R., R. Gudi and S. Patwardhan (2012). Advanced state estimation techniques for packed bed reactors. In: *Proceedings of the 8th IFAC Symposium on Advanced Control of Chemical Processes*. Singapore. pp. 519–524.

Pitt, M.K. and N. Shephard (1999). Filtering via simulation: auxiliary particle filters. *Journal of the American Statistical Association* **94**(446), 590–599.

Reams, R. (1999). Hadamard inverses, square roots and products of almost semi-definite matrices. *Linear Algebra and its Applications* **288**(1), 35–43.

Ristic, B., M.S. Arulampalam and N. Gordon (2004). *Beyond the Kalman Filter: Particle Filters for Tracking Applications*. Artech House, Boston.

Robert, C.P. and G. Casella (2004). *Monte Carlo Statistical Methods*. Chap. Monte Carlo integration. Springer–Verlag, New York.

Romanenko, A. and J.A.A.M. Castro (2004). The unscented filter as an alternative to the EKF for non-linear state estimation: a simulation case study. *Computers and Chemical Engineering* **28**(3), 347–355.

Schön, T.B., A. Wills and B. Ninness (2011). System identification of non-linear state-space models. *Automatica* **47**(1), 39–49.

Shao, X., B. Huang and J.M. Lee (2010). Constrained Bayesian state estimation–a comparative study and a new particle filter based approach. *Journal of Process Control* **20**(2), 143–157.

Shenoy, A.V., J. Prakash, V. Prasad, S.L. Shah and K.B. McAuley (2012). Practical issues in state estimation using particle filters: case studies with polymer reactors. *Journal of Process Control* **23**(2), 120–131.

Sorenson, H.W. (1974). On the development of practical non-linear filters. *Information Sciences* **7**(C), 253–270.

Tanizaki, H. (2001). Non-linear and non-Gaussian state-space modeling using sampling techniques. *Annals of the Institute of Statistical Mathematics* **53**(1), 63–81.

Tichavský, P., C. Muravchik and A. Nehorai (1998). Posterior Cramér-Rao bounds for discrete-time non-linear filtering. *IEEE Transactions on Signal Processing* **46**(5), 1386–1396.

Trees, H.L.V. (1968). *Detection, Estimation and Modulation Theory–Part I*. Chap. Classical detection and estimation theory. Wiley, New York.

Tulsyan, A., B. Huang, R.B. Gopaluni and J.F. Forbes (2012). Performance assessment of non-linear state filters. In: *Proceedings of the 8th IFAC Symposium on Advanced Control of Chemical Processes*. Singapore. pp. 371–376.

Tulsyan, A., B. Huang, R.B. Gopaluni and J.F. Forbes (2013*a*). A particle filter approach to approximate posterior Cramér-Rao lower bound: The case of hidden states. *IEEE Transactions on Aerospace and Electronic Systems, In press.*

Tulsyan, A., B. Huang, R.B. Gopaluni and J.F. Forbes (2013*b*). On simultaneous state and parameter estimation in non-linear state-space models. *Journal of Process Control* **23**(4), 516–526.

Šimandl, M., J. Královec and P. Tichavský (2001). Filtering, predictive, and smoothing Cramér-Rao bounds for discrete-time non-linear dynamic systems. *Automatica* **37**(11), 1703–1716.

Wang, H., A. Szabo, J. Bamberger, D. Brunn and U.D. Hanebeck (2008). Performance comparison of non-linear filters for indoor WLAN positioning. In: *Proceedings of the 11th International Conference on Information Fusion*. Cologne, Germany. pp. 1–7.

Xu, Z., J. Zhao, J. Qian and Y. Zhu (2009). Non-linear MPC using an identified LPV model. *Industrial & Engineering Chemistry Research* **48**(6), 3043–3051.

Chapter 9

Concluding remarks

In this chapter, the conclusions drawn from the results and analyses presented in Chapters 2 through 8 are summarized. Discussions on some future directions are also presented.

9.1 Conclusions

This thesis considers the use of Bayesian methods for state inference and identification of non-linear dynamical systems represented by discrete-time, stochastic non-linear state-space models (SSMs). The basic idea behind the simultaneous on-line state inference and identification method in Chapter 2 is augmentation of the model parameters with the process states. This approach is called the artificial dynamics approach (ADA). The ADA is an on-line Bayesian approach, which allows to cast the Bayesian identification problem as a state inference problem. The ADA is one of the most important and popular class of on-line Bayesian identification method for discrete-time, stochastic non-linear SSMs. Although the idea of state-parameter augmentation is certainly not new, there are several long standing drawbacks of ADA: (a) the dynamics of the parameters are related to the width of the kernel and the variance of the artificial noise, which are often difficult to fine tune; and (b) transforming the problem by adding artificial noise modifies the original problem, so that it becomes hard to quantify the bias introduced in the resulting parameter estimates. In this thesis, an attempt to solve the aforementioned problems associated with

ADA has been made.

To address the first problem, in Chapter 2, an adaptive sequential-importance-resampling (Ad-SIR) filter for ADA based on-line state inference and identification of general non-linear SSMs with non-Gaussian state and measurement noise is presented. The usual variance inflation problem introduced by adding artificial parameter dynamics is corrected, using a kernel smoothing algorithm. An optimal tuning rule for the kernel smoothing parameter is presented under an on-line optimization framework. The usual degeneracy issues with sequential-importance-resampling filter under different process-to-measurement noise ratios are also avoided through the kernel smoothing process based on Kullback-Leibler divergence. The proposed Ad-SIR method is an 'optimization-free' estimator, making it efficient and computationally fast. This is a major advantage over the traditional maximum-likelihood based methods. The extension of Ad-SIR method to handle missing measurements in real-time is also presented in Chapter 2.

For the second problem, a posterior Cramér-Rao lower bound (PCRLB) based approach is proposed in Chapter 4 for error analysis in ADA. The proposed tool has wide applicability, as it can be used to perform error analysis for an entire class of on-line Bayesian identification methods and for a general class of non-linear systems represented by discrete-time, stochastic non-linear SSMs. Using the PCRLB based analysis tool, in Chapter 4, it is illustrated how the quality of the parameter estimates obtained with Ad-SIR filter can be assessed in terms of bias, mean square error (MSE) and efficiency.

Another important problem considered in this thesis is that of optimal selection of on-line Bayesian identification methods. Considering the large number of on-line Bayesian identification methods available at our disposal, it is often in our interest to select the right identification method for our system. A PCRLB inequality based tool for performance assessment of on-line Bayesian identification methods is developed in Chapter 3. Based on the developed measure, an average-optimal and optimal minimum (MMSE) strategy

for state inference in non-linear SSMs with non-Gaussian noise and unknown model parameters is proposed. An approach to monitoring the quality of the the state estimates obtained under unknown model parameters is also provided. The utility of the tools is illustrated on a ballistic target tracking system with unknown ballistic coefficient.

In this thesis, the input design problem for on-line Bayesian identification of stochastic non-linear SSM is also considered. An input design procedure based on minimization of the PCRLB with respect to inputs is developed in Chapter 5. This development is critical since to the best of authors' knowledge, no known Bayesian input design methods are available for a class of general stochastic non-linear SSMs. One of the distinct advantages of the proposed method is that the designed input is independent of the on-line Bayesian method used for identification. Simulation results in Chapter 5 suggest that the method can be used to deliver accurate inference on the parameter estimates.

The problem of prior design is considered in Chapter 6. This study is performed in the context of organization of a priori information amassed from previous experiments to design informed future experiments. Different prior designs relating to organization and use of available information are discussed from a theoretical viewpoint. Development of these prior designs arises based on the need to project a priori parameter information onto the constrained space for achieving efficient integration of available process information with the input design algorithm. Results in Chapter 6 suggest superior identification capabilities of Bayesian methods with appropriate prior design.

Besides the above developments, in Chapter 7, a numerical method to recursively approximate the PCRLB for general discrete-time, non-linear SSMs is proposed. The presented method is effective in approximating the PCRLB, when the true states are hidden or unavailable. This has practical relevance in situations wherein the test-data consist of only sensor readings. The proposed approach makes use of the sensor readings to estimate the hidden true states, using a sequential Monte Carlo (SMC) method. The

method is general and can be used to compute the lower bound on the MSE for non-linear dynamical systems, with non-Gaussian state and sensor noise. The quality and utility of the SMC based PCRLB approximation was validated on two simulation examples, including a practical problem for ballistic target tracking at re-entry phase. The numerical quality of the SMC based PCRLB approximation was analysed for a range of target state and sensor noise variances, and with different number of particles. The proposed method exhibited acceptable and consistent performance in all the simulations. Increasing the number of particles was found to be effective in reducing the errors in the PCRLB estimates. Strategies to improve the quality of SMC estimates were also discussed.

In Chapter 8, the use of a PCRLB inequality as a performance benchmark for non-linear state filters is proposed. Using PCRLB inequality, an assessment measure is developed to monitor and evaluate the MSE performance of multiple non-linear state filters. A diagnosis procedure based on second-order filter error decomposition is also developed to improve the non-linear filtering performance. Using this assessment and diagnosis tool, a minimum MSE non-linear filter switching strategy is proposed for state estimation in general non-linear SSMs. According to the proposed strategy, at each sampling-time, the performance of a pre-determined bank of Kalman and SMC based non-linear filters is first assessed using the PCRLB based measure and then, the filter with the highest performance measure is selected for delivering the state estimate. The complex integrals involved in the computation of the PCRLB inequality and the tools developed therefrom are approximated using SMC methods. The utility and efficiency of the SMC based filter assessment and diagnosis tool in devising an optimal filter switching strategy was illustrated with an example.

To summarize, in this thesis, an attempt to develop a unified framework for state inferencing (see Figure 9.1) and Bayesian identification (see Figure 9.2) of general discrete-time, stochastic non-linear SSMs has been made. According to Figure 9.1, given a SSM
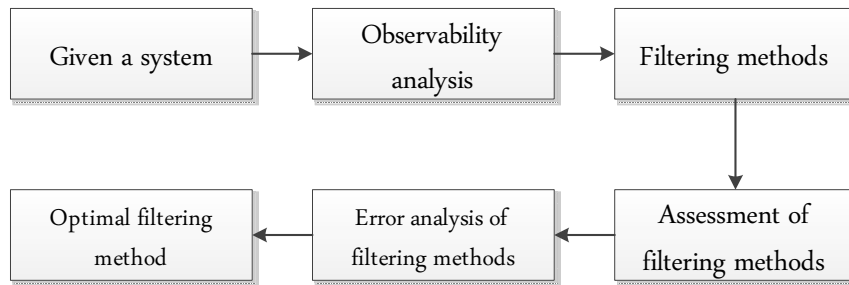
Figure 9.1: A unified framework for state inferencing in non-linear systems.
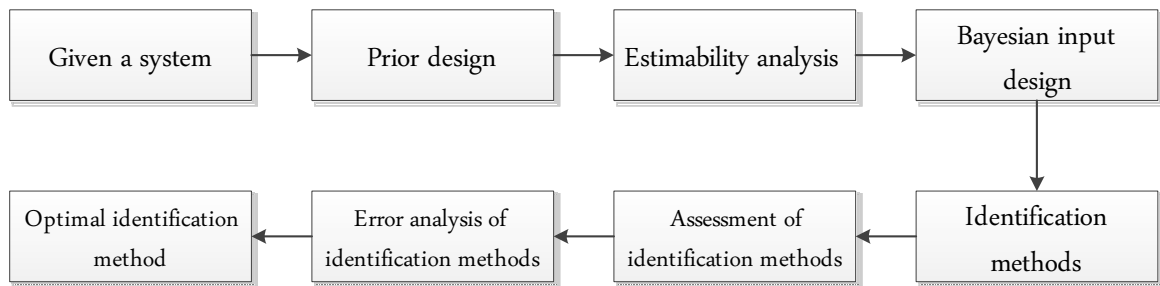

Figure 9.2: A unified framework for Bayesian identification of non-linear systems.

representation of a non-linear system, the first step to develop efficient state inferencing method is to perform observability analysis. This step helps determine whether it is theoretically possible to design state inferencing methods for the given system. Once it is determined that inferencing is possible, use of different state filters can be investigated along with assessment of their individual filtering performance. If required, error analysis of filters can be performed to diagnose and improve their filtering performance. After error analysis, the best filtering method for state inferencing can be selected for a given system.

Similarly, for Bayesian identification of non-linear systems, a unified approach, as given in Figure 9.2, can be adopted. Given an SSM representation of a non-linear system and some a priori process and parameter information, prior density for the parameters can be designed. This can be followed by estimability analysis, to determine whether it is theoretically possible to identify the model parameters for the given prior design and SSM representation. If the model parameters are estimable, optimal input design and performance assessment of different identification methods can be performed. If

needed, error analysis on the identification methods can also be performed to improve their performance. Finally, based on the assessment and analyses results, an optimal method can be selected, which would allow identification of the given system.

To fully realize the benefits of the proposed unified framework for state inferencing and Bayesian identification of general discrete-time, stochastic non-linear SSMs, much work remains to be done, which is discussed in the next section.

9.2   Future work

Throughout this thesis a range of different problems surfaced, which require further attention. The most notable being the observability and estimability analysis for stochastic non-linear systems. Working on these two topics would complete the unified framework illustrated in Figures 9.1 and 9.2. Note that observability and estimability analyses for stochastic non-linear systems are not only the important links, which are currently missing in this thesis, but are also, in general, two notoriously difficult unsolved problems in non-linear estimation theory. Currently, a detailed research on these two topics is being worked out, and because of the premature results, it has not been included in the thesis.

The simultaneous state inferencing and identification method discussed in Chapter 2 can be improved in several ways. First, the method used to solve the optimization problem in Proposition 2.5.8 can be improved. Currently, simple non-linear programming methods are used to solve it, but due to the non-convex objective function, the use of effective stochastic optimization methods may be expected to yield superior results. Convergence proof for the proposed Ad-SIR filter is currently missing, but can be a significant future addition.

The PCRLB based error analysis method developed in this thesis for state inferencing and Bayesian identification methods is based on comparing the first two moments of the approximate posterior density with the true posterior density. Now since a non-Gaussian posterior density requires an infinite number of moments for its exact representation, clearly

developing the analysis based on only the first two moments is certainly not sufficient. The same arguments also hold for the PCRLB based performance assessment and selection tools developed in this thesis. A possible future direction to expand this work would be to investigate entropy based performance assessment, diagnosis and filter selection.

The prior design strategy presented in this thesis is only valid for non-linear SSMs, with zero state noise. This is because all the prior designs developed in Chapter 6 (i.e., circular, truncated and directional prior design), assume the posterior density to be Gaussian. This assumption may be restrictive or impractical for systems modeled by general stochastic non-linear SSMs wherein, the posterior density is generally non-Gaussian. Furthermore, the prior design strategy considered in this thesis is valid only for off-line Bayesian identification method. A possible direction for future work in this topic could be the extension of the proposed prior design methods for general stochastic non-linear SSMs and for on-line Bayesian identification methods. These extensions will help explore how effective prior can be designed for ADA and other on-line Bayesian identification methods.

An SMC based PCRLB approximation in Chapter 7 assumes the model parameters to be known a priori; however, for certain applications, this assumption might be a little restrictive. Future work will focus on extending these results to handle PCRLB approximation in situations, where parameters are unknown. Furthermore, use of the SMC method in approximating the modified versions of the PCRLB, which allows inferencing in applications, such as target generated measurements, measurement origin uncertainty, cluttered environments, and Markovian models, will also be a useful future addition.

The results in Chapter 5 appear promising; however, solving the optimization problem is non-trivial. Despite several levels of relaxation and parametrization of the input space, the optimization in (5.25) is a stochastic programming problem, as a result (5.25a) tends to be non-smooth, and has many local minima. Development of stochastic gradient-based optimization methods will definitely help design improved inputs for our system.

Finally, the tools developed in this thesis have only been tested on simple non-linear systems, with the exception of the ballistic target tracking system and the Baker's yeast fermenter example considered in Chapters 3 and 7, and Chapter 6, respectively. It would be interesting to study and analyse scalability issues with these methods. Another future extension would be practical approaches for validation of the unified framework for the state inference and identification proposed in Figures 9.1 and 9.2, respectively. Currently, validation of each of the steps in Figures 9.1 and 9.2 is done separately, but to demonstrate the true potential of the proposed work, all of the steps in Figures 9.1 and 9.2 need to be validated and studied as an integrated framework.